

Low-temperature anaerobic wastewater treatment by granulated biomass

by

Anissa Sukma Safitri

Thesis submitted in fulfilment of
the requirements for the degree of
PHILOSOPHIAE DOCTOR
(PhD)



Faculty of Science and Technology
Department of Chemistry, Bioscience and Environmental Engineering
2022

University of Stavanger
NO-4036 Stavanger
NORWAY
www.uis.no

©2022 Anissa Sukma Safitri

ISBN: 978-82-8439-087-1

ISSN: 1890-1387

PhD: Thesis UiS No. 648

Preface

The presented thesis is submitted to the University of Stavanger (Norway) to partially fulfil the requirements for the degree of *Philosophiae Doctor* (PhD). This PhD thesis comprises three years of research carried out at the University of Stavanger (Norway) and INRAE LBE (Narbonne, France). Associate Professor Roald Kommedal and Associate Professor Krista M. Kaster were supervisor and co-supervisor, respectively. This work was funded by the Norwegian Ministry of Education and Research through the university grant program (Norwegian Department of Education) and the Foundation *Stiftelsen Signe-Marie*.

Two mandatory elective courses were taken while enrolling on this PhD study: MLJ 903 Applied Instrumental Analysis and MLJ 906 PhD Project Course in Environmental Science and Technology. The main objective of the instrumental analysis course (MLJ 903) was to investigate the cell growth characteristics of a microalgae strain in nutrient-limited media using a microplate reader. Then, the project chosen in MLJ 906 course was anaerobic granulated biofilm system modelling using AQUASIM 2.1 software. The main results of these two courses are incorporated in this thesis.

Two advanced external courses, Environmental Biotechnology (22 May - 1 June 2018) and Bioprocess Design (18 - 22 March 2019) in the Delft University of Technology, the Netherlands, were taken along with two inhouse courses to support and develop further understanding of the basic in microbiology, bioprocess, and biochemical engineering.

An international collaboration was done with INRAE LBE (Narbonne, France) in September 2018 - March 2019, in the framework of the experiment on methanotrophic-phototrophic interactions in oxygenic photogranules to remove dissolved methane.

Parts of this thesis have been published, with the scientific papers included in the Appendices. The following paper, manuscripts, and related publications have been produced and included in this thesis:

1. Paper/manuscripts:

- a. Paper I: Effect of low-temperatures and wastewater organic loading on UASB system performances. Anissa Sukma Safitri, Krista M. Kaster, and Roald Kommedal. *Submitted for publication*.
- b. Paper II: Microbial community development on psychrophilic granules during long-term UASB operation. Anissa Sukma Safitri, Krista M. Kaster, and Roald Kommedal. *In preparation manuscript*.
- c. Paper III: Engineered methanotrophic syntrophy in photogranule communities removes dissolved methane. Anissa Sukma Safitri, Jérôme Hamelin, Roald Kommedal, and Kim Milferstedt. Published in Water Research X journal, <https://doi.org/10.1016/j.wroa.2021.100106>.

2. Conferences:

- a. Conference I: Effect of low-temperature and municipal wastewater organic loading on UASB reactor performances. Anissa Sukma Safitri, Krista M. Kaster, and Roald Kommedal. Poster presented at IWA Biofilms: Granular Sludge Conference; Delft, the Netherlands; March 8 - 21, 2018.
- b. Conference II: Integrated wastewater treatment concept for water resource recovery. Anissa Sukma Safitri, Ali Farsi, Krista M. Kaster, and Roald Kommedal. Poster presented at IWA EcoSTP: Ecotechnologies for Wastewater Treatment Conference; London, Canada; June 25 - 27, 2018.

- c. Conference III: Low-temperature biogas production from municipal wastewater by laboratory-scale UASB granules. Anissa Sukma Safitri, Krista M. Kaster, Gopalakrishnan Kumar, and Roald Kommedal. Oral presentation at International Conference on Alternative Fuels Energy and Environment-ICAFEE; Nanjing, China; October 28 - 31, 2018.
- d. Conference IV: Anaerobic municipal wastewater treatment – The solution or part of the solution towards sustainable wastewater treatment? Roald Kommedal and Anissa Sukma Safitri. Oral presentation (virtual platform) at 1st International Conference on Pollution Prevention and Clean Technologies (ICPPCT); New Delhi, India; December 06 - 07, 2021.
- e. Conference V: Ecologically engineering methanotrophic photogranules. Anissa Sukma Safitri, Jérôme Hamelin, Roald Kommedal, and Kim Milferstedt. Extended abstract accepted for oral presentation at 13th IWA Specialist Conference on Wastewater Ponds and Algal Technologies; Melbourne, Australia; July 03 - 06, 2022.
- f. Conference VI: Anaerobic granulated biofilm system model for municipal wastewater treatment. Anissa Sukma Safitri and Roald Kommedal. Abstract accepted for full paper submission at 63rd International Conference of the Scandinavian Simulation Society, SIMS 2022; Trondheim, Norway; September 20 - 21, 2022.

Acknowledgements

All praises are to The Creator, The Lord of this world, *Allah Subhanahu wa Ta'ala*.

Undertaking this PhD has been a long journey for me, and it would not have been possible without the guidance and help of several individuals who, in one way or another, contributed and extended their valuable presence in the completion of this thesis.

First, I would like to express my deep gratitude to my supervisor, Roald Kommedal, for believing that I was a good candidate for this project, continuous guidance, fruitful discussions, and positive encouragement, along with my co-supervisor, Krista M. Kaster. Thank you for being such great mentors who have taught me not only related to this research project but also research integrity and professionalism in general. I really enjoyed working with you two.

My sincere thanks also to Kim Milferstedt and Jérôme Hamelin for the opportunity to join their team at INRAE LBE (Narbonne, France), for the collaboration, insightful comments, and inspiration. I am also grateful to Philippe Sousbie and Anaïs Bonnafous for the laboratory technical support. My stay in Narbonne was one of the highlights of this PhD journey.

I wish to gratefully acknowledge the Norwegian Ministry of Education and Research through the university grant program (Norwegian Department of Education) and the Foundation *Stiftelsen Signe-Marie* to support this research project. I would also express my gratitude to IVAR IKS (Norway), especially Elena Alventosa, Lena Pedersen, Anders Wold, Ayu Rahmi, and Leif Ydstebø, for wastewater logistics, support, and operational advice.

I thank all my colleagues at the Department of Chemistry, Bioscience and Environmental Engineering (IKBM), University of Stavanger, for their help, especially Ingunn W. Jolma, head of the department; Gro Johnsen, former head of department; Jacob C. Rørdam, office manager; Torleiv Bilstad, Gopalakrishnan Kumar, and Ilke P. Ozkok for sharing their knowledge and experience; and to all laboratory staffs: Liv Margareth A., Hans Kristian B., Erling B. Monsen, Lyudmyla Nilsen, Hong Lin, and Xiaoping Zhang, who store all the knowledge on how to do things, you are incredibly helpful.

Thanks to all my PhD fellows for the help, stimulating discussions, and sharing our ups and downs during our PhD life, especially our Environmental Engineering group: Eystein Opsahl, Daniel Basiry, Menghour Huy, and Nooshin E. Heravi. Gratitude also goes to Postdocs and all students who played important parts in this work: Ali Farsi, Remya R. Nair, Ayesha Akhtar, Nurul Aufa, Kobina A. Quansah, Rebekka T. Carlsen, Yaw Boateng, Riway Khanal, and Roberto T. Nuñez. I cannot miss mentioning Postdoc fellow, Kristin T. Ravndal, for spending time and effort reviewing my thesis.

I would like to thank all people who have motivated and prayed from across the sea: my parents (Mamah Ida Windiani & Bapak Nana Mulyana; Mamah Aisyah & Ayah Riadhun Najichin), my brothers and sisters (Fajri, Faisal, Syibli, Nadya, and Lala), relatives, and all my friends.

Last but not least, special gratitude and tremendous respect for my husband, Abdul Qohar Hadzami, for the endless prays, support, encouragement, patience, and unconditional love, and my son, Abdullah Zayn Hadzami, who is both an excellent distraction from work and a great motivation to do better each day. This is all yours.

Anissa Sukma Safitri

Stavanger, March 2022

Summary

In this study, long-term operation of up-flow anaerobic sludge blanket (UASB) system treating real municipal wastewater at decreasing temperatures (25, 16, 12, 8.5, 5.5, and 2.5 °C) and variable organic loading rates from 1.0 gCOD·l⁻¹·d⁻¹ up to 15.2 gCOD·l⁻¹·d⁻¹ was investigated over 1025 days. Experiments were performed in two parallel in-house designed laboratory-scale UASB reactors, which were operated continuously with hydraulic retention time of 16.7 h down to 1.1 h. Stable COD removal efficiencies of 50 - 70 % were achieved at 25 °C down to 8.5 °C with loading up to approximately 15.2 gCOD·l⁻¹·d⁻¹. COD removal efficiencies were reduced at temperatures below 8.5 °C, but significant methane formation was observed even at 2.5 °C at reduced loading (up to 5 gCOD·l⁻¹·d⁻¹). More than 90% of COD removed was converted to methane, and the methane yield did not change significantly with respect to temperatures. The overall COD balance closed at above 90% of the inlet COD at all operating temperatures and organic loading rates.

Temperature affected the reactor performances, microbial community structure, and the degradation pathway of organic matter with acetoclastic methanogen played significant roles. Acetate was the primary precursor of methanogenesis pathway at low-temperatures. Microbial communities proved the adaptation ability to very low-temperatures down to 2.5 °C regardless of the operating organic loading rates; psychrotolerant. Additionally, an anaerobic granulated biofilm system at 25 °C and different organic loading rates (1, 3, 8, 10, 15, and 20 gCOD·l⁻¹·d⁻¹) was modelled in AQUASIM 2.1 to predict and simulate biofilm model implementation and assumptions specific to the granules as a fixed biofilm in UASB reactor system in this study. Simulated organic loading rates scenario results showed COD removal efficiencies (62 - 69%) and methane fraction (83 - 88%) in biogas at steady-state conditions decreased with the increasing organic loading rates. All

simulations predicted an increased pH profile, from pH 7 in the outer layer to approximately pH 8.3 in the core of granules, under increasing organic loading rates, but the biomass composition and active biofilm regions were not significantly affected by organic loading rate variable.

UASB effluent post-treatment investigations, specifically on dissolved methane and nutrient removal, were performed as supplementary studies. A methanotrophic-cyanobacterial syntrophy was established in the existing oxygenic photogranules to remove dissolved methane. This syntrophy was maintained and propagated in a continuously operated reactor (hydraulic retention time of 12 h), proven by observed biomass yield and dissolved methane removal by approximately 2.4 gVSS·gCH₄⁻¹ and 85%, respectively, with COD balance closed at around 91%. Community analysis suggested methanotrophs and phototrophs syntrophy, and the cross-feeding between photogranules of different community compositions, containing methanotrophic bacteria, phototrophs, and non-methanotrophic methylotrophs.

Nutrient removal from filtered UASB secondary effluent was investigated using several microalgal strains based on a literature review: *Chlorella vulgaris*, *Chlorella sorokiniana*, *Tetradesmus obliquus*, *Haematococcus pluvialis*, and *Microchloropsis salina*. Microalgae strain *C. sorokiniana* presented the ability to grow in wastewater in all the tested culture conditions, suggesting high adaptability and viability of the strain in this specific type of filtered UASB secondary effluent. The results also implied nutrient removal achieved 62% of total nitrogen removal and 97% of total phosphorous removal, when applying *C. sorokiniana* in the batch systems with hydraulic retention time of 9 days.

The growth potential and the nutrient removal capacity of *C. sorokiniana* in a continuous laboratory-scale photobioreactor were also investigated. The system removed total nitrogen and total phosphorous by approximately 17% and 27%, respectively, with hydraulic retention time of 5.5 days. High ammonium removal yet high nitrate release indicated

microalgae-nitrifiers imbalance in the photobioreactor system. Unfavorable growth factor for microalgae in the photobioreactor could be carbon-limited media in wastewater (2C:22N:1P). Adding an external source of CO₂ to control alkalinity, pH, and provide carbon source for microalgal growth is most probably needed for further investigation. Even though nutrient removal efficiencies in continuous photobioreactor were significantly lower than the batch test, biomass yield in the photobioreactor was higher ($0.16 \pm 0.02 \text{ gTN}_{\text{removed}} \cdot \text{gSS}^{-1}$ and $0.03 \pm 0.005 \text{ gTP}_{\text{removed}} \cdot \text{gSS}^{-1}$), compared to the batch test ($0.04 \pm 0.01 \text{ gTN}_{\text{removed}} \cdot \text{gSS}^{-1}$ and $0.02 \pm 0.002 \text{ gTP}_{\text{removed}} \cdot \text{gSS}^{-1}$). High biomass production suggested that microalgal-based treatment for UASB effluent could offer a resource recovery potential.

Overall, this study demonstrated the feasibility of UASB system treating municipal wastewater at low-temperatures and variable loadings in a long-term application. In combination with suitable post-treatments, UASB system showed a viable secondary pre-treatment option unit process for achieving lower carbon footprint wastewater treatment and resource recovery at low-temperatures. The robustness exhibited to low-temperature and variable loading conditions provides a solid basis for further research and potential applications. Further advances in an integrated UASB system and post-treatment unit processes investigation will be needed for pilot- and/or full-scale applications in the future.

Table of Contents

Preface	i
Acknowledgements	iv
Summary	vi
Table of Contents	ix
List of Figures	xii
List of Tables.....	xix
Abbreviations	xxi
1 Introduction	1
1.1 Background and motivation.....	1
1.2 Scope of work	5
1.3 General objectives.....	7
1.4 Thesis structure	7
2 Literature Review	8
2.1 Anaerobic treatment.....	8
2.2 Granulated anaerobic wastewater treatment	12
2.3 Granulated anaerobic wastewater treatment at low- temperatures.....	16
2.4 Anaerobic granulated biofilm modelling.....	20
2.5 Post-treatment technology development for anaerobic treatment effluents	21
2.6 Dissolved methane removal from anaerobic effluent	23
2.7 Microalgae-based advanced wastewater treatment.....	26
2.8 Specific objectives and research questions	35
3 General Methodology.....	38
3.1 UASB systems and operation	38

3.2	Microbial community analysis on psychrophilic granules from the UASB system.....	42
3.3	Anaerobic granulated biofilm system model for municipal wastewater treatment	43
3.3.1	Model implementation.....	43
3.3.2	Simulation set-up	45
3.3.3	Inputs.....	46
3.4	Methanotrophics-photogranules experiment for dissolved methane removal.....	47
3.5	Quantification method and screening of microalgae growth potential on secondary wastewater effluent.....	49
3.5.1	Microalgal strains.....	49
3.5.2	Microalgal quantification methods	51
3.6	Screening of microalgae growth potential on UASB secondary wastewater effluent in a batch system	53
3.7	Nutrient-limited kinetic growth analysis of <i>Chlorella sorokiniana</i> in microplate well	55
3.8	Evaluation of selected microalgae strain for nutrient removal in a continuous photobioreactor (PBR) system	57
3.9	Pathogen analysis.....	58
4	Main Results and Discussions.....	59
4.1	UASB system for municipal wastewater treatment at low-temperatures.....	59
4.2	Microbial community analysis on psychrophilic granules of UASB system.....	67
4.2.1	Composition shift of bacterial community	68
4.2.2	Composition shift of methanogenic archaeal community	74
4.3	Anaerobic granulated biofilm system model for municipal wastewater treatment	80

4.4	Engineered methanotrophic syntrophy in photogranule for dissolved methane removal.....	84
4.5	Microalgal-based treatment for removing nutrient.....	92
4.5.1	Microalgal cell quantification methods	92
4.5.2	Screening the growth potential of the microalgae on secondary wastewater effluent in a batch system	95
4.5.3	Nutrient-limited kinetic growth analysis of <i>Chlorella sorokiniana</i> in microplate well	100
4.5.4	Evaluation of selected microalgae strain for nutrient removal in a continuous photobioreactor system...	102
5	Conclusions and Future Research	108
5.1	Main conclusions	108
5.2	Future research.....	110
	Bibliography.....	112
	Appendices	150
	Appendix 1 – Paper I.....	151
	Appendix 2 – Paper II	195
	Appendix 3 – Paper III.....	234
	Appendix 4 – Microalgal-based treatment for secondary wastewater effluent	280
	Appendix 5 – Pathogen analysis method	287
	Appendix 6 – Anaerobic granulated biofilm system model for municipal wastewater treatment	291

List of Figures

- Figure 1.1 The annual baseline water stress worldwide (adapted from The United Nations (2021)) 1
- Figure 1.2 Valuing wastewater as resources for reused water, renewable energy, and nutrients 2
- Figure 1.3 Conceptual process flowchart of ÅLS project (four work packages). This study (red boxes) was part of ÅLS project that was mainly focused on work package 1, UASB development at low-temperatures, and its post-treatment studies, work package 3, as supplementary studies. 6
- Figure 2.1 Multistep of anaerobic processes and chemical oxygen demand (COD) flow in percent unit (adapted from Batstone et al. (2002)) 9
- Figure 2.2 Generalized comparison between aerobic and anaerobic wastewater treatment in terms of the fate of organic carbon, expressed as COD, energy production/consumption and nutrient requirements (expressed as N-requirements) (adapted from Kleerebezem et al. (2015)) 13
- Figure 2.3 Layered structure and spatial distribution of microorganisms in granules (adapted from Satoh Hisashi et al. (2007)). A. Cross-sectional differential interference contrast images of the granules showed that the granules had a multilayered structure consisting of biomass and interstitial voids; B. FISH revealed that the outer layer was dominated by bacterial cells whereas the inner layer (below 250 μm from the surface) was occupied mainly by archaeal cells; C. Filamentous cells were observed in the uppermost layer of the granules; D. The BET42a-stained cells were also present in the outer shell of the granule; E. Firmicutes, were numerically important Bacteria in the inner layer of the granule; F. The abundance and fluorescence intensity of the

	Alphaproteobacteria-stained cells were low; G. The dense spherical microcolonies that were composed of a number of Actinobacteria in the middle layer (at a depth of ca. 200 μm) of the granule.....	15
Figure 2.4	Schematic description of anaerobic process under psychrophilic conditions. Dotted arrows represent the minor pathway. The two-step production of methane from CO_2 and H_2 via acetate is more prevalent under low-temperature (adapted from Tiwari et al. (2021)).....	19
Figure 2.5	Methane utilization potential from different sources by methanotrophs and ammonia oxidizing bacteria (adapted from AlSayed et al. (2018))	25
Figure 3.1	Flow diagram of the laboratory-scale UASB reactor. Two reactors were assembled parallelly identically with the same set-up as illustrated here. The red line represents the wastewater inlet and outlet flow; the green line represents the biogas flow; the blue line represents the distilled water flow for the cooling circulating water (Paper I).....	40
Figure 3.2	The UASB reactors were operated continuously over 1025 days by the stepwise increase of OLR at decreasing temperatures. Initially, UASB reactors were started-up at 25 °C with low OLR around 1.0 $\text{gCOD}_{\text{dissolved}} \cdot \text{l}^{-1} \cdot \text{d}^{-1}$ and increased gradually up to approximately 15 $\text{gCOD}_{\text{dissolved}} \cdot \text{l}^{-1} \cdot \text{d}^{-1}$. During operation, hydraulic retention rate (HRT) started at about 16.7 h then gradually decreased along with the increasing OLR, down to 1.1 h. The operating temperatures were then reduced to the next lower temperature experiments at 16, 12, 8.5, 5.5 and finally 2.5 °C (Paper I), and the loading procedure repeated.	41
Figure 3.3	Schematic representation of anaerobic granulated biofilm implementation into ADM1	45

Figure 3.4	Presentation of the continuous reactor set-up. The gas bag connected to the media preparation tank was used as methane reservoir during the preparation of methane-saturated batches of media. The finished media batches were transferred to the media storage tank, from where it was continuously pumped into the reactor. The gas bag connected to media storage equilibrated pressure changes resulting from filling and emptying the tank. The gas bag connected to the reactor equilibrated potential pressure changes in the reactor (Paper III).....	48
Figure 3.5	Method developed for distinguishing selected microalgae from background noise and debris using the forward scatter trigger and the fluorescence trigger FL4 (675 nm) on Flow Cytometer BD Accuri C6.....	52
Figure 3.6	Presentation of continuous PBR set-up, equipped with programmable control of lighting (including diurnal cycles), heating, and agitation.....	58
Figure 4.1	Averaged transient time to steady-state conditions at different temperatures and OLRs in reactor A and B. The student t-test revealed no significant difference ($p>0.05$) between reactor A and B transient times (Paper I).....	61
Figure 4.2	Dissolved COD removal efficiencies at steady-state under different temperatures and OLRs. Error bars represent standard errors from measurements taken during steady-state conditions in reactor A and B. The student t-test revealed no significant difference ($p>0.05$) between reactor A and B COD removal efficiencies (Paper I)	62
Figure 4.3	Specific methane production rate per volume biomass (a and b) and overall COD specific methane yield (c and d) at steady-state conditions in reactor A and B. Error bars represent standard errors from measurements taken during steady-state conditions.	65

Figure 4.4 Bacterial and archaeal diversity statistics based on Shannon Index in UASB granules at different operating temperatures and OLRs. A and B on the x-axis represent two parallel reactors, A and B. Numbers beside A and B represent OLR in $\text{gCOD}\cdot\text{l}^{-1}\cdot\text{d}^{-1}$ (Paper II).....	68
Figure 4.5 Relative abundances of microbial population structure in UASB granules at the bacterial species level at different operating temperatures and OLRs. A and B on the x-axis represents microbial population structure in two parallel reactors, A and B. Numbers beside A and B represent OLR in $\text{gCOD}\cdot\text{l}^{-1}\cdot\text{d}^{-1}$ (Paper II).	70
Figure 4.6 Relative abundances of microbial population structure in UASB granules at (a) archaeal species level and (b) methanogen groups based on methanogenesis pathway at different operating temperatures and OLRs. A and B on the x-axis represents microbial population structure in two parallel reactors, A and B. Numbers beside A and B represent OLR in $\text{gCOD}\cdot\text{l}^{-1}\cdot\text{d}^{-1}$	75
Figure 4.7 Relative abundances of genus <i>Acetoanaerobium</i> (homoacetogen) in UASB granules at different operating temperatures and OLRs. A and B on the x-axis represents microbial population structure in two parallel reactors, A and B. Numbers beside A and B represent OLR in $\text{gCOD}\cdot\text{l}^{-1}\cdot\text{d}^{-1}$ (Paper II).....	78
Figure 4.8 Anaerobic process pathway proposed under psychrophilic conditions. Dashed arrows represent hydrogen consuming and producing pathways (Paper II).	79
Figure 4.9 Simulation result of COD removal efficiencies (blue bars) compared to experimental results (orange bars) during steady-state conditions at 25 °C. There was no experimental data measured at OLR 20 $\text{gCOD}\cdot\text{l}^{-1}\cdot\text{d}^{-1}$. Error	

	bars represent standard errors from measurements taken during steady-state conditions in UASB reactors.	80
Figure 4.10	Simulation result of methane fraction in biogas (blue bars) compared to experimental results (orange bars) during steady-state conditions at 25 °C. There was no experimental data measured at OLR 20 gCOD·l ⁻¹ ·d ⁻¹ . Error bars represent standard errors from measurements taken during steady-state conditions in UASB reactors.	81
Figure 4.11	pH distribution profile along the granule in UASB reactor during steady-state conditions.....	82
Figure 4.12	Simulated active biomass composition of the granular sludge of UASB reactor at different organic loading during steady-state conditions.....	83
Figure 4.13	Removal efficiency of dissolved methane (filled circles) and concentrations of total suspended solids in the effluent (TSS, open circles) during continuous reactor operation. Mixing speed was increased on day 31. On day 40, the reactor effluent clogged. Wasting of biomass was done on days 42 and 94 (Paper III).....	86
Figure 4.14	Surface specific methane removal rates for individual photogranule sizes. Rates are plotted by (a) the average diameter of the photogranule batch, and (b) by the surface to volume ratio, derived from the average diameters of the tested photogranules. Each point represents an independent batch experiment conducted with on average six similar-sized photogranules (Paper III).	88
Figure 4.15	Relative abundances of methylotrophic and phototrophic taxa in photogranules and background material. The background material before the enrichment is the original activated sludge (AS), and an oxygenic photogranules (OPG). The inoculum after the enrichment process is represented by four photogranules. In total eight	

photogranule communities during continuous reactor operation are shown for days 15, 28 and 44. a) Putative methylotrophic bacteria (Silva SSU 132) among the non-phototrophic bacteria in the 16S rRNA amplicons. The three samples with asterisks mark photogranules in which methanotrophs are present in low abundances compared to non-methanotrophic methylotrophs. b) Major (>5% total abundance) cyanobacterial and chloroplast OTUs (Silva LSU 132) among the phototrophic taxa of the 23S rRNA amplicons (Paper III). 89

- Figure 4.16 Independent confirmation of microplate-based method, direct counting, flow cytometry, and optical density (OD) and calibration of each strain in pre-growth media..... 93
- Figure 4.17 Microalgal nutrient, COD and alkalinity removal from secondary wastewater effluent in the batch system after reaching stationary phase. Error bars show standard deviations. 98
- Figure 4.18 Growth rates vs. nutrient concentrations showing single nutrient limitation (phosphate limited-blue circle, ammonium limited-orange triangle). Error bars represent standard deviations..... 100
- Figure 4.19 Lineweaver-Burk plot on microalgal kinetic experiment (phosphate limited-blue circle. ammonium limited-orange triangle) after five replications of experiment. Error bars represent standard deviations. 101
- Figure 4.20 PO₄-P concentration profiles at the inlet and effluent of the PBR throughout 109 days continuous operation. Error bars represent standard deviations from triplicate samples from PBR (n=3). 104
- Figure 4.21 Ammonium (A) and nitrate (B) concentration profiles at the inlet and effluent of the PBR throughout 109 days

continuous operation. Error bars represent standard deviations from triplicate samples from PBR (n=3). 105

Figure 4.22 (A) Microalgae culture under the microscope (optics x40) in PBR at day 11 indicating *C. sorokiniana*, (B) Microalgae culture in PBR at day 21, *T. obliquus* within the blue circles and *C. sorokiniana* within red circles..... 107

List of Tables

Table 2.1 Main anaerobic bioreactions during the anaerobic treatment (adapted from Liu & Whitman (2008) and Pan et al. (2021)).	12
Table 2.2 Representative results of pilot- and full-scale UASB system for municipal wastewater.	16
Table 2.3 Specific growth rates (day^{-1}) of methanogenic and acetogenic bacteria at low-temperatures calculated with two times diluted soil and H_2/CO_2 as a substrate. Q_{10} estimates over the psychrotolerant temperature range to the right (adapted from Kotsyurbenko et al. (1996)).	18
Table 2.4 Examples of applied granulated anaerobic treatment of different types wastewater at low-temperatures (adapted from Aquino et al. (2019), Dev et al. (2019), Lettinga et al. (2001), Trego et al. (2021), and Wu et al. (2017)).	20
Table 2.5 Microalgae-based treatment in different types of wastewater, adapted from Kong et al. (2021).	28
Table 3.1 Granule samples on microbial community analysis from the UASB system.	42
Table 3.2 COD input used for simulations of anaerobic granulated biofilm.	46
Table 3.3 Characteristics of selected microalgal strains for wastewater treatment	50
Table 3.4 Experimental scenarios on kinetics of nutrient-limited growth analysis. Five replications were used for each concentration	56
Table 4.1 Secondary effluent wastewater characteristics after UASB reactor and tight-micro filtration (T-MF) treatment that was used in screening microalgal-based treatment in batch system for nutrient removal.	96

Table 4.2 Established microalgal growth rates cultivated in pre-growth media and filtered UASB secondary effluent	97
Table 4.3 TSS production and yield of microalgal strains cultivated in wastewater after reaching the stationary phase (\pm standard deviation)	99
Table 4.4 The values of <i>C. sorokiniana</i> kinetic parameters of Monod equation were determined by regression analysis of the linearized Lineweaver-Burk equation (mean \pm standard deviation)	101
Table 4.5 Secondary effluent wastewater characteristics after UASB reactor and tight-micro filtration (T-MF) treatment that was used in microalgal-based treatment in a continuous PBR system for nutrient removal	103

Abbreviations

ABR	Anaerobic Baffled Reactor
ADM1	Anaerobic Digestion Model No.1
ADP	Adenosine Diphosphate
AFB	Anaerobic Fluidized Bed
ÅLS	<i>Åge Lærdal Stiftelsen</i>
AMB	Acetoclastic Methanogenic Bacteria
AS	Activated Sludge
ASBR	Anaerobic Sequencing Batch Reactor
ATP	Adenosine Triphosphate
COD	Chemical Oxygen Demand
COVID-19	Coronavirus Disease
CSTR	Continuous Stirred-Tank Reactor
DAE	Differential-Algebraic Equation
DAF	Dissolved Air Flotation
DE	Differential Equation
DNA	Deoxyribonucleic Acid
DO	Dissolved Oxygen
EGSB	Expanded Granular Sludge Blanket
EPS	Extracellular Polymeric Substances
F/M	Food Mass Ratio
FL	Fluorescence
FISH	Fluorescence In Situ Hybridization
FLASH	Fast Length Adjustment of Short reads
FSC	Forward Scatter
GWP	Global Warming Potential

HRT	Hydraulic Retention Time
IVAR	<i>Interkommunalt Vann Avløp og Renovasjon</i>
LCFA	Long-Chain Fatty Acid
LED	Light-Emitting Diode
LSU	Large Subunit
NCBI	National Center for Biotechnology Information
NLR	Nitrogen Loading Rate
OD	Optical Density
OLR	Organic Loading Rate
OPG	Oxygenic Photogranule
OTU	Operational Taxonomic Unit
PAR	Photosynthetically Active Radiation
PBR	Photobioreactor
PBS	Phosphate-Buffered Saline
PLR	Phosphorous Loading Rate
rRNA	Ribosomal Ribonucleic Acid
RPM	Revolutions per Minute
RQ	Research Question
SBR	Sequencing Batch Reactor
SCFA	Short Chain Fatty Acid
SMP	Soluble Microbial Products
SRT	Solid/Sludge Retention Time
SSC	Side Scatter
SSU	Small Subunit
T-MF	Tight-Micro Filtration
TN	Total Nitrogen
TP	Total Phosphorous
TSS	Total Suspended Solid

UASB	Up-flow Anaerobic Sludge Blanket
UV	Ultraviolet
VFA	Volatile Fatty Acid
VSS	Volatile Suspended Solid

1 Introduction

1.1 Background and motivation

The world's water demand has been consistently increasing and will continue to do so over the coming decades. The United Nations predicted the world would face a global clean water deficit of 40% by 2030 (The United Nations, 2021) and will be worsened by global challenges such as climate change and COVID-19 pandemic (Boretti, 2020). According to Mekonnen & Hoekstra (2016), two-thirds of the world's population live in areas that experience water scarcity for at least one month a year, and about 500 million people live in areas where water consumption exceeds locally renewable water resources by a factor of two. Furthermore, the increasing world population makes it more challenging to access adequate and good quality water supplies. Figure 1.1 shows the annual baseline water stress worldwide (The United Nations, 2021), measured by the ratio of total water withdrawals to available renewable water supplies.

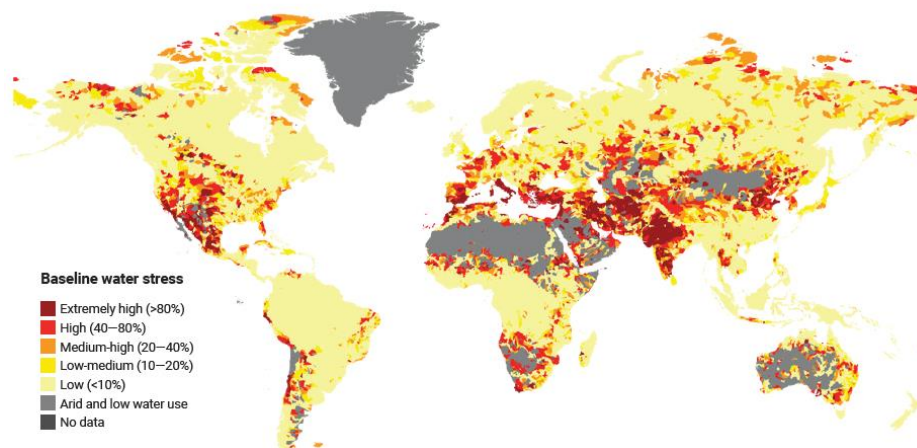


Figure 1.1 The annual baseline water stress worldwide (adapted from The United Nations (2021))

Water availability is closely associated with water quality, as water pollution may restrain use. Increasing untreated domestic wastewater discharges, combined with agricultural runoff along with inadequately treated industrial wastewater have resulted in deterioration of water quality. Globally, an estimated 48% of wastewater is released into the environment without any prior treatment (WHO & UNICEF, 2021), which contributes to detrimental effects on human health and ecosystems.

Wastewater has often been claimed as an undervalued water source to be discharged and/or ignored. It is essential to develop a more circular and sustainable wastewater treatment and value wastewater as a potential resource with a low carbon footprint. Mainly, three resource components in raw wastewater may be identified: Organic material is a potential energy source (about 2 kWh·m⁻³ according to Heidrich et al., 2011), dissolved and particulate bound macronutrients representing a potential for nutritional recovery, while the liquid fraction represents a potential for water reclamation. Figure 1.2 presents the illustration of resource recovery potential from wastewater.

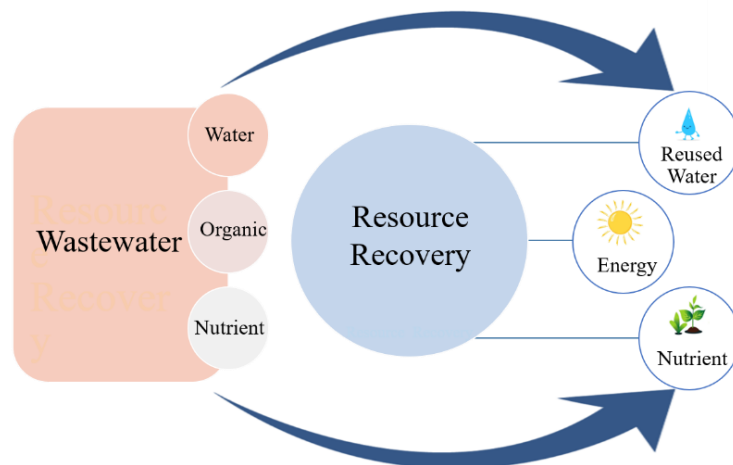


Figure 1.2 Valuing wastewater as resources for reused water, renewable energy, and nutrients

Most wastewater treatment technologies are relatively energy-intensive and become increasingly expensive over time (Rojas & Zhelev, 2012). In principle, energy-neutral or even net energy-positive wastewater treatment can be developed by bioconversion of the organic material into biogas via anaerobic treatment. Wastewater as a carbon-rich source could be converted to biogas, transforming an assumed low-value water source into a substantial renewable form of energy (Aiyuk et al., 2004; Rosa et al., 2018). Biogas produced can be used to compensate a portion (25 - 50%) of energy requirements in the activated sludge process (Ghimire et al., 2021).

Among several anaerobic treatment technologies that have been implemented, up-flow anaerobic sludge blanket (UASB) system using granulated biomass offers a great alternative. The use of UASB for biological wastewater treatment was introduced 40 years ago (Lettinga et al., 1980) and is now regarded as an adequate technology and a robust system for municipal wastewater treatment and energy recovery (Rosa et al., 2018). Chernicharo et al. (2019) summarized six full-scale UASB-based domestic wastewater treatment applications, which were currently operated in Brazil. The overall organic removal efficiencies as chemical oxygen demand (COD) of their full-scale UASB systems were within the range 56 - 91% with approximately 75% methane fraction in the biogas produced, which was recovered and used as an energy source for thermal sludge drying system (Chernicharo et al., 2019).

Despite the excellent performance of the UASB system in removing organic carbon (in wastewater treatment up to 90%), the relatively slow-growth rate and sensitivity of methanogens to environmental conditions have often been claimed to limit the process, particularly under psychrophilic conditions (Lettinga et al., 2001). Anaerobic treatment is also vulnerable to organic overloading, disturbing the bioconversion stability and affecting the microbial community (Cardinali-Rezende et al., 2013; da Silva Martins et al., 2017). Low-temperature anaerobic bioreactor operation offers economic advantages, especially for some

high latitude countries, due to reduce heating requirement and bioenergy production potential. One critical factor to assure stable granulated anaerobic treatment performance at low-temperatures and high loading is the development of well-balanced community substrate-product interactions within the granules (McKeown et al., 2009).

An often-overlooked or under communicated drawback of anaerobic wastewater treatment is the loss of dissolved methane. Souza et al. (2011) and Wu et al. (2017) found that dissolved methane was supersaturated in the liquid phase of an anaerobic bioreactor effluent (saturation factor of 1.03 - 1.67), increasing with the increased methane solubility at decreasing temperatures. Even at equilibrium, considerable amounts of methane are lost with the liquid effluent, and even more predominant when treating wastewater at low-temperatures and/or in high-flow through situations (low hydraulic retention time) (Brandt et al., 2019). Once the effluent is discharged and exposed to ambient methane partial pressures, methane degasses into the atmosphere. This methane loss significantly reduces, and even offsets, the positive climate effect of energy recovery from anaerobic wastewater treatment.

In addition, UASB reactor systems have limited removal potential for nitrogen and phosphorus (Li et al., 2007). The removal of nutrients in UASB systems is usually negligible due to low growth yields and normally mobilizing nutrients due to ammonification and phosphatases (Elmitwalli & Otterpohl, 2011). Hence, anaerobic process has potential for nutrient recovery enhancement as pre-treatment for nutrient uptake unit processes. The suitability of pre-treatment, post-treatment, and by-product treatment would influence the applicability of anaerobic treatment by UASB systems of municipal wastewater treatment, especially at low-temperatures and variable loadings. To conclude, UASB systems for municipal wastewater treatment at low-temperatures under typical variable loading conditions is attractive for resource recovery. Limited knowledge and experiences with low-temperature applications may cause the limited use of anaerobic, including granulated

sludge wastewater treatment, and may explain the reluctance of anaerobic technology providers to market their process solutions for low mesophilic and psychrotolerant use (Lettinga, 2018). The green shift, however, calls for sustainable wastewater management, and the resource recovery potential of anaerobic technology will also comply with the societal move towards a circular economy. Hence, the motivation both relies on sustainable wastewater treatment and resource recovery, as embedded in several United Nations sustainability goals.

1.2 Scope of work

This study was part of the ÅLS project (*Åge Lærdal Stiftelsen*, currently *Stiftelsen Signe Marie*), which aims to combine energy-efficient wastewater treatment unit processes with resource economical/extensive water treatment methods for resource recovery. Figure 1.3 presents the conceptual flowchart of the selected unit processes in ÅLS project: 1. UASB system for organic removal; 2. Membrane treatment for anaerobic effluents for solids and pathogens removal; 3. Microalgal-based technologies for nutrient removal; 4. Polishing treatment with a constructed wetland. The project was funded by the Norwegian Ministry of Education and Research through the university grant program (Norwegian Department of Education) and by the aforementioned foundation *Stiftelsen Signe-Marie*. In addition, IVAR IKS served as an associated industry partner with in-kind contributions and financial support through the UNIVAR project.

The presented study has mainly focused on low-temperature anaerobic wastewater treatment using UASB system for organic removal and biogas production (work package 1). Additionally, post-treatment development studies specifically on dissolved methane and nutrients removal were investigated as supplementary studies (work package 3). Initially, dissolved methane removal study was not included in the initial

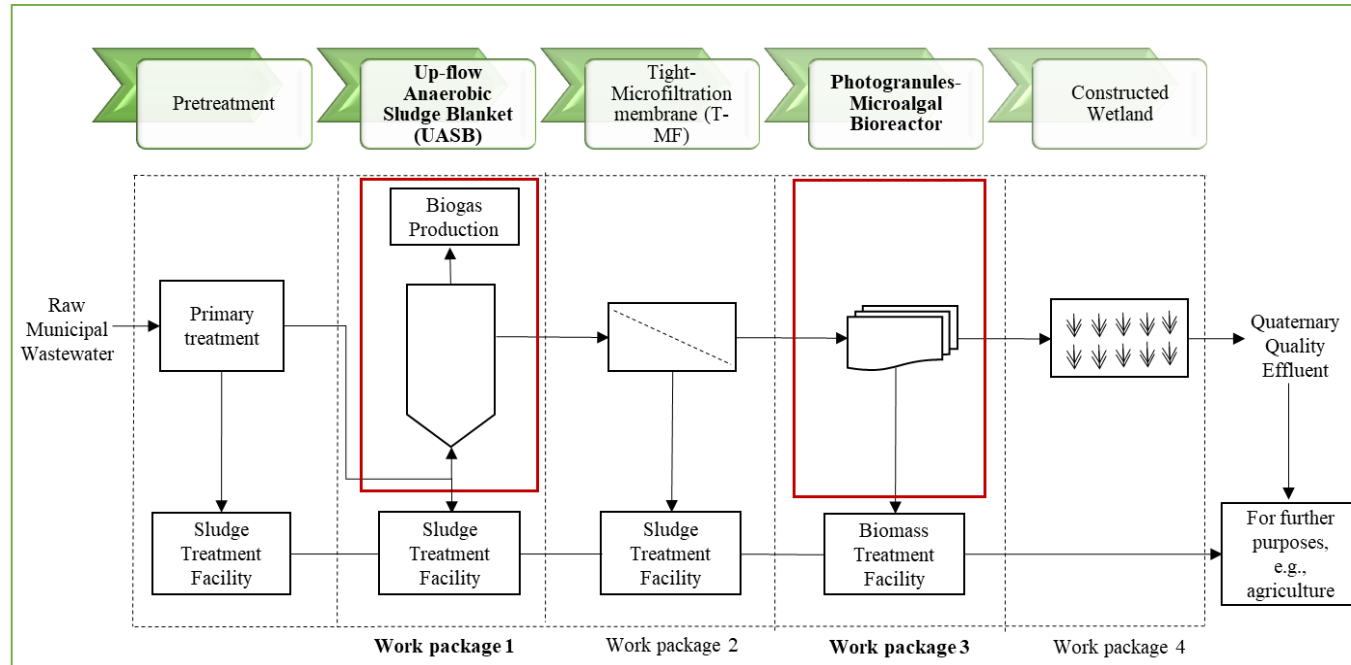


Figure 1.3 Conceptual process flowchart of ÅLS project (four work packages). This study (red boxes) was part of ÅLS project that was mainly focused on work package 1, UASB development at low-temperatures, and its post-treatment studies, work package 3, as supplementary studies.

concept. However, this challenge was identified to be crucial for the ambitions towards sustainable anaerobic wastewater treatment with lower carbon footprint. While the current work studied the selected unit processes individually, an integration evaluation in the laboratory- and pilot-scale system is currently under investigation and subject for the future research in our group.

1.3 General objectives

The main objective of this research was to investigate the effectiveness of anaerobic treatment of municipal wastewater in anaerobic granular sludge reactors (UASB) at low-temperatures and variable loadings. Furthermore, insightful information such as the functional microbial community involved in the anaerobic granules will be addressed to explain this work findings. In addition, this research aimed to demonstrate novel phototroph-based methods for UASB effluent post-treatment removal of dissolved methane and nutrient. More specific research objectives and research questions are defined in Chapter 2.8 after a critical review of existing literature and identifying relevant knowledge gaps for the overall scope of this work.

1.4 Thesis structure

The thesis consists of five chapters. Chapter 1 introduces the research background and motivation, identifies the scope of work, and presents the general objectives. In Chapter 2, literature within the topics is critically reviewed, knowledge gaps are identified which conclude into specific research questions. Chapter 3 describes the general methodology adopted for experimental studies. Chapter 4 summarizes research results and discuss them in the context of the research questions. Chapter 5 contains overall conclusions and corollaries, and suggestions for future research. Appendices include published and submitted research articles, and hitherto unpublished supplementary materials. Papers and manuscripts are reformatted to fit the thesis' structure and layout.

2 Literature Review

This chapter describes theoretical understanding of anaerobic process basic as well as defines anaerobic wastewater treatment. The development of anaerobic treatment for municipal wastewater processing using high-rate granulated reactors at low-temperatures is also reviewed. Furthermore, anaerobic biofilm model implementation is addressed. In addition, post-treatment technology developed for anaerobic effluent treatment is reviewed including a description of methanotroph-photogranule syntrophy removing dissolved methane and nutrient removal using microalgal-based treatment. Based on this literature review and theoretical background, key knowledge gaps are identified and used to define specific objectives.

2.1 Anaerobic treatment

Anaerobic treatment is a process by which microorganisms convert biodegradable material in the absence of molecular oxygen (low redox potential) (Grady et al., 2011). The metabolic pathways involve in carbon conversion and energy generation are the same for both aerobic and anaerobic process, but with two basic differences: (a) the terminal fate of electrons produced in the oxidation reactions; and (b) the amount of ATP produced by phosphorylation. More ATP will be released from aerobic respiration (Benefield & Randall, 1980).

Anaerobic carbon conversion is a complex biological process involving four basic steps (i.e. hydrolysis, acidogenesis, acetogenesis and methanogenesis), which rely on the natural activity of mixed methanogenic anaerobic consortia (Angelidaki et al., 2011), as depicted in Figure 2.1. Two basic bacteria groups (acidogens and acetogens) and one archaeal group (methanogens) are recognized in this process. The cumulative actions of these groups of bacteria ensure process continuity and stability.

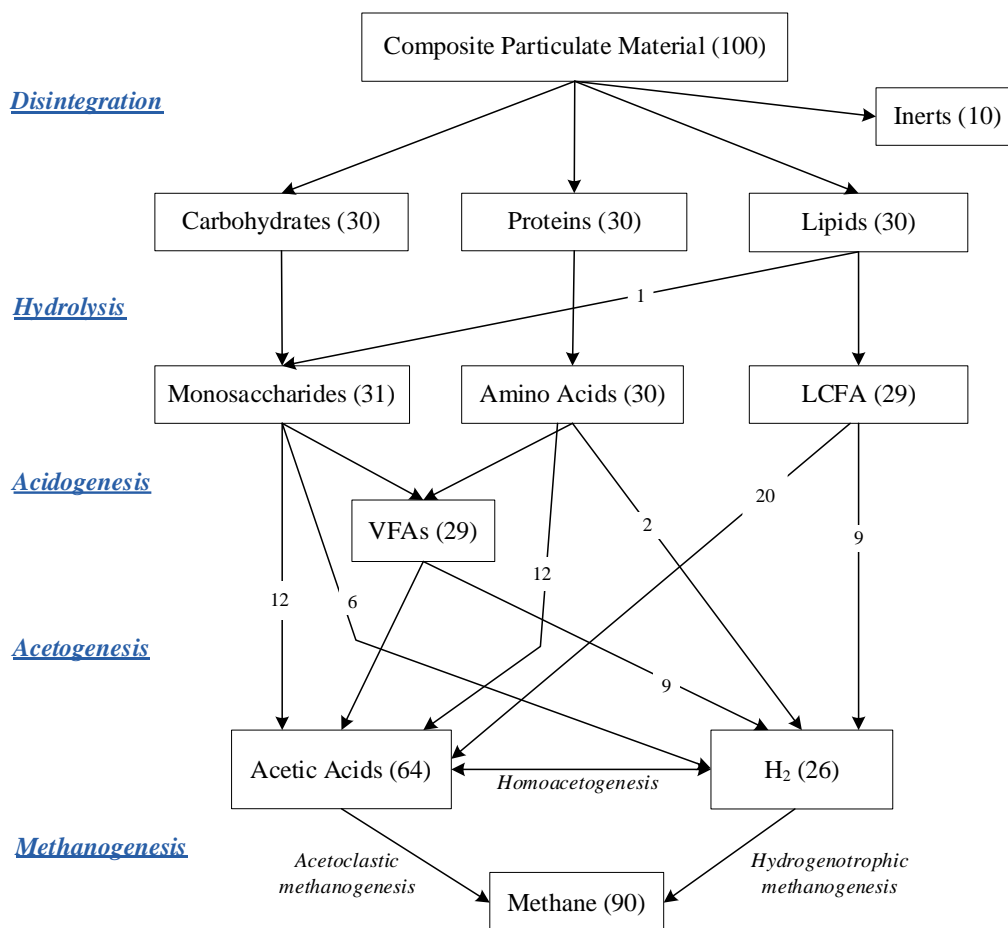


Figure 2.1 Multistep of anaerobic processes and chemical oxygen demand (COD) flow for a particulate composite, consisted of 10% inerts and 30% of each carbohydrates, proteins, and lipids (in the term of COD) (adapted from Batstone et al. (2002))

Disintegration and hydrolysis are extracellular biological and non-biological processes mediating the breakdown and solubilization of complex organic material to soluble substrates. The substrates are complex composite particulates and polymeric carbohydrates, proteins, and lipids. The last three substrates are also products from disintegration of composite particulates. Hydrolysis is understood as any mechanism leading to the degradation of a defined particulate or macromolecular substrate to its soluble monomers (depolymerization). Large polymeric

materials, e.g., carbohydrates, proteins, and lipids, cannot be directly degraded by microorganisms, and their size must be reduced to small molecules that allow for their passage across the cell membrane for metabolic conversion. The products are their respective mono- and oligomers among the monosaccharides, amino acids, nucleosides, and long-chain fatty acids (LCFA).

Acidogenesis (fermentation) is defined as an anaerobic acid-producing microbial process without an additional electron acceptor or donor. This includes the degradation of soluble sugars (monosaccharides) and amino acids to several simpler products. Fermentation is carried out by a range of obligate and facultative procaryotes and is relatively fast. The growth rate of acidogenic bacteria is comparable to slow-growing aerobic bacteria with maximum rates, μ_{\max} , of 2 - 7 d⁻¹ (Angelidaki et al., 2011). Because acidogenesis can occur without an additional electron acceptor, and free energy yields are normally higher, the reactions can occur at high hydrogen or formate concentrations and provide high biomass yields. The end products of acidogenesis are mainly short chain fatty acids (SCFA), also called volatile fatty acids (VFA), such as acetic, propionic, and butyric acids. Alcohols such as ethanol, propanol and butanol may also be produced in addition to lactic and formic acid. The composition of fermentation products depends on a range of growth factors such as substrate composition, environmental factors (pH, temperature, etc.) and operational factors (loading rate, retention time, etc.). The large fraction of energy associated with the excreted fermentation products cause the remaining energy for growth to be limited, and thus the growth yield is low, typically 0.1 - 0.2 gVSS·gCOD⁻¹ (Henze et al., 2008; McHugh et al., 2003).

The VFAs, other than acetate, which are produced in acidogenesis step, are further converted to acetate, hydrogen, and carbon dioxide by the acetogenic bacteria. The essential acetogenic substrates are propionate and butyrate, key-intermediates in anaerobic processes (Henze et al., 2008). Acetic acid and H₂ are used directly by the methanogens while the

other fermentation products are converted into acetic acid and H₂ in acetogenesis. Acetogenesis is also required for VFAs formation during lipase activity on lipids and glycerol. The products (H₂ and formic acid) must be kept at a low concentration in order to favor thermodynamically their formation reaction ($\Delta G^0 < 0$). This low concentration is maintained by the hydrogen utilizing methanogens (McHugh et al., 2003). There is an important role in anaerobic process by homoacetogens that convert H₂ and CO₂ to acetate via the acetyl-CoA pathway (Pan et al., 2021). Methanogens and homoacetogens are the primary H₂-consumers in anaerobic system, and methanogens are commonly dominant. However, homoacetogens outcompete hydrogenotrophic methanogens at low-temperatures, and homoacetogens could also grow under both acidic and alkaline conditions (Kotsyurbenko et al., 2001; Nozhevnikova et al., 2007).

The last step is methanogenesis. There are three main methanogenesis pathways: (1) CO₂-reducing (hydrogenotrophic methanogenesis), (2) acetoclastic methanogenesis, and (3) methylotrophic methanogenesis (Söllinger & Urich, 2019). Energy generation in methanogens is not driven by substrate level phosphorylation, but reversed electron transport and ATPase. Methanogens are significantly more sensitive to their environmental requirements than acidogens and their rates of metabolism are also lower. The maximum growth rate (μ_{\max}) of methanogens is as low as 0.3 - 0.5 d⁻¹, and long retention is required for methane producing processes to sustain (Henze et al., 2008). The growth yield is also very low, as the majority of the energy in the substrate is converted into methane gas with typical growth yield of 0.05 - 0.1 gVSS·gCOD⁻¹ (Henze et al., 2008). Free energies of central anaerobic bioreactions are presented in Table 2.1.

Literature Review

Table 2.1 Main anaerobic bioreactions during the anaerobic treatment (adapted from Liu & Whitman (2008) and Pan et al. (2021)).

Bioreactions	ΔG^0 (kJ·mol ⁻¹)
Acidogenic reactions:	
(1) Acetate: $C_6H_{12}O_6 + 2H_2O \rightarrow 2CH_3COOH + 4H_2 + 2CO_2$	-206
(2) Butyrate: $C_6H_{12}O_6 \rightarrow CH_3CH_2CH_2COOH + 2CO_2 + 2H_2$	-254
(3) Propionate: $C_6H_{12}O_6 + 2H_2 \rightarrow 2CH_3CH_2COOH + 2H_2O$	-279.4
(4) Lactate: $C_6H_{12}O_6 \rightarrow 2CH_3CHOHCOOH + H^+$	-225.4
(5) Ethanol: $C_6H_{12}O_6 \rightarrow 2CH_3CH_2OH + 2CO_2$	-164.8
(6) Butyrate: $2CH_3CHOHCOOH + 2H_2O \rightarrow CH_3CH_2CH_2COOH + 2HCO_3^- + 2H^+ + 2H_2$	-56.3
(7) Valerate: $CH_3CH_2COO^- + 2CO_2 + 6H_2 \rightarrow CH_3(CH_2)_3COO^- + 4H_2O$	-143.3
(8) Valerate: $3CH_3COO^- + 3H_2 + 2H^+ \rightarrow CH_3(CH_2)_3COO^- + 4H_2O$	-96.7
(9) Valerate: $CH_3(CH_2)_2COO^- + CH_3COO^- + 2H_2 + H^+ \rightarrow CH_3(CH_2)_3COO^- + 2H_2O$	-48.0
(10) Caproate: $CH_3(CH_2)_2COO^- + 2CO_2 + 6H_2 \rightarrow CH_3(CH_2)_4COO^- + 4H_2O$	-143.3
Acetogenic reactions:	
(11) Propionate: $CH_3CH_2COOH + 2H_2O \rightarrow CH_3COOH + 3H_2 + CO_2$	+76.2
(12) Butyrate: $CH_3CH_2CH_2COOH + 2H_2O \rightarrow 2CH_3COOH + 2H_2$	+48.4
(13) Lactate: $CH_3CHOHCOOH + 2H_2O \rightarrow CH_3COOH + HCO_3^- + 2H_2$	-4.2
(14) Ethanol: $CH_3CH_2OH + H_2O \rightarrow CH_3COOH + 2H_2$	+9.6
Methanogenic reactions:	
(15) Hydrogen: $4H_2 + CO_2 \rightarrow CH_4 + 2H_2O$	-135.0
(16) Acetate: $CH_3COOH \rightarrow CH_4 + CO_2$	-31.0
(17) Formate: $4HCOOH \rightarrow CH_4 + 3CO_2 + 2H_2O$	-304.2
(18) Methanol: $4CH_3OH \rightarrow 3CH_4 + CO_2 + 2H_2O$	-312.8
(19) Ethanol: $2CH_3CH_2OH + CO_2 \rightarrow CH_4 + 2CH_3COOH$	-31.6
Syntrophic acetate oxidizing reaction:	
(20) $CH_3COOH + 2H_2O \rightarrow 2CO_2 + 4H_2$	+104.6
Homoacetogenic reactions:	
(21) Autotrophic: $4H_2 + 2CO_2 \rightarrow CH_3COOH + 2H_2O$	-104.6
(22) Heterotrophic: $C_6H_{12}O_6 \rightarrow 3CH_3COO^- + 3H^+$	-310.9

Note: ΔG^0 represents changes of Gibbs free energies under standard conditions (1 atm and 298 K)

2.2 Granulated anaerobic wastewater treatment

Anaerobic process has been widely used for wastewater treatment for more than a century (van Lier et al., 2015). The simplest and oldest form of anaerobic wastewater treatment is the septic tank. An anaerobic tank designed to retain solids, similar to a septic tank, was first reported in 1857 (McCarty, 2001). In the mid-seventies of the last century, a steep increase in energy demand and prices reduced the attractiveness of

aerobic wastewater treatment (Lettinga, 2014). Figure 2.2 presents carbon and energy fate in both aerobic and anaerobic wastewater treatment. Essentially, the main advantage of anaerobic wastewater treatment is bio-converting the organics into biogas as renewable energy. In addition, anaerobic wastewater treatment has lower energy demand due to the absence of aeration requirements and the lower biomass production and associated nutrient requirements (Figure 2.2).

Among several anaerobic treatment technologies that have been implemented, the high-rate up-flow anaerobic sludge blanket (UASB) system using granulated biomass offers several advantages (Seghezzi et al., 1998; Singh et al., 1996). The interest and popularity of anaerobic technology as secondary wastewater treatment were scarce until the development of UASB reactor system. The biomass in UASB systems is in the form of compact granules that contain a complex community of microorganisms embedded in the extracellular polymeric substances (EPS) matrix, i.e., biofilm.

Anaerobic granules were first observed in the Dorr Oliver Clarifiers installed in South Africa in the 1950s but were not scientifically reported until 1979 when detected in samples taken from these up-flow digesters (Lettinga, 2014). His discovery marked a turning point for engineered

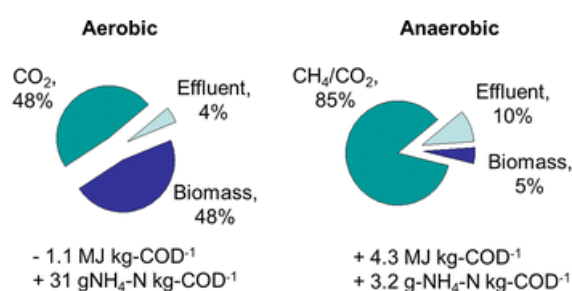


Figure 2.2 Generalized comparison between aerobic and anaerobic wastewater treatment in terms of the fate of organic carbon, expressed as COD, energy production/consumption and nutrient requirements (expressed as N-requirements) (adapted from Kleerebezem et al. (2015))

anaerobic systems, opening the door to high-rate treatment using an anaerobic reactor. High-rate treatment relies upon decoupling the solid retention time (SRT) from the hydraulic retention time (HRT), often achieved by effective sedimentation.

The ability of granules to settle meant that the active biomass driving the treatment process did not get washed out of the system. High volumetric rates are achieved by the retention of elevated densities of active biomass which allows for application of high organic loading rates (OLR), thereby facilitating compact and reduced design costs of wastewater treatment plants. Additionally, granular structure facilitates efficient mass transport of substrates between various trophic groups and provides protection from microclimate changes for the more sensitive microorganisms (Hulshoff Pol et al., 2004).

Size distribution of granules has long been an important characteristic of anaerobic granules. Coupled with the density of the aggregate, this determines the settleability and consequently retention. Many studies have analyzed and identified hydrodynamics to be decisive for the size of an anaerobic granule (Arcand et al., 1994; Wu et al., 2016). Furthermore, other research suggested that physico-chemical characteristics of anaerobic granules are strongly influenced by the type of feed (Batstone & Keller, 2001). Generally, the diameter of anaerobic granules ranges from 0.1 mm to 5 mm (Trego et al., 2020; Wu et al., 2016). They are usually dark in color, spherical, and have settling velocities around $60 \text{ m}\cdot\text{h}^{-1}$ (Hulshoff Pol et al., 2004) which is 20 - 30 times the critical velocity of activated sludge flocs. They are naturally porous and layered (Hisashi et al., 2007), as shown in Figure 2.3. Porosity was found to increase with granule size and this is important for mass transfer and activity (Wu et al., 2016).

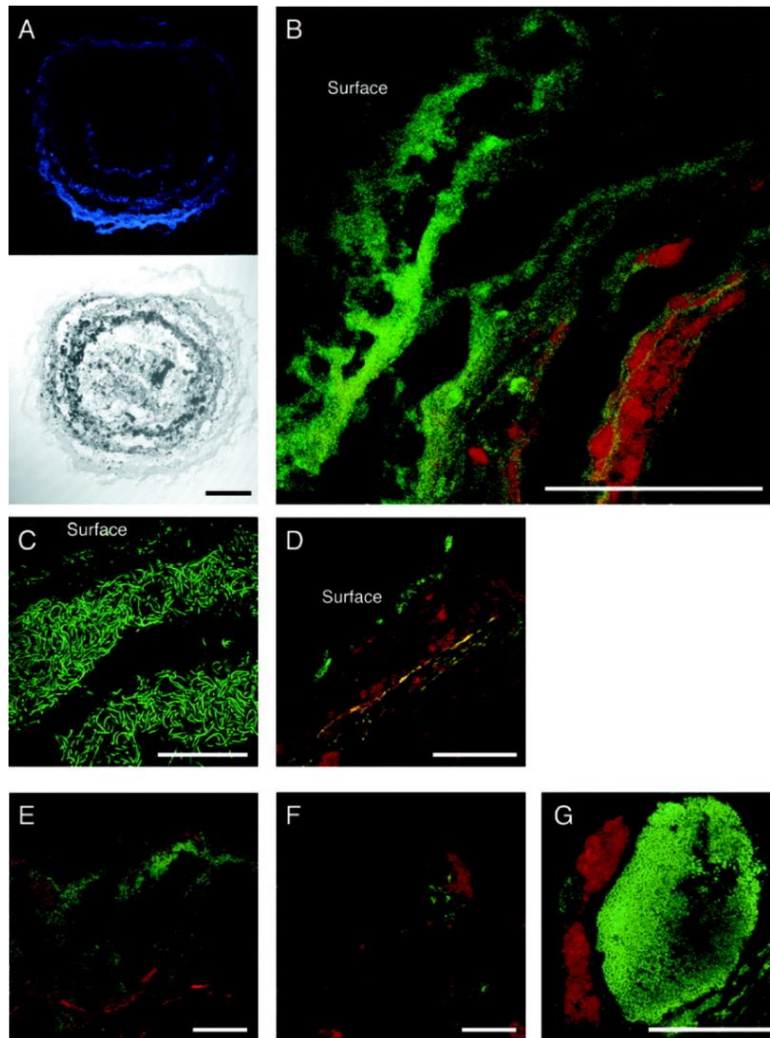


Figure 2.3 Layered structure and spatial distribution of microorganisms in granules (adapted from Satoh Hisashi et al. (2007)). A. Cross-sectional differential interference contrast images of the granules showed that the granules had a multilayered structure consisting of biomass and interstitial voids; B. FISH revealed that the outer layer was dominated by bacterial cells whereas the inner layer (below 250 μm from the surface) was occupied mainly by archaeal cells; C. Filamentous cells were observed in the uppermost layer of the granules; D. The BET42a-stained cells were also present in the outer shell of the granule; E. Firmicutes, were numerically important Bacteria in the inner layer of the granule; F. The abundance and fluorescence intensity of the Alphaproteobacteria-stained cells were low; G. The dense spherical microcolonies that were composed of a number of Actinobacteria in the middle layer (at a depth of ca. 200 μm) of the granule.

Table 2.2 Representative results of pilot- and full-scale UASB system for municipal wastewater.

Country	Volume (m³)	Temperature (°C)	HRT (h)	COD removal (%)	References
Brazil	67.5	16-23	7	74	(Vieira et al., 1995)
Brazil	120	18-28	4.4-14.5	54-65	(Vieira & Garcia, 1992)
Brazil	9	ambient	5.5	45	(Chernicharo & Nascimento, 2001)
Brazil	810	30-31	8.8-9.7	59-75	(Florencio et al., 2001)
Columbia	35	ambient	5-19	66-72	(Schellinkhout & Collazos, 1992)
Columbia	2x3300	ambient	5.2	18-44	(Schellinkhout & Collazos, 1992)
India	1200	20-30	6	74	(Draaijer et al., 1992)
Jordan	60	18-25	23-27	51-62	(Halalsheh et al., 2005)
Jordan	96	18-26	5-10	57-60	(Halalsheh et al., 2005)
Mexico	2200	20	20.3	75-80	(Monroy et al., 2000)
Mexico	5x16740	22.5	18.6	80	(Monroy et al., 2000)
UK	88	ambient	3-7	>85 (BOD)	(Trego et al., 2021)

In the 40 years following the discovery of anaerobic granules, the technology has transitioned from focused laboratory-scale experiments to successful full-scale implementation (van Lier et al., 2015). Even though most UASB applications are treating industrial wastewater, the application of full-scale UASB reactors treating municipal wastewater has largely increased over the last decade, especially in warm climate regions, such as Brazil and Columbia. Table 2.2 shows some selected representative results of pilot- and full-scale UASB systems for municipal wastewater.

2.3 Granulated anaerobic wastewater treatment at low-temperatures

The relatively slow growth rate and sensitivity of methanogens have often been claimed to limit anaerobic municipal wastewater treatment, including environmental conditions, such as temperature, pH, OLR, and HRT (Cardinali-Rezende et al., 2013; Dague et al., 1998; Lettinga et al., 2001; Lew et al., 2009). These environmental conditions influence the

kinetics and thermodynamics of microbial growth and substrate utilization. Anaerobic processing of complex municipal wastewater involves two relatively slow steps; hydrolysis and methanogenesis. For low strength municipal wastewater ($<1000 \text{ mgCOD}\cdot\text{l}^{-1}$) under tropical conditions, methanogenesis is the stage limiting the overall process (Aquino et al., 2019), while hydrolysis has been reported as the rate-limiting step at low-temperatures (Petropoulos et al., 2017). Removing suspended solids prior to anaerobic treatment has been proposed as a solution to overcome the lower hydrolysis rate at low-temperatures (Elmitwalli et al., 2002; Elmitwalli & Otterpohl, 2011).

As mentioned in Chapter 2.2, majority of anaerobic full-scale applications treating wastewater have been concentrated on using high-rate anaerobic systems within the mesophilic temperature ranges for concentrated wastewater and sludges. This was largely due to the assumption that psychrophilic ($<20 \text{ }^\circ\text{C}$) anaerobic treatment was not viable because of low methanogenic activity. Methanogenic conversion becomes even further limited for low strength municipal wastewater. Studies on the metabolic activity of mesophilic methanogens at low-temperatures confirmed this assumption (Bowen et al., 2014; Kettunen & Rintala, 1997; Koster & Lettinga, 1985; Rebac et al., 1995, 1999). Despite the observed reduction in activity at temperatures below $20 \text{ }^\circ\text{C}$, conflicting results have been reported in a few studies conducted in the range of $10 - 15^\circ\text{C}$ (Akila & Chandra, 2007; Collins et al., 2006; Kettunen & Rintala, 1997). Furthermore, promising results have also been reported for the anaerobic community of granulated sludge systems adapted to temperatures in the obligate psychrophilic range down to $4 - 10 \text{ }^\circ\text{C}$ (McKeown et al., 2009; Petropoulos et al., 2017).

Successful operation of high rate anaerobic treatment at low-temperatures benefit from inoculation by cold-adapted granules through improved conversion performance and shorter adaptation time (Collins et al., 2006; McKeown et al., 2009). Moreover, psychrophilic seeds from low nutrient environments might add a further advantage for application

in low strength wastewater (Cavicchioli, 2006). Interestingly, Cavicchioli (2006) found that methanogens are the most abundant archaea in many samples from cold environments. This is not surprising as methane accumulation is common in globally large psychrophilic environments/biomes, like the Eurasian tundra and the deep oceanic sediments. Recently, it has also been confirmed that active methanogens are abundant in extreme cold natural environments, such as lake sediments, high Arctic peats, permafrost, or in the tundra (Kwon et al., 2019; Varsadiya et al., 2021). Hence, growth and multiplication of methanogenic organisms at low-temperatures are common in natural environments, and growth in biotechnological environments should be equally possible.

To assure stable operation and optimization of anaerobic wastewater treatment at low-temperatures, a fine-balance between the various steps in anaerobic processing is critically important. Hence, detailed understanding of the coupled bioconversion mechanisms is necessary. Normally, acetoclastic methanogenesis is commonly reported as the dominant mesophilic methanogenic pathway at a ratio of >67% (Conrad, 2020), as well as under low-temperature conditions (Fey et al., 2004; Kotsyurbenko et al., 1996).

At low-temperatures, homoacetogens have an important role as they are more competitive than hydrogenotrophic methanogens (Pan et al., 2021). Table 2.3 shows specific growth rates (day^{-1}) of methanogenic and acetogenic bacteria at low-temperatures, and at below 10 °C the latter

Table 2.3 Specific growth rates (day^{-1}) of methanogenic and acetogenic bacteria at low-temperatures calculated with two times diluted soil and H_2/CO_2 as a substrate. Q_{10} estimates over the psychrotolerant temperature range to the right (adapted from Kotsyurbenko et al. (1996)).

Bacteria	Substrate	Specific growth rates (day^{-1})					Q_{10} (6 - 20 °C)
		28 °C	20 °C	15 °C	10 °C	6 °C	
Acetogens	H_2/CO_2	0.27	0.28	0.23	0.16	0.09	2.2
Methanogens	H_2/CO_2	0.25	0.23	0.20	0.10	0.04	4.1
	Acetate	0.06	0.22	0.14	0.11	0.07	2.3

grow twice as fast as the autotrophic methanogens. Kotsyurbenko et al. (1996) also found that acetogens were less sensitive to decreasing temperatures compared to hydrogenotrophic methanogens (Q_{10} of 2.2 and 4.1, respectively) over the psychrotolerant and into the psychrophilic growth regime. Furthermore, thermodynamic calculations also confirmed the predominance of acetogens at low-temperatures (Nozhevnikova et al., 1997). Tiwari et al. (2021) proposed a schematic description of anaerobic process under psychrophilic conditions, which by acetate is the main precursor of methanogenesis pathway Figure 2.4. Table 2.4 presents examples of applied granulated anaerobic treatment of different wastewaters at low-temperatures using several types of anaerobic reactors, such as up-flow anaerobic sludge blanket reactor (UASB), anaerobic fluidized bed (AFB), expanded granular sludge bed (EGSB), anaerobic baffled reactor (ABR), and anaerobic sequencing batch reactor (ASBR).

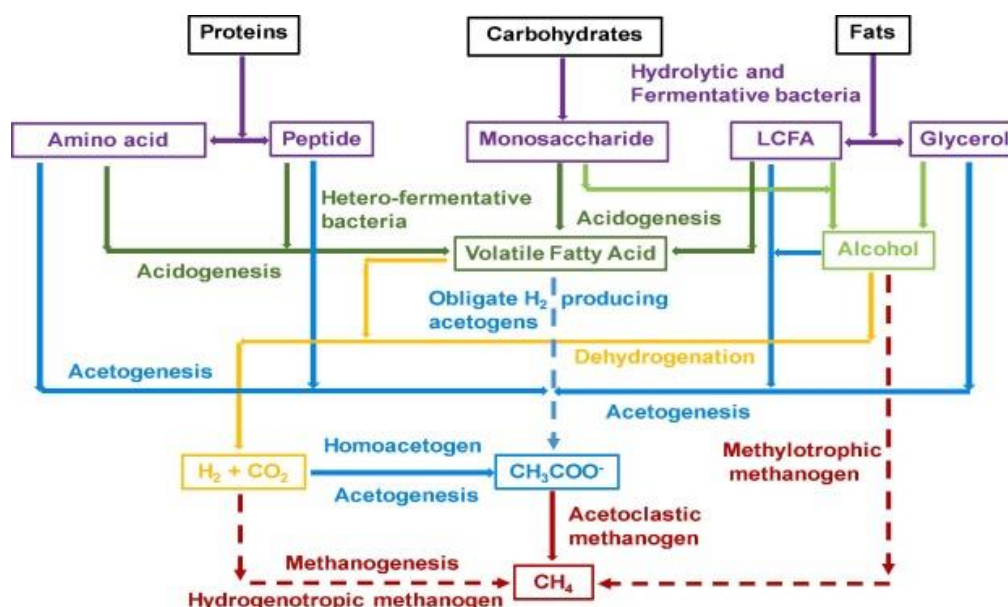


Figure 2.4 Schematic description of anaerobic process under psychrophilic conditions. Dotted arrows represent the minor pathway. The two-step production of methane from CO_2 and H_2 via acetate is more prevalent under low-temperature (adapted from Tiwari et al. (2021)).

Table 2.4 Examples of applied granulated anaerobic treatment of different types wastewater at low-temperatures (adapted from Aquino et al. (2019), Dev et al. (2019), Lettinga et al. (2001), Trego et al. (2021), and Wu et al. (2017)).

Reactor type	Wastewater type	Temperature (°C)	HRT (h)	COD removal (%)
UASB	Sugar vinasse	8	1.5-14	32-65
UASB	Beef consommé	10	16	49-80
UASB	Wine vinasse	4-11	12-38	15-92
UASB	Wine vinasse	4-10	19-31	16-80
UASB	Raw wastewater	8-20	12	67
UASB	Raw Wastewater	11-12	8	30-50
UASB	Raw wastewater	12-20	7-8	30-75
UASB	Raw wastewater	12-18	18	73
UASB	Municipal wastewater	2-18	3-7	>85 (BOD)
AFB	Raw wastewater	10	1.7-2.3	53-85
EGSB	Pre-settled wastewater	9-11	2.1	20-48
UASB	Raw wastewater	13-25	4.7	64-70
UASB+EGSB	Raw wastewater	8-13	5	45-57
ABR	Synthetic wastewater	20	10	70
ABR	Synthetic wastewater	10	10	60
ASBR	Synthetic wastewater	15	16	80

UASB: Up-flow anaerobic sludge blanket reactor, AFB: Anaerobic fluidized bed, EGSB: Expanded granular sludge bed, ABR: Anaerobic baffled reactor, ASBR: Anaerobic sequencing batch reactor

2.4 Anaerobic granulated biofilm modelling

Modelling is a recognized tool for fundamental process understanding, data analysis and hypothesis testing, as well as for design and optimization of wastewater treatment processes (Henze et al., 2008). Considerable effort has gone into developing mathematical models for anaerobic granular technology. Baeten et al. (2019) have recently published a comprehensive review of modelling anaerobic granular sludge reactors. Two main approaches are used for anaerobic granular modelling: The intragranular transport models (biofilm models) and the suspended biomass liquid phase models using apparent kinetics. Granular biofilm models are used for any redox system, while the apparent kinetic models are more commonly used for anaerobic systems (Baeten et al., 2019). Wanner & Gujer (1986) identified several

beneficial objectives attainable by using biofilm models: Understanding the mechanisms fundamental to how a biofilm forms or performs; Integration of different mechanisms occurring at different spatial and temporal scales; pre-model the system to generate expected results; and evaluating novel process designs.

Biofilm modelling on anaerobic granules has been conducted by several researchers who have focused on mass transfer limitations and single as well as multiple limiting substrates (Batstone et al., 2004; Buffière et al., 1995; Doloman et al., 2020; Feldman et al., 2017; Flora et al., 1995; Odriozola et al., 2016; Sun et al., 2016). Granulated biofilm models have been implemented in several programs, such as AQUASIM (Batstone et al., 2004) and MATLAB (Odriozola et al., 2016). An extended Anaerobic Digestion Model No.1 (ADM1) model was also developed with sulfate reduction and sulfide oxidation to elemental sulfur (Pokorna-Krayzelova et al., 2017). In biofilm reactors, substrate transport rate from the bulk liquid to the microbial population is often controlled by diffusion of substrates within the biofilm. Hence to extend ADM1 for biofilm systems, substrate utilization kinetics of single-cell system must be replaced with a biofilm model. The integration of the flow and biofilm models for these biofilm reactors with ADM1 can result in a robust model, which can be a tool for design purposes.

2.5 Post-treatment technology development for anaerobic treatment effluents

Despite the capacity of UASB system to remove organic carbon in wastewater treatment up to 90% in full-scale applications (Chernicharo et al., 2019), a variety of organic compounds, nutrients, and pathogens still remain in the anaerobic effluent above traditional effluent limits. Therefore, UASB reactors usually require a post-treatment unit process to adapt the treated effluent to the requirement water quality standards, protect the receiving water bodies, and/or making the effluent suitable for water reuse (such as, agricultural irrigation).

Most residual particulate COD is composed of less readily biodegradable COD from inlet wastewater which has a slow hydrolysis rate and cannot be entrapped in the reactors. The dissolved fraction of residual COD contains fermentation intermediates, mainly VFAs used as substrate for slow growing methanogens and synergistic consortia and dissolved inert COD. In addition, a bulk phase substrate (dissolved and polymeric) concentration is required as a driving force for substrate diffusion. This is an intrinsic nature of diffusion limited surface systems like biofilms and granulated biomass (Kommedal, 2003). VFA accumulation in UASB reactor system occurs during shock loads and/or stress conditions (e.g., abrupt changes in pH or temperature) due to kinetic limitations of methanogenic microorganisms, which often is enhanced by covariances (e.g., pH and temperature reductions). In a well-operated reactor, the residual COD in the effluent is low in VFA, but still contain bulk phase substrates and non- and/or slowly biodegradable soluble COD that originate from the raw municipal wastewater. Another frequently cited cause for a residual COD during low-temperatures operation is a significant amount of dissolved methane in the effluent (Souza et al., 2011; Wu et al., 2017).

The unspecific soluble microbial products (SMP) have also been mentioned as sources of soluble organic matter in the effluent released from biomass decay or excreted metabolic products (Barker & Stuckey, 1999; Jarusutthirak & Amy, 2007). In contrast to the high removal capacity of organics, anaerobic reactors show limited removal of nitrogen and phosphorus (Li et al., 2007) partly due to low biomass yields and the requirements for obligate aerobic conversions. The removal of nutrients in the UASB systems is therefore usually negligible and sometimes even negative (Elmitwalli & Otterpohl, 2011) due to the hydrolysis of proteins, lipids and nucleic acids. The typical nutrient concentrations range from 0.01 to 4.6 gN·l⁻¹ and 11 to 303 mgP·l⁻¹ for total nitrogen (mostly ammonium) and total phosphorous, respectively (Torres-Franco et al., 2021). These high nutrient concentrations in

anaerobic effluent are nutrient net release for nutrient resource recovery potential.

Another important anaerobic effluent characteristic is low pathogen removal (Espinosa et al., 2021; Uemura et al., 2002). Removal of fecal coliforms by UASB system are reported to range from 40 - 79% (Espinosa et al., 2021; Henze et al., 2008), which is much less compared to activated sludge treatment (80 - 99%) (Henze et al., 2008). The one-stage UASB reactors are not designed to remove the pathogens, again due to the lack of aerobic conditions, and pathogen removal requirements prevent this reactor type from use as a stand-alone unit process. It has been reported that high pathogenic bacteria and virus removal in aerobic wastewater systems, such as activated sludge system, are associated with adsorption to or encapsulation within flocs sludge; virus inactivation bacteria; and ingestion by protozoa and small nematodes (Henze et al., 2008).

Several unit operations have been proposed for anaerobic effluent post-treatments, such as activated sludge systems (Cao & Ang, 2009; Mungray & Patel, 2011), microalgal-based treatments (Ángeles et al., 2021; Torres-Franco et al., 2021), membrane filtrations (Bailey et al., 1994; Ozgun et al., 2015; Rivera et al., 2022), and other biofilm-based treatments like trickling filters and rotating biological contactors (Tawfik et al., 2003; Vieira et al., 2013). Comprehensive reviews on post-treatment technologies for anaerobic effluents for discharge and recycling wastewater have been done by several researchers (Chernicharo, 2006; Mai et al., 2018; Mungray et al., 2010).

2.6 Dissolved methane removal from anaerobic effluent

Dissolved methane in the anaerobic effluent is an often-overlooked hurdle for anaerobic treatment of municipal wastewater (Liu et al., 2014). Theoretically, 381 ml of methane are produced per gram COD removed at standard ambient conditions (25 °C, 1 atm) (Tchobanoglous

et al., 2003). By assuming 80% COD removal efficiency for a typical high strength municipal wastewater with an average soluble COD concentration of $450 \text{ g}\cdot\text{m}^{-3}$ (Henze et al., 2008), $137 \text{ l CH}_4\cdot\text{m}^{-3}$ is produced, equivalent to $90 \text{ g CH}_4\cdot\text{m}^{-3}$. At an equilibrium methane solubility of approximately $20 \text{ g}\cdot\text{m}^{-3}$ at $25 \text{ }^\circ\text{C}$ (Liu et al., 2014), approximately 22% of all produced methane would be in its dissolved form and leave the digester by the liquid effluent. Of the $90 \text{ g CH}_4\cdot\text{m}^{-3}$ formed, a methane gas volume of $107 \text{ l CH}_4\cdot\text{m}^{-3}$, which in energy equivalents is equal to 100 l natural gas or a CO_2 equivalent of 248 g (or 137 l CO_2), degassing of the dissolved methane to the atmosphere, would contribute approximately $500 \text{ g CO}_2\text{equiv}\cdot\text{m}^{-3}$ (100 years global warming potential (GWP) of 25), equivalent to $278 \text{ l CO}_2\cdot\text{m}^{-3}$. Therefore, the greenhouse gas contribution of methane loss through the liquid effluent is about 2.5 times greater than the positive effects from generating a renewable energy from the produced biogas (Safitri et al., 2021). This methane loss is significantly reducing and, as in the given example above, even offsetting the positive effect of energy recovery from anaerobic wastewater treatment. Therefore, a post-treatment process is required to remove dissolved methane, reducing the environmental impact of anaerobic wastewater treatment. Several methods have been proposed for removing or recovering dissolved methane from anaerobic effluents. These include air stripping oxidation (Hatamoto et al., 2010; Matsuura et al., 2015) and degassing membrane-based recovery (Bandara et al., 2011; Cookney et al., 2016).

Dissolved methane can be biologically oxidized by methanotrophs (Ruiz-Ruiz et al., 2020). Methanotrophs are part of a larger group of bacteria called methylotrophs that typically utilize single-carbon compounds like methane, methanol, formic acid or even formaldehyde as carbon and energy source (Chistoserdova et al., 2009). Methanotrophs may fully oxidize methane to CO_2 or partially to oxidation intermediates like methanol (Hanson & Hanson, 1996). In nature, methanotrophs often co-occur with non-methanotrophic methylotrophs that feed on partially

oxidized methane intermediates like methanol (Takeuchi et al., 2019; Yu et al., 2017).

Methanotrophs have recently emerged as a prominent solution for methane mitigation and value-added resources recovery platform in wastewater treatment technology (AlSayed et al., 2018). A recent published study also demonstrated methane bioconversion into ectoine, a valuable compound in the cosmetic and medical industry, using mixed methanotrophic consortia (Carmona-Martínez et al., 2021). AlSayed et al. (2018) summarized the potential of biogas utilization by methanotrophs in comparison with ammonia-oxidizing bacteria that can also utilize methane and activate its stable C–H bond, as shown in Figure 2.5.

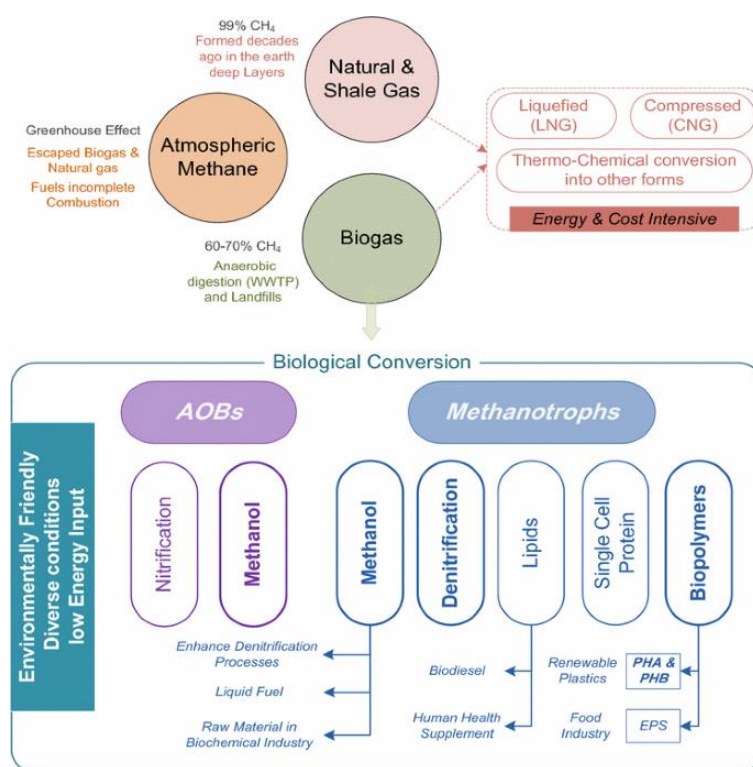


Figure 2.5 Methane utilization potential from different sources by methanotrophs and ammonia oxidizing bacteria (adapted from AlSayed et al. (2018))

Oxygen is required for methane conversion. Through the coupled activities of eukaryotic algae or photosynthetic bacteria and methanotrophs in syntrophic bio-aggregates, i.e., photogranule, oxygen may be provided by direct, or at least local transfer. The produced oxygen is then immediately utilized by the methanotrophs to convert organic matter to CO₂, which is in turn used by phototrophs for autotrophic CO₂ fixation. Oxygenic photogranules are a light-driven consortium of phototrophic and non-phototrophic microorganisms which are embedded in a matrix of extracellular polymeric substances (EPS). The phototrophic microorganisms in photogranules are a mix of algae and/or mostly filamentous cyanobacteria (Milferstedt et al., 2017).

The methane conversion relies on syntrophic interactions between phototrophic cyanobacteria and methanotrophic bacteria aggregated in oxygenic photogranules. These interactions are found in natural systems, for example, at the chemocline between anaerobic and aerobic water layers in freshwater lakes (Milucka et al., 2015), and are also utilized in engineered systems, e.g., by van der Ha et al. (2012) to produce lipids or polyhydroxy butyrate using co-cultured eukaryotic algae and methanotrophs. Rasoulie et al. (2018) also investigated a co-culture of green microalgae and methanotrophs for removing methane and recovering nutrients (Rasouli et al., 2018).

2.7 Microalgae-based advanced wastewater treatment

Many studies have shown that microalgae have great potential for removing nutrients from wastewater (Torres-Franco et al., 2021). Microalgae have been used to treat wastewater for a long time, as W.J Oswald proposed the high-rate algal ponds in the 1950s (Oswald & Golueke, 1960). A desirable property of microalga used in wastewater treatment is rapid growth coupled to high uptake rates. Small, single planktonic cells grown in suspension will grow faster compared to larger, colonial, or filamentous cells or cells that grow attached to surfaces due to intrinsic transport limitations. However, larger filamentous and

colonial cells are easier to harvest (Chisti, 2007). Ideal microalgal strains for wastewater treatment have properties such as a high nutrient requirement and high uptake affinity (Torres-Franco et al., 2021; Wang et al., 2017). Several applications of microalgae in wastewater treatments using several types of photobioreactor (PBR), such as flat-plate membrane and bubble column PBR, are summarized in Table 2.5.

Microalgae-based systems removing nutrients in wastewater treatment rather than conventional treatment methods have several advantages. These include cost-effectiveness, low-energy use, decreased greenhouse gas emissions, and production of high-value microalgal biomass, for example, fatty acids for nutraceutical productions (Huy et al., 2022). Microalgae-based systems leave low residual nutrient concentrations without adding extra chemicals. Some limitations of microalgae-based treatment of wastewaters, specifically anaerobic wastewater treatment effluent, have been addressed by Torres-Franco et al. (2021). Besides operational and practical issues, such as high energy demand for light and large area requirement for open ponds, ammonia inhibition, light blockage, and unbalanced macronutrients ratio are the main challenges that directly affect the ability of microalgae to grow in anaerobic effluent (Torres-Franco et al. 2021). Furthermore, drawbacks include a relatively long hydraulic retention time (HRT), complicated processes for separating microalgae within treated wastewater and reduced performance under contamination and predation (Wang et al., 2017).

Literature Review

Table 2.5 Microalgae-based treatment in different types of wastewater, adapted from Kong et al. (2021)

Feed	Microalgae	Reactor	CO₂ (%)	R_{CO2} (g·l⁻¹·d⁻¹)	C_N (mg·l⁻¹)	R_N (mg·l⁻¹)	C_P (mg·l⁻¹)	R_P (mg·l⁻¹·d⁻¹)	C_C (mg·l⁻¹)	R_C (mg·l⁻¹·d⁻¹)	Ref.(s)
Synthetic wastewater	<i>Spirulina platensis</i> UTEX 2340	Bench-scale PBR	0.038	n.a.	TN: 412	23-49 [#]	TP: 90	64-81 [#]	n.a.	n.a.	Yuan et al. (2011)
	<i>Spirulina platensis</i>	Hollow fiber membrane PBR	2	0.912-1.44	NO ₃ ⁻	82 [#]	n.a.	n.a.	n.a.	n.a.	Kumar et al. (2010)
Treated domestic wastewater	<i>Chlorella vulgaris</i> <i>Botryococcus braunii</i> <i>Spirulina platensis</i>	Flat-plate membrane PBR	1% CO ₂ 20% O ₂ 79% N ₂	1.5-22.4 g·m ⁻³ ·d ⁻¹	0.62-2.4	1.4-6.9	0.08-0.89	0-0.071	TOC: 1.7-3.6	n.a.	Honda et al. (2012)
Municipal wastewater	<i>Chlorella</i> strains (10 strains)	Erlenmeyer flasks	10	26.14%- 35.51%	TN: 29.32 NH ₄ ⁺ - N:26.13	n.a.	TP: 3.62	n.a.	COD: 52.42	n.a.	Hu et al. (2016)

PBR, photobioreactor; R_{CO2}, CO₂ fixation rate; C_N, initial nitrogen concentrations; R_N, nitrogen removal rate; C_P, initial phosphorus concentrations; R_P, phosphorus removal rate; C_C, initial organic carbon concentrations; R_C, organic carbon removal rate; n.a., not available; [#] represents the unit of nitrogen, phosphorus and organic carbon removal rate is %.

Literature Review

Table 2.5 Microalgae-based treatment in different types of wastewater, adapted from Kong et al. (2021) (continued)

Feed	Microalgae	Reactor	CO ₂ (%)	R _{CO2} (g·l ⁻¹ ·d ⁻¹)	C _N (mg·l ⁻¹)	R _N (mg·l ⁻¹)	C _P (mg·l ⁻¹)	R _P (mg·l ⁻¹ ·d ⁻¹)	C _C (mg·l ⁻¹)	R _C (mg·l ⁻¹ ·d ⁻¹)	Ref.(s)
Domestic wastewater	<i>Scenedesums</i> sp.	Bubble column PBR	0.03-10	0.239-0.368	NH ₄ ⁺ -N: 38.6 NO ₃ ⁻ -N: 17.1	5.16-5.42 1.38-1.71	9.24	0.96-1.08	COD: 142.2	14-19.5	Nayak et al. (2016)
	<i>Chlorella</i> sp. <i>Scenedesmus</i> sp. <i>Sphaerocystis</i> sp. <i>Spirulina</i> sp.	Flask	20-50	150-291 mg·g ⁻¹	NH ₄ ⁺ -N	39 [#]	PO ₄ ³⁻ P	59 [#]	n.a.	n.a.	Bhakta et al. (2015)
	<i>Chlorella minutissima</i>	Assembly based on fish aquarium	5.36-86.4% Biogas	486.2-210.76 g·m ⁻³ ·d ⁻¹	n.a.	n.a.	n.a.	n.a.	n.a.	n.a.	Khan et al. (2018)
	<i>Spirulina platensis</i> mixed indigenous microalgae	Pilot plant	2.5-20	0.05-0.60	NH ₄ ⁺ -N: 42 NO ₂ ⁻ : 0.81 NO ₃ ⁻ : 10.5	50-95 [#]	TP: 9.3±0.3	50-90 [#]	52.0±0.5	50-100 [#]	Almomani et al. (2019)

PBR, photobioreactor; R_{CO2}, CO₂ fixation rate; C_N, initial nitrogen concentrations; R_N, nitrogen removal rate; C_P, initial phosphorus concentrations; R_P, phosphorus removal rate; C_C, initial organic carbon concentrations; R_C, organic carbon removal rate; n.a., not available; # represents the unit of nitrogen, phosphorus and organic carbon removal rate is %.

Literature Review

Table 2.5 Microalgae-based treatment in different types of wastewater, adapted from Kong et al. (2021) (continued)

Feed	Microalgae	Reactor	CO ₂ (%)	R _{CO2} (g·l ⁻¹ ·d ⁻¹)	C _N (mg·l ⁻¹)	R _N (mg·l ⁻¹)	C _P (mg·l ⁻¹)	R _P (mg·l ⁻¹ ·d ⁻¹)	C _C (mg·l ⁻¹)	R _C (mg·l ⁻¹ ·d ⁻¹)	Ref.(s)
Synthetic domestic wastewater	<i>Chlorella vulgaris</i>	Flask	0.038	0.075-0.471	NaNO ₃ :	6.75-	KH ₂ PO ₄ :	0.68-2.67	n.a.	n.a.	Gonçalves et al. (2014)
	<i>Pseudokirchneriella subcapitata</i>				250	18.18		0.55-2.22			
	<i>Synechocystis salina</i>					6.79-		0.38-1.92			
	<i>Microcystis aeruginosa</i>					17.82		0.50-1.67			
						7.04-					
Synthetic municipal wastewater	<i>Scenedesmus obliquus</i>	Flasks; Cylindrical plexiglass PBR	0.03-15	0.257	11-14	97.8 [#]	1-1.5	95.6 [#]	TOC: 20-120	59.1-93.3 [#]	Shen et al. (2015)
	<i>Scenedesmus obliquus</i>	Erlenmeyer flasks	0.038-10	n.a.	NH ₄ ⁺ -N: 30-70	20-100 [#]	PO ₄ ³⁻ -P: 13	n.a.	50	n.a.	Liu et al. (2019)
Aquaculture wastewater	<i>Chlorella</i> sp. GD	Glass-fabricated PBR	2-8% Flue gas	2.333	TN: 60	40-90 [#]	TP: 6.8	87-99 [#]	COD: 112	61-80 [#]	Kuo et al. (2016)

PBR, photobioreactor; R_{CO2}, CO₂ fixation rate; C_N, initial nitrogen concentrations; R_N, nitrogen removal rate; C_P, initial phosphorus concentrations; R_P, phosphorus removal rate; C_C, initial organic carbon concentrations; R_C, organic carbon removal rate; n.a., not available; [#] represents the unit of nitrogen, phosphorus and organic carbon removal rate is %.

Literature Review

Table 2.5 Microalgae-based treatment in different types of wastewater, adapted from Kong et al. (2021) (continued)

Feed	Microalgae	Reactor	CO ₂ (%)	R _{CO2} (g·l ⁻¹ ·d ⁻¹)	C _N (mg·l ⁻¹)	R _N (mg·l ⁻¹)	C _P (mg·l ⁻¹)	R _P (mg·l ⁻¹ ·d ⁻¹)	C _C (mg·l ⁻¹)	R _C (mg·l ⁻¹ ·d ⁻¹)	Ref.(s)
Tequila vinasses and culture media	<i>Chlorella</i> <i>vulgaris</i> U162 <i>Chlorella</i> sp. <i>Scenedesmus</i> <i>obliquus</i> U169 <i>Scenedesmis</i> sp.	Flasks	25% CO ₂ 75% CH ₄ (Biogas)	0.15- 0.91	39-50 for tequila vinasses; 0.075-5 for media	n.a.	80.04- 83.3	n.a.	TOC: 12.9- 9024	n.a.	Choix et al. (2018)
Effluent of cattle farm and manure leachate	<i>Coelastrum</i> sp. SM	Airlift PBR:	6-16	0.153- 0.302 g·l ⁻¹	TKN: about 62	7.548- 9.471	TP: 4-9	3.45-6.90	sCOD: n.a.	71.749- 98.192	Mousavi et al. (2018)
Palm oil mill effluent	<i>Chlorella</i> sp.	Transparent glass bottles	10-25	0.02- 0.14	TN: 330±30	28- 92.11	PO ₄ ³⁻ : 273±17	n.a.	COD 2900±1 10	n.a.	Hariz et al. (2018)
Seafood processing industry wastewater	<i>Chlorella</i> <i>vulgaris</i> NIOCCV	Tubular PBR	5-20	0.149- 0.430 mg·l ⁻¹ ·d ⁻¹	n.a.	79.68- 82.42 [#]	n.a.	63.64 [#]	TOC: n.a.	23.46 [#]	Jain et al. (2019)

PBR, photobioreactor; R_{CO2}, CO₂ fixation rate; C_N, initial nitrogen concentrations; R_N, nitrogen removal rate; C_P, initial phosphorus concentrations; R_P, phosphorus removal rate; C_C, initial organic carbon concentrations; R_C, organic carbon removal rate; n.a., not available; # represents the unit of nitrogen, phosphorus and organic carbon removal rate is %.

Literature Review

Table 2.5 Microalgae-based treatment in different types of wastewater, adapted from Kong et al. (2021) (continued)

Feed	Microalgae	Reactor	CO ₂ (%)	R _{CO2} (g·l ⁻¹ ·d ⁻¹)	C _N (mg·l ⁻¹)	R _N (mg·l ⁻¹)	C _P (mg·l ⁻¹)	R _P (mg·l ⁻¹ ·d ⁻¹)	C _C (mg·l ⁻¹)	R _C (mg·l ⁻¹ ·d ⁻¹)	Ref.(s)
Textile and food processing wastewater	<i>Chlorella vulgaris</i>	Bubble column PBR	0.03-10%	0.103-0.187	NH ₄ ⁺ -N: 153.1	85.3-95.9 [#]	PO ₄ ³⁻ P: 11	89.5-98.8 [#] 80.4-85.8 [#]	850	71.4-91.9 [#] 65.1-85.2 [#]	Yadav et al. (2019)
	<i>Chlorococcum infusionum</i>		Coal-fired flue gas	0.543-0.947		65.3-75.5 [#]		80.4-85.8 [#]			
Ossein effluent	<i>Phormidium valderianum</i> BDU 20041	Open tank	15% Coal burning flue gas	0.0564-0.0658	60.24	66.35 [#]	56.67	35.66 [#]	n.a.	n.a.	Dineshbabu et al. (2017)
Steel-making facility wastewater	<i>Chlorella vulgaris</i> UTEX 259	PBR	0.03-15	0.624	NH ₃ : 50	0.86-0.92 gNH ₃ ·m ⁻³ ·h ⁻¹	PO ₄ ³⁻ P: 400 g·m ⁻³	n.a.	n.a.	n.a.	Yun et al. (2018)
Petroleum wastewater	<i>Spongiochloris</i> sp.	Airlift bioreactor	0.038	2.9205	63.5	n.a.	17	n.a.	COD: 285	97 [#]	Abid et al. (2017)
Oil sands tailings water	<i>Chlorella pyrenoidosa</i> CCCM 7066	Erlenmeyer flask	n.a.	0.11	NH ₃ : 23.9-68	n.a.	PO ₄ ³⁻ P: 0.02-0.4	n.a.	n.a.	n.a.	Yewalkar et al. (2011)

PBR, photobioreactor; R_{CO2}, CO₂ fixation rate; C_N, initial nitrogen concentrations; R_N, nitrogen removal rate; C_P, initial phosphorus concentrations; R_P, phosphorus removal rate; C_C, initial organic carbon concentrations; R_C, organic carbon removal rate; n.a., not available; # represents the unit of nitrogen, phosphorus and organic carbon removal rate is %.

Microalgal-based wastewater treatment is often not only performed by microalgae but also by natural consortia of microalgae and bacteria, naturally developed or specifically inoculated from cultures (Muñoz & Guieysse, 2006). Photosynthetic activity of microalgae can provide oxygen to support bacterial needs and therefore avoid the energy consumption associated with external aeration (Casagli et al., 2021). There are three mechanisms for nutrient removal, specifically nitrogen and phosphorous, in microalgal-bacterial systems: Assimilatory nutrient recovery into biomass production; abiotic nutrient removal by elevated pH during microalgal photosynthesis, removing $\text{NH}_3\text{-N}$ and enhancing phosphate precipitation; and dissimilatory nutrient removal by nitrification-denitrification (Posadas et al., 2017). Hence, complex interactions between microalgae and bacteria during wastewater treatment can support an efficient removal of nutrients and/or other pollutants.

The type of wastewater and its characteristics affect the microalgal-based wastewater treatment performance. The initial carbon (C), nitrogen (N), and phosphorus (P) ratio in wastewater is often correlated with its biodegradability by microalgal-based treatment. For this, the Redfield ratio of 106C:16N:1P is widely used to quantify possible carbon and/or nutrient limitations (Tyrrell, 2019), though many studies have found the evidence of deviations from this ratio (Ación et al., 2016; Posadas et al., 2017).

Carbon is present in wastewater as inorganic carbonates and as organic molecules. Carbon dioxide can be assimilated from the atmosphere and from industrial exhaust gas by microalgae carbon fixation (Richmond, 2003). Some microalgae are also capable of using organic carbon through heterotrophic assimilation, while others are mixotrophic using both inorganic and organic carbon sources (Cai et al., 2013). Additional carbon supply in the form of CO_2 or bicarbonate is needed to allow for the complete assimilation of N and P contained within the wastewater. Moreover, even if the wastewater composition does not necessitate CO_2

injection to supply carbon, it is still important to do so in order to control the pH (Acién et al., 2016).

Nitrogen is present in wastewater in various forms, including ammonium (NH_4^+), nitrate (NO_3^-), nitrite (NO_2^-) and organically bound nitrogen (Wang et al., 2017). Microalgal dry mass contains around 7% nitrogen, distributed among proteins, enzymes, peptides, chlorophylls, genetic material (DNA, RNA) and energy transfer molecules (ATP, ADP) (Richmond, 2003). Nitrate, ammonia and urea are widely applied nitrogen sources for microalgal cultivation. Changes in nitrogen supply can potentially influence metabolic pathways, leading to altered composition of the microalgae. Bacterial nitrification-denitrification leads to some nitrogen being lost as nitrogen gas (N_2) and minute amounts of NH_3 may also escape by volatilization at elevated pH, temperature and mixing intensities (Wang et al., 2017).

Autotrophs assimilate dissolved phosphorous into intracellular energy transfer molecules, nucleic acids and nucleotides, cell membrane phospholipids, proteins (Richmond, 2003), and phosphorylated metabolic intermediates. Some cyanobacteria and eukaryotic coccal green microalgae can accumulate phosphate as polyphosphate granules. Phosphorous is commonly removed from wastewater by trivalent metallic cation precipitation or by Ca_2^+ , Mg_2^+ , precipitation at high pH, as struvite and apatite (Wang et al., 2017). Dry microalgal biomass contains approximately 1% phosphorous (Becker, 2007).

Beside, wastewater chemical composition, microalgal growth can be affected by biotic factors, such as the presence of pathogens and competition by other microalgal species, and abiotic factors, such as temperature, light, pH, salinity and mixing (Gonçalves et al., 2017). Optimal culture temperature will vary with type of media and microalgal strains used for culturing. The most common cultured species tolerates temperatures from 16 - 27 °C, where 18 - 20 °C is commonly utilized for culturing (Richmond, 2003). Light is essential for cultivation of

microalgae as it is the main source of energy. The intensity of illumination varies with depth and density of the microalgal culture. High depth and cell density increase attenuation, however, if the light intensity is too high this can cause photo-inhibition or even overheating. Typical light intensity used in laboratory studies range from 100 to 200 $\mu\text{E}\cdot\text{s}^{-1}\cdot\text{m}^{-2}$ (5-10% of full daylight) and diurnal cycles are often applied as many microalgal species do not grow well under constant illumination (Richmond, 2003).

While some microalgal species grow in acidic environments, the optimal pH for the cultivation of most species ranges from 7 to 9 (Posadas et al., 2015). Aeration and/or addition of CO_2 can be used to control pH in cultures (Richmond, 2003). High partial pressure of CO_2 can lead to acidification of culture conditions, inhibiting microalgal growth. A sufficient supply of carbon is vital for microalgal growth due to microalgal biomass carbon content of 50% (w/w) (Becker, 2007). pH affects microalgal carbon uptake. At pH values ranging from 5 to 7, CO_2 is taken up through diffusion, while bicarbonate is taken up by active transport at pH values above 7 (Gonçalves et al., 2017). Agitation of microalgal cultures is essential to avoid sedimentation of microalgae. Proper mixing provides illumination and enhances gas transfer between culture medium and the gaseous headspace (Richmond, 2003).

2.8 Specific objectives and research questions

Continuous anaerobic reactors (e.g., UASB, EGSB, anaerobic filter and hybrid system, anaerobic membrane reactor) treating real wastewater at low-temperature, down to 3 °C, for 140 - 540 days have been published (Bandara et al., 2012; Elmitwalli et al., 2002; Kettunen & Rintala, 1998; Mahmoud et al., 2004; Petropoulos et al., 2021; Smith et al., 2012; Zhang et al., 2018). However, investigation of long term UASB reactor operation on real municipal wastewater at temperatures below 20 °C and variable OLR effect is scarce. For anaerobic wastewater treatment to become a viable and preferred treatment strategy for municipal

wastewater in the northern temperate and sub-arctic populated regions, stable operation and acceptable treatment performance must be demonstrated, and operational stability needs to be documented. Further, if psychrophilic wastewater treatment is possible, an important design and operational question is whether such performance is a result of microbial community adaptations or phenotypic adaptations of a mesophilic generic sludge. In addition, a UASB biofilm model can be used to predict and simulate biofilm model implementation and assumptions specific to the granules in the UASB reactor system.

UASB post-treatments are required to remove dissolved methane and nutrient. Engineered systems using suspended phototrophic-methanotrophic consortia to remove methane has been proposed (Rasouli et al., 2018; van der Ha et al., 2012). Removal by syntrophic methanotrophs in oxygenic photogranule communities (Milferstedt et al., 2017) is a novel technique with beneficial attributes, and potential and performance needs to be demonstrated. Furthermore, many studies have shown that microalgae can utilize the reduced nutrients in anaerobic wastewater treatment effluent. In this study, the growth potential and the nutrient removal capacity of selected microalgal strain(s) in specific UASB effluent should be investigated.

The research questions (RQs) and hypotheses proposed in this study are stated as follows:

UASB system on municipal wastewater treatment at low-temperatures and variable loadings

- a. RQ1. Can UASB system be used for municipal wastewater treatment at low-temperatures and variable loadings?
Hypothesis: UASB reactor stability at low-temperatures and variable loadings can be maintained and significant COD removal efficiency and methane production are sustained.

- b. RQ2. Can microbial community show mesophilic anaerobic granules adaptation to psychrophilic conditions in a long-term UASB operation?

Hypothesis: Microbial community adaptation explains the low-temperature performance in a long-term UASB operation.

- c. RQ3. Can the anaerobic granulated biofilm model predict the effect of organic loading on reactor performances and biofilm characteristic(s)?

Hypothesis: Simulation can predict the effect of organic loading on reactor performances and biofilm characteristic(s).

Methanotrophs-photogranules experiment for dissolved methane removal

- d. RQ4. Can an engineered cyanobacterial-methanotrophic photogranule community remove dissolved methane?

Hypothesis: Cyanobacterial-methanotrophic syntrophy in photogranule community removes dissolved methane.

- e. RQ5. Can microbial communities show methanotrophs and cyanobacteria syntrophy in photogranules to remove dissolved methane?

Hypothesis: The community composition suggests methanotrophs and cyanobacteria syntrophy in photogranules to remove dissolved methane.

Microalgae-based wastewater treatment for nutrient removal

- f. RQ6. Can the selected microalgae strain(s) grow and remove nutrients in specific UASB effluent in this study?

Hypothesis: The selected microalgae strain(s) can adapt to grow and remove nutrients in specific UASB effluent in this study.

3 General Methodology

This work is the result of three different experimental studies and anaerobic granulated biomass/biofilm modelling. This chapter elaborates on the overall research approach, followed by details on the general methodology of laboratory-scale experiments: Long term studies of UASB system at low-temperatures and different loadings; post-treatment potential of UASB effluent using methanotroph-photogranules experiment for dissolved methane removal; and microalgal treatment for nutrient removal. This chapter also describes UASB biofilm model implementation.

3.1 UASB systems and operation

In this study, long-term temperature effects (25, 16, 12, 8.5, 5.5, and 2.5 °C) on a laboratory-scale UASB reactor performance under increasing organic loading rates of municipal wastewater was investigated over 1025 days. The performance of this anaerobic granular sludge system was evaluated by determining its COD conversion and removal efficiency, measuring its specific methane production rate, and methane yield. Observations were interpreted by COD mass balance analysis to determine reactor performance. Nutrients (N and P), VFA and alkalinity variability during UASB operation were also investigated in order to determine granular biomass activity and stability.

Two parallel in-house designed temperature-controlled laboratory-scale UASB reactors (reactor A and B) were operated continuously, receiving primary treated municipal wastewater from the Grødaland wastewater treatment plant operated by IVAR IKS, Norway. The wastewater may be characterized as a municipal wastewater with significant contributions from agricultural and food industries like (a) Animal residual recovery plant (Biosirk Protein: 167 m³·d⁻¹); (b) Municipal wastewater of approximately 3000 houses of the community Varhaug (3000 m³·d⁻¹) and food processing plant (Fjordland: 1910 m³·d⁻¹); (c) Dairy and

chicken slaughterhouse (Kviamarka: $3020 \text{ m}^3 \cdot \text{d}^{-1}$); and (d) Reject water from thickening and dewatering of digested sludge from the Grødalund biogas plant ($345 \text{ m}^3 \cdot \text{d}^{-1}$). The dissolved COD concentrations of inlet wastewater during UASB reactor operation fluctuated in the range 439 - $1473 \text{ mgCOD}_{\text{dissolved}} \cdot \text{l}^{-1}$ with the mean concentration being $741 \pm 7 \text{ mgCOD}_{\text{dissolved}} \cdot \text{l}^{-1}$ (\pm standard error). Approximately 30 % (v/v) of UASB granule inoculum, kindly provided by the late Professor Rune Bakke (University of South-Eastern, Norway), were transferred to the UASB reactors with 1000 ml of total volume. The inoculum was originated from a mesophilic active pilot-scale bioreactor treating a combination of municipal wastewater, industrial pulp factory effluents, and a non-specific effluent from the Rafnes Industrial Park (Hærøya, Porsgrunn, Norway).

Figure 3.1 presents a schematic view and flow diagram of the reactor set-up. The reactors were air-tight glass-type reactors capped with a natural rubber stopper (custom made by glassblower Mellum AS, Aurskog Norway: www.friedel.no). Reactor temperature was controlled using a Lauda Alpha RA8 refrigerated water circulation unit (Lauda, Germany), circulating water through reactor jackets at a high rate ($>200 \text{ ml} \cdot \text{min}^{-1}$). Glycol was added to the circulating unit to avoid freezing at reactor temperature $2.5 \text{ }^\circ\text{C}$ from day 842. External foam insulators were mounted to maintain the desired temperatures of $8.5 \text{ }^\circ\text{C}$ operations (day 520) and below. An external digital thermometer was installed inside the circulating unit as an additional temperature confirmation, and temperatures inside the reactors were measured manually on a regular basis. Cooled wastewater ($2 - 4 \text{ }^\circ\text{C}$) was fed by a peristaltic pump (Ismatec, Germany) with adjustable flow rates. Continuous recirculation to sustain mixing and a constant up-flow was achieved by pumping effluent from the top to the bottom of the reactors providing an up-flow velocity of $1.8 \pm 0.7 \text{ m} \cdot \text{h}^{-1}$.

Methane and CO_2 produced were measured using Milligas counters (Dr.-Ing. RITTER Apparatebau GmbH & Co., Bochum, Germany) serially

General Methodology

connected to the UASB gas outlet and equipped with a bubble-through CO₂-absorber, containing NaOH 3 M and 0.4% Thymolphthalein pH-indicator solution. A pH probe (Hanna Instruments, HI 9025C, Norway) was installed in the recirculation line allowing an inline measurement of the bulk liquid pH. A 1000 µm Sefar® Flourtex filter (Sefar AG, Switzerland) was installed inside the reactor exit section to retain biomass from being washed out and potentially clog pump and gas exit tubes.

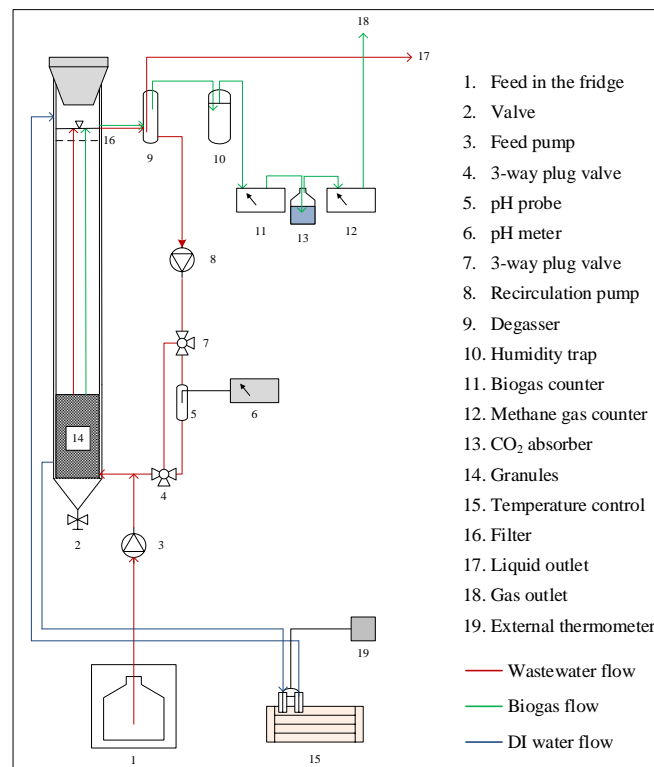


Figure 3.1 Flow diagram of the laboratory-scale UASB reactor. Two reactors were assembled parallelly identically with the same set-up as illustrated here. The red line represents the wastewater inlet and outlet flow; the green line represents the biogas flow; the blue line represents the distilled water flow for the cooling circulating water (Paper I).

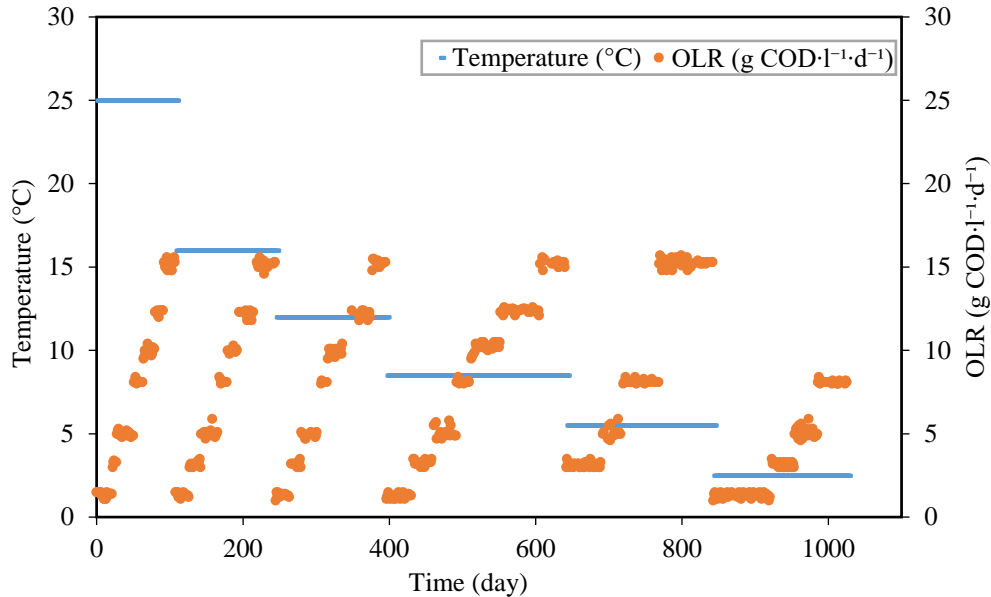


Figure 3.2 The UASB reactors were operated continuously over 1025 days by the stepwise increase of OLR at decreasing temperatures. Initially, UASB reactors were started-up at 25 °C with low OLR around 1.0 $\text{gCOD}_{\text{dissolved}}\cdot\text{l}^{-1}\cdot\text{d}^{-1}$ and increased gradually up to approximately 15 $\text{gCOD}_{\text{dissolved}}\cdot\text{l}^{-1}\cdot\text{d}^{-1}$. During operation, hydraulic retention rate (HRT) started at about 16.7 h then gradually decreased along with the increasing OLR, down to 1.1 h. The operating temperatures were then reduced to the next lower temperature experiments at 16, 12, 8.5, 5.5 and finally 2.5 °C (Paper I), and the loading procedure repeated.

Operational conditions during continuous UASB system operation are shown in Figure 3.2. The UASB reactors were operated continuously by applying a stepwise increase of organic loading rate (OLR) starting from 1.3 ± 0.1 by intermittent increases to 15.2 ± 0.2 $\text{gCOD}_{\text{dissolved}}\cdot\text{l}^{-1}\cdot\text{d}^{-1}$ following the establishment of a steady-state following a decrease in reactor temperatures (25, 16, 12, 8.5, 5.5, and 2.5 °C). Steady-state was achieved in the reactors when the parameters, i.e., the COD removal efficiencies and the daily gas production remained relatively constant at the same temperature and OLR. OLR was controlled by adjusting the inlet flow rate according to the dissolved COD concentration of inlet wastewater. Both reactors were identical and operated with the same loading and inlet. At each operating temperature, the gradual increment

of OLR was used to ensure that granules would not washed out of the system while the microorganisms were acclimating to the higher loading. Severe deterioration (dissolution) of granules occurred in reactor A when applying OLR of $15 \text{ gCOD}\cdot\text{l}^{-1}\cdot\text{d}^{-1}$ at $5.5 \text{ }^\circ\text{C}$, and the reactor stopped operating at day 738, and investigations continued on reactor B only. Further details on UASB reactor system set-up and methods are presented in Appendix (Paper I).

3.2 Microbial community analysis on psychrophilic granules from the UASB system

Molecular characterization of the temperature responding community gradients was performed. This study investigated the microbial community changes resulting from temperature reductions and organic loading increments from the low mesophilic into obligate psychrophilic conditions. In short, granule samples were obtained from UASB reactors during 12, 8.5, 5.5 and 2.5°C reactor operation at selected OLRs, as shown in Table 3.1. Community DNA was extracted using a DNeasy PowerWater Kit (Qiagen, Germany). After extraction, DNA was checked via agarose gel electrophoresis and DNA concentration was determined using the NanoVue™ Plus Spectrophotometer (GE Healthcare, USA) before external sequencing.

Table 3.1 Granule samples on microbial community analysis from the UASB system

Temperature (°C)	Reactor A			Reactor B		
	*OLR 3	OLR 8	OLR 15	OLR 3	OLR 8	OLR 15
12	-	√	√	-	√	√
8.5	√	√	√	√	√	√
5.5	√	-	√	√	-	√
2.5	-	-	-	√	-	-

*OLR in $\text{gCOD}\cdot\text{l}^{-1}\cdot\text{d}^{-1}$

For polymerase chain reaction (PCR) amplification, the DNA was amplified using primers the v3–4 region of the 16S rRNA gene; B-341F (5'-CCTACGGGNGGCWGCAG) and B-805R (5'-GACTACNVGGGTATCTAAKCC) amplifying 465 base pairs (bp) for bacterial DNA, A-340F (CCCTAYGGGGYGCASCAG) and A-760R (GGACTACCSGGGTATCTAATCC) for archaeal DNA (Nordgård et al., 2017). Pair end sequencing was done by Macrogen Europe B.V, Maastricht (Netherlands), using the MiSeq™ platform. FLASH (fast length adjustment of short reads) software was used to assembly reading data by merging paired-end reads from next-generation sequencing experiments (Magoč and Salzberg, 2011). CD-HIT-OTU was utilized to preprocess and cluster the data with a three-step clustering to identify operational taxonomic units (OTU) and rDnaTools (Li et al., 2012). Details on the microbial community analysis methods are presented in Appendix (Paper II).

3.3 Anaerobic granulated biofilm system model for municipal wastewater treatment

This chapter presents the model used to predict the behavior of a granule biofilm representative of the UASB reactor described in Chapter 3.1 (and Paper I). Model implementation, simulation set up, and inputs are described herein. Additionally, scenario analyses were carried out to assess the effect of organic loading rates (OLRs) at 1, 3, 8, 10, 15, and 20 gCOD·l⁻¹·d⁻¹.

3.3.1 Model implementation

The two main model structures implemented are: biochemical and physico-chemical conversion processes as described in the Anaerobic Digestion Model No. 1 (ADM1) by Batstone et al. (2002) and diffusive mass-transfer model for granulated biomass (the biofilm compartment) based on Wanner and Gujer (1986). The biochemical conversions included a. disintegration of particulates to biopolymers

(polysaccharides, proteins, and lipids); b. hydrolysis of biopolymers to sugars, amino acids, and long-chain fatty acids (LCFA); c. acidogenesis from sugars and amino acids to volatile fatty acids (VFAs) and hydrogen; d. acetogenesis of LCFA and VFAs to acetate; and e. separate methanogenesis steps from acetate and hydrogen/CO₂ (Hulshoff Pol et al., 2004). The physico-chemical equations describe ion association and dissociation, and gas–liquid mass transfer. Inhibition kinetics have been integrated in relevant biochemical process. Detailed stoichiometric matrix and kinetic expressions used in the model are presented in Appendix 6.

The diffusion limited biogeochemical model was implemented in AQUASIM 2.1 (Reichert, 1994). The ADM1 conversions were implemented in the biofilm compartment using 20 vertical grid points evenly distributed over biofilm depth. The bulk liquid is modelled as a fully mixed reactor, with in- and out-flows and bulk liquid biochemical reaction equal to the biofilm matrix reactions. An additional mixed compartment was implemented to represent the gas phase, connected by a diffusive link to simulate the gaseous transfer of methane, carbon dioxide, and hydrogen. Figure 3.3 presents the schematic of biofilm implementation into ADM1.

Acid-base reactions in the ADM1 model can either be implemented as a combination of differential and algebraic sets of equations (DAE) or by time dependent differential equations (DE). The standard (commonly available) ADM1 simulators implemented for CSTR (using AQUASIM 2.1) use the DAE approach. However, the acid-base biofilm model is implemented by solving individual acids and conjugated bases separately, as dynamic state variables. All ionic species were implemented as differential variables and a pH model construction followed a step-by-step procedure based on Hofmann et al. (2008). Detailed equations used to calculate pH are given in Appendix 6.

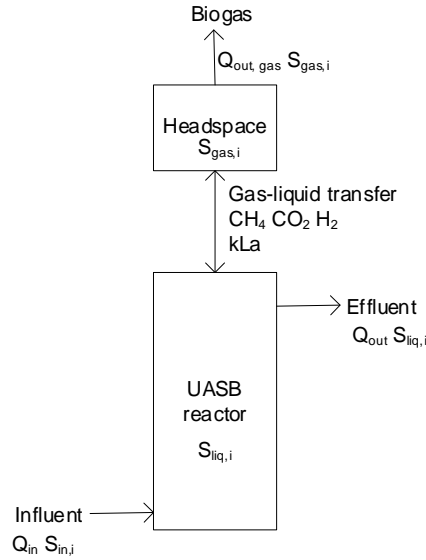


Figure 3.3 Schematic representation of anaerobic granulated biofilm implementation into ADM1

3.3.2 Simulation set-up

The simulated reactor model consisted of a liquid (0.8 l) and a gas phase (0.2 l), assumed to be completely mixed. The biofilm matrix corresponded to experimental data from this work and consisted of approximately 300 ml of granular sludge of assumed uniform spherical granules with a diameter of 2 mm. The number of granules ($n_{sp} \approx 21500$) was calculated based on the predefined total granule volume. Granules were assumed to have no diffusive solid transport (rigid biofilm matrix) and no suspended solids within biofilm matrix pores (pore volume contains only liquid phase). External mass transfer limitation was for simplicity reasons neglected (no diffusion limitations in the stagnant surface layer). Based on the above assumptions, this gave a biofilm surface area of 1.08 m^2 . Detachment of biomass (Equation 1) is based on the non-linear biofilm thickness dependency proposed by Stewart et al. (1996):

$$r_{det} = k_{det} \cdot L_f^2 \quad \text{Equation 1}$$

where k_{det} is an empirical detachment coefficient, (here: $0.024 \text{ kg}\cdot\text{m}^{-2}\cdot\text{d}^{-1}$), and L_f is the program variable representing biofilm thickness (m). Biomass density within the granules was set at $180 \text{ kgCOD}\cdot\text{m}^{-3}$, a typical anaerobic granules density based on Batstone and Keller (2001). Details on other parameters used in the biofilm model in the UASB reactor is presented in Appendix 6.

Initial conditions were defined for the biofilm matrix and the bulk liquid volume. All modelled microorganisms were considered to have equal initial bulk phase concentrations of 0.05% v/v ($9 \text{ kgCOD}\cdot\text{m}^{-3}$) equal to the biomass fractions in the biofilm matrix. The initial biofilm thickness was set at 0.03 mm and bulk phase initial biomass, initial VFAs and pH was chosen at $10^{-5} \text{ kgCOD}\cdot\text{m}^{-3}$, $10^{-6} \text{ kgCOD}\cdot\text{m}^{-3}$ and $10^{-7} \text{ kmol}\cdot\text{m}^{-3}$, respectively. Approximate steady-state pore and bulk liquid concentrations were used as initial state variables. The simulations were operated through out 600 days at 25 °C.

3.3.3 Inputs

The COD influent to the UASB reactor is defined in the model as presented in Table 3.2 and assumed to be primarily polysaccharides, proteins, and fats, taking into consideration that IVAR Grørdaland wastewater treatment plant receives wastewater from food, animal, and dairy industries as described in Chapter 3.1. A feed bicarbonate alkalinity of 0.01 M and inorganic nitrogen of 0.007 M were used which were in line with analysis of the wastewater applied in the UASB laboratory experiment.

Table 3.2 COD input used for simulations of anaerobic granulated biofilm

Variable	Description	Fraction	Value	Unit
input_S_aa_in	Input amino acid	0.002	0.003	$\text{kgCOD}\cdot\text{m}^{-3}$
input_S_ac_in	Input acetic acid	0.08	0.1	$\text{kgCOD}\cdot\text{m}^{-3}$
input_S_bu_in	Input butyrate	0.08	0.1	$\text{kgCOD}\cdot\text{m}^{-3}$
input_S_pro_in	Input propionate	0.08	0.1	$\text{kgCOD}\cdot\text{m}^{-3}$

Table 3.2 COD input used for simulations of anaerobic granulated biofilm (continued)

Variable	Description	Fraction	Value	Unit
input_S_va_in	Input valerate	0.08	0.1	kgCOD·m ⁻³
input_S_fa_in	Input LCFA	0.14	0.175	kgCOD·m ⁻³
input_S_su_in	Input sugar	0.1	0.075	kgCOD·m ⁻³
input_X_ch_in	Input carbohydrate	0.1	0.125	kgCOD·m ⁻³
input_S_I_in	Input soluble inert	0.07	0.088	kgCOD·m ⁻³
input_X_pr_in	Input protein	0.1	0.15	kgCOD·m ⁻³
input_X_li_in	Input lipid	0.1	0.15	kgCOD·m ⁻³
input_X_I_in	Input particulate inert	0.06	0.075	kgCOD·m ⁻³
input_X_c_in	Input composite/complex	0.005	0.006	kgCOD·m ⁻³
Input_COD_t	Input total COD	1.00	1.26	kgCOD·m⁻³

3.4 Methanotrophics-photogranules experiment for dissolved methane removal

This experiment was carried out at INRAE LBE (Narbonne, France). The possibility of using an aggregated granular biomass engineered to contain a cyanobacterial-methanotrophic community for the aeration-free removal of dissolved methane was investigated, as post-treatment for UASB effluents. The conversion relied on syntrophic interactions between wastewater isolates of phototrophic cyanobacteria and methanotrophic bacteria that aggregated into oxygenic photogranules.

Initially, methanotrophs were enriched under batch conditions from municipal activated sludge from the local wastewater treatment plant in Narbonne. After harvesting the enriched suspended methanotrophic cultures, it was transferred to new batch systems containing fresh media and oxygenic photogranules from a sequencing batch photobioreactor treating synthetic wastewater. The oxygenic photogranules development, sequencing batch photobioreactor configuration, and experimental set-up are described in more detail in Milferstedt et al. (2017). After one week, the active methanotrophic photogranules were separated from the suspended biomass and rinsed. Only the solid

methanotrophic photogranule biomass was used to inoculate the continuous reactor. Further details on methanotroph enrichment methods are presented in Safitri et al. (2021) (Paper III).

Figure 3.4 shows a schematic view of the continuous reactor set-up. Methanotrophic photogranules were transferred to a continuous reactor with 1.8 l of liquid volume and mixed by 100 rpm during the first 30 days of reactor operation, increased to 125 - 128 rpm on day 31 for the remainder of the experiment. The illuminated light intensity was approximately $45 \mu\text{mol}\cdot\text{m}^{-2}\cdot\text{s}^{-1}$ photosynthetically active radiation (PAR). The reactor was operated at an average room temperature of $23.2\pm 1.0 \text{ }^\circ\text{C}$ (\pm standard deviation) without active temperature control.

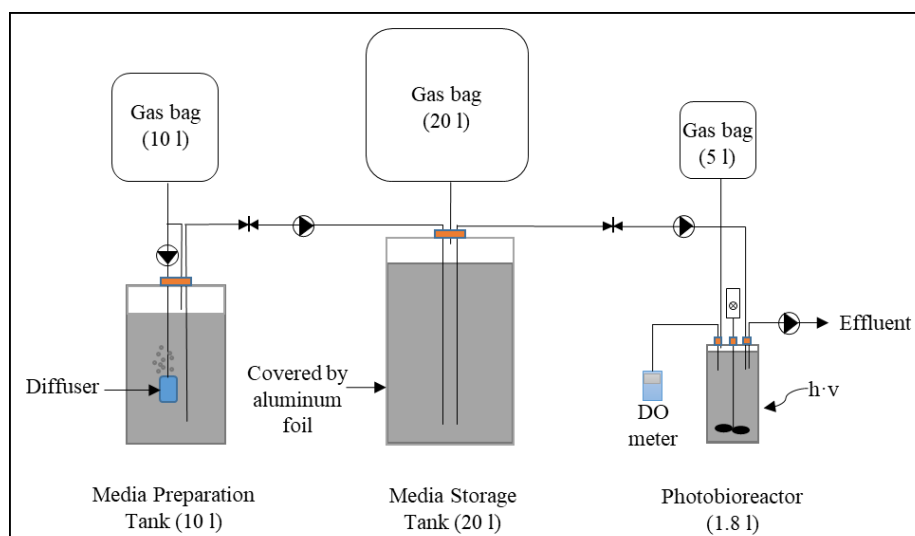


Figure 3.4 Presentation of the continuous reactor set-up. The gas bag connected to the media preparation tank was used as methane reservoir during the preparation of methane-saturated batches of media. The finished media batches were transferred to the media storage tank, from where it was continuously pumped into the reactor. The gas bag connected to media storage equilibrated pressure changes resulting from filling and emptying the tank. The gas bag connected to the reactor equilibrated potential pressure changes in the reactor (Paper III).

The reactor was operated at a hydraulic retention time of 12 h. The media contained on average $17.6 \pm 2.2 \text{ mgCH}_4 \cdot \text{l}^{-1}$, and the volumetric organic loading rate was approximately $35.1 \pm 4.5 \text{ mgCH}_4 \cdot \text{l}^{-1} \cdot \text{d}^{-1}$. COD, TSS, total number of photogranules, and the overall observed biomass yield were determined to evaluate reactor performance. In addition, size-specific metabolic activity was determined in batch experiments. The media composition for the batch experiments (i.e., enrichment and size-specific analysis) and the continuously operated reactor were identical; A modified nitrate mineral salt (NMS). Microbial community analysis of methanotrophs-photogranules was performed to evaluate community stability and document the heterotrophic-phototrophic co-culture. Details on growth conditions and microbial community analysis are described in Safitri et al. (2021) (Paper III).

3.5 Quantification method and screening of microalgae growth potential on secondary wastewater effluent

This experiment aimed at identifying microalgal strains that are able to efficiently grow in the UASB specific secondary wastewater effluent and investigate nutrients and residual soluble chemical oxygen demand (COD) removal. Part of this work also included establishment and evaluation of different microalgal quantification technologies as drawbacks have been linked to many commonly used methods (Griffiths et al., 2011; Peniuk et al., 2016). The methods tested included flow cytometer, optical density (OD) measurement, counting chambers and microplate-based fluorescence method. All methods were tested and compared to identify the most efficient microalgal growth quantification technique using independent methodological confirmation.





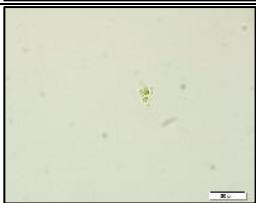
3.5.1 Microalgal strains

The following microalgal species; *Chlorella vulgaris*, *Chlorella sorokiniana*, *Tetrademus obliquus* (synonym: *Scenedesmus obliquus*), *Haematococcus pluvialis*, and *Microchloropsis salina* (synonym:

General Methodology

Nannochloropsis salina) were selected for this study based on a literature review, focusing on their suitability to remove nutrient in wastewater and potential for microalgal biomass product recovery. Characteristics for selected microalgal strains are described in Table 3.3.

Table 3.3 Characteristics of selected microalgal strains for wastewater treatment

Microalgae strain	Growth rate (d ⁻¹)	Composition ^a (%)	Morphology ^b	Average diameter (µm)	References
<i>C. vulgaris</i>	1.61	P: 24-58 L: 5-58 C:12-55		2-5	(Safi et al., 2014; Yeh et al., 2010)
<i>T. obliquus</i>	1.13	P: 50-56 L: 12-14 C:10-17		5-10	(Becker, 2007; Martínez et al., 1999)
<i>C. sorokiniana</i>	4.32	P: 37.7 L: 20.9 C: 27.5		3	(Janssen et al., 1999; Kumar et al., 2014; Xu et al., 2013)
<i>H. pluvialis</i>	0.72	P: 21.1 L: 22.2 C: 38.0		4-50	(Boussiba & Vonshak, 1991; Katsuda et al., 2006; Kim et al., 2015)
<i>M. Salina</i>	1.30	P: 17.8 L: 16.9 C: 8.9		2.5	(Coustets et al., 2013; van Wagenen et al., 2012; Volkman et al., 1993)

^aP: Protein; L: Lipid; C: Carbohydrates

^bImages were taken by the author using microscope (Olympus BX61, Japan)

Freshwater microalgal suspension, *C. vulgaris* (CCAP 211/11B), *T. obliquus* (CCAP 276/3A), *H. pluvialis* (CCAP 34/7), *C. sorokiniana* (CCAP 211/8K), and marine microalgae in agar, *M. salina* (CCAP 849/3) were obtained from the Culture Collection of Algae and Protozoa (CCAP) in Scotland. Before testing in filtered UASB secondary effluent, the freshwater and marine species were cultivated and maintained initially in MWC+Se (Guillard & Lorenzen, 1972) and L1 (Davis et al., 2015) growth media, respectively. Details on MWC+Se, L1 media recipes, and pre-culturing methods are presented in Appendix 4A.

3.5.2 Microalgal quantification methods

Four methods, flow cytometry, OD measurements, direct counting, and microplate-based methods, were investigated and compared for quantification of microalgal cell concentration. All methods were calibrated and cross-validated against cultured microalgal cell concentration.

- Flow cytometry

Flow cytometric cell counting was performed on a BD Accuri C6 flow cytometer (BD Biosciences, USA) to provide absolute cell counts (analyzed sample volume was quantified). The Accuri C6 contains two lasers of 488 and 640 nm and four signal detectors of 533 nm (FL1), 585 nm (FL2), 670 nm (FL3) and 675 nm (FL4). Size beads were used for calibration of cell size determination by the forward scatter. Twice a day, 1.0 ml of microalgal suspension was added to sample vials and vortexed quickly to homogenize the sample before analysis on the flow cytometer. All samples were run using a flow rate of $14 \mu\text{l}\cdot\text{min}^{-1}$ with a $10 \mu\text{m}$ core size. As the C6 quantitatively measured the sample volume analyzed, cell concentration was determined directly from the BD Accuri C6 Plus software (BD Biosciences, USA).

General Methodology

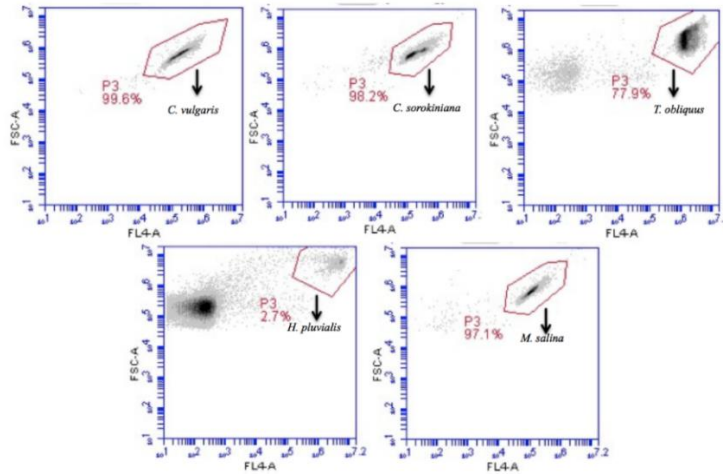


Figure 3.5 Method developed for distinguishing selected microalgae from background noise and debris using the forward scatter trigger and the fluorescence trigger FL4 (675 nm) on Flow Cytometer BD Accuri C6.

All five microalgal species showed a high fluorescence on detector FL4 (red fluorescence 675 nm), the signature emission wavelength of Chlorophyll A. By using the size of the microalgae, combined with fluorescence, microalgae were easily distinguished from background noise and other particles such as bacteria and debris by combined gating on forward scatter and FL4, as illustrated in Figure 3.5.

- Optical density (OD) measurement

OD measurement of microalgal cells growing in MWC+Se and L1 media was used to establish a relationship between absorbance and the number of cells in the culture. One ml of homogenized microalgal cell suspension from the microalgal batch cultures were added to disposable UV cuvettes and quantified twice a day by absorbance at 750 nm (UV-1600PC, VWR International AS, Norway).

- Microplate-based method

A procedure was developed based on previously suggested assay by van Wagenen et al. (2014). Two ml of homogenized microalgal cell

suspension was added to a transparent wall and clear bottomed Corning® Costar® TC-treated 24-well plate (Sigma Aldrich, Germany). Microplates were incubated in a shaker at 18 - 20 °C, mixed at 150 rpm and illuminated at a light intensity of 100 - 135 $\mu\text{mol}\cdot\text{m}^{-2}\cdot\text{s}^{-1}$ part of a light/dark regime of 16/8 hours. PAR was measured at the top of the microplate using the light meter LI-250A (LI-COR, USA). The microplates were read 2 - 4 times a day using Tecan Infinite F200 PRO microplate reader (Tecan, Switzerland), and growth was determined by measuring fluorescence intensity at 430/690 nm.

- Direct counting method

The Improved Neubauer counting chamber (Improved Neubauer, 0.100 mm depth, 0.0025 mm², Germany) was used for direct cell counting. A glass coverslip was added to the chamber's central area after a homogenous microalgal suspension was pipetted into the counting chamber. Dense cultures were diluted with distilled water prior to analysis. The sample was enumerated manually bright field microscopy (VisiScope series 200, VWR international AS, Norway), with a 40x objective. After each sample, the counting chamber and coverslip were carefully cleaned with 70% ethanol and wiped dry using lens paper.

3.6 Screening of microalgae growth potential on UASB secondary wastewater effluent in a batch system

Membrane filtered UASB secondary effluent was evaluated for microalgal growth potential. Details on the UASB reactor system and operation is presented in Appendix (Paper I). Following the UASB system, a ceramic membrane filtration system with a nominal pore size of 100 nm (tight-micro filtration, T-MF) manufactured by Atech (Neu-Ulm, Germany) was evaluated for particulate and microbial removal potential. The membrane system was designed and operated by Postdocs, Ali Farsi and Remya R. Nair. Permeate was collected in sterile bottles and directly used for microalgal cultivation without any amendments.

Cultivation procedure was as follows: 100 ml secondary effluent wastewater, including microalgae strain inoculum (approximately 50 - 100 cell·ml⁻¹), was transferred to a 250 ml of Erlenmeyer flasks (VWR International AS, Norway) with four-five replications. The Erlenmeyer flasks were incubated at 20 °C and 150 rpm in a shaking incubator (Innova S44i Eppendorf, Germany) equipped with fluorescent light providing photoactive radiation (PAR) at approximately 80 - 120 μmol·m⁻²·s⁻¹ in a light/dark regime of 16/8 hours. PAR was measured inside the empty flasks and on the outside by a hand-held light meter LI-250A (LI-COR, USA). Blank samples constituted microalgae inoculum and deionized water in Erlenmeyer and microplate covered with aluminum foil. *C. vulgaris*, *C. sorokiniana*, *T. obliquus*, *M. Salina*, and *H. pluvialis* were cultivated in wastewater over 9 - 14 days for determination of nutrient removal potential. Growth was quantified, as described in Chapter 3.5.2.

The ability of microalgae to provide tertiary treatment of filtered UASB secondary effluent was evaluated by measuring removal of COD, phosphate, total phosphorous, nitrite, nitrate, ammonium, total nitrogen, and alkalinity under cultivation. Production of total suspended solid (TSS) was measured as an indicator of microalgal biomass productivity. Spectroquant® test kits (Merck, Germany) were used for quantification of COD (kit no: 109773, measuring range: 100 - 1500 mg·l⁻¹), phosphate and total phosphorous (kit no: 114729, measuring range: 0.5 - 25.0 mg·l⁻¹ PO₄-P), nitrite (kit no: 114547, measuring range: 0.010 - 0.700 mg·l⁻¹ NO₂-N), nitrate (kit no: 114563, measuring range: 0.5 - 25.0 mg·l⁻¹ NO₃-N), ammonium (kit no: 114544, measuring range: 0.5 - 16.0 mg·l⁻¹ NH₄-N), total nitrogen (kit no: 11473, measuring range: 10 - 150 mg·l⁻¹ N) according to the manufacturer's instructions. TSS was analyzed by standard methods 2540D (Rice et al., 2013). Production of TSS was compared to a negative control for indication of microalgal biomass production.

Dissolved COD, ammonium, nitrate, phosphate, and TSS was determined by filtration through a GF/C glass microfiber filter (Whatman, UK). Conductivity was measured using a WTW Multi340i, equipped with a conductivity probe (WTW Tetra Con® 325, Geotech Environmental Equipment, Inc., USA). This parameter was needed for analytical determination of alkalinity and VFA concentration which were titrimetrically determined using a TitroLine® 5000 titrator (SI Analytics, Germany) following the five-pH point titration method (Moosbrugger et al., 1993). Total VFA and alkalinity were calculated concomitantly using the TITRA5 software (brouckae@ukzn.ac.za). Samples were taken in duplicates for each measurement.

3.7 Nutrient-limited kinetic growth analysis of *Chlorella sorokiniana* in microplate well

Based on the microalgal screening, *C. sorokiniana* showed high viability for growth on the membrane filtered UASB secondary effluent and a high ability to remove nutrients in the batch system. This experiment aimed to determine the cell growth kinetic characteristics of *C. sorokiniana* in a nutrient-limited media using a microplate reader calibrated as described in section 3.5.2. MWC+Se media was again used as a basic media in which the concentration of the phosphate and ammonium were varied (Table 3.4). *C. sorokiniana* cultures (100 µl) were transferred to fresh media in a 96 sterilized clear wall microplate (Corning® Costar® TC-treated, Sigma Aldrich, Germany). It was then covered with sterile gas permeable membrane and incubated at 20 - 25 °C at 100 rpm in the same incubator (Innova S44i Eppendorf, Germany) and photoactive radiation (PAR) at approximately $135 \mu\text{mol}\cdot\text{m}^{-2}\cdot\text{s}^{-1}$ with a light/dark regime of 16/8 hours. Blank samples were used by adding microalgal cultures and deionized water. Five replications of each concentration were made to reduce variability in experimental results, increasing statistical significance and data confidence level. The cultures were allowed to grow approximately 140 hours through their exponential

General Methodology

period. Cell quantification using fluorescent reads on a Tecan Infinite F200 PRO microplate reader (Tecan, Switzerland) set at 430/690 nm were made at intervals of two hours or more, between 2 - 4 times per day. Regression analysis of the linearized multiple Monod growth model was used to determine kinetic constants (Kumar et al., 2014). Statistical analysis was done using SigmaPlot V14.0 for Windows (SyStat Inc., USA).

Table 3.4 Experimental scenarios on kinetics of nutrient-limited growth analysis. Five replications were used for each concentration

Phosphate Limited Experiment		Ammonium Limited Experiment		Blank	
PO ₄ -P (mg·l ⁻¹)	NH ₄ -N (mg·l ⁻¹)	PO ₄ -P (mg·l ⁻¹)	NH ₄ -N (mg·l ⁻¹)	PO ₄ -P (mg·l ⁻¹)	NH ₄ -N (mg·l ⁻¹)
0			0		
0.5			1		
1			5		
2			10		
5	100	50	20	0	0
10			30		
20			50		
30			80		

Specific growth rate was calculated from Equation 2 (Madigan et al., 2009).

$$\mu = \frac{\ln N_2 - \ln N_1}{t_2 - t_1} \quad \text{Equation 2}$$

where, $t_2 - t_1$ (t_d) is the doubling time. Minimum doubling time t_d (min) was calculated by replacing μ by μ_{max} . The linearized Monod equation, equivalent to the Lineweaver-Burk equation (Equation 3) (Kumar et al., 2014).

$$\frac{1}{\mu} = \frac{1}{\mu_{max}} + \frac{K}{\mu_{max}} \cdot \frac{1}{(\text{nutrient})} \quad \text{Equation 3}$$

3.8 Evaluation of selected microalgae strain for nutrient removal in a continuous photobioreactor (PBR) system

In this study, *C. sorokiniana* was chosen for further examination of growth in a continuous photobioreactor (PBR) system. Approximately $6 \cdot 10^3$ cell·ml⁻¹ of *C. sorokiniana* strains were transferred to a 550 ml borosilicate flask PBR (Phenometrics 101 PBR, Algae Metrics, US) operated in continuous mode. The reactor system was semi-automated, with programmable control of lighting (including diurnal cycles), heating, and agitation (via magnetic stir bar). Temperature and stirring were set at 15 °C and 150 rpm, respectively. Bubbling with air was applied to enhance mixing and transfer additional CO₂. PBR was equipped with top-mounted fluorescent light bulbs providing photoactive radiation (PAR) set at approximately 179 $\mu\text{mol}\cdot\text{m}^{-2}\cdot\text{s}^{-1}$.

Figure 3.6 shows a schematic view of the PBR set-up, which was operated for a period of 109 days. Hydraulic retention time (HRT) started at 2.25 days and then increased to 5.5 days at day 90. Organic, nitrogen and phosphorous loading rates applied were 0.4 ± 0.2 gCOD·l⁻¹·d⁻¹, 145 ± 24 gN·l⁻¹·d⁻¹, and 14 ± 4 gP·l⁻¹·d⁻¹, respectively, giving an N/P ratio slightly above the Redfield ratio of 10 ± 2 g·g⁻¹ (equivalent to approximately 22 molN·molP⁻¹). The wastewater fed the PBR was similar to the batch test system set-up, however, the effluent compositions were not identical as the experiments were not conducted simultaneously. Nutrients (TP, TN, phosphate, nitrite, nitrate, and ammonium), COD, pH, alkalinity, TSS were measured before and after microalgal treatment, using analytical method as described in Chapter 3.6. The microalgal cultures were regularly examined and checked for cell viability by microscopy.

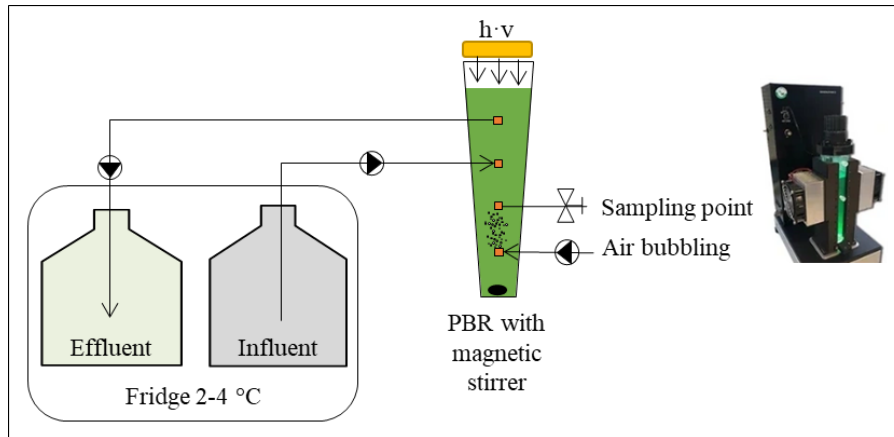


Figure 3.6 Presentation of continuous PBR set-up, equipped with programmable control of lighting (including diurnal cycles), heating, and agitation

3.9 Pathogen analysis

One of the primary concepts of the overall project is to reuse water. Hence, pathogen removal from the effluent is also essential. In this study, pathogen analysis was conducted to assess the combined UASB-membrane system for pathogenic bacteria removal, limited to total coliforms and *E. coli*. The viable count method was used for enumeration of pathogens, and pathogen reduction was limited to a single study (due to time limitations) and only indicates the hygienic barrier potential of the UASB-membrane system. Detail methods of pathogen analysis are described in Appendix 5.

4 Main Results and Discussions

In this chapter, the research results leading up to the three appended papers/manuscripts are summarized. Some unpublished results are also reported and discussed in this chapter: The presentation of an anaerobic granulated biofilm system model (Chapter 4.3) and microalgal-based treatment for nutrient removal (Chapter 4.5).

4.1 UASB system for municipal wastewater treatment at low-temperatures

This study has shown that efficient municipal wastewater treatment was achieved in long term UASB reactors operated at temperatures of 25 down to 12 °C and OLR up to $15.2 \pm 0.2 \text{ gCOD} \cdot \text{l}^{-1} \cdot \text{d}^{-1}$ (\pm standard error). Besides, the remarkable operation of the long-term treatment UASB reactors at 8.5, 5.5, 2.5 °C serves to confirm the feasibility of this treatment at low-temperatures and high organic loading, not only for degrading the organic carbon but also for a positive energy balance potential achieving sustainable wastewater treatment. Detailed results and discussions on UASB system for municipal wastewater treatment at low-temperatures are presented in the appendix (Paper I).

In this study, the two parallel UASB reactors (reactor A and B), operated continuously with the same operational conditions. Based on statistical analysis (student t-test at 95% confidence level) the two reactors demonstrated no significant difference in terms of transient response times, COD removal efficiency, methane fraction in biogas, methane production, COD balance, and nutrient variability.

Biomass retention is critically important for successful high-rate anaerobic bioreactors operation at low-temperatures (Lettinga et al., 2001). There was a significant difference in retention of granules at 5.5 °C. In reactor A, severe granule washout occurred as the sludge bed floated, presumably due to gas entrapment at high OLR and subsequent

high biogas production. This resulted in diminishing gas production and loss of COD removal capacity, and reactor A loading was stopped on day 738. Sludge bed expansion also occurred at higher temperatures, but this was counteracted by variable recirculation flow and mechanical wall tapping. Different granule sizes could explain the difference in reactor sludge behavior. Granule size was observed during the experiment and larger granules were initially applied in reactor B by roughly 2 - 3 mm of diameter compared to 1 - 2 mm of diameter in reactor A, likely due to fractionation during transport and storage. A distinct decrease in the granule diameter was observed during operation of reactors, whereby the average granule size reduced from approximately 3 to 1 - 2 mm in reactor B. In reactor A, granules became even smaller constituting fine particles by approximately 0.5 mm of granules size towards the end of the period. In reactor B, even though granules expanded several times, granules could be still retained and wash out was prevented.

Wu et al. (2016) and Owusu-Agyeman et al. (2019) has observed large granules (3 - 3.5 mm) and claim higher mass transfer due to their internal structure, including big pore size, high porosity and short diffusion distance compared to medium and small granules. Small granules (<1 mm) appeared to be weaker and more easily washed-out from the system (Wu et al., 2016; Owusu-Agyeman et al., 2019). Moreover, Singh et al. (2019) investigated UASB reactor operation treating dairy wastewater at 20 °C and found that LCFA-containing feed stimulated granule flotation and wash out from the reactors due to LCFA-encapsulated granular sludge (Singh et al., 2019). This could also explain the frequent granule expansion in the system as parts of the wastewater inlet at IVAR Grødaland originates from a dairy and a slaughterhouse.

UASB reactor performance was analyzed and evaluated by investigating two main parameters: COD removal and methane production. From Figure 4.1, the rapid transient times (the adaptation time of the system until steady-state) of 5, 9, and 14 days at temperatures 25, 16, and 12 °C, respectively, indicated that the granules adapted quickly to decreased

operating temperatures, adaptations that would not require community structure changes.

The ability of the UASB system to recover rapidly from temperature and loading shock perturbations demonstrates the robustness of the system, which is an important consideration for pilot- and even full-scale applications. At lower temperatures (8.5, 5.5, and 2.5 °C), more extended periods (up to 68 days) were required to adapt and achieve new steady-states. Furthermore, during 8.5, 5.5, and 2.5 °C operation, lower inlet COD concentration at high OLRs effectively reduced the liquid HRT and consequently the COD removal efficiency. Decreasing HRT leads to insufficient contact time of wastewater with the granules and less organic matter utilized (Zhang et al., 2015).

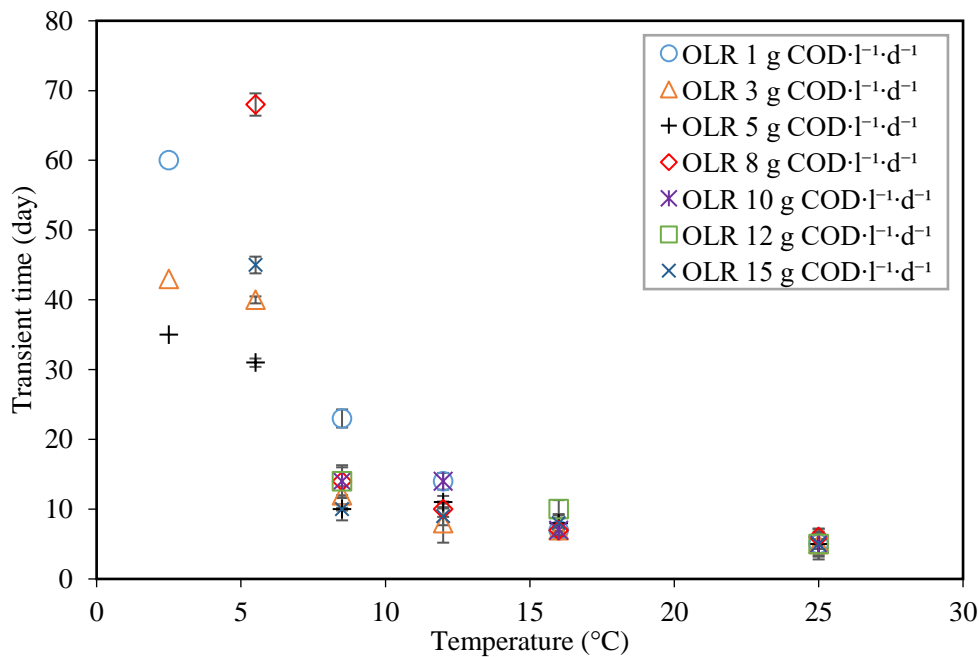


Figure 4.1 Averaged transient time to steady-state conditions at different temperatures and OLRs in reactor A and B. The student *t*-test revealed no significant difference ($p > 0.05$) between reactor A and B transient times (Paper I).

In addition, washout of fermentation intermediates increases. Therefore, the effluent COD temporarily increased during the first days after increasing the OLR. During this acclimatization period, VFA accumulation and reduced alkalinity were also observed, especially at low-temperatures and when applying higher OLRs ($>8.0 \text{ gCOD}\cdot\text{l}^{-1}\cdot\text{d}^{-1}$) (Paper I). This was temporarily augmented by dosing of additional buffer (e.g., NaHCO_3) to assure process stability during transitions. Upon controlled buffering, the effluent COD and VFA accumulation started decreasing until a new steady-state condition was achieved. Steady state COD removal efficiencies in excess of 50 - 60 % could be maintained at 25 - 12 °C for all operating OLRs, and at 8.5 °C up to an OLR of $8.0 \text{ gCOD}\cdot\text{l}^{-1}\cdot\text{d}^{-1}$ (Figure 4.2).

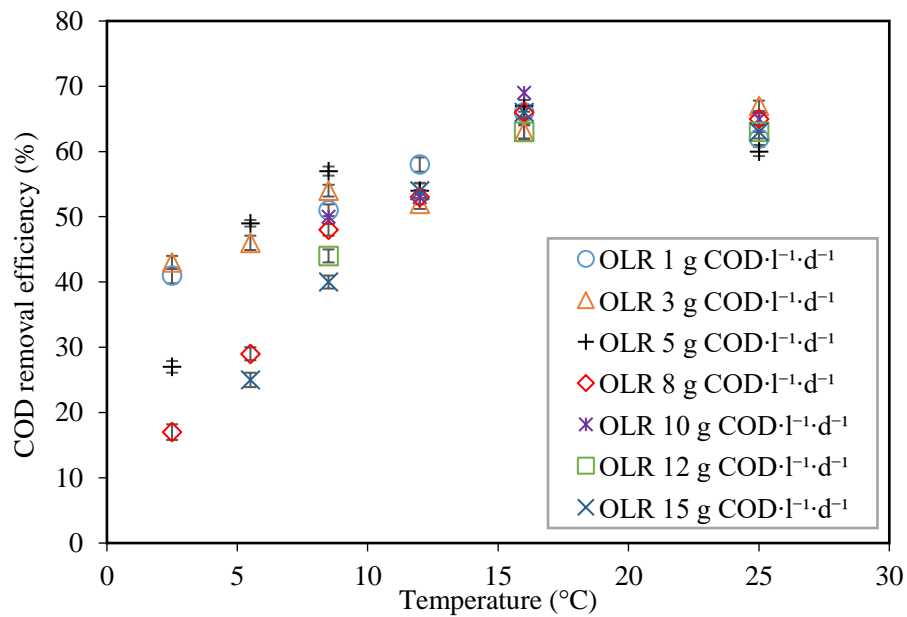


Figure 4.2 Dissolved COD removal efficiencies at steady-state under different temperatures and OLRs. Error bars represent standard errors from measurements taken during steady-state conditions in reactor A and B. The student *t*-test revealed no significant difference ($p>0.05$) between reactor A and B COD removal efficiencies (Paper I)

At steady-state conditions, alkalinity and VFA were stable in both reactors, and external buffering not necessary. Gradual increments in OLRs and recirculation did not destabilize reactors. However, at low-temperatures (<8.5 °C) and high OLRs, above 12 gCOD·l⁻¹·d⁻¹, VFA accumulation, decreasing alkalinity and reduced COD removal efficiencies (below 30%) were observed more frequently (Paper I), indicating the reactors to be close to become overloaded. This is comparable to the result by Dague et al. (1998), whereby lower temperatures resulted in reduced rates of substrate removal when treating synthetic wastewater at 5 - 25 °C (Dague et al., 1998). Similar findings have also been reported by Mahmoud et al. (2004) and Bandara et al. (2012) using UASB reactors treating real municipal wastewater at lower temperatures over a shorter periods (<400 days) and relatively low OLR <3 gCOD·l⁻¹·d⁻¹. Using a single stage UASB, the COD removal efficiencies were 44% at 15 °C (Mahmoud et al., 2004) and 40% during wintertime at 6 °C (Bandara et al., 2012). Contrary to these and more concurrent with this present result, a long-term anaerobic granular sludge reactor operation (1243 days) at 4 - 15 °C and OLR up to 10 gCOD·l⁻¹·d⁻¹ demonstrated >80% COD removal efficiencies with VFA-based synthetic wastewater (McKeown et al., 2009). The apparent contradictory results may be due to the different substrates used as VFA-based wastewater is more easily degradable than real municipal wastewater, suggesting hydrolysis or fermentations could be rate-limiting. Petropoulos et al. (2017) investigated the intrinsic capacity of cold-adapted communities to treat domestic wastewater at 4, 8, and 15 °C in batch systems and showed hydrolysis/fermentation to be a limiting step at low-temperature and was twice as temperature sensitive as methanogenesis, Q₁₀ values were 4.62 and 1.57 respectively (Petropoulos et al., 2017).

UASB reactor performance may also be evaluated by methane production. At each temperature, methane production rates increased with the increasing OLR, and directly proportional to the amount of

organic matter removed in the UASB reactors. Despite significantly decreased methane production under low-temperatures (5.5 and 2.5 °C), at 25, 16, 12, and 8.5 °C methane production rates were comparable for all OLRs, indicating that the reduction in operating temperature did not negatively affect methane production (Figure 4.3a and b). These findings are important for application of anaerobic municipal wastewater treatment at low-temperatures as it suggests that anaerobic granules are capable to adapt to low-temperatures and maintain system performances (COD removal and methane production) over long-term operation. The results also show the produced biogas to contain an average methane fraction above 70% (v/v), and more than 80% of COD removed was converted to methane (Figure 4.3c and d). The overall mean COD balance closure were above 90% for both UASB reactors at all operating temperature and OLRs (Paper I). Analytical uncertainty, random gas leakages, and the inaccuracy of the gas counter at low gas flow rates are possible explanations of the minor discrepancies. Henze et al. (2008) concluded that fat or LCFA-containing substrates resulting in very high COD removal efficiencies but low CH₄ production rates lead to considerable COD balance gaps (Henze et al., 2008). Singh et al. (2019; 2020) found this to be explained by lipid and/or LCFA accumulation in the granules which also associated with granules flotation and wash out. Another reason could be particulate entrapment or accumulation of COD in the sludge blanket by proteins and/or other macromolecules (Zhang et al., 2018). The COD balance gaps by around 3 - 10% in this study may therefore be the result of the high fat and protein content in the wastewater applied herein.

Main Results and Discussions

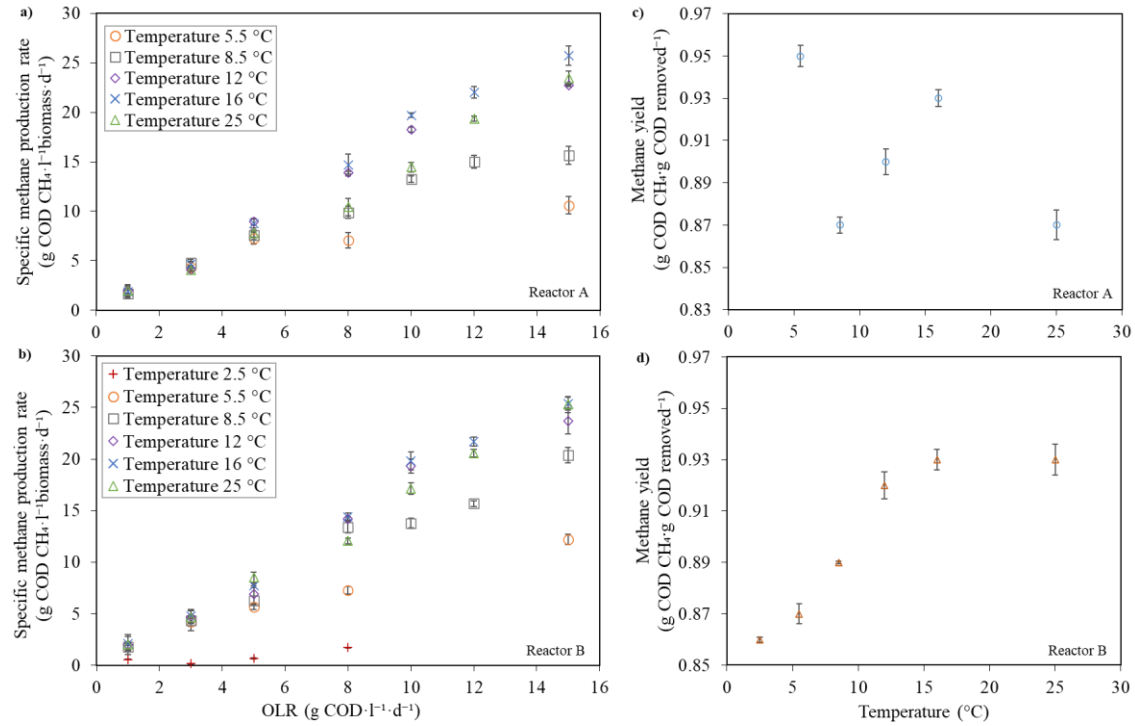


Figure 4.3 Specific methane production rate per volume biomass (a and b) and overall COD specific methane yield (c and d) at steady-state conditions in reactor A and B. Error bars represent standard errors from measurements taken during steady-state conditions.

Another frequently cited cause for a COD gap at low-temperatures is a significant amount of dissolved methane escaping through the liquid effluent. The equilibrium dissolved methane was compensated using the appropriate Henry's coefficient. However, Souza et al. (2011) and Wu et al. (2017) found that dissolved methane was supersaturated in the liquid phase of an anaerobic bioreactor effluent (saturation factor of 1.03 - 1.67), increasing with the increased methane solubility at decreasing temperatures, and the missing COD could putatively be explained by this.

Besides organic conversion and methane production, nutrient (N and P) availability in the anaerobic reactors is important to assure bioreactor performance, and potential removal is of interest. The UASB reactors removed mainly particulate nutrients, in the literature explained by sedimentation and granule entrapment (Elmitwalli and Otterpohl, 2011). Additionally, some nutrients were assimilated during microbial growth. Although the UASB reactors removed total nitrogen and phosphorous in the range of 10 - 33% and 4 - 20 %, respectively, the reactors displayed limited removal of dissolved nutrients, especially ammonium (Paper I). In fact, negative ammonium removal was common which must be the result of ammonification during fermentation of small amine containing organic molecules (such as, amino acids, amino sugars, urea, and nucleotides).

Low-temperature anaerobic bioreactor operation offers economic benefits, especially for high latitude countries due to reduced heating requirements and sustained bioenergy production potential. Despite stable and robust reactor performance at low-temperatures demonstrated in this study, a significant fraction of organic matter remained in the effluent. Furthermore, the methane loss by the liquid effluent could also offset the positive effect of low carbon footprint from anaerobic wastewater treatment (Liu et al., 2014). Moreover, this study also demonstrated that the UASB system had limited potential for nutrient

removal. In full-scale applications, post-treatments are required to remove residual COD, dissolved methane, and nutrients.

In conclusion (with respect to research question, RQ1), significant COD removal and methane production at low-temperatures could be maintained, even down to 2.5 °C. In combination with suitable post-treatment, granulated anaerobic biomass unit processes offer a viable secondary treatment option for municipal wastewater achieving energy recovery and lower carbon footprint wastewater treatment at low-temperatures.

4.2 Microbial community analysis on psychrophilic granules of UASB system

The feasibility of long-term anaerobic bioreactor operation using UASB system treating municipal wastewater has been demonstrated in psychrophilic condition down to 2.5 °C (Paper I). Stable long-term UASB performance suggests development of well-balanced and stable community interactions in the granules, and psychrophilic community adaptation is a putative explanation for the observed low-temperature process performance observed. Hence, microbial community characterization of the low-temperature loading gradients were pursued in order to test this hypothesis (RQ2).

Microbial community analysis using MiSeq amplicon sequencing produced high quality data by on average more than 89% coverage, representing the percentage of sample sequences aligned to a deposited sequence in National Center for Biotechnology Information (NCBI) gen bank. Based on sequencing data (weighted unfrac), the overall similarity of the communities between samples are shown in a split matrix (Paper II, Table S1). Results showed that granule samples had no significant common features between the two samples within UASB granules; the similarity index was in the range 0.50 - 0.71.

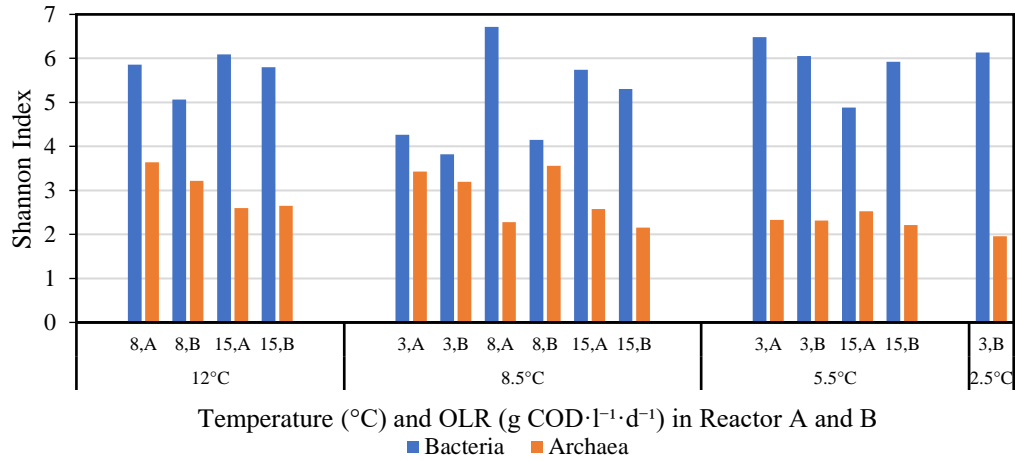


Figure 4.4 Bacterial and archaeal diversity statistics based on Shannon Index in UASB granules at different operating temperatures and OLRs. A and B on the x-axis represent two parallel reactors, A and B. Numbers beside A and B represent OLR in $\text{g COD}\cdot\text{l}^{-1}\cdot\text{d}^{-1}$ (Paper II).

Figure 4.4 shows the bacterial and archaeal Shannon diversity index under different temperatures and OLRs. For the archaeal communities, the Shannon index was reduced at lower temperatures (2.5 and 5.5 °C), indicative of a less diverse and specialized community. Higher OLR also resulted in a decrease of archaeal diversity. The lower community diversities probably resulted from long-term acclimation that could be selective for specific microorganisms and caused a significant change in the microbial community in the reactor. However, there is no trend within bacterial community diversity. Based on statistical analysis (student t-test at 95% confidence level) the two reactors demonstrated no significant difference in terms of bacterial and archaeal community diversity at the different temperatures and loadings ($p>0.05$).

4.2.1 Composition shift of bacterial community

Microbial community analysis resulted in an average of 257917 ± 26324 reads (\pm standard deviations) for the bacterial community, while

727217±65465 reads were obtained for the archaeal community. Chlorobi, Bacteroidetes, Proteobacteria, and Firmicutes were identified as the four most dominant phyla within the bacterial community in granules. The most abundant bacterial species in granules are shown in Figure 4.5. Five dominant species were found in all granules these include, *Chlorobium limicola*, *Lentimicrobium saccharophilum*, *Hydrogenispora ethanolica*, *Anaerophaga thermohalophila*, and *Anaerocella delicata*. However, there was a dynamic in the bacterial community structure, with shifts at the bacterial species level following decreasing temperatures and increasing OLRs.

At 12 and 8.5 °C, the species *C. limicola* dominated the bacterial community by 38 - 46% relative abundance especially at low to medium OLR, 3 - 8 gCOD·l⁻¹·d⁻¹. However, it decreased remarkably to 2 - 20% relative abundance when applying higher OLR, 15 gCOD·l⁻¹·d⁻¹. On the contrary, *L. saccharophilum* contributions to the bacterial community increased along with the increasing OLR from were 3 - 10% to 12 - 28% in 3 - 8 gCOD·l⁻¹·d⁻¹ and 15 gCOD·l⁻¹·d⁻¹, respectively. A significant shift was observed on the predominant species when decreasing temperature to 5.5 and 2.5 °C in both reactors. The relative abundance of *L. saccharophilum* increased up to 10 - 28%, and the relative abundance of *C. limicola* decreased to less than 5%.

C. limicola is an auto- and mixotrophic, green phototrophic bacterium belonging to the *Chlorobiaceae* family. This species carries out anaerobic photosynthesis in which reduced sulfur compounds are used as electron donor to fix carbon dioxide (Verté et al., 2002), in particular sulfide ions (Henshaw et al., 1998). Cabral et al. (2020) and Aida et al. (2015) revealed the presence of green sulfur bacteria in UASB reactor system related to sulfide oxidation (Cabral et al., 2020) and low-temperature conditions (Aida et al., 2015). Their results showed that this group played a significant role in anaerobic sulfur oxidation in low-temperatures (10 - 26 °C) consortia (Aida et al., 2015). A significant decrement of *C. limicola* abundance in this current study was observed

Main Results and Discussions

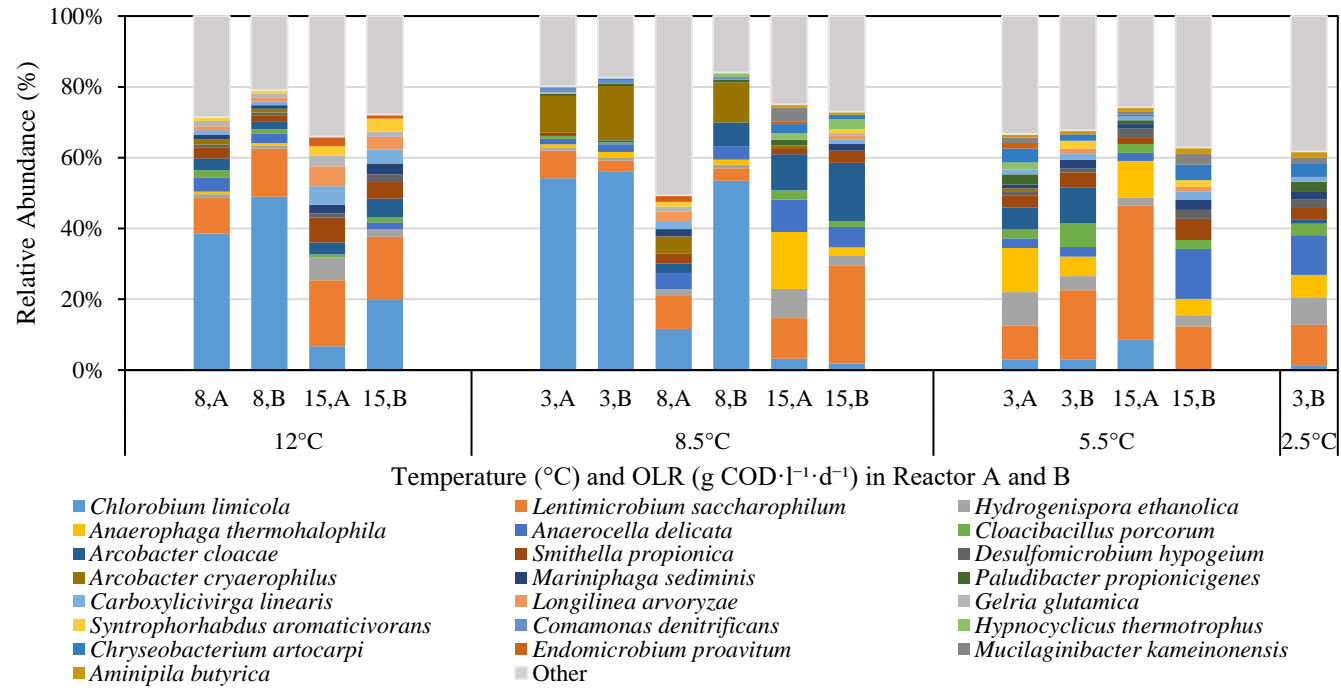


Figure 4.5 Relative abundances of microbial population structure in UASB granules at the bacterial species level at different operating temperatures and OLRs. A and B on the x-axis represents microbial population structure in two parallel reactors, A and B. Numbers beside A and B represent OLR in gCOD·l⁻¹·d⁻¹ (Paper II).

when decreasing temperature to 5.5 and 2.5 °C. This coincided with the insulation of the reactors by opaque external foam covers at the end of the 8.5 °C experiment. Hence, their reduced abundance most likely resulted from lack of photons rather than reduced temperature. *L. saccharophilum* is a strictly anaerobic bacteria which belongs to the *Lentimicrobiaceae* family. It is a chemo-organotrophic fermenter which is widely found in the environment, and it is especially common in organic-rich anoxic ecosystems, such as animal gut and anaerobic waste/wastewater treatment systems. Their major fermentative products are acetate, malate, propionate, formate and hydrogen (Sun et al., 2016), filling the major niche of fermenters in the consortia of anaerobic organic carbon converters.

The mesophile *H. ethanolica* also emerged as a predominant community member at all operating conditions with relative abundance increasing with decreasing temperatures from approximately 1% (around 1000 OTU counts) at 12 °C to approximately 8% (around 5000 OTU counts) at 2.5 °C. As for the previously described specie, *L. saccharophilum*, *H. ethanolica* is commonly found in anaerobic wastewater systems as an ethanol-hydrogen-coproducing bacteria which co-culture with the hydrogenotrophic methanogens in syntrophic substrate utilization (Liu et al., 2014). Their major end-products of glucose fermentation are acetate, ethanol and hydrogen (Yang et al., 2016). Two other predominant species in the granule bacterial communities were *A. thermohalophila*, and *A. delicata* that appeared at 8.5, 5.5, and 2.5 °C. *A. thermohalophila* and *A. delicata* are strictly anaerobic bacteria and live where they may show both fermentative and acetogenic metabolism (Abe et al., 2012; Denger et al., 2002). *A. thermohalophila* is classified as a thermophilic bacteria and has not been reported to play a significant role at low-temperature conditions (Denger et al., 2002). Presence at low-temperatures might be due to novel biological capabilities (and re-classification) or an indication of psychrotolerance. As only a single species is characterized among the *Anaerophaga*, by an isolated study

from an anaerobic sludge, only putative conclusions to their role and growth are possible. *A. delicata* can grow down to 10 °C (Abe et al., 2012) and the relative abundances of *A. delicata* increased from 3% (approximately 1500 OTU counts) at 12 °C to 11% at 2.5 °C (approximately 7500 OTU counts). Eco-physiological studies by Abe et al. (2012) showed the species to be able to ferment some amino acids to acetate, butyrate and valerate, and a limited ability to reduce sulfate. The relative increase in abundance indicated psychrotolerant ecophysiology concurrent with reduced general diversity. In addition to the dominant and omnipresent species, several predominant species emerged at more obligate psychrophilic (5.5 and 2.5 °C) conditions and represented interesting and relevant ecological capabilities as suggested by the literature: *Paludibacter propionicigenes*, *Chryseobacterium artocarp*, *Mucilaginibacter kameinonensis*, and *Aminipila butyr* should be mentioned. *P. propionicigenes* is a natural occurring mesophilic fermentative bacteria which utilized various sugars and produce propionate and acetate as major products (Kim et al., 2015; Ueki et al., 2006). *C. artocarp* have been known as a psychrotolerant and halotolerant bacteria (Venil et al., 2014) and is known to produce mucoid colonies suggesting a role in granule formation. Likewise, *M. kameinonensis* are extracellular polymeric substances (EPS)-producing bacteria, including fatty acids containing EPS and could live in a wide range environment at 5 - 30 °C (Urai et al., 2008). *A. butyr* fermented amino acids as growth substrates and produced acetate and butyrate (Ueki et al., 2018).

Among the top predominant species identified from granule communities, three pathogenic species were identified: *Cloacibacillus porcorum* (0 - 7% relative abundance), *Arcobacter cryaerophilus* (0 - 15% relative abundance), and *Citrobacter gill* (0 - 1% relative abundance). *C. porcorum* can cause soft tissue infections, abscesses, blood, peritoneal fluid, and dental infections (Domingo et al., 2015; Looft et al., 2013). *A. cryaerophilus* is a globally emerging foodborne

pathogen which is a dominant member in wastewater causing diarrhea, mastitis and abortion in animals, and bacteremia, endocarditis, peritonitis, gastroenteritis and diarrhea in humans (Müller et al., 2020). Finally, *C. gillanii* is an opportunistic human pathogen that can lead to invasive diseases, including infections of the urinary tract and respiratory tract (Samonis et al., 2008). There was no significant trend of *C. gillanii* observed at decreasing temperatures and different loadings. Based on this result, there was a slight increase of *C. porcorum* relative abundance with decreasing temperature from 1 - 2 % at 12 °C to 3 - 7% at 5.5 °C, suggesting of psychrotolerance. Significant increases of *A. cryaerophilus* relative abundance was observed from 1% at 12 °C to approximately 15% when applying 8.5 °C. However, they were only detected in traces below 0.01% relative abundance at 5.5 and 2.5 °C. There was no significant trend observed in *C. gillanii* relative abundance (0 - 1%) at the different temperatures and loadings.

The original wastewater showed a significant dissimilarity of the predominant bacterial species compared to granule samples. The wastewater was dominated by *Trichococcus paludicola* with 14767 OTUs count (31.2±0.08% relative abundance ± standard deviation), *Aliarcobacter cryaerophilus* with 4494 OTUs count (10.0±0.01%), and *Lactococcus raffinolactis* with 3954 OTUs count (8.4±0.08%). *T. paludicola* is psychrotolerant facultative anaerobes and alkaliphilic with optimum growth at pH 9.0 (Dai et al., 2018). *L. raffinolactis* is a non-starter lactic acid bacterium in a wide range of environments downstream of dairy effluents (Meslier et al., 2012), indicative of the food processing industrial origin of the wastewater applied. OTU counts of these three species in the granules were insignificant (0 - 293 OTUs count) suggesting them to be functionally lacking the ability to attach and grow in the granule biofilm and/or adapt to psychrophilic conditions. Furthermore, it also indicated the communities in the granules to be autochthonous, or at least selected from minor abundances of inlet origin. Hence, significant changes observed in the granule communities must

therefore be the result of adaptations to growth conditions, rather than changes induced by invasive inlet species. Details on sequencing data of predominant species in original wastewater are presented in Appendix 2 (Paper II).

4.2.2 Composition shift of methanogenic archaeal community

The relative abundances of predominant archaeal species in the granules at different operating temperatures and OLRs are presented in Figure 4.6a. The archaeal community structure was dynamic, with shifts at the archaeal species level following decreasing temperatures and increasing OLRs. Figure 4.6a shows predominant species contributing to at least 97% relative abundance. The most predominant methanogen species in all granule samples were *Methanothrix soehngeni*, *Methanomassiliicoccus luminyensis*, *Methanocorpusculum aggregans*, and *Methanobacterium beijingense* contributing to more than 90% relative abundance in the archaeal communities. Similar to the granule's communities, the predominant species in the original wastewater are *M. luminyensis* (27 % relative abundance) and *M. soehngeni* (25 % relative abundance). Detailed predominant species in wastewater sequencing data are presented in Appendix 2 (Paper II).

At 12 °C, *M. soehngeni* and *M. luminyensis* contributions in archaeal community were 46 - 64% and 29 - 47%, respectively. A significant shift in both reactors was observed when temperature was reduced to 8.5 °C. At OLR 3 and 8 gCOD·l⁻¹·d⁻¹, the relative abundance of *M. luminyensis* increased up to 85%, and the relative abundance of *M. soehngeni* decreased down to less than 10%. However, after further reduction of the operating temperature, *M. soehngeni* abundance gradually increased to more than 82% at 2.5 °C. The relative abundance of *M. aggregans*, and *M. beijingense* fluctuated regardless of operating temperatures and OLRs in the range 2 - 10%.

Main Results and Discussions

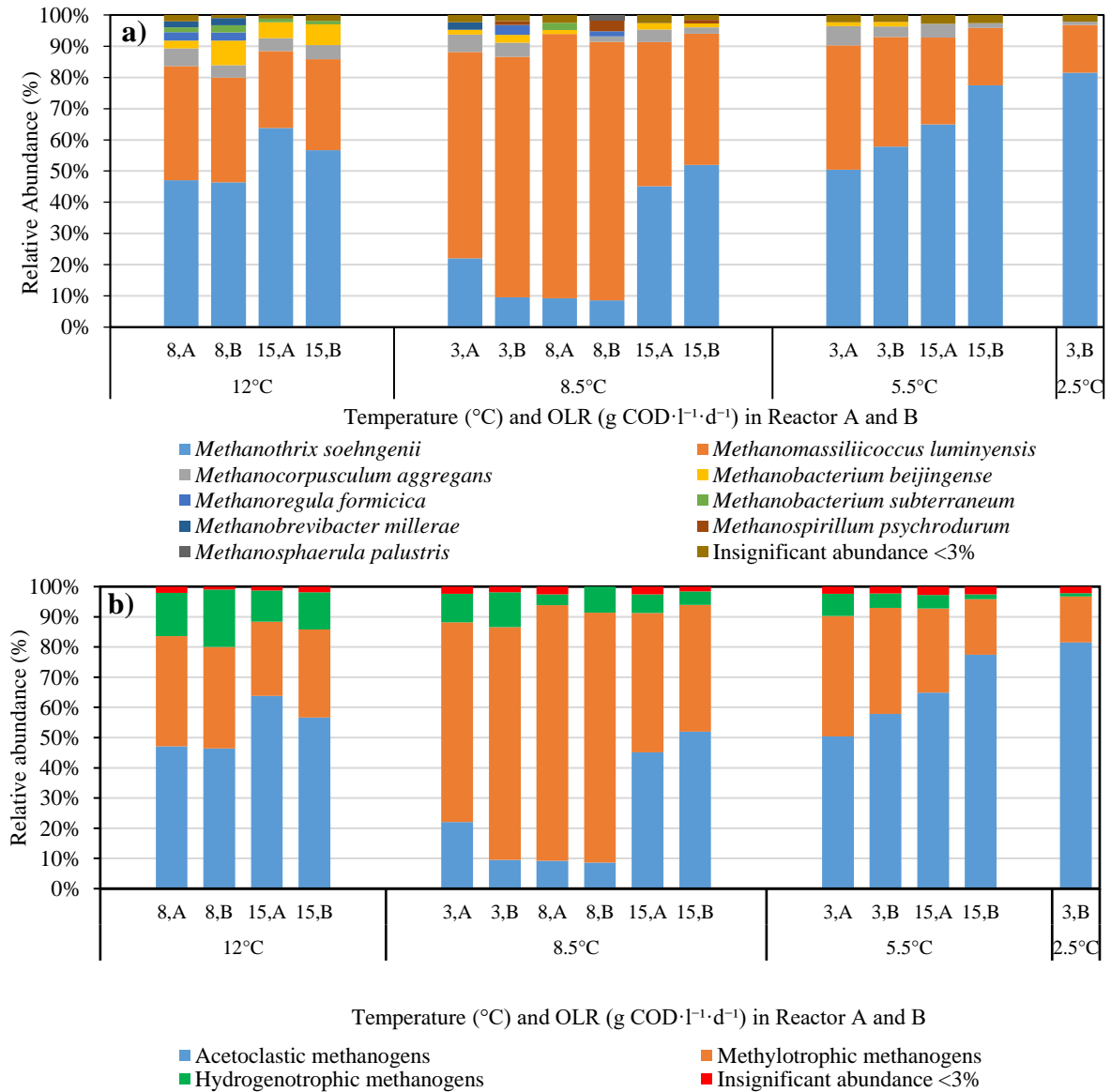


Figure 4.6 Relative abundances of microbial population structure in UASB granules at (a) archaeal species level and (b) methanogen groups based on methanogenesis pathway at different operating temperatures and OLRs. A and B on the x-axis represents microbial population structure in two parallel reactors, A and B. Numbers beside A and B represent OLR in gCOD·l⁻¹·d⁻¹.

Based on the species individual contribution to the main methanogenic pathways, the archaeal community could be divided into three methanogenic groups as presented in Figure 4.6b. At 12 °C, acetoclastic methanogens accounted for 46 - 64% and 29 - 47% of archaeal community, in reactor A and B respectively. A significant shift was observed upon temperature reduction to 8.5 °C in both reactors. At OLR 3 and 8 gCOD·l⁻¹·d⁻¹, the relative abundance of H₂-dependent methylotrophic methanogens increased to 85%. However, after further decrement of the operating temperatures, acetoclastic methanogens abundance gradually resurged to more than 82% at 2.5 °C. The relative abundance of hydrogenotrophic methanogen decreased at lower temperatures.

The most predominant methanogen species in all granule samples were: The obligate acetoclastic methanogen *M. soehngeni* belonging to the *Methanosarcinales* order which decarboxylates acetate (Huser et al., 1982); The H₂-dependant methylotrophic methanogen *M. luminyensis* of the *Methanomassiliicoccales* order which reduces methyl-groups of methylated compounds to methane using H₂ as electron donor (Söllinger & Urich, 2019) and the two autotrophic hydrogen oxidizers *M. aggregans* (heterotype *parvum*) and *M. beijingense* belong to *Methanomicrobiales* and *Methanobacteriales* order, respectively, using carbon dioxide or formate as carbon sources (Ma et al., 2005; Oren, 2014). These four species made up more than 90% of the relative abundance in the archaeal communities regardless of operating temperatures and OLRs. However, systematic shifts in the methanogen composition were observed under increasing OLR and as a response to lower temperatures, suggesting similar alteration of predominant community methanogenic pathways (Figure 4.6b).

During operating temperature of 12 °C and low OLR, acetoclastic methanogens were relatively more abundant in both reactors and acetoclastic methanogens slightly increased at high OLR (Figure 4.6b). Similar observations were reported by Zhang et al., (2018) whereby

acetoclastic *Methanosaetaceae* was abundant after 300 days of operation at 10 - 20 °C in a UASB reactor. By decreasing operating temperature to 8.5 °C, a significant methanogenic composition shifts were observed, especially at low to medium OLRs. Methylotrophic methanogens, specifically *Methanomassiliicoccales*, became more dominant contributing to more than 70% relative abundance of the archaeal community. Interestingly, *Methanomassiliicoccales* is known as a methylotrophic methanogens lacking the Wood-Ljungdahl pathway and therefore cannot oxidize methyl-groups to CO₂ (Söllinger & Urich, 2019). Consequently, they are dependent on an external electron donor (i.e. H₂) and compete with autotrophic methanogens. However, with the increased OLRs and decreased temperatures further down to 2.5 °C, the relative abundance of acetoclastic methanogen increased again to more than 70%. This has also been demonstrated by Nozhevnikova et al. (2007) reporting about 95% methane to originate from acetate at 5 °C. In this study, acetoclastic methanogens became increasingly dominant under low-temperature (2.5 °C), indicating acetoclastic growth and acetate to be the main precursor of methanogenesis pathway at low-temperatures.

In several studies, hydrogenotrophic methanogens were given an essential role in anaerobic treatment at low-temperatures (Bandara et al., 2012; McKeown et al., 2009; Petropoulos et al., 2017; Smith et al., 2015). However, the results showed the relative abundances of hydrogenotrophic methanogens to be low and decreasing with decreasing temperatures to 14%, 7.3%, 4.5% and 1.1% at 12, 8.5, 5.5, and 2.5 °C, respectively. Inferring from the high abundance of acetoclastic methanogens, homoacetogenesis is assumed to be the main hydrogen consuming reaction at low-temperatures. An increased acetate production was also observed, especially at 2.5 °C (Paper I). Furthermore, bacterial community analysis showed a slight increase in relative abundances of the genus *Acetoanaerobium* (homoacetogen) in

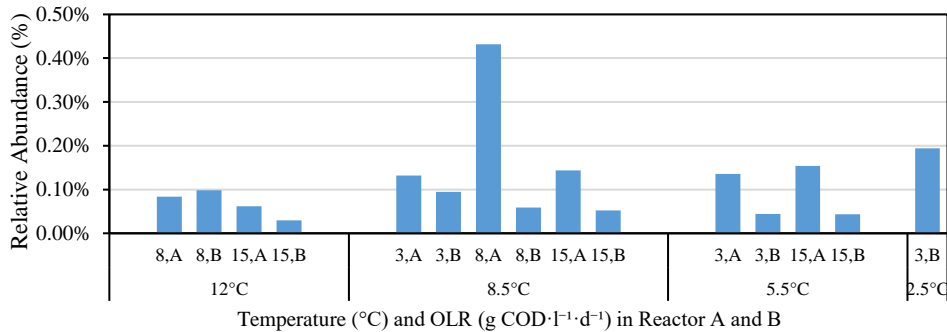


Figure 4.7 Relative abundances of genus *Acetoanaerobium* (homoacetogen) in UASB granules at different operating temperatures and OLRs. A and B on the x-axis represents microbial population structure in two parallel reactors, A and B. Numbers beside A and B represent OLR in $\text{g COD}\cdot\text{l}^{-1}\cdot\text{d}^{-1}$ (Paper II).

UASB granules at low-temperatures (Figure 4.7). Homoacetogens convert H_2 and CO_2 to acetate outcompeting hydrogenotrophic methanogens at low-temperatures (Kotsyurbenko et al. 2001; Nozhevnikova et al. 2007). Kotsyurbenko et al. (1996) showed that homoacetogens grow two times faster at 6 °C and were less temperature sensitive in the entire psychrotolerant range than hydrogenotrophic methanogens by experimentally estimated Q_{10} values of 2.2 and 4.1, respectively. Therefore, temperature and organic loading resulted in a change in the microbial community composition and through that the importance of conversion pathway of organic matter. Nucleic acids, lactate, alcohols, and C_1 -compound conversions are included in the suggested pathway scheme (Figure 4.8) which is extension of the COD flow model proposed by Batstone et al. (2002) and Tiwari et al. (2021) (see Chapter 2.1 (Figure 2.1) and 2.3 (Figure 2.4), respectively).

Sustained COD removal and methane production was demonstrated in Chapter 4.1 (Paper I) and this microbial community analysis was used to assess whether low-temperature performance is a result of genotypic adaptations or psychrotolerant capabilities of the original mesophilic community. This finding indicates that long-term adaptation of the microbial community in granulated biomass through changes in the

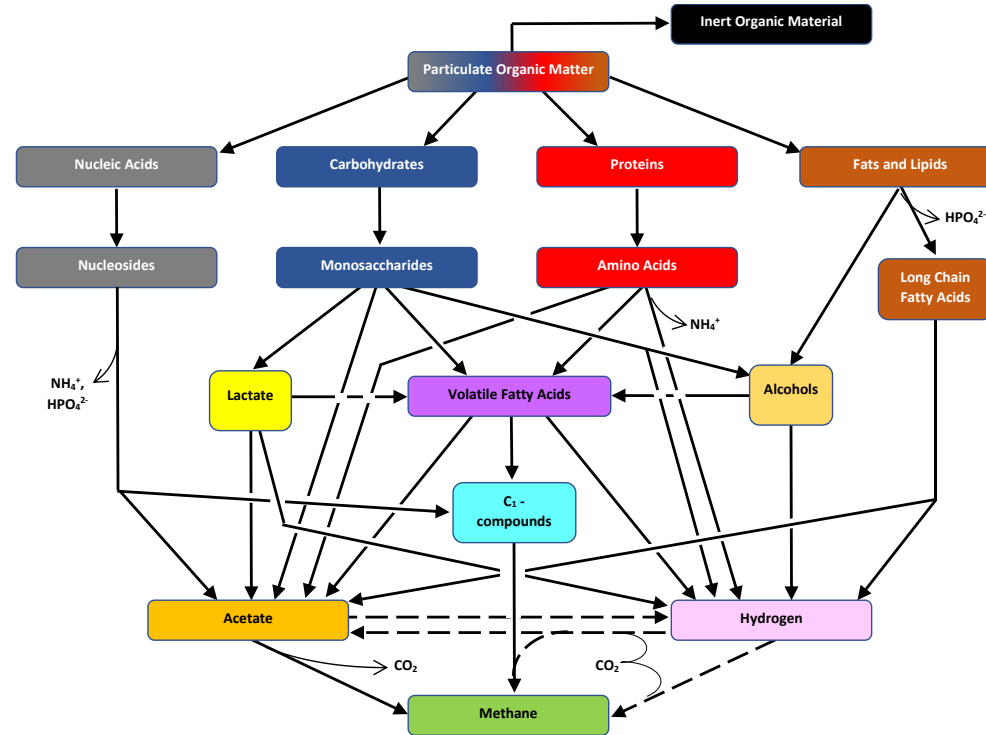


Figure 4.8 Anaerobic process pathway proposed under psychrophilic conditions. Dashed arrows represent hydrogen consuming and producing pathways (Paper II).

community structure is the most likely explanation, especially among the methanogenic community. Hence, the research hypothesis (Chapter 2.8, RQ2) is confirmed. Low-temperature anaerobic treatment seems to require methanogenic community changes. These changes are slow, and this study allowed for changes over seasonal timescales. Hence, design and operation must allow for community changes to proceed. Lack of such adaptations may also be an explanation to why many earlier studies showed inability to use anaerobic treatment at temperature below 10 °C.

4.3 Anaerobic granulated biofilm system model for municipal wastewater treatment

Simulated OLR scenario results reflected observed COD removal efficiencies. Figure 4.9 presents simulated and observed COD removal efficiencies of the UASB reactor at 25 °C. Both simulation and experimental results show decreasing COD removal efficiencies at steady-state conditions with increasing OLR. However, there was a significant difference in COD removal efficiency reductions in the simulation results (62 - 69%) compared the observed experimental reduction (63 - 66%).

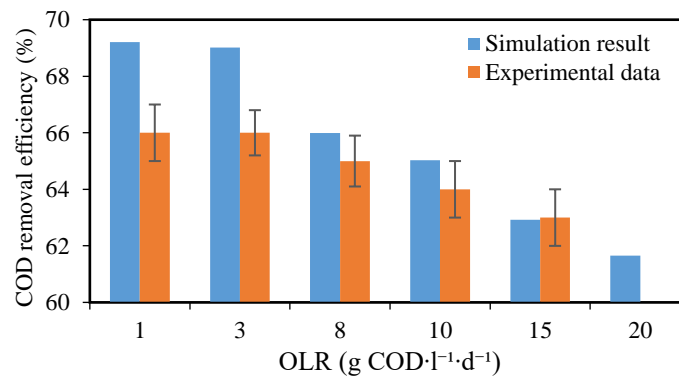


Figure 4.9 Simulation result of COD removal efficiencies (blue bars) compared to experimental results (orange bars) during steady-state conditions at 25 °C. There was no experimental data measured at OLR 20 gCOD·l⁻¹·d⁻¹. Error bars represent standard errors from measurements taken during steady-state conditions in UASB reactors.

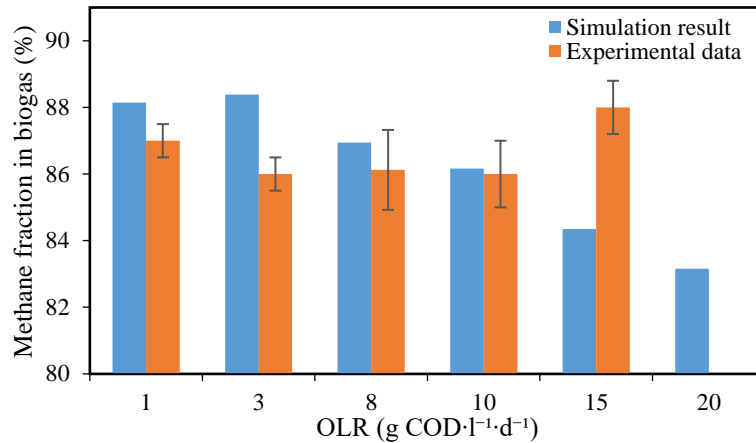


Figure 4.10 Simulation result of methane fraction in biogas (blue bars) compared to experimental results (orange bars) during steady-state conditions at 25 °C. There was no experimental data measured at OLR 20 gCOD·l⁻¹·d⁻¹. Error bars represent standard errors from measurements taken during steady-state conditions in UASB reactors.

In simulations, methane fractions in the biogas at steady-state conditions decreased with increasing OLR. However, there was no significant trend observed in experimental data (Figure 4.10). The dissolved methane concentration in the effluent (86 mgCOD·l⁻¹) was mimicked by the simulation result, and both are in line with theoretical value of dissolved methane at 25 °C (Liu et al., 2014). Considerable pH profile (approximately 7 - 8.3) through the depth of the granule were predicted, as shown in Figure 4.11. The interior increase in pH inside the granules suggest calcium phosphate (CaP) granulation. CaP precipitation is known to stimulate granule formation, and could be exploited for phosphorous recovery (Cunha et al., 2018).

Simulated composition of granular sludge active biomass fractions for the experimental UASB reactor is given in Figure 4.12. The experimental study does not provide spatial data for comparison, so the simulated values are only to be theoretically interpreted. Based on the composition, methane production was mainly performed by acetoclastic methanogens, which dominated compared to hydrogenotrophic methanogens for all

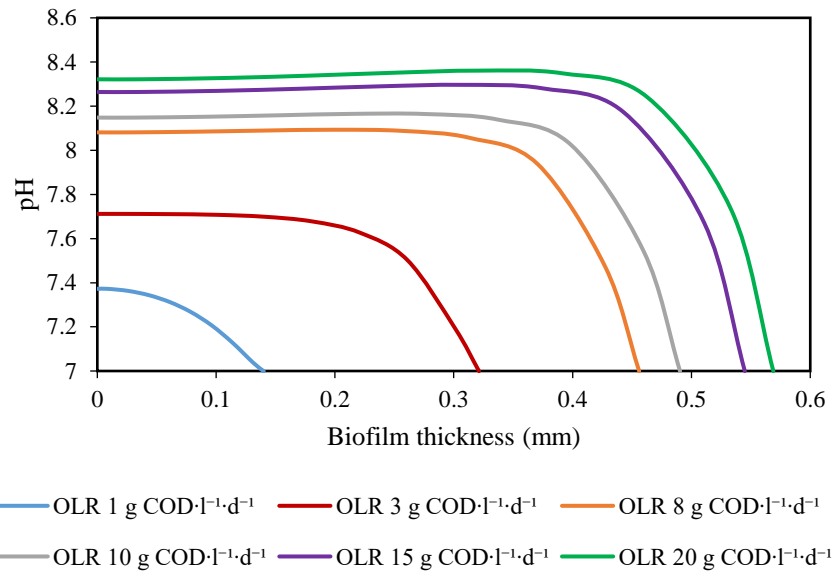


Figure 4.11 pH distribution profile along the granule in UASB reactor during steady-state conditions

selected loadings. LCFA degraders only accounted for trace quantities of the active biomass. This could be explained by too low LCFA concentration to sustain biomass. There are significant decreases on amino acid degraders with the increasing loading. However, more than 90% of the influent amino acid and LCFA was converted in the reactor at all organic loadings. There is no significant loading effect on bacterial distribution profile along the granule in UASB reactor during steady-state conditions, as shown in Appendix 6C. The sugar degraders had the highest concentration on the outer layer of granular sludge followed by butyrate and valerate degraders (X_{c4}), hydrogenotrophic (X_{h2}) and acetotrophic (X_{ac}) methanogens. The high amount of carbohydrates in the wastewater, supported these bacterial groups and resulted in a high methane concentration in the produced biogas. In the granules, the acetate degrading biomass peaked approximately 100 μm behind the biofilm-bulk boundary. Acetate concentrations were at their maximum at the biofilm boundary. The delayed front was possibly due to the faster growth of the other organisms, and a consequent high availability (not

concentration) of acetate. Substrate distribution profile into the granules during steady-state conditions are shown in Appendix 6C. Monosaccharide and VFA substrates are predicted to degrade approximately within the outer 100 - 200 μm . The granules had generally lower substrate concentrations than the bulk phase.

In general, the model can predict some bulk experimental observations, and that it may be used to investigate unobservable variables inside the granules affirmed the hypothesis in Chapter 2.8 (RQ3). Furthermore, this simulation was developed to help understand theoretical consequences inside the anaerobic biofilm granules, and that it might be used to identify new research questions and test theoretical hypothesis.

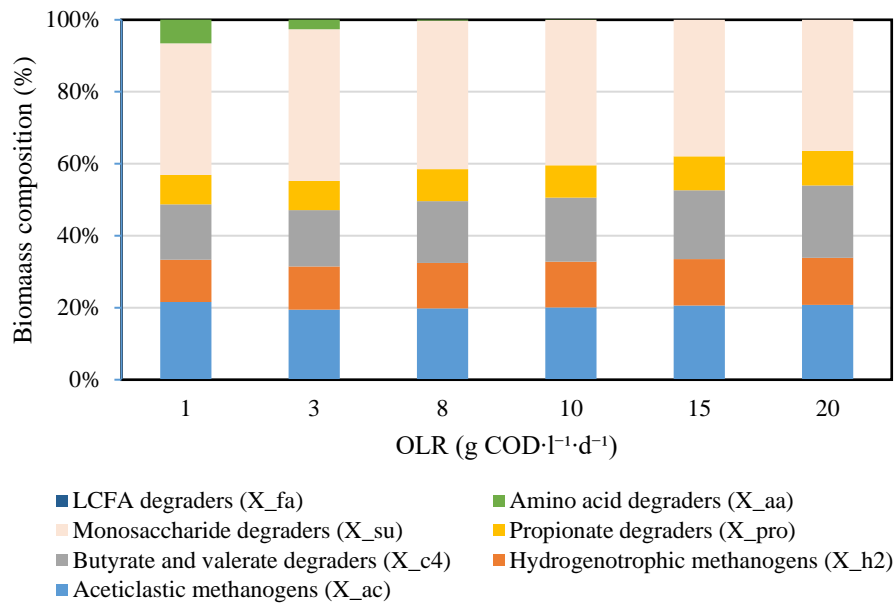


Figure 4.12 Simulated active biomass composition of the granular sludge of UASB reactor at different organic loading during steady-state conditions.

4.4 Engineered methanotrophic syntrophy in photogranule for dissolved methane removal

In this part, a process for dissolved methane removal was investigated based on the syntrophic interactions between phototrophic cyanobacteria and methanotrophic bacteria aggregated in oxygenic photogranules. This was motivated by the acknowledgment of dissolved methane to represent a major obstacle for the sustainability of anaerobic wastewater treatment. Aggregation is particularly important in the bioprocesses as it allows for efficient and fast removal of the biomass from the reactor water, and efficient intra-aggregate oxygen transfer. This study was performed using an open community of cyanobacteria and methanotrophs originating from an ordinary activated sludge reactor. The syntrophy was ecologically engineered from an enrichment culture of methanotrophs and chemoorganotrophic oxygenic photogranules converting synthetic wastewater, as described in Milferstedt et al. (2017). Furthermore, community assembly and performance characteristics of a continuously operated reactor system for the removal of dissolved methane was investigated. Detailed results and discussions on engineered methanotrophic syntrophy in photogranule for dissolved methane removal are presented in the appendix (Paper III).

A syntrophic community of methanotrophs enriched from activated sludge and cyanobacteria residing in photogranules was developed in a batch test system and maintained over a two-month period in a continuously operated reactor. Initially, methanotrophs were enriched in gas-tight, stoppered serum bottles with a mixture of oxygen and methane in the headspace. Approximately 50% of statically incubated cultures removed methane. After adding 100% methane to the headspace, methane removal was detected without externally provided oxygen. Additionally, production of oxygen and CO₂ was measured and these observations demonstrated the onset of syntrophic interactions between methanotrophs and oxygenic photogranules.

The ecologically engineered methane-converting photogranules were then used as inoculum for the continuously operated reactor.

Figure 4.13 shows the dissolved COD removal efficiency as a proxy for methane removal as well as effluent total suspended solids (TSS) over time. The novel community removed dissolved methane during stable reactor operation by on average $84.8 \pm 7.4\%$ (\pm standard deviation) with an average effluent concentration of dissolved methane of 4.9 ± 3.7 $\text{mgCH}_4 \cdot \text{l}^{-1}$. From an inlet $32 \text{ mgCH}_4 \cdot \text{l}^{-1}$, the average methane removal rate was $26 \text{ mgCH}_4 \cdot \text{l}^{-1} \cdot \text{d}^{-1}$. In van der Ha et al. (2011), an overall methane oxidation rate was reported to be $171 \text{ mg CH}_4 \cdot \text{l}^{-1} \text{ liquid phase} \cdot \text{d}^{-1}$ which appears to be 6.6 times higher than in this experiment. A major factor leading to a higher removal rate is the organic loading. In van der Ha et al. (2011), 235 ml of CH_4 were added over 72 hours, which corresponds to approximately $258 \text{ mgCH}_4 \cdot \text{l}^{-1} \cdot \text{d}^{-1}$ at 22°C . Our OLR of $35.1 \pm 4.5 \text{ mgCH}_4 \cdot \text{l}^{-1} \cdot \text{d}^{-1}$ was thus, 7.3 times lower. It is important to note that the rates are not directly comparable as van der Ha et al. (2011) worked in a batch system over 90 h, while this presented study was obtained in a CSTR with an HRT of 12 h.

The observed overall biomass yield was $0.7 \text{ gTSS} \cdot \text{gCOD}^{-1}$, equivalent to $0.6 \text{ gVSS} \cdot \text{gCOD}^{-1}$ (assuming 15 % inorganic biomass fraction). Per mass substrate (CH_4) this is equivalent to $2.4 \text{ gVSS} \cdot \text{gCH}_4^{-1}$. The observed yield represents the combination of cellular yield from methanotrophic and cyanobacterial growth. Literature values of methanotrophic yields relevant for this study have been reported by Leak & Dalton (1986) and Arcangeli & Arvin (1999). By theoretical analysis and experimental observations on suspended *Methylococcus capsulatus*, Leak & Dalton (1986) reported cellular yield of $0.6 - 0.7 \text{ gVSS} \cdot \text{gCH}_4^{-1}$ at cultivation conditions similar to this study.

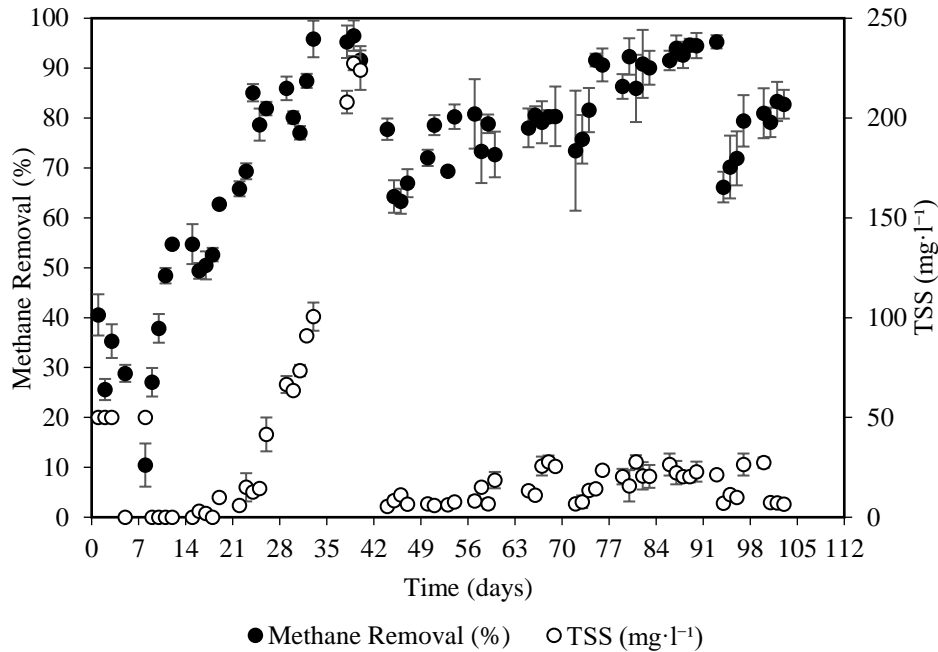


Figure 4.13 Removal efficiency of dissolved methane (filled circles) and concentrations of total suspended solids in the effluent (TSS, open circles) during continuous reactor operation. Mixing speed was increased on day 31. On day 40, the reactor effluent clogged. Wasting of biomass was done on days 42 and 94 (Paper III).

Arcangeli & Arvin (1999) studied a methanotrophic biofilm enriched from landfill soil and estimated the dry weight yield to be $0.56 \text{ gVSS} \cdot \text{gCH}_4^{-1}$. As conditions and growth technique, granular aggregation is similar to biofilms, and this present media ($0.02 \text{ mg} \cdot \text{l}^{-1}$ of $\text{CuSO}_4 \cdot 5\text{H}_2\text{O}$) was comparable to the Cu limited experiment of Leak & Dalton (1986), methanotrophic yields were estimated to be in the order of $0.5 - 0.6 \text{ gVSS} \cdot \text{gCH}_4^{-1}$, which leaves the remaining observed $1.8 \text{ gVSS} \cdot \text{gCH}_4^{-1}$ to be the autotrophic contribution. Assuming all CO_2 from the mineralization of methane to be assimilated by the phototrophic bacteria, a combined methanotrophic and phototrophic yield of $1.54 \text{ gVSS} \cdot \text{gCH}_4^{-1}$ would be theoretically possible. The observed combined yield ($2.4 \text{ gVSS} \cdot \text{gCH}_4^{-1}$) therefore indicates an additional autotrophic

growth contribution of $0.9 \text{ gVSS.gCH}_4^{-1}$ probably originating from the inlet bicarbonate. High biomass yields in this system highlight the potential for the recovery of chemical energy by, for instance, a methane-based biorefinery using photogranules.

The overall COD balance closed at 91% of the inlet COD. The unaccounted 9% COD could be explained by the reactor system still not being completely at steady-state (positive bioaccumulation), and by the negative COD contribution by phototrophically produced oxygen consumed by the methanotrophs during methane mineralization. The elevated methane removal in the absence of any external oxygen supply can only be explained by in-situ oxygen production and immediate uptake by methanotrophs. The results therefore demonstrate the establishment of syntrophic interactions between phototrophs and methanotrophs. This syntrophy was stably maintained over seven weeks during continuous reactor operation.

Photogranule size may influence the specific phototrophic and methanotrophic activities as phototrophic methane conversion is assumed to be a surface-depending process. Photogranule size affects the surface to volume ratios and diffusional lengths. The specific metabolic activity was analyzed in batch experiments for sets of on average six similar-sized photogranules in size classes between 1.3 and 5.5 mm in average diameter (Figure 4.14). Photogranules were sampled during stable reactor performance. Photogranules with diameters of approximately 1 - 2 mm gave the highest surface-specific methane removal rate of $0.53 \pm 0.02 \text{ mgCH}_4 \cdot \text{d}^{-1} \cdot \text{mm}^{-2}$ (\pm standard deviation). The methane removal rate per photogranule surface area decreased with increasing diameter (Figure 4.14a). The relation to the surface to volume ratio is presented in Figure 4.14b. An elevated surface to volume ratio is beneficial for methane removal. From a conversion perspective alone, it is favorable to engineer a size distribution within the reactor of minimal photogranule diameter. The surface dependent character of photogranule metabolism was also shown in a recent study by Abouhend et al. (2020)

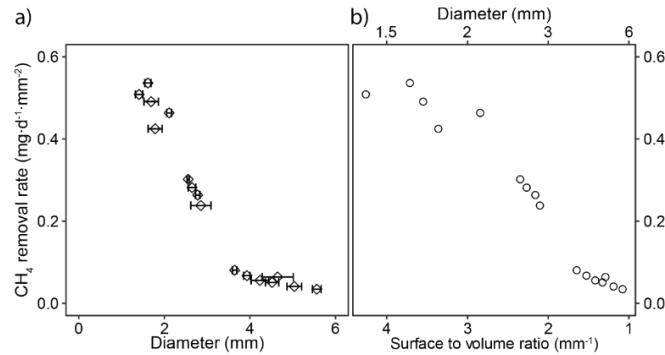


Figure 4.14 Surface specific methane removal rates for individual photogranule sizes. Rates are plotted by (a) the average diameter of the photogranule batch, and (b) by the surface to volume ratio, derived from the average diameters of the tested photogranules. Each point represents an independent batch experiment conducted with on average six similar-sized photogranules (Paper III).

in which oxygenic photogranules of 0.5 - 1.7 mm in diameter showed the highest oxygen production rate compared to bigger photogranules (Abouhend et al., 2020). Higher oxygen production rates influence the treatment potential of the biomass, in this case dissolved methane removal, due to higher oxygen availability from photosynthesis as electron acceptor. Bigger photogranules may also become less active because they lose their cyanobacteria from the core as the photo-layer appear to be limited to depth of about 700 μm (Milferstedt et al., 2017). Small granules, however, settle slower, and granule size is therefore a compromise between rate and separation.

MiSeq amplicon sequencing of 16S and 23S rRNA revealed a potential syntrophic chain between methanotrophs, non-methanotrophic methylotrophs and filamentous cyanobacteria. Figure 4.15 shows relative abundances of methylotrophic and phototrophic taxa in photogranules and background material. The enrichment process had a profound impact on the microbial community, 18.5 \pm 6.0% (\pm standard deviation) of all non-cyanobacterial bacterial 16S rRNA sequences were

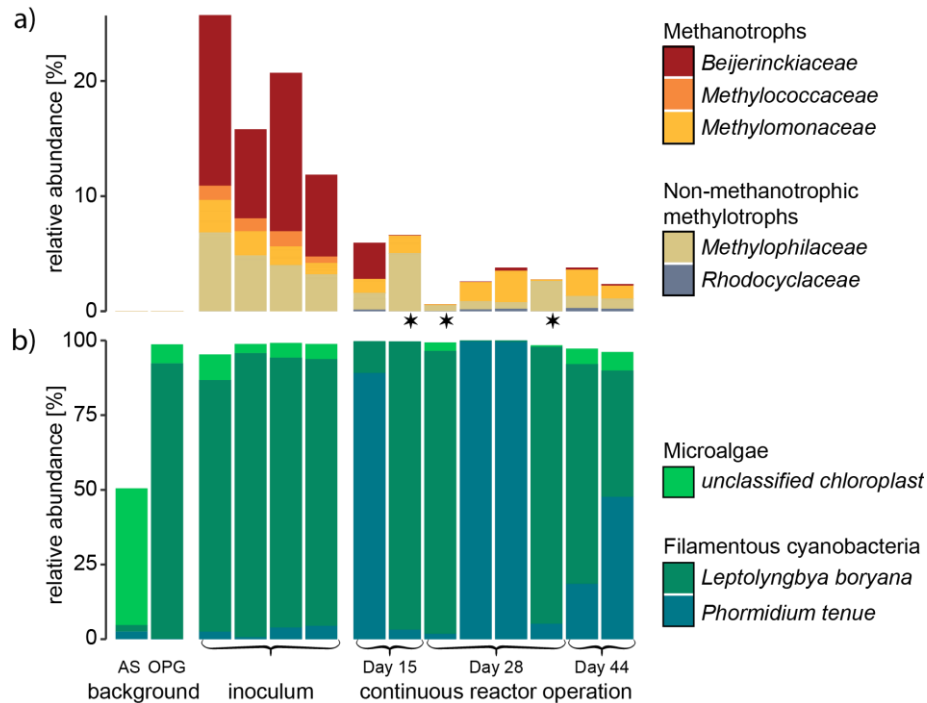


Figure 4.15 Relative abundances of methylotrophic and phototrophic taxa in photogranules and background material. The background material before the enrichment is the original activated sludge (AS), and an oxygenic photogranules (OPG). The inoculum after the enrichment process is represented by four photogranules. In total eight photogranule communities during continuous reactor operation are shown for days 15, 28 and 44. a) Putative methylotrophic bacteria (Silva SSU 132) among the non-phototrophic bacteria in the 16S rRNA amplicons. The three samples with asterisks mark photogranules in which methanotrophs are present in low abundances compared to non-methanotrophic methylotrophs. b) Major (>5% total abundance) cyanobacterial and chloroplast OTUs (Silva LSU 132) among the phototrophic taxa of the 23S rRNA amplicons (Paper III).

affiliated with known methylotrophic bacterial genera. Of this methylotrophic fraction, $74.1 \pm 4.8\%$ were known methanotrophs, notably of the family of *Beijerinckiaceae*. Across all samples containing sequences of methanotrophic *Beijerinckiaceae*, $98.5 \pm 4.5\%$ were of the genus *Methylocystis*. Also present at the end of the enrichment, however, at notably lower abundances of $21.6 \pm 5.5\%$ of all methanotrophic bacteria, were members of the families of *Methylococcaceae* and

Methylomonaceae. These subdominant families belong to the Gammaproteobacteria, also known as type I methanotrophs. Traditionally, the distinction in type I and type II methanotrophs allowed the differentiation of mutually exclusive physiological traits. Over the last years, however, it was realized that the distribution of these traits was less exclusive, and the distinction has become less meaningful (Dedysh & Knief, 2018).

During photoreactor operation, the overall relative abundance of methylotrophs dropped from 18.5% in the inoculum to, on average, $3.5 \pm 2.0\%$ (\pm standard deviation), of which roughly half of all sequences were known methanotrophs ($1.8 \pm 1.4\%$). Also, the abundance of the other two methanotrophic families *Methylococcaceae* and *Methylomonaceae* decreased significantly (t-test, p-value=0.02) dropping from, on average, $2.9 \pm 1.0\%$ to $1.3 \pm 0.9\%$. After the disappearance of the *Methylocystis*, these two families presented the majority of methanotroph-affiliated sequences during reactor operation ($87.2 \pm 24.2\%$). Two photogranules, sampled at day 28, only contained about 0.1% of methanotrophic sequences, more than ten times fewer than the other samples taken during reactor operation. The overall loss of methanotrophs may be explained by a reduced substrate availability per photogranule during reactor operation with the increasing number of photogranules in the system. The overall methanotrophic performance of the reactor system was maintained even at comparably low sequence abundances of $1.8 \pm 1.4\%$ of methanotrophs.

The results also showed sequences of non-methanotrophic methylotrophs in the amplicons, notably of the family *Methylophilaceae*. Their sequences represented on average $4.7 \pm 1.6\%$ in the inoculum, and $1.7 \pm 1.5\%$ during reactor operation. In natural systems like sediments, these organisms are frequently found to respire methanol produced by methanotrophic bacteria (Yu et al., 2017). Yu et al. (2017) even suggested that among non-methanotrophic methylotrophs and methanotrophs, specific non-random pairings exist that seem to possess

an environmental advantage. The abundances of *Methylophilaceae* sequences appears to be roughly one third of the counts of known methanotrophic sequences found in the photogranules. The constant ratio in abundance between the two distinct phylogenetic groups hints towards a stoichiometric relationship between the implied organisms, possibly through metabolite dependencies.

In the reactor samples, methanotrophs are only present at a comparably low number. The exceptions indicate that metabolic heterogeneity between photogranules existed in the reactor, with the coexistence of putatively methanotrophic and non-methanotrophic photogranules. The non-methanotrophic photogranules may consume substrates provided by other methanotrophic photogranules. These substrates could be for example methanol. A complete CH₄ to CO₂ conversion chain may therefore not be required to be present within each photogranule, but the entire population of photogranules participates in the methane conversion, cross-feeding beyond the boundaries of individual photogranules. The enrichment process and the consequent transfer into the continuously operated reactor also shaped the non-methylotrophic and non-phototrophic bacteria in the community. The postulated trophic chain between the different methylotrophs in photogranules is coupled to the oxygen production by phototrophs, notably cyanobacteria. Detailed of non-methylotrophic, non-phototrophic bacteria, and phototrophs in the community are presented in appendix 3 (paper III).

Generally, the hypotheses in Chapter 2.8 (RQ4 and RQ5) were affirmed. This experiment demonstrated the removal and elimination of dissolved methane by an ecologically engineered methanotrophic community harbored in oxygenic photogranules. Methanotrophic photogranules may be a viable option for dissolved methane removal as anaerobic effluent post-treatment.

4.5 Microalgal-based treatment for removing nutrient

This chapter presents results obtained from the experiments performed to evaluate microalgal based post-treatment for nutrient removal. The result is divided into four sub-chapters: (1) Microalgal cell quantification methods, (2) screening of microalgae growth potential on secondary wastewater effluent in a batch system, and (3) evaluation of selected microalgae strain for nutrient removal in a continuous photobioreactor system.

4.5.1 Microalgal cell quantification methods

Quantitative microalgal analysis is important to determine growth and biomass yield by identifying microalgal strains with the ability to grow efficiently in specific wastewater. Several analytical methods are available for microalgal quantification, including flow cytometry, counting chambers, optical density measurement and microplate reading. It is difficult to determine the most accurate microalgal cell quantification method, as it requires the true concentration to be known. To obtain reliable microalgal quantification one should use several methods on the same samples and cross check results.

The results of the methodological cross-validation indicated that microplate-based method, direct counting, and flow cytometry can be utilized as reliable quantification methods for axenic microalgal cultures of *C. vulgaris*, *C. sorokiniana*, *T. obliquus* and *M. salina* cultivated in filtered UASB secondary effluent. All measurements (Figure 4.16) presented acceptable correlation ($R^2 > 0.9$) between the methods for all species, except for *H. pluvialis* ($R^2 < 0.7$). The t-test revealed no significant difference ($p > 0.05$) between the direct counting and flow cytometry enumeration for all strains except *H. pluvialis* ($p < 0.05$). *H. pluvialis* cultures proved very difficult to maintain in pre-growth media and it was challenging to achieve high cell density and determine

Main Results and Discussions

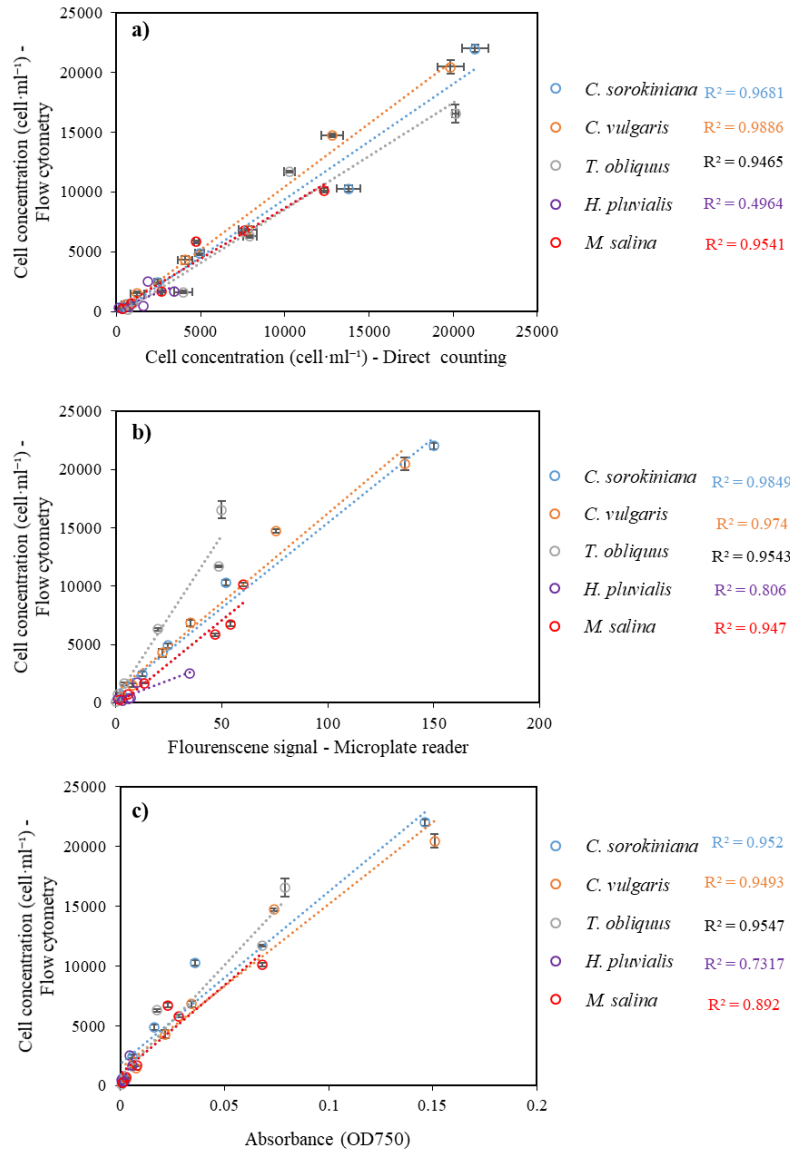


Figure 4.16 Independent confirmation of microplate-based method, direct counting, flow cytometry, and optical density (OD) and calibration of each strain in pre-growth media.

accurate cell numbers. Throughout the experiments, *H. pluvialis* were shown to be fragile and easily lysed, making quantification methods and

growth studies unreliable. Ruptured cells will result in low cell counts by flow cytometry, but still result in light scattering and/or absorbance using OD measurements. This will give false positives of microalgal growth in the culture. Therefore, *H. pluvialis* was excluded from further experiments. OD₇₅₀ measurements showed lower linearity for all species compared to microplate-based method, direct counting, and flow cytometry (Figure 4.16). Hence, OD measurement was not included in the continuation of experiments.

When applying direct cell counting, the method will simultaneously provide information about contamination and visual viability of the cells. The method is also simple and low-cost, however, direct counting is time-consuming. In addition, if the sample is not completely homogenous, counts will not represent the actual cell concentration. The microalgal cultures usually grew dense after some days and had to be diluted prior counting. This can be a source of error, as an imprecise dilution will result in unreliable cell count. Another implicit error by manual counts is the variability introduced by human visualization errors due to cell aggregation and debris. This was experienced with the small *M. salina* with diameter of approximately 2.5 μm . Therefore, counting chamber type should be considered and Guillard and Sieracki suggested the Petroff-Hausser counting device as appropriate when enumerating cells with size less than 1 - 5 μm (Andersen, 2004).

Flow cytometry has been used for estimating microalgal biomass for a long time. It provides a rapid and accurate microalgal quantification analysis, and multi-channel (multi-color) analysis can also give information about DNA, protein, pigment and lipid content (Chioccioli et al., 2014). Identifying correct cell type and discriminate particulate contamination is more difficult using flow cytometry compared to using direct counting. However, combining the fluorescence trigger (here: the red fluorescence) and the particle sensitive forward scatter (FSC) may limit the effect of false counts, as red fluorescence in microalgal suspensions is unique to total chlorophyll content (Peniuk et al., 2016).

Flow cytometry, however, is compared to counting chambers significantly more expensive. Microplate based method can be used to observe microalgal growth rates in low density microplate cultures (van Wagenen et al., 2014), but is limited in too dense cultures. As for flow cytometry, it is not possible to distinguish microalgal species from each other.

This section reports unpublished methodological work for applications in the microalgal growth studies and details are found in Appendix 4. Although the method has some limitations, the results suggest that flow cytometry, direct counting, and microplate-based method can all be used to monitor microalgal growth in wastewater accurately, and the fluorescence-based microplate method correlated well with the established techniques.

4.5.2 Screening the growth potential of the microalgae on secondary wastewater effluent in a batch system

Microalgae typically used for resource recovery was studied for their capacity to remove nutrients and residual COD following UASB treatment. Appropriate wastewater parameters were examined before and after microalgal cultivation for their removal efficiency: COD, phosphate (PO_4^{3-}), ammonium (NH_4^+), nitrate (NO_3^-), nitrite (NO_2^-), total nitrogen (TN), total phosphorous (TP) and alkalinity ($\text{mg CaCO}_3\cdot\text{l}^{-1}$). The chemical and biological composition of the secondary wastewater effluent before and after ceramic membrane filtration is presented as the mean value (\pm standard deviations), as shown in Table 4.1 (n=38). The secondary wastewater effluent composition indicates that most of the nitrogen and phosphorous in the secondary wastewater effluent after membrane treatment were present as ammonium and phosphate, respectively, readily available for microalgal assimilation. TSS was eliminated (up to 99.99% removal efficiency) by the ceramic membrane. Furthermore, total coliforms, *E. coli*, and heterotrophs were as for the particulates removed completely by the membrane.

Main Results and Discussions

Table 4.1 Secondary effluent wastewater characteristics after UASB reactor and tight-micro filtration (T-MF) treatment that was used in screening microalgal-based treatment in batch system for nutrient removal.

Parameters	Unit	Effluent Quality		
		DAF Pre-treatment	UASBR	T-MF
Physico-chemical Parameter:				
s COD	mg·l ⁻¹	721±128	240±79	272±86
t COD	mg·l ⁻¹	917±179	504±141	301±120
TSS	mg·l ⁻¹	420±83	101±9	0.02 ±0.01
NH ₄ ⁺	mg·l ⁻¹	57±8	55±8.6	55±9
NO ₃ ⁻	mg·l ⁻¹	<0.5	<0.5	<0.5
PO ₄ ³⁻	mg·l ⁻¹	24±6	24±4	24±4
TN	mg·l ⁻¹	59±7	57 ± 4	55±4
TP	mg·l ⁻¹	25±5	25±6	24±6
Alkalinity	mg CaCO ₃ ·l ⁻¹	478±69	684±128	691±45
Total VFA	mg CH ₃ COOH·l ⁻¹	143±51	182±146	112±11
Microbiological Parameters:				
Total Coliforms	log ₁₀ CFU·(100 ml) ⁻¹	6.0±0.1	5.7±0.2	0.0
<i>E. coli</i>	log ₁₀ CFU·(100 ml) ⁻¹	4.1±0.2	4.0±0.1	0.0
<i>Enterococci</i>	log ₁₀ CFU·(100 ml) ⁻¹	1.3±0.3	1.0±0.2	0.0
Heterotrophs	log ₁₀ CFU·(100 ml) ⁻¹	7.7±0.1	7.6±0.1	0.0

Filtered UASB effluent was used as media for growth studies on the pre-selected microalgal species. Calculated maximum specific growth rates based on data from identified logarithmic phases are shown in Table 4.2. Results showed that secondary wastewater effluent enhanced growth for *C. vulgaris*, *C. sorokiniana*, *T. obliquus*, but not for *H. pluvialis* and *M. salina*. Low salinity or possibly toxic substances present in the wastewater could be inhibitory for growth of *M. salina* in wastewater. As mentioned in previous section, *H. pluvialis* never reached high cell density. To make this strain grow in wastewater, one should consider different growth media and other environmental conditions (Zhu et al., 2018).

Table 4.2 Established microalgal growth rates cultivated in pre-growth media and filtered UASB secondary effluent

Algal strains	Growth rate (day ⁻¹)	
	Pre-growth media ¹	Wastewater ²
<i>C. vulgaris</i>	0.77±0.12	1.23±0.33
<i>C. sorokiniana</i>	0.63±0.11	1.46±0.39
<i>T. obliquus</i>	0.62±0.32	1.26±0.48
<i>H. pluvialis</i>	0.37±0.20	0.02±0.001
<i>M. salina</i>	0.56±0.42	0.21±0.12

¹Pre-growth media: MWC+Se media for *C. vulgaris*, *C. sorokiniana*, *T. obliquus*, *H. pluvialis*; L1 media for *M. salina*
²Wastewater: UASB+membrane effluent

The results in Figure 4.17 imply that *C. sorokiniana* was the most efficient microalgal strain for removing nutrients in the tested wastewater with hydraulic retention time of 9 days. *C. sorokiniana* was able to remove up to 97±2% TP and 70±8% TN, while *T. obliquus* removed up to 83±4% TP and 49±5% TN. *C. sorokiniana*, *C. vulgaris* and *T. obliquus* significantly reduced ammonium (>70%). Similar results were obtained by (Wang et al., 2010), where *Chlorella sp.* removed up to 83% ammonium from municipal wastewater. Nitrate was produced by the culture (+26 - 43%; Figure 4.17), indicating limited ammonium oxidation. Furthermore, almost 100 % alkalinity reduction was observed by all strains in all batch tests, suggesting the nitrification process to be alkalinity limited and microalgae used in this experiment preferred ammonium as a nitrogen source. It is possible that some ammonium could have been removed by ammonia volatilization. The low alkalinity at the end of experiments implies that pH has decreased. *C. sorokiniana* removed more than 90% of phosphate and proved to be the most efficient phosphorous removal microalgae tested, followed by *T. obliquus* (83%). *C. vulgaris* and *M. salina* removed 63% and 50% respectively in wastewater. Wang et al. (2010) reported 90 % phosphorous removal of by *Chlorella sp.* in municipal wastewater. The N/P ratio for microalgal-based wastewater

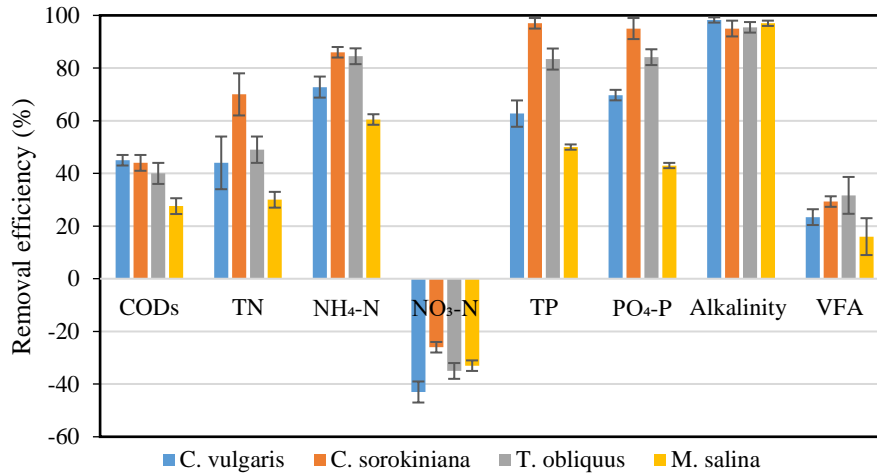


Figure 4.17 Microalgal nutrient, COD and alkalinity removal from secondary wastewater effluent in the batch system after reaching stationary phase. Error bars show standard deviations.

treatment has been proposed to be in the range of 6.8 to 10.0 (Wang et al., 2010). The measured N/P ratio in the UASB secondary wastewater effluent were slightly lower from this proposed optimal condition by 4.3, however, growth does not seem to be severely limited by phosphorous or nitrogen indicating another growth limiting factor to be decisive. Low alkalinity and limited nitrification suggest that to be CO₂.

TSS production of microalgal strains cultivated in wastewater after reaching the stationary phase represented dry microalgal biomass production. The microalgal production yield result is presented in Table 4.3. and show *C. sorokiniana* to have a relatively high yield compared to *C. vulgaris*, *M. salina*, and *T. obliquus*. The amount of TSS was measured before and after microalgal growth tests, and may be used as an indication of total microalgal biomass production (Ramaraj et al., 2015). Comparing these values with results gained in other studies indicates a high and effective biomass production (biomass per liquid volume). Ramaraj et al. (2015) reported values ranging from 0.07 gTSS·l⁻¹ to 0.26 gTSS·l⁻¹ for microalgae consortia cultivated in a natural water

Main Results and Discussions

Table 4.3 TSS production and yield of microalgal strains cultivated in wastewater after reaching the stationary phase (\pm standard deviation).

<i>C. vulgaris</i>	<i>C. sorokiniana</i>	<i>T. obliquus</i>	<i>M. salina</i>	Unit
0.75 \pm 0.23	1.05 \pm 0.34	1.35 \pm 0.18	0.60 \pm 0.12	gTSS \cdot l ⁻¹
0.03 \pm 0.01	0.04 \pm 0.01	0.02 \pm 0.005	0.02 \pm 0.01	gTN _{removed} \cdot gSS ⁻¹
0.02 \pm 0.003	0.02 \pm 0.004	0.01 \pm 0.005	0.01 \pm 0.006	gTP _{removed} \cdot gSS ⁻¹

media. Biomass productivity of microalgae cultivated in effluent from a submerged membrane anaerobic bioreactor by Ruiz-Martinez et al. (2012) resulted in a maximum biomass level of 0.6 gTSS \cdot l⁻¹.

Microalgae can remove organic carbon through mixotrophic or heterotrophic metabolism (Cai et al., 2013). As presented in Figure 4.17, *C. vulgaris* demonstrated the highest dissolved COD removal by 45 \pm 2%, followed by *C. sorokiniana* and *T. obliquus*, with removal efficiencies of 44 \pm 3% and 40 \pm 4%, respectively, likely the result of co-cultured with heterotrophs which would growth symbiotically with the microalgae. Moreover, organic and nutrient removal by *C. vulgaris* and *C. sorokiniana* indicated they are mixotrophic culture as it has been known that acetate has been used as the main carbon source in some industrial mixotrophic cultivations of *Chlorella* (Richmond, 2003). CO₂ can be the limiting nutrient in microalgal cultivation when using atmospheric CO₂ as an inorganic carbon source. As shown in Figure 4.17, all microalgal species removed all the alkalinity in the wastewater, implying nitrification. Therefore, addition of an external CO₂ or co-culturing with ordinary heterotrophic bacteria could enhance microalgal growth and nutrient removal. For example, biogas produced in the UASB system could be used as CO₂ source with a proper gas collecting system. However, in this presented study, there was no biogas handling, and CO₂ was likely stripped by the membrane system.

4.5.3 Nutrient-limited kinetic growth analysis of *Chlorella sorokiniana* in microplate well

Nutrient limitation of *C. sorokiniana* growth was evaluated by microplate reader analysis. Statistical analysis and microplate reader calibration are presented in Appendix 4B. The growth of *C. sorokiniana* was measured at various initial nutrient concentrations. Figure 4.18 presents observed growth rates at increasing nitrogen (NH_4^+) and phosphorous concentrations. The investigations were carried out to find out identify Monod growth parameters for specific nutrient-limited growth. Maximum specific growth rate (μ_{max}) and half saturation constants (K) were estimated by regression analysis of the Lineweaver-Burk linearized Monod equation. Lineweaver-Burk plot (Figure 4.19) was found to fit the growth profile of microalgae ($R^2=0.96$ and $R^2=0.93$), and the estimated kinetic coefficients are presented in Table 4.4.

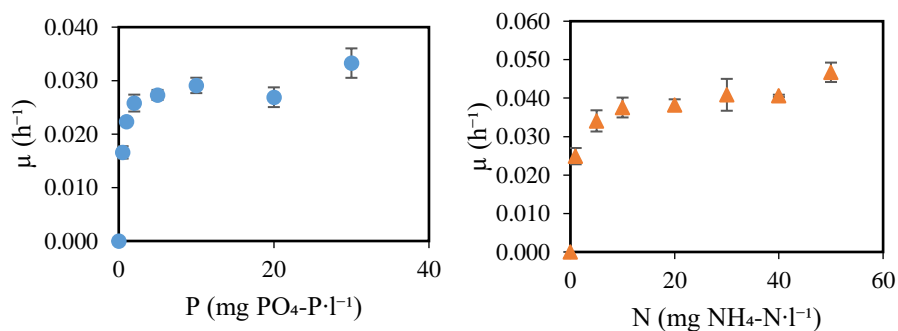


Figure 4.18 Growth rates vs. nutrient concentrations showing single nutrient limitation (phosphate limited-blue circle, ammonium limited-orange triangle). Error bars represent standard deviations.

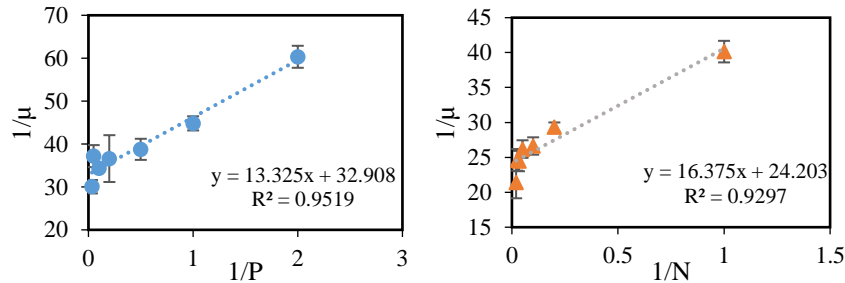


Figure 4.19 Lineweaver-Burk plot on microalgal kinetic experiment (phosphate limited-blue circle. ammonium limited-orange triangle) after five replications of experiment. Error bars represent standard deviations.

Maximum specific growth rate (μ_{\max}) was approximately $0.03 \pm 0.01 \text{ h}^{-1}$. Literature values of *C. sorokiniana* maximum specific growth rate vary significantly, from $0.06 - 0.2 \text{ h}^{-1}$, the high variance probably due to media composition and experimental set up (Cuaresma et al., 2009; Negi et al., 2016; van Wagenen et al., 2015). Half saturation constants (K) were $0.41 \pm 0.25 \text{ mg} \cdot \text{l}^{-1}$ and $0.68 \pm 0.14 \text{ mg} \cdot \text{l}^{-1}$ of phosphate and ammonium limited concentration respectively. Especially for ammonium, this is higher compared to microalgal experiment in the literatures in range of $0.07 - 0.8 \text{ mgPO}_4\text{-P} \cdot \text{l}^{-1}$ and $0.08 - 0.2 \text{ mgNH}_4\text{-N} \cdot \text{l}^{-1}$ (Kumar et al., 2014; Nyholm, 1977; Sterner & Grover, 1998). This could be explained by the media composition and reduced substrate availability in batch operation (small well of microplate) with the increasing number of cells in the system. Although carbonate concentration in this experiment was increased (1 mM HCO_3^-), the basic MWC+Se media used was originally

Table 4.4 The values of *C. sorokiniana* kinetic parameters of Monod equation were determined by regression analysis of the linearized Lineweaver-Burk equation (mean \pm standard deviation).

Kinetic Constants	Phosphate Limited Experiment	Ammonium Limited Experiment
$\mu_{\max} (\text{h}^{-1})$	0.03 ± 0.01	0.03 ± 0.01
td, min (h)	22.8 ± 4.7	17.1 ± 3.5
K ($\text{mg} \cdot \text{l}^{-1}$)	0.41 ± 0.25	0.68 ± 0.14

carbon limited media without CO₂ addition (4C:15N:1P). Based on literatures, the average molar ratio of C, N, and P in microalgae is assumed to follow the Redfield ratio of 106C:16N:1P (Redfield, 1960), though many studies have found the evidence of deviations from this ratio (Hulatt et al., 2012; Townsend et al., 2008). The standard error values of kinetic constants (Table 4.4) were less than 10% which indicated high accuracy of the microplate measurement. To conclude, the microplate-based method is a fast, low-cost methodology capable of high throughput microalgae growth studies. The methodology was also useful for limited growth studies, and suitable for identification of growth kinetic parameters. Hence, the study supports the findings in section 4.5.2 and the research statement therein.

4.5.4 Evaluation of selected microalgae strain for nutrient removal in a continuous photobioreactor system

As presented in Chapter 4.5.2, screening results implied maximized nutrient removal by *C. sorokiniana* for filtered UASB secondary effluent. Therefore, *C. sorokiniana* was chosen for filtered UASB secondary effluent post-treatment in a continuous photobioreactor (PBR) system for evaluation of sustained growth in a continuous system. The effluent quality used in the PBR experiment were slightly different to the batch experiments (Table 4.1) and not conducted simultaneously. The filtered UASB effluent characteristics for the PBR feeding is presented as mean values over the growth period and shown in Table 4.5 (n=67). Similar to the batch studies, nitrogen and phosphorous in the secondary wastewater effluent are present as readily assimilable ammonium and phosphate.

Figure 4.20 presents phosphate concentration profile at the inlet and effluent of the PBR throughout 109 days of continuous operation. In general, the system removed TN and TP by 17±11% and 27±16% (±standard deviations), respectively, with hydraulic retention time of 5.5 days. The orthophosphate removal efficiency was not significant from

the TP (26±13%). Current results are comparable to removal efficiency of microalgae-bacteria consortia following digestate treatment (Pizzera et al., 2019). Furthermore, the results show that the PBR system removed ammonium by 97±3% with an almost concurrent nitrate concentration increase of 73±13%.

Table 4.5 Secondary effluent wastewater characteristics after UASB reactor and tight-micro filtration (T-MF) treatment that was used in microalgal-based treatment in a continuous PBR system for nutrient removal.

Parameters	Unit	Effluent Quality		
		DAF Pre-treatment	UASBR	T-MF
Physico-chemical Parameter:				
_s COD	mg·l ⁻¹	815±77	476±71	490±95
_t COD	mg·l ⁻¹	917±179	526±118	511±104
TSS	mg·l ⁻¹	368±53	12.5±5.5	0.15 ±0.21
NH ₄ ⁺	mg·l ⁻¹	157±28	155±36	155±44
NO ₃ ⁻	mg·l ⁻¹	<0.5	1.5±0.7	2.1±0.4
PO ₄ ³⁻	mg·l ⁻¹	24±7	20±2	19±2
TN	mg·l ⁻¹	216±17	200±32	198±47
TP	mg·l ⁻¹	25±5	22±4	20±2
Alkalinity	mg CaCO ₃ ·l ⁻¹	356±36	434±127	409±88
Total VFA	mg CH ₃ COOH·l ⁻¹	143±29	328±66	368±45
Microbiological Parameters^a:				
Total Coliforms	log ₁₀ CFU·(100 ml) ⁻¹	3.3±0.3	3.3±0.4	0
<i>E. coli</i>	log ₁₀ CFU·(100 ml) ⁻¹	1.6±0.1	1.5±0.3	0
<i>Enterococci</i>	log ₁₀ CFU·(100 ml) ⁻¹	1.9±0.4	1.8±0.1	0
Heterotrophs	log ₁₀ CFU·(100 ml) ⁻¹	5.5±0.2	5.3±0.3	1.29±0.6

^aAdapted from Boateng (2019) and Khanal (2019)

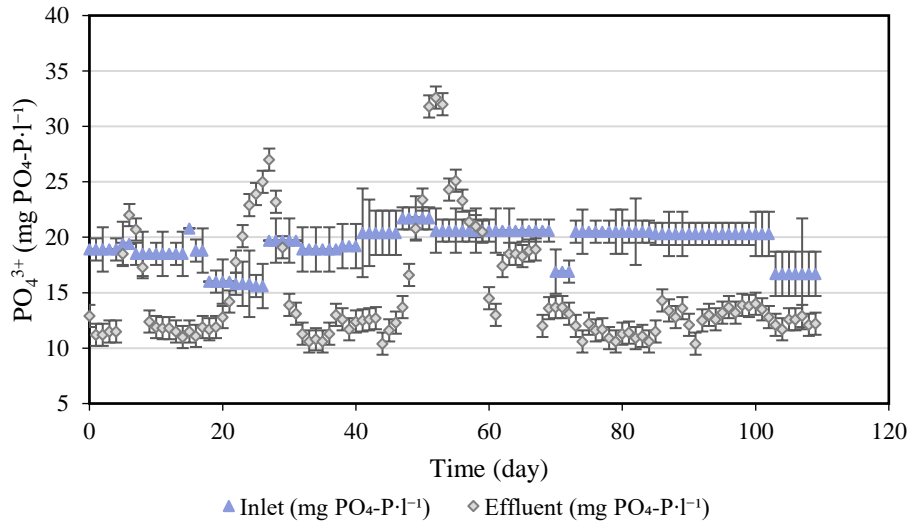


Figure 4.20 $PO_4\text{-P}$ concentration profiles at the inlet and effluent of the PBR throughout 109 days continuous operation. Error bars represent standard deviations from triplicate samples from PBR ($n=3$).

Ammonium (A) and nitrate (B) concentration profiles at the inlet and effluent of the PBR throughout 109 days of continuous operation are presented in Figure 4.21. On day 60, ammonium concentration increased, and nitrate concentration decreased significantly, indicative of predominant nitrification to microalgal assimilation. Specific biomass production in the PBR was higher ($0.16 \pm 0.02 \text{ gTN}_{\text{removed}} \cdot \text{gSS}^{-1}$ and $0.03 \pm 0.005 \text{ gTP}_{\text{removed}} \cdot \text{gSS}^{-1}$), compared to the batch test ($0.04 \pm 0.01 \text{ gTN}_{\text{removed}} \cdot \text{gSS}^{-1}$ and $0.02 \pm 0.002 \text{ gTP}_{\text{removed}} \cdot \text{gSS}^{-1}$). A major factor leading to a higher yield is nutrient loading, specifically nitrogen loading. As shown in Table 4.1 and Table 4.5, TN concentration in batch test was significantly lower ($56 \text{ mgN} \cdot \text{l}^{-1}$) compared to continuous PBR system ($216 \text{ mgN} \cdot \text{l}^{-1}$). Furthermore, longer hydraulic retention time was used in batch tests (9 days), compared to continuous PBR system (5.5 days). In this experiment, high ammonium removal but low nitrate removal was seen. This could indicate that the microalgae used in this experiment prefer ammonium as nitrogen source, and compete for ammonium with nitrifiers. Pizzera et al. (2019) found more than 50% of the nitrogen load

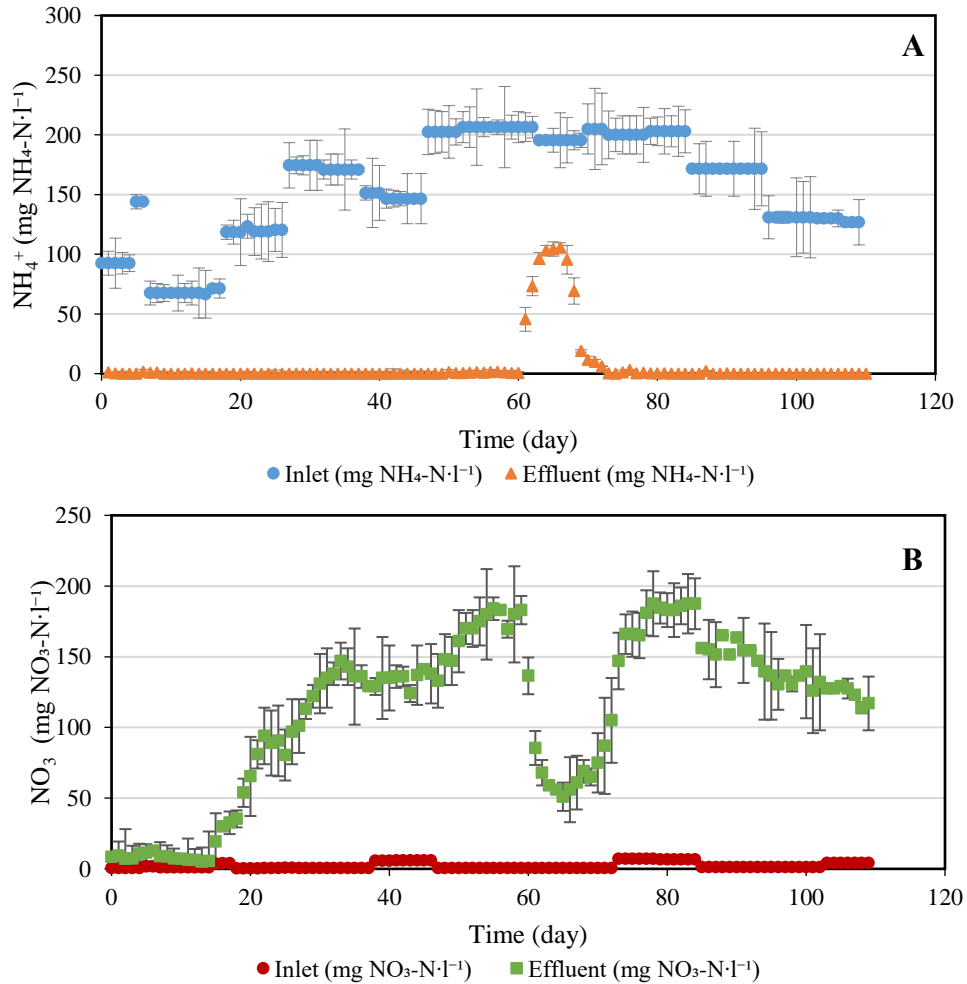


Figure 4.21 Ammonium (A) and nitrate (B) concentration profiles at the inlet and effluent of the PBR throughout 109 days continuous operation. Error bars represent standard deviations from triplicate samples from PBR ($n=3$).

was oxidized by nitrification when applying microalgae-bacteria consortia for digestate treatment. Microalgae/nitrifier consortia can syntrophically enhance the nitrogen conversion capacity of the system. By providing oxygen to nitrifiers, microalgae substantially increase the overall ammonium removal capacity of the system, while nitrifiers reduce oxygen levels below the inhibition thresholds for microalgae

(Bilanovic et al., 2016). Nitrification, in turn, helps by keeping the ammonium concentration low, thus reducing the risk of free ammonia inhibition on microalgae, especially when high strength wastewaters are to be treated (Rossi et al., 2020). The consortia, however, compete for the same carbon source, unless mixotrophic microalgae predominates.

The consortia may also compete for micronutrients (Delgadillo-Mirquez et al., 2016) and experience amensalism by inhibition of bacterial growth by photosynthetic increase of pH (van Hulle et al., 2010). These complex interplays make the overall dynamics of nitrifiers/microalgae especially challenging to understand and predict, as well as highly dependent on the composition of the wastewater to be treated and on the operation parameters (Unnithan et al., 2014).

Lower nutrient removal could also be explained by carbon limitations in the experiment. Although carbonate (alkalinity) in this experiment was available from secondary wastewater effluent, the wastewater used was originally carbon limited media (2C:22N:1P), and an almost 100% removal of alkalinity was observed. The average molar ratio of C, N, and P in microalgae is assumed to follow the Redfield ratio of 106C:16N:1P (Redfield, 1960), though many studies have found evidence of slight deviations (Hulatt et al., 2012; Townsend et al., 2008). Posadas et al. (2015) showed a great effect of applying an external source of CO₂ for pH and alkalinity control, as well as increasing removal of COD, TP and TN. Furthermore, alkalinity was revealed to be a hidden process parameter that must be controlled to operate the system under optimal conditions for microalgae-bacteria consortia (Casagli et al., 2021). COD removal in the PBR system was significant at 48±15% (Appendix 4B). Either aerobic heterotrophic bacteria degradation or mixotrophic microalgal is the likely cause of this COD removal, however, available data are insufficient in order to distinguish between them.

As mentioned in Chapter 3.6, the microalgal cultures were regularly examined and checked for cell viability under a microscope. The results

showed that *T. obliquus* was found on day 19 in the PBR, even though it was originally inoculated only with an axenic culture of *C. sorokiniana*. Two signals, typical for the two species, were also identified in flow cytometry while quantifying microalgal cells after day 19. Figure 4.22 shows the comparison of microalgae culture in PBR under a microscope before and after *T. obliquus* emerging. *C. sorokiniana* and *T. obliquus* are species able to coexist within the same environment (Kong et al., 2021; Shen et al., 2015b), and long term cultivation showed a stable coculture.

The experiment showed that *C. sorokiniana* could sustain growth and remove nutrients in UASB effluent over the 110 days studied, but optimization of is necessary to enhance nutrient removal. Invasion of *T. obliquus* did not deteriorate nutrient removal, indicate that *C. Sorokiniana* may be sustained also in open cultures (with reference to research question, RQ6).

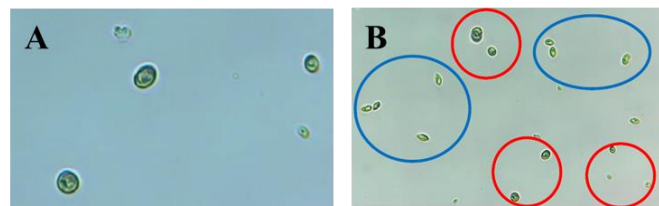


Figure 4.22 (A) Microalgae culture under the microscope (optics $\times 40$) in PBR at day 11 indicating *C. sorokiniana*, (B) Microalgae culture in PBR at day 21, *T. obliquus* within the blue circles and *C. sorokiniana* within red circles.

5 Conclusions and Future Research

The research presented in this thesis demonstrates the potential of applying up-flow anaerobic sludge blanket (UASB) technology for municipal wastewaters under low-temperature conditions and variable loadings. The performed long-term evaluation brought novel insights into the feasibility and limitations of anaerobic bioconversion of municipal wastewater under these conditions while applying several post-treatment unit processes to ensure sustainable wastewater treatment and resource recovery. The developed UASB technology opens interesting perspectives for such municipal wastewaters at low-temperatures. This chapter outlines the conclusion of the research study as well as future research directions.

5.1 Main conclusions

The main conclusions of the presented work based on the research questions (Chapter 2.8) are stated as follows:

UASB system for municipal wastewater treatment at low-temperatures and variable loadings

- a. The long term UASB system was established treating real municipal wastewater at the decreasing temperatures (25 - 2.5 °C) and increasing OLRs (1.0 - 15.0 gCOD·l⁻¹·d⁻¹). The sustained UASB reactor performance was maintained and confirmed by COD removal and methane production. This study demonstrated the feasibility of UASB system application treating municipal wastewater at low-temperatures and variable loadings.
- b. Long-term operation under low-temperature conditions lead to the selection of a less dynamic cold-adapted consortium, including psychrotolerant bacteria and methanogens. Temperature affected the reactor performances and the structure of the microbial community. Microbial community proved the adaptation ability to low-

- temperatures down to 2.5 °C regardless of the operating OLR; psychrotolerant communities. Acetoclastic methanogens became important members of the methanogenic community and acetate was the main precursor organic degradation pathway at low-temperatures.
- c. The simulation results could predict and simulate biofilm model implementation and assumptions specific to the granules as a fixed biofilm in UASB reactor system. Furthermore, it simulated the effect of organic loading on reactor performances and biofilm characteristic(s).

Methanotrophs-photogranules experiment for dissolved methane removal

- d. A methanotrophic-cyanobacterial syntrophy was established in the existing oxygenic photogranules. This syntrophy was maintained and propagated in a continuously operated reactor, proven by biomass growth and the removal of dissolved methane as potential biocatalyst for anaerobic effluents post-treatment.
- e. The community composition suggested methanotrophs and cyanobacteria syntrophy in photogranules to remove dissolved methane, not only contained methanotrophic bacteria and phototrophs, but also non-methanotrophic methylotrophs.

Microalgae-based wastewater treatment for nutrient removal

- f. Microalgae strain *C. sorokiniana* presented ability to grow in specific filtered UASB secondary effluent. The results implied nutrient removal achieved when applying microalgae *C. sorokiniana* in the batch test and a continuous photobioreactor (PBR) system. High ammonium removal yet high nitrate release indicated microalgae-nitrifiers imbalance in the PBR system. Unfavorable growth factor for microalgae in the PBR could be carbon limited media in wastewater (2C:22N:1P).

5.2 Future research

This study showed that anaerobic treatment systems using UASB reactor for treating high strength municipal wastewater represent a feasible and attractive alternative treatment for removing organics even at low-temperatures and high loading. In addition, the system contributed to energy recovery by converting organic matter into economically valuable methane. Furthermore, UASB system followed by other unit processes as post-treatments, in this case, membrane treatment, microalgal-based treatment, and methanotroph-photogranule system, gave a promising step to achieve sustainable wastewater treatment for resource recovery, i.e., energy, nutrient, and reused water. Still, there are many research and practical questions as natural progressions to this work:

- a. This study was approached by a performance study of the selected unit processes individually. An integration evaluation in the laboratory- and pilot-scale system investigation in the future would bring the endeavor closer to a real application at actual temperature conditions.
- b. The presence of other possible ions, e.g., SO_4^{2-} , could also be significant in anaerobic processes. VFA specification is also essential for UASB performance analysis and understanding changes in trophic structure and redistribution of carbon flow along with microbial community development on anaerobic granules.
- c. Despite the usefulness of the model as described in Chapter 4.3, available data are insufficient to validate the model simulation. Biofilm profile data and non-steady-state data from the UASB reactor are needed for validation. Furthermore, several specific modifications are required to produce a tool for applications such as growth and accumulation, prediction of inhibitor profiles, and advanced parameter identification. These modifications include assessment of the in-granule physico-chemical system, microbial pH buffering, the influence of hydrogen sulfide production, and particle population

- modelling, which should include shear, surface attachment, and granule breakage.
- d. In the present methanotrophic-photogranule study, the presence of non-methanotrophic methylotrophs is not problematic if the biotechnological aim was the removal of dissolved methane as post-treatment of anaerobic effluent. If simultaneous molecule recovery was the intention, e.g., methanol production, work on more specific ways for controlling the activity of the open microbial community would be needed.
 - e. Methanotrophic-photogranule reactor system should focus on treating real anaerobic wastewaters effluent in a long-term continuous mode. Nutrient recovery and an increased loading rate need to be studied as a function of temperature. Photogranules may be suitable to remove methane after psychrophilic anaerobic wastewater treatment with increased methane solubility and decreased biological kinetics. Furthermore, one essential consideration is maximizing natural light for the co-culture to reduce electricity costs. Due to diurnal cycles, a mixture of natural light and artificial light can be used to maintain high productivities and efficiencies depending on the process requirements.
 - f. Some scenarios on microalgal-based wastewater treatment could be applied for better performances in continuous PBR systems, such as mixotrophy, cyclic heterotrophy/autotrophy approach investigation, and/or additional anoxic system. In addition, the effect of adding an external source of CO₂ to control alkalinity, pH, and provide carbon for microalgal growth should be studied.

Bibliography

- Abe, K., Ueki, A., Ohtaki, Y., Kaku, N., Watanabe, K., & Ueki, K. (2012). *Anaerocella delicata* gen. Nov., sp. Nov., a strictly anaerobic bacterium in the phylum Bacteroidetes isolated from a methanogenic reactor of cattle farms. *The Journal of General and Applied Microbiology*, 58(6), 405–412. <https://doi.org/10.2323/jgam.58.405>
- Abid, A., Saidane, F., & Hamdi, M. (2017). Feasibility of carbon dioxide sequestration by *Spongiochloris* sp microalgae during petroleum wastewater treatment in airlift bioreactor. *Bioresource Technology*, 234, 297–302. <https://doi.org/10.1016/j.biortech.2017.03.041>
- Abouhend, A. S., Milferstedt, K., Hamelin, J., Ansari, A. A., Butler, C., Carbajal-González, B. I., & Park, C. (2020). Growth progression of oxygenic photogranules and its impact on bioactivity for aeration-free wastewater treatment. *Environmental Science & Technology*, 54(1), 486–496. <https://doi.org/10.1021/acs.est.9b04745>
- Acién, F. G., Gómez-Serrano, C., Morales-Amaral, M. M., Fernández-Sevilla, J. M., & Molina-Grima, E. (2016). Wastewater treatment using microalgae: How realistic a contribution might it be to significant urban wastewater treatment? *Applied Microbiology and Biotechnology*, 100(21), 9013–9022. <https://doi.org/10.1007/s00253-016-7835-7>
- Aida, A. A., Kuroda, K., Yamamoto, M., Nakamura, A., Hatamoto, M., & Yamaguchi, T. (2015). Diversity Profile of Microbes Associated with Anaerobic Sulfur Oxidation in an Upflow Anaerobic Sludge Blanket Reactor Treating Municipal Sewage. *Microbes and Environments*, 30(2), 157–163. PubMed. <https://doi.org/10.1264/jsme2.ME14105>

- Aiyuk, S., Amoako, J., Raskin, L., van Haandel, A., & Verstraete, W. (2004). Removal of carbon and nutrients from domestic wastewater using a low investment, integrated treatment concept. *Water Research*, 38(13), 3031–3042. <https://doi.org/10.1016/j.watres.2004.04.040>
- Akila, G., & Chandra, T. S. (2007). Performance of an UASB reactor treating synthetic wastewater at low-temperature using cold-adapted seed slurry. *Process Biochemistry*, 42(3), 466–471. <https://doi.org/10.1016/j.procbio.2006.09.010>
- Almomani, F., Al Ketife, A., Judd, S., Shurair, M., Bhosale, R. R., Znad, H., & Tawalbeh, M. (2019). Impact of CO₂ concentration and ambient conditions on microalgal growth and nutrient removal from wastewater by a photobioreactor. *Science of The Total Environment*, 662, 662–671. <https://doi.org/10.1016/j.scitotenv.2019.01.144>
- AlSayed, A., Fergala, A., & Eldyasti, A. (2018). Sustainable biogas mitigation and value-added resources recovery using methanotrophs intergrated into wastewater treatment plants. *Reviews in Environmental Science and Bio/Technology*, 17(2), 351–393. <https://doi.org/10.1007/s11157-018-9464-3>
- Andersen, R. A. (2004). *Algal culturing techniques* (1st ed.). Academic Press.
- Ángeles, R., Vega-Quiel, M. J., Batista, A., Fernández-Ramos, O., Lebrero, R., & Muñoz, R. (2021). Influence of biogas supply regime on photosynthetic biogas upgrading performance in an enclosed algal-bacterial photobioreactor. *Algal Research*, 57, 102350. <https://doi.org/10.1016/j.algal.2021.102350>
- Angelidaki, I., Karakashev, D., Batstone, D. J., Plugge, C. M., & Stams, A. J. M. (2011). Chapter sixteen—Biomethanation and Its Potential. In A. C. Rosenzweig & S. W. Ragsdale (Eds.), *Methods in Enzymology* (Vol. 494, pp. 327–351). Academic Press. <https://doi.org/10.1016/B978-0-12-385112-3.00016-0>

- Aquino, S. F., Araújo, J. C., Passos, F., Curtis, T. P., & Foresti, E. (2019). Fundamentals of anaerobic sewage treatment. In C. A. de Lemos Chernicharo & T. Bressani-Ribeiro (Eds.), *Anaerobic Reactors for Sewage Treatment: Design, Construction and Operation* (p. 0). IWA Publishing. https://doi.org/10.2166/9781780409238_0023
- Arcand, Y., Guiot, S. R., Desrochers, M., & Chavarie, C. (1994). Impact of the reactor hydrodynamics and organic loading on the size and activity of anaerobic granules. *The Chemical Engineering Journal and the Biochemical Engineering Journal*, 56(1), B23–B35. [https://doi.org/10.1016/0923-0467\(94\)87028-4](https://doi.org/10.1016/0923-0467(94)87028-4)
- Arcangeli, J.-P., & Arvin, E. (1999). Modelling the growth of a methanotrophic biofilm: Estimation of parameters and variability. *Biodegradation*, 10(3), 177–191. <https://doi.org/10.1023/A:1008317906069>
- Baeten, J. E., Batstone, D. J., Schraa, O. J., van Loosdrecht, M. C. M., & Volcke, E. I. P. (2019). Modelling anaerobic, aerobic and partial nitrification-anammox granular sludge reactors—A review. *Water Research*, 149, 322–341. <https://doi.org/10.1016/j.watres.2018.11.026>
- Bailey, A. D., Hansford, G. S., & Dold, P. L. (1994). The enhancement of upflow anaerobic sludge bed reactor performance using crossflow microfiltration. *Water Research*, 28(2), 291–295. [https://doi.org/10.1016/0043-1354\(94\)90266-6](https://doi.org/10.1016/0043-1354(94)90266-6)
- Bandara, W. M. K. R. T. W., Kindaichi, T., Satoh, H., Sasakawa, M., Nakahara, Y., Takahashi, M., & Okabe, S. (2012). Anaerobic treatment of municipal wastewater at ambient temperature: Analysis of archaeal community structure and recovery of dissolved methane. *Water Research*, 46(17), 5756–5764. <https://doi.org/10.1016/j.watres.2012.07.061>
- Bandara, W. M. K. R. T. W., Satoh, H., Sasakawa, M., Nakahara, Y., Takahashi, M., & Okabe, S. (2011). Removal of residual

- dissolved methane gas in an upflow anaerobic sludge blanket reactor treating low-strength wastewater at low temperature with degassing membrane. *Water Research*, 45(11), 3533–3540. <https://doi.org/10.1016/j.watres.2011.04.030>
- Barker, D. J., & Stuckey, D. C. (1999). A review of soluble microbial products (SMP) in wastewater treatment systems. *Water Research*, 33(14), 3063–3082. [https://doi.org/10.1016/S0043-1354\(99\)00022-6](https://doi.org/10.1016/S0043-1354(99)00022-6)
- Batstone, D. J. (2006). Mathematical Modelling of Anaerobic Reactors Treating Domestic Wastewater: Rational Criteria for Model Use. *Reviews in Environmental Science and Bio/Technology*, 5(1), 57–71. <https://doi.org/10.1007/s11157-005-7191-z>
- Batstone, D. J., & Keller, J. (2001). Variation of bulk properties of anaerobic granules with wastewater type. *Water Research*, 35(7), 1723–1729. [https://doi.org/10.1016/S0043-1354\(00\)00446-2](https://doi.org/10.1016/S0043-1354(00)00446-2)
- Batstone, D. J., Keller, J., Angelidaki, I., Kalyuzhnyi, S. V., Pavlostathis, S. G., Rozzi, A., Sanders, W. T. M., Siegrist, H., & Vavilin, V. A. (2002). The IWA Anaerobic Digestion Model No 1 (ADM1). *Water Science and Technology*, 45(10), 65–73. <https://doi.org/10.2166/wst.2002.0292>
- Batstone, D. J., Keller, J., & Blackall, L. L. (2004). The influence of substrate kinetics on the microbial community structure in granular anaerobic biomass. *Water Research*, 38(6), 1390–1404. <https://doi.org/10.1016/j.watres.2003.12.003>
- Becker, E. W. (2007). Micro-algae as a source of protein. *Biotechnology Advances*, 25(2), 207–210. <https://doi.org/10.1016/j.biotechadv.2006.11.002>
- Benfield, L. D., & Randall, C. W. (1980). *Biological process design for wastewater treatment*. Prentice-Hall; /z-wcorg/. <http://books.google.com/books?id=rSVSAAAAMAAJ>
- Bhakta, J. N., Lahiri, S., Pittman, J. K., & Jana, B. B. (2015). Carbon dioxide sequestration in wastewater by a consortium of elevated

- carbon dioxide-tolerant microalgae. *Journal of CO2 Utilization*, 10, 105–112. <https://doi.org/10.1016/j.jcou.2015.02.001>
- Bilanovic, D., Holland, M., Starosvetsky, J., & Armon, R. (2016). Co-cultivation of microalgae and nitrifiers for higher biomass production and better carbon capture. *Bioresource Technology*, 220, 282–288. <https://doi.org/10.1016/j.biortech.2016.08.083>
- Boateng, Y. (2019). Pathogenic Bacteria and Antibiotic Resistance Gene Removal Using Up-flow Anaerobic Sludge Blanket (UASB). *University of Stavanger, Norway*. <http://hdl.handle.net/11250/2623654>
- Boretti, A. (2020). Covid19 pandemic as a further driver of water scarcity in Africa. *GeoJournal*. <https://doi.org/10.1007/s10708-020-10280-7>
- Boussiba, S., & Vonshak, A. (1991). Astaxanthin Accumulation in the Green Alga *Haematococcus pluvialis*1. *Plant and Cell Physiology*, 32, 1077–1082.
- Bowen, E. J., Dolfing, J., Davenport, R. J., Read, F. L., & Curtis, T. P. (2014). Low-temperature limitation of bioreactor sludge in anaerobic treatment of domestic wastewater. *Water Science and Technology*, 69(5), 1004. <https://doi.org/10.2166/wst.2013.821>
- Brandt, E. M. F., Noyola, A., & McAdam, E. J. (2019). Control of diffuse emissions in UASB reactors treating sewage. In C. A. de Lemos Chernicharo & T. Bressani-Ribeiro (Eds.), *Anaerobic Reactors for Sewage Treatment: Design, Construction and Operation* (p. 0). IWA Publishing. https://doi.org/10.2166/9781780409238_0237
- Buffière, P., Steyer, J.-P., Fonade, C., & Moletta, R. (1995). Comprehensive modeling of methanogenic biofilms in fluidized bed systems: Mass transfer limitations and multisubstrate aspects. *Biotechnology and Bioengineering*, 48(6), 725–736. <https://doi.org/10.1002/bit.260480622>

- Cabral, C. S., Sanson, A. L., Afonso, R. J. C. F., Chernicharo, C. A. L., & Araújo, J. C. (2020). Impact of microaeration bioreactor on dissolved sulfide and methane removal from real UASB effluent for sewage treatment. *Water Science and Technology*, *81*(9), 1951–1960. <https://doi.org/10.2166/wst.2020.250>
- Cai, T., Park, S. Y., & Li, Y. (2013). Nutrient recovery from wastewater streams by microalgae: Status and prospects. *Renewable and Sustainable Energy Reviews*, *19*, 360–369. <https://doi.org/10.1016/j.rser.2012.11.030>
- Cao, Y. S., & Ang, C. M. (2009). Coupled UASB-activated sludge process for COD and nitrogen removals in municipal sewage treatment in warm climate. *Water Science and Technology*, *60*(11), 2829–2839. <https://doi.org/10.2166/wst.2009.725>
- Cardinali-Rezende, J., Araújo, J. C., Almeida, P. G. S., Chernicharo, C. A. L., Sanz, J. L., Chartone-Souza, E., & Nascimento, A. M. A. (2013). Organic loading rate and food-to-microorganism ratio shape prokaryotic diversity in a demo-scale up-flow anaerobic sludge blanket reactor treating domestic wastewater. *Antonie van Leeuwenhoek*, *104*(6), 993–1003. <https://doi.org/10.1007/s10482-013-0018-y>
- Carmona-Martínez, A. A., Marcos-Rodrigo, E., Bordel, S., Marín, D., Herrero-Lobo, R., García-Encina, P. A., & Muñoz, R. (2021). Elucidating the key environmental parameters during the production of ectoines from biogas by mixed methanotrophic consortia. *Journal of Environmental Management*, *298*, 113462. <https://doi.org/10.1016/j.jenvman.2021.113462>
- Casagli, F., Rossi, S., Steyer, J. P., Bernard, O., & Ficara, E. (2021). Balancing Microalgae and Nitrifiers for Wastewater Treatment: Can Inorganic Carbon Limitation Cause an Environmental Threat? *Environmental Science & Technology*, *55*(6), 3940–3955. <https://doi.org/10.1021/acs.est.0c05264>

- Cavicchioli, R. (2006). Cold-adapted archaea. *Nature Reviews Microbiology*, 4, 331.
- Chernicharo, C. A. L. (2006). Post-Treatment Options for the Anaerobic Treatment of Domestic Wastewater. *Reviews in Environmental Science and Bio/Technology*, 5(1), 73–92. <https://doi.org/10.1007/s11157-005-5683-5>
- Chernicharo, C. A. L., Lobato, L. C. S., Bressani-Ribeiro, T., Pereira, R. A. S., Lermontov, A., & Francisco, L. L. (2019). Experience with full-scale uasb reactors treating sewage. In C. A. de Lemos Chernicharo & T. Bressani-Ribeiro (Eds.), *Anaerobic Reactors for Sewage Treatment: Design, Construction and Operation* (p. 0). IWA Publishing. https://doi.org/10.2166/9781780409238_0159
- Chernicharo, C. A. L., & Nascimento, M. C. P. (2001). Feasibility of a pilot-scale UASB/trickling filter system for domestic sewage treatment. *Water Science and Technology*, 44(4), 221–228. <https://doi.org/10.2166/wst.2001.0227>
- Chioccioli, M., Hankamer, B., & Ross, I. L. (2014). Flow Cytometry Pulse Width Data Enables Rapid and Sensitive Estimation of Biomass Dry Weight in the Microalgae *Chlamydomonas reinhardtii* and *Chlorella vulgaris*. *PLOS ONE*, 9(5), e97269. <https://doi.org/10.1371/journal.pone.0097269>
- Chisti, Y. (2007). Biodiesel from microalgae. *Biotechnology Advances*, 25(3), 294–306. <https://doi.org/10.1016/j.biotechadv.2007.02.001>
- Choix, F. J., Ochoa-Becerra, M. A., Hsieh-Lo, M., Mondragón-Cortez, P., & Méndez-Acosta, H. O. (2018). High biomass production and CO₂ fixation from biogas by *Chlorella* and *Scenedesmus* microalgae using tequila vinasses as culture medium. *Journal of Applied Phycology*, 30(4), 2247–2258. <https://doi.org/10.1007/s10811-018-1433-2>

- Collins, G., Mahony, T., & O’Flaherty, V. (2006). Stability and reproducibility of low-temperature anaerobic biological wastewater treatment. *FEMS Microbiology Ecology*, *55*(3), 449–458. <https://doi.org/10.1111/j.1574-6941.2005.00034.x>
- Collins, G., McHugh, S., Connaughton, S., Enright, A.-M., Kearney, A., Scully, C., Mahony, T., Madden, P., & O’Flaherty, V. (2006). New Low-Temperature Applications of Anaerobic Wastewater Treatment. *Journal of Environmental Science and Health, Part A*, *41*(5), 881–895. <https://doi.org/10.1080/10934520600614504>
- Conrad, R. (2020). Importance of hydrogenotrophic, acetoclastic and methylotrophic methanogenesis for methane production in terrestrial, aquatic and other anoxic environments: A mini review. *Pedosphere*, *30*(1), 25–39. [https://doi.org/10.1016/S1002-0160\(18\)60052-9](https://doi.org/10.1016/S1002-0160(18)60052-9)
- Cookney, J., Mcleod, A., Mathioudakis, V., Ncube, P., Soares, A., Jefferson, B., & McAdam, E. J. (2016). Dissolved methane recovery from anaerobic effluents using hollow fibre membrane contactors. *Journal of Membrane Science*, *502*, 141–150. <https://doi.org/10.1016/j.memsci.2015.12.037>
- Coustets, M., Al-Karablieh, N., Thomsen, C., & Teissié, J. (2013). Flow Process for Electroextraction of Total Proteins from Microalgae. *The Journal of Membrane Biology*, *246*(10), 751–760. <https://doi.org/10.1007/s00232-013-9542-y>
- Cuaresma, M., Janssen, M., Vílchez, C., & Wijffels, R. H. (2009). Productivity of *Chlorella sorokiniana* in a short light-path (SLP) panel photobioreactor under high irradiance. *Biotechnology and Bioengineering*, *104*(2), 352–359. <https://doi.org/10.1002/bit.22394>
- Cunha, J. R., Tervahauta, T., van der Weijden, R. D., Temmink, H., Hernández Leal, L., Zeeman, G., & Buisman, C. J. N. (2018). The Effect of Bioinduced Increased pH on the Enrichment of Calcium Phosphate in Granules during Anaerobic Treatment of

- Black Water. *Environmental Science & Technology*, 52(22), 13144–13154. <https://doi.org/10.1021/acs.est.8b03502>
- da Silva Martins, A., Ornelas Ferreira, B., Ribeiro, N. C., Martins, R., Rabelo Leite, L., Oliveira, G., Colturato, L. F., Chernicharo, C. A., & de Araujo, J. C. (2017). Metagenomic analysis and performance of a mesophilic anaerobic reactor treating food waste at various load rates. *Environmental Technology*, 38(17), 2153–2163. <https://doi.org/10.1080/09593330.2016.1247197>
- Dague, R. R., Banik, G. C., & Ellis, T. G. (1998). Anaerobic Sequencing Batch Reactor Treatment of Dilute Wastewater at Psychrophilic Temperatures. *Water Environment Research*, 70(2), 155–160.
- Dai, Y.-M., Zhang, L.-L., Li, Y., Li, Y.-Q., Deng, X.-H., Wang, T.-T., Yang, F., Tian, Y.-Q., Li, N., Zhou, X.-M., Liu, X.-F., & Li, W.-J. (2018). Characterization of *Trichococcus paludicola* sp. Nov. And *Trichococcus alkaliphilus* sp. Nov., isolated from a high-elevation wetland, by phenotypic and genomic analyses. In *International Journal of Systematic and Evolutionary Microbiology* (Vol. 68, Issue 1, pp. 99–105). Microbiology Society. <https://doi.org/10.1099/ijsem.0.002464>
- Davis, R. W., Siccardi, A. J., Huysman, N. D., Wyatt, N. B., Hewson, J. C., & Lane, T. W. (2015). Growth of mono- and mixed cultures of *Nannochloropsis salina* and *Phaeodactylum tricorutum* on struvite as a nutrient source. *Bioresource Technology*, 198, 577–585. <https://doi.org/10.1016/j.biortech.2015.09.070>
- De Vrieze, J., Hennebel, T., Boon, N., & Verstraete, W. (2012). Methanosarcina: The rediscovered methanogen for heavy duty biomethanation. *Bioresource Technology*, 112, 1–9. <https://doi.org/10.1016/j.biortech.2012.02.079>
- Dedysh, S. N., & Knief, C. (2018). Diversity and phylogeny of described aerobic methanotrophs. In M. G. Kalyuzhnaya & X.-H. Xing (Eds.), *Methane biocatalysis: Paving the way to sustainability*

- (pp. 17–42). Springer International Publishing.
https://doi.org/10.1007/978-3-319-74866-5_2
- Delgadillo-Mirquez, L., Lopes, F., Taidi, B., & Pareau, D. (2016). Nitrogen and phosphate removal from wastewater with a mixed microalgae and bacteria culture. *Biotechnology Reports*, *11*, 18–26. <https://doi.org/10.1016/j.btre.2016.04.003>
- Denger, K., Warthmann, R., Ludwig, W., & Schink, B. (2002). *Anaerophaga thermohalophila* gen. Nov., sp. Nov., a moderately thermohalophilic, strictly anaerobic fermentative bacterium. *International Journal of Systematic and Evolutionary Microbiology*, *52*(1), 173–178. <https://doi.org/10.1099/00207713-52-1-173>
- Dev, S., Saha, S., Kurade, M. B., Salama, E.-S., El-Dalatony, M. M., Ha, G.-S., Chang, S. W., & Jeon, B.-H. (2019). Perspective on anaerobic digestion for biomethanation in cold environments. *Renewable and Sustainable Energy Reviews*, *103*, 85–95. <https://doi.org/10.1016/j.rser.2018.12.034>
- Dineshababu, G., Uma, V. S., Mathimani, T., Deviram, G., Arul Ananth, D., Prabaharan, D., & Uma, L. (2017). On-site concurrent carbon dioxide sequestration from flue gas and calcite formation in ossein effluent by a marine cyanobacterium *Phormidium valderianum* BDU 20041. *Sustainable Biofuels*, *141*, 315–324. <https://doi.org/10.1016/j.enconman.2016.09.040>
- Dolejs, P., El Tayar, G., Vejmelkova, D., Pecenka, M., Polaskova, M., & Bartacek, J. (2018). Psychrophilic anaerobic treatment of sewage: Biomethane potential, kinetics and importance of inoculum selection. *Journal of Cleaner Production*, *199*, 93–100. <https://doi.org/10.1016/j.jclepro.2018.07.134>
- Doloman, A., Mahajan, A., Pererva, Y., Flann, N. S., & Miller, C. D. (2020). A Model for Bioaugmented Anaerobic Granulation. *Frontiers in Microbiology*, *11*, 2239. <https://doi.org/10.3389/fmicb.2020.566826>

- Domingo M.-C., Yansouni C., Gaudreau C., Lamothe F., Lévesque S., Tremblay C., Garceau R., & Richter S. S. (2015). Cloacibacillus sp., a Potential Human Pathogen Associated with Bacteremia in Quebec and New Brunswick. *Journal of Clinical Microbiology*, 53(10), 3380–3383. <https://doi.org/10.1128/JCM.01137-15>
- Draaijer, H., Maas, J. A. W., Schaapman, J. E., & Khan, A. (1992). Performance of the 5 MLD UASB Reactor for Sewage Treatment at Kanpur, India. *Water Science and Technology*, 25(7), 123–133. <https://doi.org/10.2166/wst.1992.0145>
- Elmitwalli, T. A., Oahn, K. L. T., Zeeman, G., & Lettinga, G. (2002). Treatment of domestic sewage in a two-step anaerobic filter/anaerobic hybrid system at low temperature. *Water Research*, 36(9), 2225–2232. [https://doi.org/10.1016/S0043-1354\(01\)00438-9](https://doi.org/10.1016/S0043-1354(01)00438-9)
- Elmitwalli, T., & Otterpohl, R. (2011). Grey water treatment in upflow anaerobic sludge blanket (UASB) reactor at different temperatures. *Water Science and Technology*, 64(3), 610–617. <https://doi.org/10.2166/wst.2011.616>
- Espinosa, M. F., Verbyla, M. E., Vassalle, L., Rosa-Machado, A. T., Zhao, F., Gaunin, A., & Mota, C. R. (2021). Reduction and partitioning of viral and bacterial indicators in a UASB reactor followed by high rate algal ponds treating domestic sewage. *Science of The Total Environment*, 760, 144309. <https://doi.org/10.1016/j.scitotenv.2020.144309>
- Feldman, H., Flores-Alsina, X., Ramin, P., Kjellberg, K., Jeppsson, U., Batstone, D. J., & Gernaey, K. V. (2017). Modelling an industrial anaerobic granular reactor using a multi-scale approach. *Water Research*, 126, 488–500. <https://doi.org/10.1016/j.watres.2017.09.033>
- Fey, A., Claus, P., & Conrad, R. (2004). Temporal change of ^{13}C -isotope signatures and methanogenic pathways in rice field soil incubated anoxically at different temperatures. *Geochimica et*

- Cosmochimica Acta*, 68(2), 293–306.
[https://doi.org/10.1016/S0016-7037\(03\)00426-5](https://doi.org/10.1016/S0016-7037(03)00426-5)
- Flora, J. R. V., Suidan, M. T., Biswas, P., & Sayles, G. D. (1995). A modeling study of anaerobic biofilm systems: I. Detailed biofilm modeling. *Biotechnology and Bioengineering*, 46(1), 43–53.
<https://doi.org/10.1002/bit.260460107>
- Florencio, L., Kato, M. T., & de Moraes, J. C. (2001). Domestic sewage treatment in full-scale UASBB plant at Mangueira, Recife, Pernambuco. *Water Science and Technology*, 44(4), 71–77.
- Ghimire, U., Sarpong, G., & Gude, V. G. (2021). Transitioning Wastewater Treatment Plants toward Circular Economy and Energy Sustainability. *ACS Omega*, 6(18), 11794–11803.
<https://doi.org/10.1021/acsomega.0c05827>
- Gonçalves, A. L., Pires, J. C. M., & Simões, M. (2017). A review on the use of microalgal consortia for wastewater treatment. *Wastewater and Algae; Opportunities, Challenges and Long Term Sustainability*, 24, 403–415.
<https://doi.org/10.1016/j.algal.2016.11.008>
- Gonçalves, A. L., Simões, M., & Pires, J. C. M. (2014). The effect of light supply on microalgal growth, CO₂ uptake and nutrient removal from wastewater. *Energy Conversion and Management*, 85, 530–536. <https://doi.org/10.1016/j.enconman.2014.05.085>
- Grady, C. P. L., Daigger, G. T., & Lim, H. C. (2011). *Biological wastewater treatment* (3rd ed.). IWA Publishing.
- Griffiths, M. J., Garcin, C., van Hille, R. P., & Harrison, S. T. L. (2011). Interference by pigment in the estimation of microalgal biomass concentration by optical density. *Journal of Microbiological Methods*, 85(2), 119–123.
<https://doi.org/10.1016/j.mimet.2011.02.005>
- Guillard, R. R. L., & Lorenzen, C. J. (1972). Yellow-green algae with chlorophyllide C_{1,2}. *Journal of Phycology*, 8(1), 10–14.
<https://doi.org/10.1111/j.1529-8817.1972.tb03995.x>

- Halalsheh, M., Sawajneh, Z., Zu'bi, M., Zeeman, G., Lier, J., Fayyad, M., & Lettinga, G. (2005). Treatment of strong domestic sewage in a 96 m³ UASB reactor operated at ambient temperatures: Two-stage versus single-stage reactor. *Bioresource Technology*, *96*(5), 577–585. <https://doi.org/10.1016/j.biortech.2004.06.014>
- Hanson, R. S., & Hanson, T. E. (1996). Methanotrophic bacteria. *Microbiological Reviews*, *60*(2), 439.
- Hariz, H. B., Takriff, M. S., Ba-Abbad, M. M., Mohd Yasin, N. H., & Mohd Hakim, N. I. N. (2018). CO₂ fixation capability of *Chlorella* sp. And its use in treating agricultural wastewater. *Journal of Applied Phycology*, *30*(6), 3017–3027. <https://doi.org/10.1007/s10811-018-1488-0>
- Hatamoto, M., Yamamoto, H., Kindaichi, T., Ozaki, N., & Ohashi, A. (2010). Biological oxidation of dissolved methane in effluents from anaerobic reactors using a down-flow hanging sponge reactor. *Water Research*, *44*(5), 1409–1418. <https://doi.org/10.1016/j.watres.2009.11.021>
- Heidrich, E. S., Curtis, T. P., & Dolfing, J. (2011). Determination of the Internal Chemical Energy of Wastewater. *Environmental Science & Technology*, *45*(2), 827–832. <https://doi.org/10.1021/es103058w>
- Henshaw, P. F., Bewtra, J. K., & Biswas, N. (1998). Hydrogen sulphide conversion to elemental sulphur in a suspended-growth continuous stirred tank reactor using *Chlorobium limicola*. *Water Research*, *32*(6), 1769–1778. [https://doi.org/10.1016/S0043-1354\(97\)00393-X](https://doi.org/10.1016/S0043-1354(97)00393-X)
- Henze, M., van Loosdrecht, M. C. M., Ekama, G. A., & Brdjanovic, D. (2008). *Biological Wastewater Treatment: Principles, Modelling and Design*. IWA Publishing. <https://doi.org/10.2166/9781780401867>
- Hofmann, A. F., Meysman, F. J. R., Soetaert, K., & Middelburg, J. J. (2008). A step-by-step procedure for pH model construction in

- aquatic systems. *Biogeosciences*, 5(1), 227–251. <https://doi.org/10.5194/bg-5-227-2008>
- Høj, L., Olsen, R. A., & Torsvik, V. L. (2008). Effects of temperature on the diversity and community structure of known methanogenic groups and other archaea in high Arctic peat. *The ISME Journal*, 2(1), 37–48. <https://doi.org/10.1038/ismej.2007.84>
- Honda, R., Boonnorat, J., Chiemchaisri, C., Chiemchaisri, W., & Yamamoto, K. (2012). Carbon dioxide capture and nutrients removal utilizing treated sewage by concentrated microalgae cultivation in a membrane photobioreactor. *Bioresource Technology*, 125, 59–64. <https://doi.org/10.1016/j.biortech.2012.08.138>
- Hu, X., Zhou, J., Liu, G., & Gui, B. (2016). Selection of microalgae for high CO₂ fixation efficiency and lipid accumulation from ten *Chlorella* strains using municipal wastewater. *Journal of Environmental Sciences*, 46, 83–91. <https://doi.org/10.1016/j.jes.2015.08.030>
- Hulatt, C. J., Lakaniemi, A.-M., Puhakka, J. A., & Thomas, D. N. (2012). Energy Demands of Nitrogen Supply in Mass Cultivation of Two Commercially Important Microalgal Species, *Chlorella vulgaris* and *Dunaliella tertiolecta*. *BioEnergy Research*, 5(3), 669–684. <https://doi.org/10.1007/s12155-011-9175-x>
- Hulshoff Pol, L. W., de Castro Lopes, S. I., Lettinga, G., & Lens, P. N. L. (2004). Anaerobic sludge granulation. *Water Research*, 38(6), 1376–1389. <https://doi.org/10.1016/j.watres.2003.12.002>
- Huser, B. A., Wuhrmann, K., & Zehnder, A. J. B. (1982). *Methanotrix soehngenii* gen. Nov. Sp. Nov., a new acetotrophic non-hydrogen-oxidizing methane bacterium. *Archives of Microbiology*, 132(1), 1–9. <https://doi.org/10.1007/BF00690808>
- Huy, M., Kristin Vatland, A., & Kumar, G. (2022). Nutraceutical productions from microalgal derived compounds via circular

- bioeconomy perspective. *Bioresource Technology*, 347, 126575.
<https://doi.org/10.1016/j.biortech.2021.126575>
- Jain, D., Ghonse, S. S., Trivedi, T., Fernandes, G. L., Menezes, L. D., Damare, S. R., Mamatha, S. S., Kumar, S., & Gupta, V. (2019). CO₂ fixation and production of biodiesel by *Chlorella vulgaris* NIOCCV under mixotrophic cultivation. *Bioresource Technology*, 273, 672–676.
<https://doi.org/10.1016/j.biortech.2018.09.148>
- Janssen, M., Kuijpers, T. C., Veldhoen, B., Ternbach, M. B., Tramper, J., Mur, L. R., & Wijffels, R. H. (1999). Specific growth rate of *Chlamydomonas reinhardtii* and *Chlorella sorokiniana* under medium duration light/dark cycles: 13–87 s. *Biotechnological Aspects of Marine Sponges*, 70(1), 323–333.
[https://doi.org/10.1016/S0168-1656\(99\)00084-X](https://doi.org/10.1016/S0168-1656(99)00084-X)
- Jarusutthirak, C., & Amy, G. (2007). Understanding soluble microbial products (SMP) as a component of effluent organic matter (EfOM). *Water Research*, 41(12), 2787–2793.
<https://doi.org/10.1016/j.watres.2007.03.005>
- Katsuda, T., Shimahara, K., Shiraishi, H., Yamagami, K., Ranjbar, R., & Katoh, S. (2006). Effect of flashing light from blue light emitting diodes on cell growth and astaxanthin production of *Haematococcus pluvialis*. *Journal of Bioscience and Bioengineering*, 102(5), 442–446.
<https://doi.org/10.1263/jbb.102.442>
- Kettunen, R. H., & Rintala, J. A. (1997). The effect of low temperature (5–29 °C) and adaptation on the methanogenic activity of biomass. *Applied Microbiology and Biotechnology*, 48(4), 570–576. <https://doi.org/10.1007/s002530051098>
- Kettunen, R. H., & Rintala, J. A. (1998). Performance of an on-site UASB reactor treating leachate at low temperature. *Water Research*, 32(3), 537–546. [https://doi.org/10.1016/S0043-1354\(97\)00319-9](https://doi.org/10.1016/S0043-1354(97)00319-9)

- Khan, S. A., Malla, F. A., Rashmi, Malav, L. C., Gupta, N., & Kumar, A. (2018). Potential of wastewater treating *Chlorella minutissima* for methane enrichment and CO₂ sequestration of biogas and producing lipids. *Energy*, *150*, 153–163. <https://doi.org/10.1016/j.energy.2018.02.126>
- Khanal, R. (2019). *Pathogen Removal form Domestic Wastewater Using Membrane Filter*.
- Kim, W., Shin, S. G., Han, G., Cho, K., & Hwang, S. (2015). Structures of microbial communities found in anaerobic batch runs that produce methane from propionic acid—Seeded from full-scale anaerobic digesters above a certain threshold. *Journal of Biotechnology*, *214*, 192–198. <https://doi.org/10.1016/j.jbiotec.2015.09.040>
- Kleerebezem, R., Joosse, B., Rozendal, R., & Van Loosdrecht, M. C. M. (2015). Anaerobic digestion without biogas? *Reviews in Environmental Science and Bio/Technology*, *14*(4), 787–801. <https://doi.org/10.1007/s11157-015-9374-6>
- Kommedal, R. (2003). *Degradation of polymeric and particulate organic carbon in biofilms: Vol. 2003:101*. Fakultet for naturvitenskap og teknologi, NTNU.
- Kong, W., Shen, B., Lyu, H., Kong, J., Ma, J., Wang, Z., & Feng, S. (2021). Review on carbon dioxide fixation coupled with nutrients removal from wastewater by microalgae. *Journal of Cleaner Production*, *292*, 125975. <https://doi.org/10.1016/j.jclepro.2021.125975>
- Koster, I. W., & Lettinga, G. (1985). Application of the upflow anaerobic sludge bed (UASB) process for treatment of complex wastewaters at low temperatures. *Biotechnology and Bioengineering*, *27*(10), 1411–1417. <https://doi.org/10.1002/bit.260271004>
- Kotsyurbenko, O. R., Glagolev, M. V., Nozhevnikova, A. N., & Conrad, R. (2001). Competition between homoacetogenic bacteria and

- methanogenic archaea for hydrogen at low temperature. *FEMS Microbiology Ecology*, 38(2–3), 153–159. <https://doi.org/10.1111/j.1574-6941.2001.tb00893.x>
- Kotsyurbenko, O. R., Nozhevnikova, A. N., Soloviova, T. I., & Zavarzin, G. A. (1996). Methanogenesis at low temperatures by microflora of tundra wetland soil. *Antonie van Leeuwenhoek*, 69(1), 75–86. <https://doi.org/10.1007/BF00641614>
- Kumar, A., Yuan, X., Sahu, A. K., Dewulf, J., Ergas, S. J., & Van Langenhove, H. (2010). A hollow fiber membrane photobioreactor for CO₂ sequestration from combustion gas coupled with wastewater treatment: A process engineering approach. *Journal of Chemical Technology & Biotechnology*, 85(3), 387–394. <https://doi.org/10.1002/jctb.2332>
- Kumar, K., Dasgupta, C. N., & Das, D. (2014). Cell growth kinetics of *Chlorella sorokiniana* and nutritional values of its biomass. *Bioresource Technology*, 167, 358–366. <https://doi.org/10.1016/j.biortech.2014.05.118>
- Kuo, C.-M., Jian, J.-F., Lin, T.-H., Chang, Y.-B., Wan, X.-H., Lai, J.-T., Chang, J.-S., & Lin, C.-S. (2016). Simultaneous microalgal biomass production and CO₂ fixation by cultivating *Chlorella* sp. GD with aquaculture wastewater and boiler flue gas. *Bioresource Technology*, 221, 241–250. <https://doi.org/10.1016/j.biortech.2016.09.014>
- Kwon, M. J., Jung, J. Y., Tripathi, B. M., Göckede, M., Lee, Y. K., & Kim, M. (2019). Dynamics of microbial communities and CO₂ and CH₄ fluxes in the tundra ecosystems of the changing Arctic. *Journal of Microbiology*, 57(5), 325–336. <https://doi.org/10.1007/s12275-019-8661-2>
- Leak, D. J., & Dalton, H. (1986). Growth yields of methanotrophs. *Applied Microbiology and Biotechnology*, 23(6), 470–476. <https://doi.org/10.1007/BF02346062>

- Leitão, R. C., van Haandel, A. C., Zeeman, G., & Lettinga, G. (2006). The effects of operational and environmental variations on anaerobic wastewater treatment systems: A review. *Bioresource Technology*, 97(9), 1105–1118. <https://doi.org/10.1016/j.biortech.2004.12.007>
- Lettinga, G. (2014). *My anaerobic sustainability story* (pp. 196–197). LeAF. <https://research.wur.nl/en/publications/my-anaerobic-sustainability-story>
- Lettinga, G. (2018, March 20). Personal Communication, Delft.
- Lettinga, G., Rebac, S., & Zeeman, G. (2001). Challenge of psychrophilic anaerobic wastewater treatment. *Trends in Biotechnology*, 19(9), 363–370. [https://doi.org/10.1016/S0167-7799\(01\)01701-2](https://doi.org/10.1016/S0167-7799(01)01701-2)
- Lettinga, G., Van Lier, J. B., Van Buuren, J. C. L., & Zeeman, G. . (2001). Sustainable development in pollution control and the role of anaerobic treatment. *Water Science and Technology*, 44(6), 181–188. <https://doi.org/10.2166/wst.2001.0370>
- Lettinga, G., van Velsen, A. F. M., Hobma, S. W., de Zeeuw, W., & Klapwijk, A. (1980). Use of the upflow sludge blanket (USB) reactor concept for biological wastewater treatment, especially for anaerobic treatment. *Biotechnology and Bioengineering*, 22(4), 699–734. <https://doi.org/10.1002/bit.260220402>
- Lew, B., Tarre, S., Beliavski, M., & Green, M. (2009). Anaerobic degradation pathway and kinetics of domestic wastewater at low temperatures. *Bioresource Technology*, 100(24), 6155–6162. <https://doi.org/10.1016/j.biortech.2009.06.073>
- Li, W., Fu, L., Niu, B., Wu, S., & Wooley, J. (2012). Ultrafast clustering algorithms for metagenomic sequence analysis. *Briefings in Bioinformatics*, 13(6), 656–668. PubMed. <https://doi.org/10.1093/bib/bbs035>
- Li, X.-M., Guo, L., Yang, Q., Zeng, G.-M., & Liao, D.-X. (2007). Removal of carbon and nutrients from low strength domestic

- wastewater by expanded granular sludge bed-zeolite bed filtration (EGSB-ZBF) integrated treatment concept. *Process Biochemistry*, 42(8), 1173–1179. <https://doi.org/10.1016/j.procbio.2007.04.001>
- Liu, X., Wang, K., Wang, J., Zuo, J., Peng, F., Wu, J., & San, E. (2019). Carbon dioxide fixation coupled with ammonium uptake by immobilized *Scenedesmus obliquus* and its potential for protein production. *Bioresource Technology*, 289, 121685. <https://doi.org/10.1016/j.biortech.2019.121685>
- Liu, Y., Qiao, J.-T., Yuan, X.-Z., Guo, R.-B., & Qiu, Y.-L. (2014). *Hydrogenispora ethanolica* gen. Nov., sp. Nov., an anaerobic carbohydrate-fermenting bacterium from anaerobic sludge. *International Journal of Systematic and Evolutionary Microbiology*, 64(5), 1756–1762. <https://doi.org/10.1099/ijs.0.060186-0>
- Liu, Y., & Whitman, W. B. (2008). Metabolic, Phylogenetic, and Ecological Diversity of the Methanogenic Archaea. *Annals of the New York Academy of Sciences*, 1125(1), 171–189. <https://doi.org/10.1196/annals.1419.019>
- Liu, Z., Yin, H., Dang, Z., & Liu, Y. (2014). Dissolved methane: A hurdle for anaerobic treatment of municipal wastewater. *Environmental Science & Technology*, 48(2), 889–890. <https://doi.org/10.1021/es405553j>
- Looft, T., Levine, U. Y., & Stanton, T. B. (2013). *Cloacibacillus porcorum* sp. Nov., a mucin-degrading bacterium from the swine intestinal tract and emended description of the genus *Cloacibacillus*. *International Journal of Systematic and Evolutionary Microbiology*, 63(6), 1960–1966. <https://doi.org/10.1099/ijs.0.044719-0>
- Ma, K., Liu, X., & Dong, X. (2005). *Methanobacterium beijingense* sp. Nov., a novel methanogen isolated from anaerobic digesters. In *International Journal of Systematic and Evolutionary*

- Microbiology* (Vol. 55, Issue 1, pp. 325–329). Microbiology Society. <https://doi.org/10.1099/ijms.0.63254-0>
- Madigan, M. T., Brock, T. D., Martinko, J. M., Dunlap, P. V., & Clark, D. P. (2009). *Brock biology of microorganisms* (12th ed.). Pearson/Benjamin Gummings.
- Magoč, T., & Salzberg, S. L. (2011). FLASH: fast length adjustment of short reads to improve genome assemblies. *Bioinformatics (Oxford, England)*, 27(21), 2957–2963. PubMed. <https://doi.org/10.1093/bioinformatics/btr507>
- Mahmoud, N., Zeeman, G., Gijzen, H., & Lettinga, G. (2004). Anaerobic sewage treatment in a one-stage UASB reactor and a combined UASB-Digester system. *Water Research*, 38(9), 2348–2358. <https://doi.org/10.1016/j.watres.2004.01.041>
- Mai, D. T., Kunacheva, C., & Stuckey, D. C. (2018). A review of posttreatment technologies for anaerobic effluents for discharge and recycling of wastewater. *Critical Reviews in Environmental Science and Technology*, 48(2), 167–209. <https://doi.org/10.1080/10643389.2018.1443667>
- Martínez, M. E., Jiménez, J. M., & El Yousfi, F. (1999). Influence of phosphorus concentration and temperature on growth and phosphorus uptake by the microalga *Scenedesmus obliquus*. *Bioresource Technology*, 67(3), 233–240. [https://doi.org/10.1016/S0960-8524\(98\)00120-5](https://doi.org/10.1016/S0960-8524(98)00120-5)
- Matsuura, N., Hatamoto, M., Sumino, H., Syutsubo, K., Yamaguchi, T., & Ohashi, A. (2015). Recovery and biological oxidation of dissolved methane in effluent from UASB treatment of municipal sewage using a two-stage closed downflow hanging sponge system. *Journal of Environmental Management*, 151, 200–209. <https://doi.org/10.1016/j.jenvman.2014.12.026>
- McCarty, P. L. (2001). The development of anaerobic treatment and its future. *Water Science and Technology*, 44(8), 149–156. <https://doi.org/10.2166/wst.2001.0487>

- McHugh, S., Carton, M., Mahony, T., & O'Flaherty, V. (2003). Methanogenic population structure in a variety of anaerobic bioreactors. *FEMS Microbiology Letters*, *219*(2), 297–304. [https://doi.org/10.1016/S0378-1097\(03\)00055-7](https://doi.org/10.1016/S0378-1097(03)00055-7)
- McKeown, R. M., Scully, C., Mahony, T., Collins, G., & O'Flaherty, V. (2009). Long-term (1243 days), low-temperature (4–15°C), anaerobic biotreatment of acidified wastewaters: Bioprocess performance and physiological characteristics. *Water Research*, *43*(6), 1611–1620. <https://doi.org/10.1016/j.watres.2009.01.015>
- McKeown, R., Scully, C., Enright, A.-M., Chinalia, F., Lee, C., Mahony, T., Collins, G., & O'Flaherty, V. (2009). Psychrophilic methanogenic community development during long-term cultivation of anaerobic granular biofilms. *The ISME Journal*, *3*(11), 1231–1242. <https://doi.org/10.1038/ismej.2009.67>
- Mekonnen, M. M., & Hoekstra, A. Y. (2016). Four billion people facing severe water scarcity. *Science Advances*, *2*(2), e1500323. <https://doi.org/10.1126/sciadv.1500323>
- Meslier, V., Loux, V., & Renault, P. (2012). Genome sequence of *Lactococcus raffinolactis* strain 4877, isolated from natural dairy starter culture. *Journal of Bacteriology*, *194*(22), 6364–6364. PubMed. <https://doi.org/10.1128/JB.01697-12>
- Milferstedt, K., Kuo-Dahab, W. C., Butler, C. S., Hamelin, J., Abouhend, A. S., Stauch-White, K., McNair, A., Watt, C., Carbajal-González, B. I., Dolan, S., & Park, C. (2017). The importance of filamentous cyanobacteria in the development of oxygenic photogranules. *Scientific Reports*, *7*(1), 17944. <https://doi.org/10.1038/s41598-017-16614-9>
- Monroy, O., Famá, G., Meraz, M., Montoya, L., & Macarie, H. (2000). Anaerobic digestion for wastewater treatment in Mexico: State of the technology. *Water Research*, *34*(6), 1803–1816. [https://doi.org/10.1016/S0043-1354\(99\)00301-2](https://doi.org/10.1016/S0043-1354(99)00301-2)

- Moosbrugger, R. E., Wentzel, M. C., Ekama, G. A., & Marais, G. v. R. (1993). A 5 pH Point Titration Method for Determining the Carbonate and SCFA Weak Acid/Bases in Anaerobic Systems. *Water Science and Technology*, 28(2), 237–245. <https://doi.org/10.2166/wst.1993.0112>
- Mousavi, S., Najafpour, G. D., Mohammadi, M., & Seifi, M. H. (2018). Cultivation of newly isolated microalgae *Coelastrum* sp. In wastewater for simultaneous CO₂ fixation, lipid production and wastewater treatment. *Bioprocess and Biosystems Engineering*, 41(4), 519–530. <https://doi.org/10.1007/s00449-017-1887-7>
- Müller, E., Hotzel, H., Ahlers, C., Hänel, I., Tomaso, H., & Abdel-Glil, M. Y. (2020). Genomic Analysis and Antimicrobial Resistance of *Aliarcobacter cryaerophilus* Strains From German Water Poultry. *Frontiers in Microbiology*, 11, 1549. <https://doi.org/10.3389/fmicb.2020.01549>
- Mungray, A. K., Murthy, Z. V. P., & Tirpude, A. J. (2010). Post treatment of up-flow anaerobic sludge blanket based sewage treatment plant effluents: A review. *Desalination and Water Treatment*, 22(1–3), 220–237. <https://doi.org/10.5004/dwt.2010.1788>
- Mungray, A. K., & Patel, K. (2011). Coliforms removal in two UASB + ASP based systems. *International Biodeterioration & Biodegradation*, 65(1), 23–28. <https://doi.org/10.1016/j.ibiod.2010.04.011>
- Muñoz, R., & Guieysse, B. (2006). Algal–bacterial processes for the treatment of hazardous contaminants: A review. *Water Research*, 40(15), 2799–2815. <https://doi.org/10.1016/j.watres.2006.06.011>
- Nayak, M., Karemore, A., & Sen, R. (2016). Performance evaluation of microalgae for concomitant wastewater bioremediation, CO₂ biofixation and lipid biosynthesis for biodiesel application. *Algal*

- Research*, 16, 216–223.
<https://doi.org/10.1016/j.algal.2016.03.020>
- Negi, S., Barry, A., Friedland, N., Sudasinghe, N., Subramanian, S., Pieris, S., Holguin, F., Dungan, B., Schaub, T., & Sayre, R. (2016). Impact of nitrogen limitation on biomass, photosynthesis, and lipid accumulation in *Chlorella sorokiniana*. *Journal of Applied Phycology*, 28(2), 803–812.
<https://doi.org/10.1007/s10811-015-0652-z>
- Nordgård, A. S. R., Bergland, W. H., Vadstein, O., Mironov, V., Bakke, R., Østgaard, K., & Bakke, I. (2017). Anaerobic digestion of pig manure supernatant at high ammonia concentrations characterized by high abundances of *Methanosaeta* and non-euryarchaeotal archaea. *Scientific Reports*, 7(1), 15077.
<https://doi.org/10.1038/s41598-017-14527-1>
- Nozhevnikova, A. N., Holliger, C., Ammann, A., & Zehnder, A. J. B. (1997). Methanogenesis in sediments from deep lakes at different temperatures (2–70°C). *Water Science and Technology*, 36(6–7), 57–64. <https://doi.org/10.2166/wst.1997.0575>
- Nozhevnikova, A. N., Nekrasova, V., Ammann, A., Zehnder, A. J. B., Wehrli, B., & Holliger, C. (2007). Influence of temperature and high acetate concentrations on methanogenesis in lake sediment slurries. *FEMS Microbiology Ecology*, 62(3), 336–344.
<https://doi.org/10.1111/j.1574-6941.2007.00389.x>
- Nyholm, N. (1977). Kinetics of phosphate limited algal growth. *Biotechnology and Bioengineering*, 19(4), 467–492.
<https://doi.org/10.1002/bit.260190404>
- Odriozola, M., López, I., & Borzacconi, L. (2016). Modeling granule development and reactor performance on anaerobic granular sludge reactors. *Journal of Environmental Chemical Engineering*, 4(2), 1615–1628.
<https://doi.org/10.1016/j.jece.2016.01.040>

- Oren, A. (2014). The Family Methanocorpusculaceae. In E. Rosenberg, E. F. DeLong, S. Lory, E. Stackebrandt, & F. Thompson (Eds.), *The Prokaryotes: Other Major Lineages of Bacteria and The Archaea* (pp. 225–230). Springer Berlin Heidelberg. https://doi.org/10.1007/978-3-642-38954-2_314
- Oswald, W. J., & Golueke, C. G. (1960). Biological Transformation of Solar Energy. In W. W. Umbreit (Ed.), *Advances in Applied Microbiology* (Vol. 2, pp. 223–262). Academic Press. [https://doi.org/10.1016/S0065-2164\(08\)70127-8](https://doi.org/10.1016/S0065-2164(08)70127-8)
- Owusu-Agyeman, I., Eyice, Ö., Cetecioglu, Z., & Plaza, E. (2019). The study of structure of anaerobic granules and methane producing pathways of pilot-scale UASB reactors treating municipal wastewater under sub-mesophilic conditions. *Bioresource Technology*, 290, 121733. <https://doi.org/10.1016/j.biortech.2019.121733>
- Ozgun, H., Tao, Y., Ersahin, M. E., Zhou, Z., Gimenez, J. B., Spanjers, H., & van Lier, J. B. (2015). Impact of temperature on feed-flow characteristics and filtration performance of an upflow anaerobic sludge blanket coupled ultrafiltration membrane treating municipal wastewater. *Water Research*, 83, 71–83. <https://doi.org/10.1016/j.watres.2015.06.035>
- Pan, X., Zhao, L., Li, C., Angelidaki, I., Lv, N., Ning, J., Cai, G., & Zhu, G. (2021). Deep insights into the network of acetate metabolism in anaerobic digestion: Focusing on syntrophic acetate oxidation and homoacetogenesis. *Water Research*, 190, 116774. <https://doi.org/10.1016/j.watres.2020.116774>
- Peniuk, G., Schnurr, P., & Allen, D. (2016). Identification and quantification of suspended algae and bacteria populations using flow cytometry: Applications for algae biofuel and biochemical growth systems. *Journal of Applied Phycology*, 28(1), 95–104. <https://doi.org/10.1007/s10811-015-0569-6>

- Petropoulos, E., Dolfing, J., Davenport, R. J., Bowen, E. J., & Curtis, T. P. (2017). Developing cold-adapted biomass for the anaerobic treatment of domestic wastewater at low temperatures (4, 8 and 15 °C) with inocula from cold environments. *Water Research*, *112*, 100–109. <https://doi.org/10.1016/j.watres.2016.12.009>
- Petropoulos, E., Shamurad, B., Tabraiz, S., Yu, Y., Davenport, R., Curtis, T. P., & Dolfing, J. (2021). Sewage treatment at 4 °C in anaerobic upflow reactors with and without a membrane – performance, function and microbial diversity. *Environmental Science: Water Research & Technology*, *7*(1), 156–171. <https://doi.org/10.1039/DOEW00753F>
- Pizzera, A., Scaglione, D., Bellucci, M., Marazzi, F., Mezzanotte, V., Parati, K., & Ficara, E. (2019). Digestate treatment with algae-bacteria consortia: A field pilot-scale experimentation in a sub-optimal climate area. *Bioresource Technology*, *274*, 232–243. <https://doi.org/10.1016/j.biortech.2018.11.067>
- Pokorna-Krayzelova, L., Mampaey, K. E., Vannecke, T. P. W., Bartacek, J., Jenicek, P., & Volcke, E. I. P. (2017). Model-based optimization of microaeration for biogas desulfurization in UASB reactors. *Biochemical Engineering Journal*, *125*, 171–179. <https://doi.org/10.1016/j.bej.2017.06.009>
- Posadas, E., Alcántara, C., García-Encina, P. A., Gouveia, L., Guieysse, B., Norvill, Z., Acién, F. G., Markou, G., Congestri, R., Koreiviene, J., & Muñoz, R. (2017). 3—Microalgae cultivation in wastewater. In C. Gonzalez-Fernandez & R. Muñoz (Eds.), *Microalgae-Based Biofuels and Bioproducts* (pp. 67–91). Woodhead Publishing. <https://doi.org/10.1016/B978-0-08-101023-5.00003-0>
- Posadas, E., Morales, M. del M., Gomez, C., Acién, F. G., & Muñoz, R. (2015). Influence of pH and CO₂ source on the performance of microalgae-based secondary domestic wastewater treatment in

- outdoors pilot raceways. *Chemical Engineering Journal*, 265, 239–248. <https://doi.org/10.1016/j.cej.2014.12.059>
- Ramaraj, R., Tsai, D. D.-W., & Chen, P. H. (2015). Biomass of algae growth on natural water medium. *Journal of Photochemistry and Photobiology B: Biology*, 142, 124–128. <https://doi.org/10.1016/j.jphotobiol.2014.12.007>
- Rasouli, Z., Valverde-Pérez, B., D’Este, M., De Francisci, D., & Angelidaki, I. (2018). Nutrient recovery from industrial wastewater as single cell protein by a co-culture of green microalgae and methanotrophs. *Biochemical Engineering Journal*, 134, 129–135. <https://doi.org/10.1016/j.bej.2018.03.010>
- Rebac, S., Ruskova, J., Gerbens, S., van Lier, J. B., Stams, A. J. M., & Lettinga, G. (1995). High-rate anaerobic treatment of wastewater under psychrophilic conditions. *Journal of Fermentation and Bioengineering*, 80(5), 499–506. [https://doi.org/10.1016/0922-338X\(96\)80926-3](https://doi.org/10.1016/0922-338X(96)80926-3)
- Rebac, S., Van Lier, J. B., Lens, P., Stams, A. J. M., Dekkers, F., Swinkels, K. Th. M., & Lettinga, G. (1999). *Psychrophilic anaerobic treatment of low strength wastewaters* (Vol. 39). Scopus. [https://doi.org/10.1016/S0273-1223\(99\)00103-1](https://doi.org/10.1016/S0273-1223(99)00103-1)
- Redfield, A. C. (1960). The biological control of chemical factors in the environment. *Science Progress*, 11, 150–170. PubMed.
- Reichert, P. (1994). AQUASIM – A TOOL FOR SIMULATION AND DATA ANALYSIS OF AQUATIC SYSTEMS. *Water Science and Technology*, 30(2), 21–30. <https://doi.org/10.2166/wst.1994.0025>
- Rice, E. W., Baird, R. B., Eaton, A. D., & Clesceri, L. S. (2013). *Standard methods for the examination of water and wastewater*, 20th edn. (23rd ed.). APHA, AWWA, WEF.

- Richmond, A. (2003). *Handbook of microalgal culture: Biotechnology and applied phycology*. United Kingdom: Blackwell Publishing. <https://doi.org/10.1002/9780470995280>
- Rivera, F., Muñoz, R., Prádanos, P., Hernández, A., & Palacio, L. (2022). A Systematic Study of Ammonia Recovery from Anaerobic Digestate Using Membrane-Based Separation. *Membranes*, *12*(1). <https://doi.org/10.3390/membranes12010019>
- Rojas, J., & Zhelev, T. (2012). Energy efficiency optimisation of wastewater treatment: Study of ATAD. *Computers & Chemical Engineering*, *38*, 52–63. <https://doi.org/10.1016/j.compchemeng.2011.11.016>
- Rosa, A. P., Chernicharo, C. A. L., Lobato, L. C. S., Silva, R. V., Padilha, R. F., & Borges, J. M. (2018). Assessing the potential of renewable energy sources (biogas and sludge) in a full-scale UASB-based treatment plant. *SI: Waste Biomass to Biofuel*, *124*, 21–26. <https://doi.org/10.1016/j.renene.2017.09.025>
- Rossi, S., Díez-Montero, R., Rueda, E., Castillo Cascino, F., Parati, K., García, J., & Ficara, E. (2020). Free ammonia inhibition in microalgae and cyanobacteria grown in wastewaters: Photorespirometric evaluation and modelling. *Bioresource Technology*, *305*, 123046. <https://doi.org/10.1016/j.biortech.2020.123046>
- Ruiz-Martinez, A., Martin Garcia, N., Romero, I., Seco, A., & Ferrer, J. (2012). Microalgae cultivation in wastewater: Nutrient removal from anaerobic membrane bioreactor effluent. *Advances in Biological Waste Treatment and Bioconversion Technologies*, *126*, 247–253. <https://doi.org/10.1016/j.biortech.2012.09.022>
- Ruiz-Ruiz, P., Gómez-Borraz, T. L., Revah, S., & Morales, M. (2020). Methanotroph-microalgae co-culture for greenhouse gas mitigation: Effect of initial biomass ratio and methane concentration. *Chemosphere*, *259*, 127418. <https://doi.org/10.1016/j.chemosphere.2020.127418>

- Safi, C., Zebib, B., Merah, O., Pontalier, P.-Y., & Vaca-Garcia, C. (2014). Morphology, composition, production, processing and applications of *Chlorella vulgaris*: A review. *Renewable and Sustainable Energy Reviews*, *35*, 265–278. <https://doi.org/10.1016/j.rser.2014.04.007>
- Safitri, A. S., Hamelin, J., Kommedal, R., & Milferstedt, K. (2021). Engineered methanotrophic syntrophy in photogranule communities removes dissolved methane. *Water Research X*, *12*, 100106. <https://doi.org/10.1016/j.wroa.2021.100106>
- Safitri, A. S., Kaster, K. M., & Kommedal, R. (n.d.). Effect of low temperature and municipal wastewater organic loading on UASB system performance. *Submitted*.
- Safitri, A. S., Kommedal, R., & Kaster, K. M. (n.d.). Microbial community development on psychrophilic granules during long-term UASB operation. *In Preparation*.
- Samonis, G., Karageorgopoulos, D. E., Kofteridis, D. P., Matthaïou, D. K., Sidiropoulou, V., Maraki, S., & Falagas, M. E. (2008). *Citrobacter* infections in a general hospital: Characteristics and outcomes. *European Journal of Clinical Microbiology & Infectious Diseases*, *28*(1), 61. <https://doi.org/10.1007/s10096-008-0598-z>
- Satoh Hisashi, Miura Yuki, Tsushima Ikuo, & Okabe Satoshi. (2007). Layered Structure of Bacterial and Archaeal Communities and Their In Situ Activities in Anaerobic Granules. *Applied and Environmental Microbiology*, *73*(22), 7300–7307. <https://doi.org/10.1128/AEM.01426-07>
- Schellinkhout, A., & Collazos, C. J. (1992). Full-Scale Application of the UASB Technology for Sewage Treatment. *Water Science and Technology*, *25*(7), 159–166. <https://doi.org/10.2166/wst.1992.0148>
- Seghezze, L., Zeeman, G., van Lier, J. B., Hamelers, H. V. M., & Lettinga, G. (1998). A review: The anaerobic treatment of

sewage in UASB and EGSB reactors. *Bioresource Technology*, 65(3), 175–190. [https://doi.org/10.1016/S0960-8524\(98\)00046-7](https://doi.org/10.1016/S0960-8524(98)00046-7)

- Shen, Q.-H., Jiang, J.-W., Chen, L.-P., Cheng, L.-H., Xu, X.-H., & Chen, H.-L. (2015a). Effect of carbon source on biomass growth and nutrients removal of *Scenedesmus obliquus* for wastewater advanced treatment and lipid production. *Bioresource Technology*, 190, 257–263. <https://doi.org/10.1016/j.biortech.2015.04.053>
- Shen, Q.-H., Jiang, J.-W., Chen, L.-P., Cheng, L.-H., Xu, X.-H., & Chen, H.-L. (2015b). Effect of carbon source on biomass growth and nutrients removal of *Scenedesmus obliquus* for wastewater advanced treatment and lipid production. *Bioresource Technology*, 190, 257–263. <https://doi.org/10.1016/j.biortech.2015.04.053>
- Show, K.-Y., Yan, Y., Yao, H., Guo, H., Li, T., Show, D.-Y., Chang, J.-S., & Lee, D.-J. (2020). Anaerobic granulation: A review of granulation hypotheses, bioreactor designs and emerging green applications. *Bioresource Technology*, 300, 122751. <https://doi.org/10.1016/j.biortech.2020.122751>
- Singh, K. S., Harada, H., & Viraraghavan, T. (1996). Low-strength wastewater treatment by a UASB reactor. *Bioresource Technology*, 55(3), 187–194. [https://doi.org/10.1016/0960-8524\(96\)86817-9](https://doi.org/10.1016/0960-8524(96)86817-9)
- Singh, S., Holohan, B. C., Mills, S., Castilla-Archilla, J., Kokko, M., Rintala, J., Lens, P. N. L., Collins, G., & O’Flaherty, V. (2020). Enhanced Methanization of Long-Chain Fatty Acid Wastewater at 20°C in the Novel Dynamic Sludge Chamber–Fixed Film Bioreactor. *Frontiers in Energy Research*, 8, 166. <https://doi.org/10.3389/fenrg.2020.00166>
- Singh, S., Rinta-Kanto, J. M., Kettunen, R., Tolvanen, H., Lens, P., Collins, G., Kokko, M., & Rintala, J. (2019). Anaerobic treatment

- of LCFA-containing synthetic dairy wastewater at 20 °C: Process performance and microbial community dynamics. *Science of The Total Environment*, 691, 960–968. <https://doi.org/10.1016/j.scitotenv.2019.07.136>
- Slanetz L. W. & Bartley Clara H. (1957). Numbers of Enterococci in water, sewage, and feces determined by the membrane filter technique with an improved medium. *Journal of Bacteriology*, 74(5), 591–595. <https://doi.org/10.1128/jb.74.5.591-595.1957>
- Smith, A. L., Skerlos, S. J., & Raskin, L. (2012). Psychrophilic anaerobic membrane bioreactor treatment of domestic wastewater. *Water Research*. <https://doi.org/10.1016/j.watres.2012.12.028>
- Smith, A. L., Skerlos, S. J., & Raskin, L. (2015). Anaerobic membrane bioreactor treatment of domestic wastewater at psychrophilic temperatures ranging from 15 °C to 3 °C. *Environmental Science: Water Research & Technology*, 1(1), 56–64. <https://doi.org/10.1039/C4EW00070F>
- Söllinger, A., & Urich, T. (2019). Methylophilic methanogens everywhere—Physiology and ecology of novel players in global methane cycling. *Biochemical Society Transactions*, 47(6), 1895–1907. <https://doi.org/10.1042/BST20180565>
- Souza, C. L., Chernicharo, C. A. L., & Aquino, S. F. (2011). Quantification of dissolved methane in UASB reactors treating domestic wastewater under different operating conditions. *Water Science and Technology*, 64(11), 2259–2264. <https://doi.org/10.2166/wst.2011.695>
- Sterner, R. W., & Grover, J. P. (1998). Algal growth in warm temperate reservoirs: Kinetic examination of nitrogen, temperature, light, and other nutrients. *Water Research*, 32(12), 3539–3548. [https://doi.org/10.1016/S0043-1354\(98\)00165-1](https://doi.org/10.1016/S0043-1354(98)00165-1)
- Stewart, P. S., Hamilton, M. A., Goldstein, B. R., & Schneider, B. T. (1996). Modeling biocide action against biofilms. *Biotechnology and Bioengineering*, 49(4), 445–455.

[https://doi.org/10.1002/\(SICI\)1097-0290\(19960220\)49:4<445::AID-BIT12>3.0.CO;2-9](https://doi.org/10.1002/(SICI)1097-0290(19960220)49:4<445::AID-BIT12>3.0.CO;2-9)

- Sun, J., Dai, X., Wang, Q., Pan, Y., & Ni, B.-J. (2016). Modelling Methane Production and Sulfate Reduction in Anaerobic Granular Sludge Reactor with Ethanol as Electron Donor. *Scientific Reports*, 6(1), 35312. <https://doi.org/10.1038/srep35312>
- Sun, L., Toyonaga, M., Ohashi, A., Turlousse, D. M., Matsuura, N., Meng, X.-Y., Tamaki, H., Hanada, S., Cruz, R., Yamaguchi, T., & Sekiguchi, Y. (2016). *Lentimicrobium saccharophilum* gen. Nov., sp. Nov., a strictly anaerobic bacterium representing a new family in the phylum Bacteroidetes, and proposal of Lentimicrobiaceae fam. Nov. *International Journal of Systematic and Evolutionary Microbiology*, 66(7), 2635–2642. <https://doi.org/10.1099/ijsem.0.001103>
- Tawfik, A., Zeeman, G., Klapwijk, A., Sanders, W., El-Gohary, F., & Lettinga, G. (2003). Treatment of domestic sewage in a combined UASB/RBC system. Process optimization for irrigation purposes. *Water Science and Technology*, 48(1), 131–138. <https://doi.org/10.2166/wst.2003.0034>
- Tchobanoglous, G., Burton, F. L., Stensel, H. D., Metcalf, & Eddy. (2003). *Wastewater engineering: Treatment and reuse* (4th ed. revised by George Tchobanoglous, Franklin L. Burton, H. David Stensel.). McGraw-Hill.
- The United Nations. (2021). *Valuing Water* [The United Nations World Water Development Report]. UNESCO. <https://www.unwater.org/publications/un-world-water-development-report-2021/>
- Tiwari, B. R., Rouissi, T., Brar, S. K., & Surampalli, R. Y. (2021). Critical insights into psychrophilic anaerobic digestion: Novel strategies for improving biogas production. *Waste Management*, 131, 513–526. <https://doi.org/10.1016/j.wasman.2021.07.002>

- Torres-Franco, A., Passos, F., Figueredo, C., Mota, C., & Muñoz, R. (2021). Current advances in microalgae-based treatment of high-strength wastewaters: Challenges and opportunities to enhance wastewater treatment performance. *Reviews in Environmental Science and Bio/Technology*, 20(1), 209–235. <https://doi.org/10.1007/s11157-020-09556-8>
- Townsend, S. A., Schult, J. H., Douglas, M. M., & Skinner, S. (2008). Does the Redfield ratio infer nutrient limitation in the macroalga *Spirogyra fluviatilis*? *Freshwater Biology*, 53(3), 509–520. <https://doi.org/10.1111/j.1365-2427.2007.01916.x>
- Trego, A. C., Conall Holohan, B., Keating, C., Graham, A., O’Connor, S., Gerardo, M., Hughes, D., Ijaz, U. Z., & O’Flaherty, V. (2021). First proof of concept for full-scale, direct, low-temperature anaerobic treatment of municipal wastewater. *Bioresource Technology*, 341, 125786. <https://doi.org/10.1016/j.biortech.2021.125786>
- Trego, A. C., O’Sullivan, S., Quince, C., Mills, S., Ijaz, U. Z., & Collins, G. (2020). Size Shapes the Active Microbiome of Methanogenic Granules, Corroborating a Biofilm Life Cycle. *MSystems*, 5(5), e00323-20. <https://doi.org/10.1128/mSystems.00323-20>
- Tyrrell, T. (2019). Redfield Ratio☆. In J. K. Cochran, H. J. Bokuniewicz, & P. L. Yager (Eds.), *Encyclopedia of Ocean Sciences (Third Edition)* (pp. 461–472). Academic Press. <https://doi.org/10.1016/B978-0-12-409548-9.11281-3>
- Ueki, A., Akasaka, H., Suzuki, D., & Ueki, K. (2006). *Paludibacter propionigenes* gen. Nov., sp. Nov., a novel strictly anaerobic, Gram-negative, propionate-producing bacterium isolated from plant residue in irrigated rice-field soil in Japan. In *International Journal of Systematic and Evolutionary Microbiology* (Vol. 56, Issue 1, pp. 39–44). Microbiology Society. <https://doi.org/10.1099/ijs.0.63896-0>

- Ueki, A., Goto, K., Kaku, N., & Ueki, K. (2018). *Aminipila butyrlica* gen. Nov., sp. Nov., a strictly anaerobic, arginine-decomposing bacterium isolated from a methanogenic reactor of cattle waste. In *International Journal of Systematic and Evolutionary Microbiology* (Vol. 68, Issue 1, pp. 443–448). Microbiology Society. <https://doi.org/10.1099/ijsem.0.002534>
- Uemura, S., Takahashi, K., Takaishi, A., Machdar, I., Ohashi, A., & Harada, H. (2002). Removal of indigenous coliphages and fecal coliforms by a novel sewage treatment system consisting of UASB and DHS units. *Water Science and Technology*, 46(11–12), 303–309. <https://doi.org/10.2166/wst.2002.0754>
- Unnithan, V. V., Unc, A., & Smith, G. B. (2014). Mini-review: A priori considerations for bacteria–algae interactions in algal biofuel systems receiving municipal wastewaters. *Progress and Perspectives on Microalgal Mass Culture*, 4, 35–40. <https://doi.org/10.1016/j.algal.2013.11.009>
- Urai, M., Aizawa, T., Nakagawa, Y., Nakajima, M., & Sunairi, M. (2008). *Mucilaginibacter kameinonensis* sp., nov., isolated from garden soil. In *International Journal of Systematic and Evolutionary Microbiology* (Vol. 58, Issue 9, pp. 2046–2050). Microbiology Society. <https://doi.org/10.1099/ijms.0.65777-0>
- van der Ha, D., Bundervoet, B., Verstraete, W., & Boon, N. (2011). A sustainable, carbon neutral methane oxidation by a partnership of methane oxidizing communities and microalgae. *Water Research*, 45(9), 2845–2854. <https://doi.org/10.1016/j.watres.2011.03.005>
- Van Hulle, S. W. H., Vandeweyer, H. J. P., Meesschaert, B. D., Vanrolleghem, P. A., Dejans, P., & Dumoulin, A. (2010). Engineering aspects and practical application of autotrophic nitrogen removal from nitrogen rich streams. *Chemical Engineering Journal*, 162(1), 1–20. <https://doi.org/10.1016/j.cej.2010.05.037>

- van Lier, J. B., van der Zee, F. P., Frijters, C. T. M. J., & Ersahin, M. E. (2015). Celebrating 40 years anaerobic sludge bed reactors for industrial wastewater treatment. *Reviews in Environmental Science and Bio/Technology*, 14(4), 681–702. <https://doi.org/10.1007/s11157-015-9375-5>
- Van Wagenen, J., Holdt, S. L., De Francisci, D., Valverde-Perez, B., Plosz, B. G., & Angelidaki, I. (2014). Microplate-based method for high-throughput screening of microalgae growth potential. *Bioresource Technology*, 169, 566.
- Van Wagenen, J., Miller, T. W., Hobbs, S., Hook, P., Crowe, B., & Huesemann, M. (2012). Effects of Light and Temperature on Fatty Acid Production in *Nannochloropsis Salina*. *Energies*, 5(3). <https://doi.org/10.3390/en5030731>
- Van Wagenen, J., Pape, M. L., & Angelidaki, I. (2015). Characterization of nutrient removal and microalgal biomass production on an industrial waste-stream by application of the deceleration-stat technique. *Water Research*, 75, 301–311. <https://doi.org/10.1016/j.watres.2015.02.022>
- Varsadiya, M., Urich, T., Hugelius, G., & Bárta, J. (2021). Microbiome structure and functional potential in permafrost soils of the Western Canadian Arctic. *FEMS Microbiology Ecology*, fiab008. <https://doi.org/10.1093/femsec/fiab008>
- Venil, C. K., Nordin, N., Zakaria, Z. A., & Ahmad, W. A. (2014). *Chryseobacterium artocarpi* sp. Nov., isolated from the rhizosphere soil of *Artocarpus integer*. In *International Journal of Systematic and Evolutionary Microbiology* (Vol. 64, Issue Pt_9, pp. 3153–3159). Microbiology Society. <https://doi.org/10.1099/ijss.0.063594-0>
- Verté, F., Kostanjevecki, V., De Smet, L., Meyer, T. E., Cusanovich, M. A., & Van Beeumen, J. J. (2002). Identification of a Thiosulfate Utilization Gene Cluster from the Green Phototrophic Bacterium

- Chlorobium limicola,. *Biochemistry*, 41(9), 2932–2945.
<https://doi.org/10.1021/bi011404m>
- Vieira, P. C., von Sperling, M., Nogueira, L. C. M., & Assis, B. F. S. (2013). Performance evaluation of a novel open trickling filter for the post-treatment of anaerobic effluents from small communities. *Water Science and Technology*, 67(12), 2746–2752. <https://doi.org/10.2166/wst.2013.195>
- Vieira, S. M. M., Carvalho, J. L., Barijan, F. P. O., & Rech, C. M. (1995). Application of the UASB technology for sewage treatment in a small community at Sumare, Sao Paulo State. *Water Science and Technology*, 12, 203–210. [https://doi.org/0273-1223\(95\)00126-3](https://doi.org/0273-1223(95)00126-3)
- Vieira, S. M. M., & Garcia, A. D., Jr. (1992). Sewage Treatment by UASB-Reactor. Operation Results and Recommendations for Design and Utilization. *Water Science and Technology*, 25(7), 143–157. <https://doi.org/10.2166/wst.1992.0147>
- Volkman, J. K., Brown, M. R., Dunstan, G. A., & Jeffrey, S. W. (1993). The biochemical composition of marine microalgae from the class Eustigmatophyceae1. *Journal of Phycology*, 29(1), 69–78. <https://doi.org/10.1111/j.1529-8817.1993.tb00281.x>
- Wainaina, S., Awasthi, M. K., Sarsaiya, S., Chen, H., Singh, E., Kumar, A., Ravindran, B., Awasthi, S. K., Liu, T., Duan, Y., Kumar, S., Zhang, Z., & Taherzadeh, M. J. (2020). Resource recovery and circular economy from organic solid waste using aerobic and anaerobic digestion technologies. *Bioresource Technology*, 301, 122778. <https://doi.org/10.1016/j.biortech.2020.122778>
- Wang, J.-H., Zhang, T.-Y., Dao, G.-H., Xu, X.-Q., Wang, X.-X., & Hu, H.-Y. (2017). Microalgae-based advanced municipal wastewater treatment for reuse in water bodies. *Applied Microbiology and Biotechnology*, 101(7), 2659–2675. <https://doi.org/10.1007/s00253-017-8184-x>
- Wang, L., Min, M., Li, Y., Chen, P., Chen, Y., Liu, Y., Wang, Y., & Ruan, R. (2010). Cultivation of Green Algae Chlorella sp. In

- Different Wastewaters from Municipal Wastewater Treatment Plant. *Applied Biochemistry and Biotechnology*, 162(4), 1174–1186. <https://doi.org/10.1007/s12010-009-8866-7>
- Wanner, O., & Gujer, W. (1986). A multispecies biofilm model. *Biotechnology and Bioengineering*, 28(3), 314–328. <https://doi.org/10.1002/bit.260280304>
- WHO, & UNICEF. (2021). *Progress on household drinking water, sanitation and hygiene 2000-2020: Five years into the SDGs*. <https://washdata.org/sites/default/files/2021-07/jmp-2021-wash-households.pdf>
- Wilhelm, Emmerich., Battino, Rubin., & Wilcock, R. J. (1977). Low-pressure solubility of gases in liquid water. *Chemical Reviews*, 77(2), 219–262. <https://doi.org/10.1021/cr60306a003>
- Wu, J., Afridi, Z. U. R., Cao, Z. P., Zhang, Z. L., Poncin, S., Li, H. Z., Zuo, J. E., & Wang, K. J. (2016). Size effect of anaerobic granular sludge on biogas production: A micro scale study. *Bioresource Technology*, 202, 165–171. <https://doi.org/10.1016/j.biortech.2015.12.006>
- Wu, P.-H., Ng, K. K., Hong, P.-K. A., Yang, P.-Y., & Lin, C.-F. (2017). Treatment of low-strength wastewater at mesophilic and psychrophilic conditions using immobilized anaerobic biomass. *Chemical Engineering Journal*, 311, 46–54. <https://doi.org/10.1016/j.cej.2016.11.077>
- Xu, Y., Purton, S., & Baganz, F. (2013). Chitosan flocculation to aid the harvesting of the microalga *Chlorella sorokiniana*. *Bioresource Technology*, 129, 296–301. <https://doi.org/10.1016/j.biortech.2012.11.068>
- Yadav, G., Dash, S. K., & Sen, R. (2019). A biorefinery for valorization of industrial waste-water and flue gas by microalgae for waste mitigation, carbon-dioxide sequestration and algal biomass production. *Science of The Total Environment*, 688, 129–135. <https://doi.org/10.1016/j.scitotenv.2019.06.024>

- Yang, Z., Guo, R., Shi, X., He, S., Wang, L., Dai, M., Qiu, Y., & Dang, X. (2016). Bioaugmentation of *Hydrogenispora ethanolica* LX-B affects hydrogen production through altering indigenous bacterial community structure. *Bioresource Technology*, *211*, 319–326. <https://doi.org/10.1016/j.biortech.2016.03.097>
- Yeh, K.-L., Chang, J.-S., & Chen, W.-M. (2010). Effect of light supply and carbon source on cell growth and cellular composition of a newly isolated microalga *Chlorella vulgaris* ESP-31. *Engineering in Life Sciences*, *10*(3), 201–208.
- Yewalkar, S., Li, B., Posarac, D., & Duff, S. (2011). Potential for CO₂ Fixation by *Chlorella pyrenoidosa* Grown in Oil Sands Tailings Water. *Energy & Fuels*, *25*(4), 1900–1905. <https://doi.org/10.1021/ef101503h>
- Yu, Z., Beck, D. A. C., & Chistoserdova, L. (2017). Natural Selection in Synthetic Communities Highlights the Roles of Methylococcaceae and Methylophilaceae and Suggests Differential Roles for Alternative Methanol Dehydrogenases in Methane Consumption. *Frontiers in Microbiology*, *8*, 2392. <https://doi.org/10.3389/fmicb.2017.02392>
- Yuan, X., Kumar, A., Sahu, A. K., & Ergas, S. J. (2011). Impact of ammonia concentration on *Spirulina platensis* growth in an airlift photobioreactor. *Bioresource Technology*, *102*(3), 3234–3239. <https://doi.org/10.1016/j.biortech.2010.11.019>
- Yun, J.-H., Cho, D.-H., Lee, S., Heo, J., Tran, Q.-G., Chang, Y. K., & Kim, H.-S. (2018). Hybrid operation of photobioreactor and wastewater-fed open raceway ponds enhances the dominance of target algal species and algal biomass production. *Algal Research*, *29*, 319–329. <https://doi.org/10.1016/j.algal.2017.11.037>
- Zhang, D., Zhu, W., Tang, C., Suo, Y., Gao, L., Yuan, X., Wang, X., & Cui, Z. (2012). Bioreactor performance and methanogenic population dynamics in a low-temperature (5–18°C) anaerobic

- fixed-bed reactor. *Bioresource Technology*, 104, 136–143. <https://doi.org/10.1016/j.biortech.2011.10.086>
- Zhang, L., De Vrieze, J., Hendrickx, T. L. G., Wei, W., Temmink, H., Rijnaarts, H., & Zeeman, G. (2018). Anaerobic treatment of raw domestic wastewater in a UASB-digester at 10 °C and microbial community dynamics. *Chemical Engineering Journal*, 334, 2088–2097. <https://doi.org/10.1016/j.cej.2017.11.073>
- Zhang, Y., Wang, X., Hu, M., & Li, P. (2015). Effect of hydraulic retention time (HRT) on the biodegradation of trichloroethylene wastewater and anaerobic bacterial community in the UASB reactor. *Applied Microbiology and Biotechnology*, 99(4), 1977–1987. <https://doi.org/10.1007/s00253-014-6096-6>
- Zhu, X., Luo, J., Zhou, C., Wang, J., Meng, R., Xu, J., Chen, J., Luo, Q., & Yan, X. (2018). Changes of pigments and lipids composition in *Haematococcus pluvialis* vegetative cell as affected by monochromatic red light compared with white light. *Journal of Oceanology and Limnology*, 36(6), 2257–2267. <https://doi.org/10.1007/s00343-019-7195-0>

Appendices

- Appendix 1 – Paper I
- Appendix 2 – Paper II
- Appendix 3 – Paper III
- Appendix 4 – Microalgal-based treatment for secondary wastewater effluent
- Appendix 5 – Pathogen analysis method
- Appendix 6 – Anaerobic granulated biofilm system model for municipal wastewater treatment

Appendix 1 – Paper 1

Effect of low-temperatures and wastewater organic loading on UASB system performances. Anissa Sukma Safitri, Krista M. Kaster, and Roald Kommedal. *Submitted for publication in Water Research Journal.*

Effect of low-temperatures and municipal wastewater organic loading on UASB system performance

Anissa Sukma Safitri, Krista M. Kaster, and Roald Kommedal*

Institute of Chemistry, Bioscience and Environmental Engineering,
University of Stavanger, 4036 Stavanger, Norway

*Corresponding Author. Email address: roald.kommedal@uis.no

Abstract

Up-flow anaerobic sludge blanket (UASB) reactors were operated continuously over 1025 days by applying a stepwise increase of organic loading rate (OLR) starting from $1.3 \pm 0.1 \text{ gCOD} \cdot \text{l}^{-1} \cdot \text{d}^{-1}$ (\pm standard error) by intermittent increases to $15.2 \pm 0.2 \text{ gCOD} \cdot \text{l}^{-1} \cdot \text{d}^{-1}$ at decreasing temperatures (25, 16, 12, 8.5, 5.5 and 2.5 °C). The sustained UASB reactor performance was maintained and proven by COD removal efficiency, methane production, and microbial community analysis. Stable COD removal efficiencies of 50 - 70 % was achieved down to 8.5 °C with loading up to $15.0 \text{ gCOD} \cdot \text{l}^{-1} \cdot \text{d}^{-1}$. Below 8.5 °C, COD removal efficiencies and methane yields reduced, but significant methane formation was observed even at 2.5 °C at reduced loading (up to $5 \text{ gCOD} \cdot \text{l}^{-1} \cdot \text{d}^{-1}$). In general, more than 90% of COD removed was converted to methane, and the methane yield did not change significantly with respect to temperatures. The overall COD balance closed at above 90% of the inlet COD at all operating temperatures and OLRs. Transient times indicated that temperature reductions down to 12 °C did not initiate community shifts, but below 10 °C methanogenic adaptations were observed. Methanogen communities showed temperature and loading change effected the degradation pathway of organic matter with acetoclastic methanogen and H₂-dependent methylotrophic methanogens

played significant roles. Methanogenic archaea communities proved the adaptation ability to very low-temperatures down to 2.5 °C regardless of the operating OLR.

Keywords:

UASB system; municipal wastewater treatment; low-temperature; organic loading rate; methanogen community

1. Introduction

Anaerobic treatment has been recognized as an attractive alternative and more sustainable to traditional aerobic processes for municipal wastewater treatment, especially for high strength wastewater (Lettinga et al., 2001). Wastewater as carbon organic-rich sources could be converted to methane by anaerobic treatment, transforming an assumed low-value source into a substantial renewable form of energy (Aiyuk et al., 2004) contributing to the circular bio-economy (Show et al., 2020; Wainaina et al., 2020). Among several anaerobic treatment technologies that have been implemented, the up-flow anaerobic sludge blanket (UASB) system using granulated biomass offers several advantages (Seghezzi et al., 1998; Singh, Harada, and Viraraghavan, 1996). The use of anaerobic granulated biomass for biological wastewater treatment was introduced about 40 years ago (Lettinga et al., 1980) and is now regarded as an adequate methodology and a robust system for municipal wastewater treatment and energy recovery (Schellinkhout and Collazos, 1992; Rosa et al., 2018).

The relatively slow-growth rate and putative sensitivity of methanogens to environmental conditions have often been claimed to limit anaerobic wastewater treatment, particularly towards psychrophilic condition (Lettinga et al., 2001). It has been reported that anaerobic treatment is also vulnerable to overloading, which could disturb the process stability

and affected the microbial community (Cardinali-Rezende et al., 2013; de Vrieze, et al. 2012; Martins et al., 2017). Several researcher in previous studies showed a significant adverse effect on the metabolic activity of mesophilic methanogens at decreasing temperatures (Kettunen and Rintala 1997; Koster and Lettinga 1985; Rebac et al. 1999; Rebac et al. 1995). The degree of influence is, however, not consensually agreed upon, and positive results have already been reported for the 10 - 15°C range (Kettunen and Rintala, 1997; Collins et al., 2006; Akila and Chandra, 2007). Furthermore, results have also been reported that anaerobic communities of granulated sludge systems could adapt to low-temperatures even down to 4 - 10°C (Petropoulos et al., 2017; Bowen et al., 2014; McKeown et al., 2009). This is not surprising as abundant methanogens have been isolated from extreme cold natural environments, such as in lake sediment, high arctic peat, permafrost, and the northern tundra (Høj, Olsen, and Torsvik, 2008; Varsadiya et al., 2021; Kwon et al., 2019).

Bowen et al. (2014) reported anaerobic treatment of low strength domestic wastewater in a batch system at low-temperatures. Methanogenesis was inhibited due to inhibition of activity rather than the absence of methanogen population, while the acidogenic reactions still occur at all temperatures studied; 4, 8 and 15 °C (Bowen et al., 2014). One long term study (1243 days) also observed acidified wastewater treatment at low-temperatures (4 - 15 °C) using an expanded granular sludge bed reactor. This published report also suggested that mesophilic inoculum could physiologically adapt to psychrophilic operational temperatures (McKeown et al., 2009). More recently, Petropoulos et al. (2017) studied communities from environments that have been exposed to low-temperatures (4, 8 and 15 °C) for 400 days in a batch system receiving domestic wastewater. Their results implied that inoculating reactors with cold-adapted communities was a promising way to develop biomass capable of treating anaerobic wastewater treatment at low-

temperatures, indicating that low-temperature anaerobic wastewater treatment is possible using adapted cultures (Petropoulos et al., 2017).

Even though real wastewater treatment in various continuous anaerobic reactors (UASB, anaerobic filter and hybrid system, anaerobic membrane reactor) at low-temperature, down to 3 °C, for 140 - 540 days is well documented (Kettunen and Rintala, 1998; Elmitwalli et al., 2002; Mahmoud et al., 2004; Bandara et al., 2012; Smith, Skerlos, and Raskin, 2012; Zhang et al., 2018; Petropoulos et al., 2021), long term UASB reactor operation treating real municipal wastewater at low-temperatures below 20 °C in the combination of organic loading rate (OLR) effect investigation is scarce. For anaerobic wastewater treatment to become a viable and preferred treatment strategy for municipal wastewater in the northern temperate and sub-arctic populated regions, stable operation and acceptable treatment performance must be demonstrated, and operational stability needs to be documented. Further, if psychrophilic wastewater treatment is possible, an important design and operational question is whether such performance is a result of microbial community adaptations or phenotypic adaptations of a mesophilic generic sludge.

In this work, we investigated long-term (1025 days) temperature effects (2.5, 5.5, 8.5, 12, 16, and 25 °C) on UASB reactor performance treating municipal wastewater over typical operational organic loading rates. The productivity of this anaerobic granular sludge system was studied by determining its COD removal efficiency, measuring its specific methane production rate, and methane yield. The COD balance analysis was conducted as well to evaluate reactor performance by investigating COD recovery and COD loss during operation. Nutrient, VFA and alkalinity dynamics was closely monitored for inference on UASB operational stability. The effect of temperature and loading was investigated in an operational regime allowing for seasonal adaptations of microbial communities. Hence, this work also included microbial community characterization of the low-temperature and loading gradients.

2. Materials and Methods

2.1. Granule inoculum source

Granulated inoculum was kindly provided by the late Professor Rune Bakke, University of South-Eastern Norway (USN). Granules were made from diverse sources: (a) pulp and paper company treating cellulose and lignin-containing (Moss, Norway); (b) agriculture pilot-plant treating swine and cow manure supernatant (Skien, Norway); and (c) hydrocarbon oil-containing wastewater at Bamble Industrial Park (Telemark, Norway).

2.2. Experimental set-up and operation of continuous reactors

Approximately 30 % (v/v) of granules inoculum were transferred to the UASB reactors with 1000 ml of total volume. Two parallel in-house designed laboratory-scale UASB reactors (reactor A and B) were operated continuously, receiving primary treated municipal wastewater, from the Grødalund wastewater treatment plant (WWTP), Norway. The wastewater may be characterized as a municipal wastewater with significant contributions from agricultural and food industries like (a) Animal residual recovery plant (Biosirk Protein: $167 \text{ m}^3 \cdot \text{d}^{-1}$); (b) Municipal wastewater of approximately 3000 houses of the community Varhaug ($3000 \text{ m}^3/\text{d}$) and food processing plant (Fjordland: $1910 \text{ m}^3 \cdot \text{d}^{-1}$); (c) Dairy + Chicken slaughterhouse (Kviamarka: $3020 \text{ m}^3 \cdot \text{d}^{-1}$); and (d) Reject water from thickening and dewatering of digested sludge from the Grødalund biogas plant ($345 \text{ m}^3 \cdot \text{d}^{-1}$). The dissolved COD concentrations of inlet wastewater during UASB reactor operation fluctuated in the range $439 - 1473 \text{ mgCOD}_{\text{dissolved}} \cdot \text{l}^{-1}$ with the mean dissolved concentration of $741 \pm 7 \text{ mgCOD}_{\text{dissolved}} \cdot \text{l}^{-1}$ (\pm standard error). Samples were collected weekly and stored in the dark at $4 \text{ }^\circ\text{C}$ before use (average storage time 5 days).

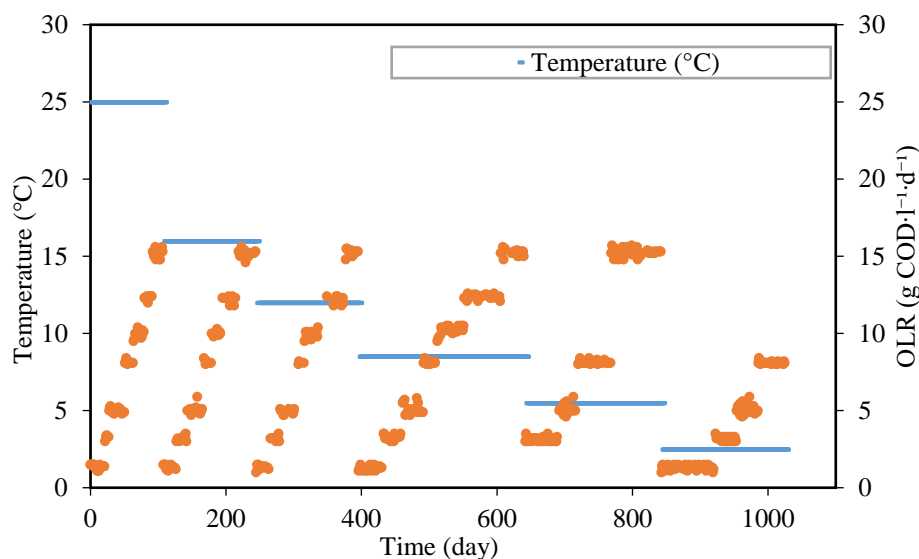


Figure 1 The UASB reactors were operated continuously over 1025 days by the stepwise increase of OLR at decreasing temperatures. Initially, UASB reactors were started-up at 25 °C with low OLR around 1.0 $\text{gCOD}_{\text{dissolved}}\cdot\text{l}^{-1}\cdot\text{d}^{-1}$ and increased gradually up to approximately 15 $\text{gCOD}_{\text{dissolved}}\cdot\text{l}^{-1}\cdot\text{d}^{-1}$. During operation, hydraulic retention rate (HRT) started at about 16.7 h then gradually decreased along with the increasing OLR, down to 1.1 h. The operating temperatures were then reduced to the next lower temperature experiments at 16, 12, 8.5, 5.5 and finally 2.5 °C.

The UASB reactors were operated continuously by applying a stepwise increase of organic loading rate (OLR) starting from 1.3 ± 0.1 by intermittent increases to 15.2 ± 0.2 $\text{gCOD}_{\text{dissolved}}\cdot\text{l}^{-1}\cdot\text{d}^{-1}$ following steady-state tests at decreasing temperatures (25, 16, 12, 8.5, 5.5 and 2.5 °C). A steady-state was achieved in the reactors when the parameters, e.g., the COD removal efficiencies and the daily gas production remained relatively constant at the same temperature and OLR. OLR was controlled by adjusting the inlet flow rate based on batchwise analysis of the dissolved COD concentration of inlet wastewater. Operational characteristic during continuous UASB system operation for both reactors is shown in Figure 1. Both reactors were identical and operated with the same loading and inlet. The gradual increment of OLR was used to ensure that granules would not wash out of the system while the

microorganisms were acclimating to the higher loading. Severe deterioration of granules occurred in reactor A when applying OLR of $15 \text{ gCOD}\cdot\text{l}^{-1}\cdot\text{d}^{-1}$ at $5.5 \text{ }^{\circ}\text{C}$ and the reactor stopped operating at day 738. The occurrence will be discussed further in Results and Discussions.

Figure 2 presents a schematic view and flow diagram of the reactor set-up. The reactors used were air-tight glass-type reactors capped with a natural rubber stopper (custom made by glass blower Mellum AS, Aurskog Norway: www.friedel.no). The total volume of the reactor is 1000 ml with 4.5 cm inner diameter and 66 cm height. The reactors were temperature controlled using a Lauda Alpha RA8 refrigerated water circulation unit (Lauda, Germany), circulating water through reactor jackets at a high rate ($>200 \text{ ml}\cdot\text{min}^{-1}$). Glycol was added to the circulating unit to avoid freezing when applying $2.5 \text{ }^{\circ}\text{C}$ in operation on day 842. An external foam insulator was mounted to maintain the desired temperatures of $8.5 \text{ }^{\circ}\text{C}$ operations (day 520) and below. An external digital thermometer was installed inside the circulating unit as an additional temperature confirmation, and temperatures inside the reactors were measured manually on a regular basis. Cooled wastewater was fed by a peristaltic pump (Ismatec, Germany) with adjustable flow rates. Continuous recirculation to sustain mixing and a constant up-flow was achieved by pumping effluent from the top to the bottom of the reactors by $1.8\pm 0.7 \text{ m}\cdot\text{h}^{-1}$ (\pm standard error).

Methane and CO_2 produced were measured using Milligas counters (Dr.-Ing. RITTER Apparatebau GmbH & Co., Bochum, Germany) serially connected to the UASB gas-outlet and equipped with a bubble-through CO_2 -absorber, containing NaOH 3 M and 0.4 % Thymolphthalein pH-indicator solution. A pH probe (Hanna Instruments, HI 9025C, Norway) was installed in the recirculation line allowing an inline measurement of the bulk liquid pH. A $1000 \text{ }\mu\text{m}$ Sefar® Flourtex filter (Sefar AG, Switzerland) was installed inside the reactor exit section to retain biomass from being washed out and potentially clog pump and gas exit tubes.

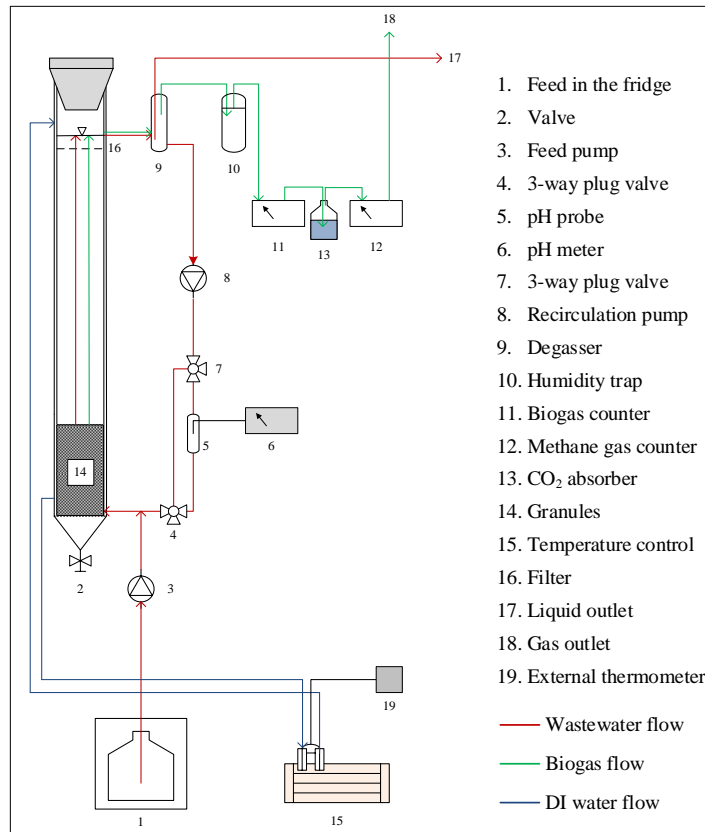


Figure 2 Flow diagram of the laboratory-scale UASB reactor. Two reactors were assembled parallelly identically with the same set-up as illustrated here. The red line represents the wastewater inlet and outlet flow; the green line represents the biogas flow; the blue line represents the distilled water flow for the cooling circulating water.

2.3. Analytical methods

Dissolved and total COD were determined daily using standard COD Spectroquant® test kits with a detection range of 100 - 1500 mg·l⁻¹ (Merck, Germany) along with nutrients (total phosphorous, orthophosphate, total nitrogen, ammonium, and nitrate, all measured using standard Spectroquant® test kits (Merck, Germany). Sample filtration was conducted prior to determining the dissolved components by a 1.2 µm glass microfiber filter (GF/C, Whatman, UK). Conductivity

was measured using WTW Multi340i, which was connected to conductivity probe WTW Tetra Con® 325 (Geotech Environmental Equipment, Inc., USA). This parameter was needed for determination of alkalinity and VFA concentrations which were determined using a TitroLine® 5000 titrator (SI Analytics, Germany) following the pH based five point titration method (Moosbrugger et al., 1993). Total VFA and alkalinity were calculated concomitantly using the TITRA5 software (brouckae@ukzn.ac.za). Samples were taken and analyzed independently in duplicates for each measurement.

Biogas methane was primarily determined using gas counters and volume percentages intermittently confirmed by Agilent 7890B gas chromatography (Agilent, USA). Biogas was collected in Tedlar® gas sampling bags (Sigma Aldrich, Germany), and 100-200 µl of biogas were withdrawn using a gas-tight syringe (SGE-Europe) and injected onto the GC equipped with a thermal conductivity detector (TCD) (Agilent column, 0.32 mm diameter, 30 m length and 0.25 µm film). Helium was used as the carrier gas at a flow rate of 54 ml·min⁻¹, and the oven temperature was 50 °C. In the effluent, dissolved methane was estimated using the temperature adjusted Henry's coefficient for determination of the total methane produced from the UASB system (Wilhelm et al., 1977).

2.4. Microbial community analysis

Approximately 0.25 g (wet weight) of granule samples were obtained from the reactor during 12, 8.5, 5.5 and 2.5°C reactor operation carried out at different OLRs at each temperature. DNA was extracted using a DNeasy PowerWater Kit (Qiagen, Germany) as described by the manufacturer. Samples were homogenized in PowerBead tubes using the FastPrep-24™ bead beater (MPBio, USA) for 60s prior to extraction. After extraction, DNA was checked via agarose gel electrophoresis. The DNA concentration was determined using the NanoVue™ Plus Spectrophotometer (GE Healthcare, USA) at absorbance 260 nm before

sending samples for external sequencing (Macrogen Europe B.V., Netherlands). The averaged DNA concentration was approximately $100 \text{ ng}\cdot\mu\text{l}^{-1}$. The isolated DNA was stored at $-20 \text{ }^\circ\text{C}$ until further processing.

For polymerase chain reaction (PCR) amplification, the DNA was amplified using primers the v3–4 region of the 16S rRNA gene; B-341F (5'-CCTACGGGNGGCWGCAG) and B-805R (5'-GACTACNVGGGTATCTAAKCC) amplifying 465 base pairs (bp) for bacterial DNA, A-340F (CCCTAYGGGGYGCASCAG) and A-760R (GGACTACCSGGGTATCTAATCC) for archaeal DNA (Nordgård et al., 2017). Pair end sequencing was done by Macrogen Europe B.V, Netherlands, using the MiSeq™ platform. FLASH (fast length adjustment of short reads) software was used to assembly reading data by merging paired-end reads from next-generation sequencing experiments (Magoč and Salzberg, 2011). CD-HIT-OTU was utilized to preprocess and cluster the data with a three-step clustering to identify operational taxonomic units (OTU) and rDnaTools (Li et al., 2012).

2.5. Statistical analysis

Statistical analyses, standard errors and student t-tests at 95% confidence were calculated and applied using Excel and SigmaPlot V14.0 for Windows (SyStat Inc., USA).

3. Results

3.1. COD removal efficiencies

UASB reactors were started-up at $25 \text{ }^\circ\text{C}$ at a low OLR of $1.0 \text{ gCOD}\cdot\text{l}^{-1}\cdot\text{d}^{-1}$, and an acclimatization period over the first five days was monitored until the reactors reached a steady-state condition. The adaptation time of the system (transient time) until steady-state was confirmed increased with decreasing temperature in both reactor (Figure 3). Statistical

analysis, student t-test, revealed no significant difference ($p>0.05$) between reactor A and B transient times. At 12, 16 and 25 °C, the transient time at different OLR were in the same range at 14, 9 and 5 days, respectively. As the temperature was reduced, and especially at 2.5 and 5.5 °C, there was an acclimatization period of up to 68 days. Acclimation also seemed to be slower for the lower loading rates, especially at low-temperatures. A significant level of granule disintegration and effluent/bulk phase suspended particles was observed several times throughout reactor operation during the acclimatization periods, especially at high OLR $>8.0 \text{ gCOD}\cdot\text{l}^{-1}\cdot\text{d}^{-1}$. Severe deterioration of granules occurred in reactor A when applying $15 \text{ gCOD}\cdot\text{l}^{-1}\cdot\text{d}^{-1}$ at 5.5 °C with an estimated $>90\%$ loss of the granular sludge from the sludge bed. Granules became smaller, down to 0.5 mm in diameter, and along with finer particles got washed-out from the reactor. Hence, reactor A was stopped on day 738, and investigations continued on reactor B only.

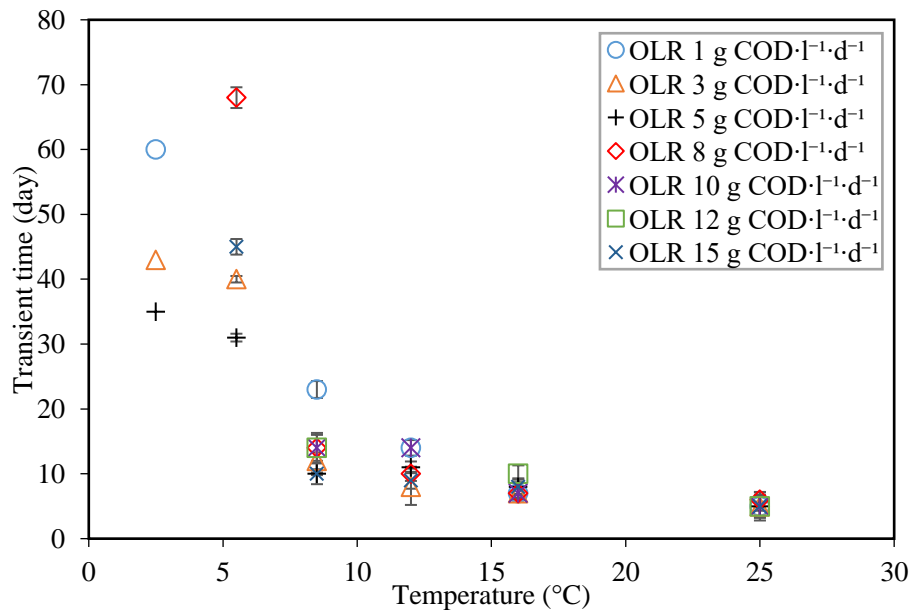


Figure 3 Averaged transient time to steady-state conditions at different temperatures and OLRs in reactor A and B. The student t-test revealed no significant difference ($p>0.05$) between reactor A and B transient times.

Figure 4 presents dissolved COD removal efficiencies when reaching steady-state conditions at different temperatures and OLRs. At each OLR increment and change of reactor temperature, COD removal efficiency temporarily decreased before gradually increasing towards the new steady-state. The COD removal efficiency (steady-state condition) declined with the temperature and increased OLR, especially at lower temperatures. At higher temperatures, 16 and 25 °C, the COD removal efficiency for all OLRs remained the same in the 60 - 70% range. Even at temperatures as low as 12 °C, at all operating OLRs, the methanogenic capacity of the UASB reactor was sufficient to maintain a COD removal efficiency above 50%.

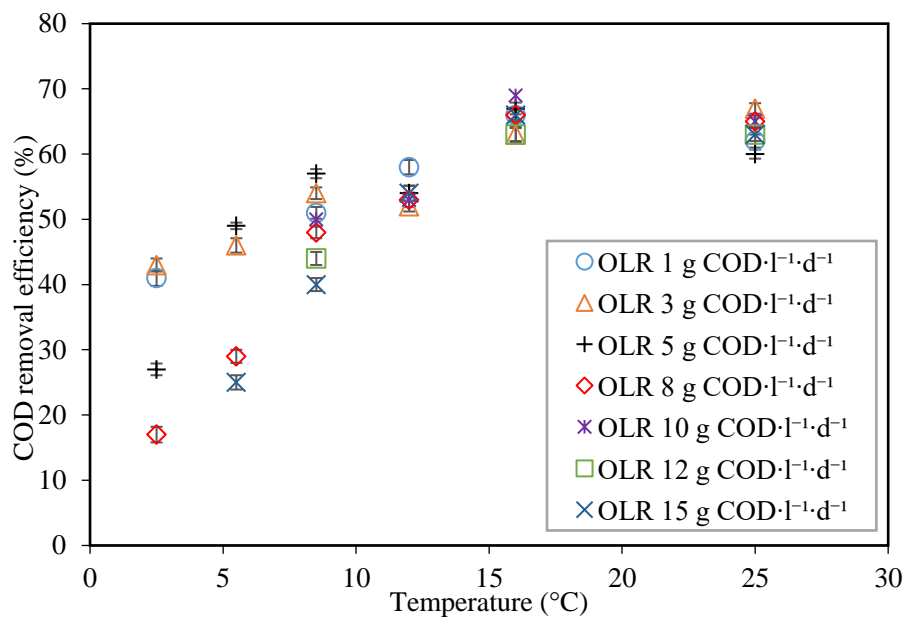


Figure 4 Dissolved COD removal efficiencies at steady-state conditions in the function of different temperatures and OLRs. Error bars represent standard errors from measurements taken during steady-state conditions in reactor A and B. The student *t*-test revealed no significant difference ($p > 0.05$) between reactor A and B COD removal efficiencies.

There was a significant change in COD removal efficiency at lower temperatures (8.5, 5.5 and 2.5 °C). At 8.5 °C, COD removal efficiency was also above 50% for OLR up to 8 gCOD·l⁻¹·d⁻¹, however, a systematic decrease started to appear for the 10 - 15 gCOD·l⁻¹·d⁻¹ range. Low-temperatures (5.5 and 2.5 °C) accompanied by higher OLR resulted in overloading the UASB reactor and higher COD effluent concentrations resulted.

At steady-state during UASB reactor operation, the mean effluent COD concentration fluctuated corresponding to the fluctuations in the inlet COD concentration. It was observed that COD removal efficiency corresponded with inlet COD concentration, especially at low-temperatures (8.5, 5.5 and 2.5 °C) and high OLRs (8.0 - 15.0 gCOD·l⁻¹·d⁻¹). Typically, COD removal efficiency above 40% could be achieved with a COD inlet >500 mgCOD_{dissolved}·l⁻¹. Low inlet COD concentrations (<500 mgCOD_{dissolved}·l⁻¹) at high OLRs (8.0 - 15.0 gCOD·l⁻¹·d⁻¹) resulted in an increased inlet flow rate to achieve the desired OLR, resulting in lower HRTs (down to 1.1 h) in the system. Lower HRT resulted in lower COD removal efficiencies at low-temperatures (8.5, 5.5, and 2.5 °C). While at higher temperatures (25, 16, and 12 °C), lower HRTs in the system did not significantly affect COD removal efficiencies.

3.2. Methane productions

Figure 5 presents the methane fraction at different operating temperatures and OLRs. Overall, biogas composition was mainly methane above 70% at all operating temperatures and OLRs. There were slight decreases in methane fraction in biogas following the decreasing temperatures from above 80% at 25 °C to approximately 75% at 5.5 °C. However, methane fractions increased by above 80% again at operating temperature by 2.5 °C.

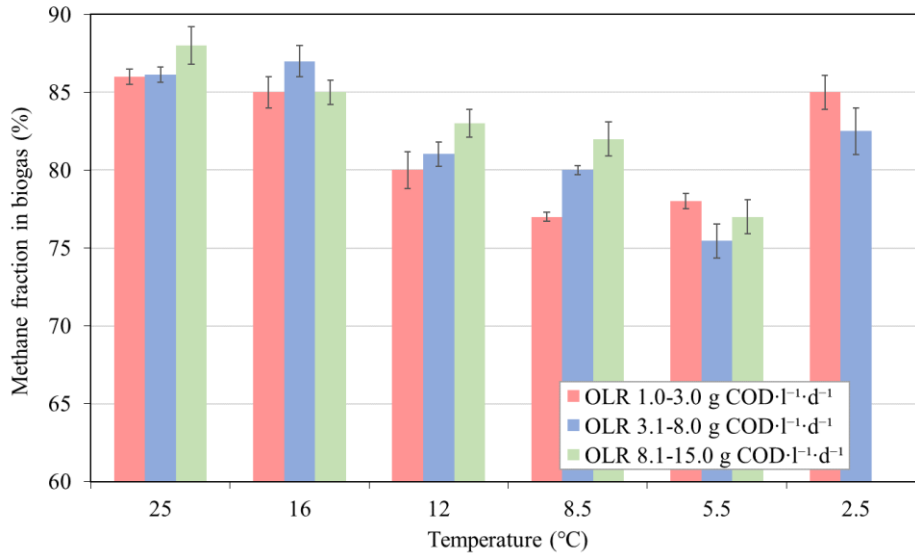


Figure 5 Methane fractions at steady-state conditions with different temperatures and OLRs. Error bars represent standard errors from measurements taken during steady-state conditions in reactor A and B. The student t-test revealed no significant difference ($p > 0.05$) between reactor A and B COD methane fraction.

Figure 6a and 6b show biomass volume specific methane production rates in reactor A and B as COD equivalent as depending on temperatures and OLRs. As shown in Figure 6a and 6b, at each temperature, methane production rates increased with the increasing OLR. Significantly decreased methane productions were observed under low-temperatures (8.5, 5.5 and 2.5 °C). On the other hand, methane productions rate at 25, 16 and 12 °C relatively were comparable in the same range and higher than at lower temperatures. In general, at higher temperatures (25, 16 and 12 °C), the methane production rate was not significantly affected by increasing OLR corresponding to the effect on COD removal efficiency. At the lowest temperature (2.5 °C) and OLR $1.3 \pm 0.1 \text{ gCOD} \cdot \text{l}^{-1} \cdot \text{d}^{-1}$ (\pm standard error), the specific methane production rate was $0.55 \pm 0.04 \text{ gCOD-CH}_4 \cdot \text{l biomass}^{-1} \cdot \text{d}^{-1}$ and then increased slightly with the increasing OLR to $8.1 \pm 0.1 \text{ gCOD} \cdot \text{l}^{-1} \cdot \text{d}^{-1}$ by $1.70 \pm 0.03 \text{ gCOD CH}_4 \cdot \text{l biomass}^{-1} \cdot \text{d}^{-1}$.

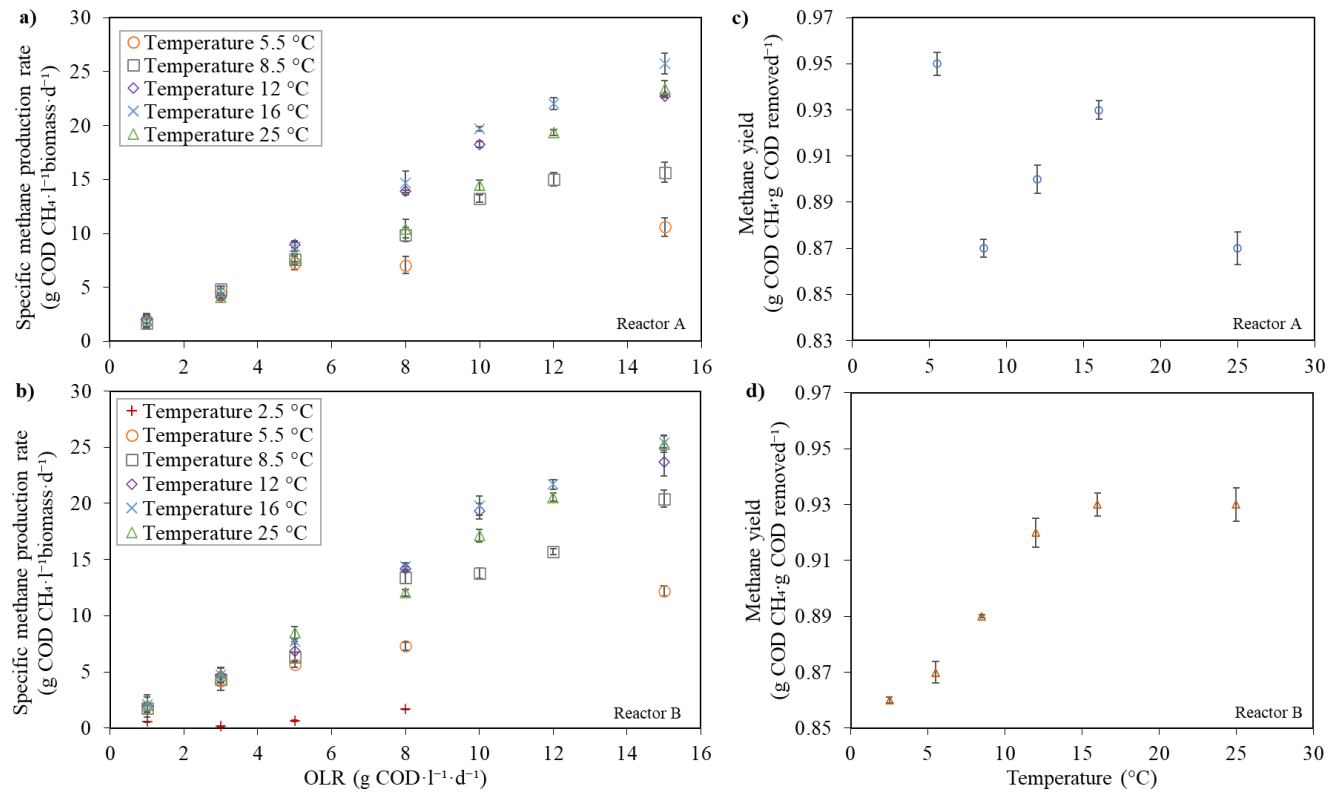


Figure 6 Specific methane production rate per volume biomass (a and b) and overall COD specific methane yield (c and d) at steady-state conditions in reactor A and B. Error bars represent standard errors from measurements taken during steady-state conditions.

Furthermore, methane yield was also investigated in this study, as presented in Figure 6c and 6d. Methane yield was calculated as gCOD methane per gCOD removed. The averaged methane yield obtained in reactor A and B were 0.86 ± 0.01 , 0.91 ± 0.01 , $0.85 \pm$, 0.91 ± 0.00 , 0.93 ± 0.01 , and 0.90 ± 0.00 gCOD-CH₄.gCOD_{removed}⁻¹ (\pm standard error) at 2.5, 5.5, 8.5, 12, 16, and 25 °C, respectively. In general, more than 90% of COD removed was converted to methane, and the methane yield did not change significantly with respect to temperatures. The overall COD balance closed at above 90% of the inlet COD at all operating temperatures and OLRs; the COD loss was 3 - 10%. The detailed COD balance profiles at different temperatures and OLRs during the experiment is presented in the Supplementary Document (Figure S3).

3.3. Nutrient variability

This study investigated the removal efficiency of nutrients (N and P) for municipal wastewater treatment in the UASB reactors. The results show that Grødaland wastewater had nitrogen mainly in particulate form (60 - 80%), while phosphorous presented mostly in dissolved form, orthophosphate (60 - 90%). No significant nutrient removal was observed during the UASB reactor operation at different temperatures and OLRs. The total nitrogen and total phosphorous removal efficiencies were in the range of 10 - 33% and 4 - 20 %, respectively. Generally, the UASB reactors removed mainly the particulate nutrients. Orthophosphate was slightly removed by less than 10% of removal efficiency. Moreover, the removal of NH₄ had negative removal efficiencies; thus, NH₄ was being released during the UASB reactor operation. Overall nutrient variability during UASB reactor operation is presented in the Supplementary Document (Figure S3).

3.4. pH, VFA and alkalinity variability

pH, VFA and alkalinity were measured daily during the experiment. pH, VFA and alkalinity profiles during UASB reactor operation are presented in the Supplementary Document (Figure S4) and expressed as

mg acetic acid·l⁻¹ for total VFA and as mgCaCO₃·l⁻¹ alkalinity. During the acclimatization period following each increment in OLR, a slight decrease in alkalinity, and consequently pH, were observed due to transient accumulation of VFA. After reaching the new steady-state conditions, alkalinity was recovered and VFA concentration decreased to stable concentrations in the range of 190 - 350 mg as acetic acid·l⁻¹ depending on inlet COD concentration. Significant VFA fluctuation was observed during the operating temperature of 8.5 and 5.5 °C (especially in reactor A) and 2.5 °C (in reactor B). The accumulation of VFA of 400 - 600 mg acetic acid·l⁻¹ in the reactors provoked the gradual drop of alkalinity concentration, and pH dropped to 5.9 - 6.7. During acclimation period, when applying high OLRs (10 - 15 gCOD·l⁻¹·d⁻¹) and low HRT of approximately 1.1 h at all temperatures, pH sometimes dropped below 6.3, and methane production ceased. Hence 1.0 g·l⁻¹ NaHCO₃ was added occasionally to the feed wastewater (Figure S4), and pH was stabilized around 7.0. The student t-test revealed a significant difference (p<0.05) between reactor A and B on pH, VFA and alkalinity variability.

3.5. Microbial community analysis

Microbial community analysis using MiSeq amplicon sequencing, produced high quality data by more than 89% of coverage on average, representing the percentage of sample sequence aligned to a sequence in gen bank (sequence reference). The relative abundances of the microbial communities in granules at archaeal species level (a) and methanogen groups based on methanogenesis pathway (b) at different operating temperatures and OLRs are presented in Figure 7. The archaeal community structure was dynamic, with shifts at the methanogen species level following decreasing temperatures and increasing OLRs. Figure 4.6a shows predominant species in the archaeal community contributing to at least 97% relative abundance. The most predominant methanogen species in all granule samples were *Methanothrix soehngenii*, *Methanomassiliicoccus luminyensis*, *Methanocorpusculum aggregans* and *Methanobacterium beijingense* making up more than 90% relative

abundance in the archaeal communities. At 12 °C, *M. soehngeni* and *M. luminyensis* contributions in archaeal community were 46 - 64% and 29 - 47%, respectively. A significant shift was observed upon temperature reduction to 8.5 °C in both reactors. At OLR 3 and 8 gCOD·l⁻¹·d⁻¹, the relative abundance of *M. luminyensis* increased up to 85%, and the relative abundance of *M. soehngeni* decreased down to less than 10%. However, after further decrement of the operating temperatures, *M. soehngeni* abundance gradually increased to more than 82% at 2.5 °C. The relative abundance of *M. aggregans*, and *M. beijingense* fluctuated regardless of operating temperatures and OLRs in the range 2 - 10%.

Based on methanogenesis pathway, our archaeal community could be divided into three methanogen groups, corresponding to archaeal dominant species in Figure 7b. At 12 °C, acetoclastic methanogen contributions in archaeal community were 46 - 64% and 29 - 47%, respectively. A significant shift was observed upon temperature reduction to 8.5 °C in both reactors. At OLR 3 and 8 gCOD·l⁻¹·d⁻¹, the relative abundance of H₂-dependent methylotrophic methanogens increased up to 85%. However, after further decrement of the operating temperatures, acetoclastic methanogens abundance gradually increased to more than 82% at 2.5 °C. The relative abundance of hydrogenotrophic methanogen decreased in decreasing temperatures.

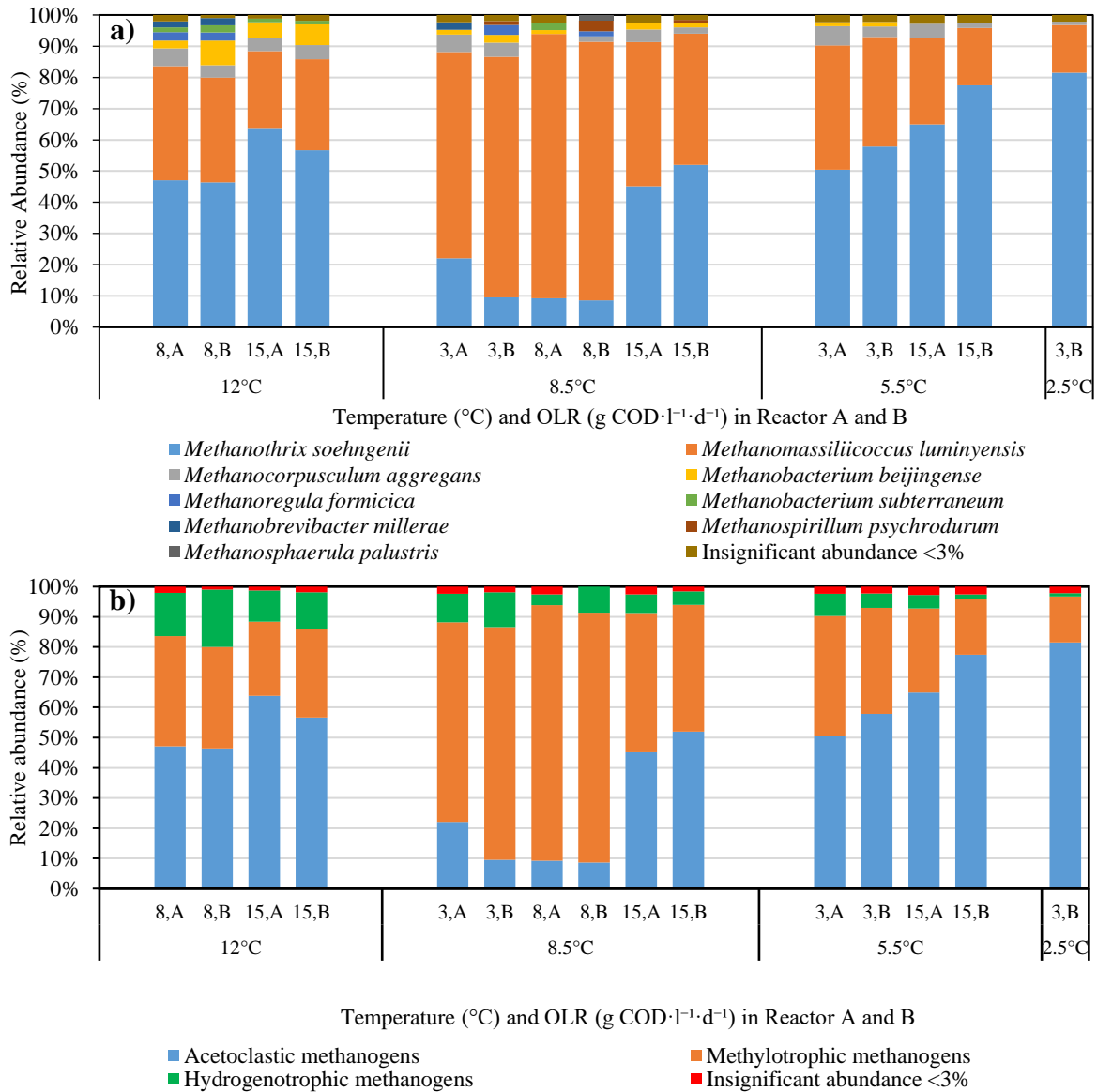


Figure 7 Relative abundances of microbial population structure in UASB granules at archaeal species level (a) and methanogen groups based on methanogenesis pathway (b) at different operating temperatures and OLRs. A and B on the x-axis represents microbial population structure in two parallel reactors, A and B. Numbers beside A and B represent OLR in gCOD·l⁻¹·d⁻¹.

4. Discussion

This current study has shown that efficient municipal wastewater treatment was achieved in long term UASB reactors operated at temperatures of 25 down to 12 °C and OLR up to $15.2 \pm 0.2 \text{ gCOD} \cdot \text{l}^{-1} \cdot \text{d}^{-1}$ (\pm standard error). Besides, the remarkable operation of the long-term treatment UASB reactors at 8.5, 5.5, 2.5 °C serves to confirm the feasibility of this treatment at low-temperatures and high organic loading, not only for degrading the organic carbon but also for a lower carbon footprint achieving sustainable wastewater treatment.

In this study, the two parallel UASB reactors (reactor A and B), operated continuously with the same operational conditions. Based on statistical analysis (student t-test at 95% confidence level) the two reactors demonstrated no significant difference in terms of transient response times, COD removal efficiency, methane fraction in biogas, methane production, COD balance, and nutrient variability.

Biomass retention is critically important for successful high-rate anaerobic bioreactors operation at low-temperatures (Lettinga et al., 2001). There was a significant difference in retention of granules at 5.5 °C. In reactor A, severe granule washout occurred as the sludge bed floated, presumably due to gas entrapment at high OLR and subsequent high biogas production. This resulted in diminishing gas production and loss of COD removal capacity, and reactor A loading was stopped on day 738. Sludge bed expansion also occurred at higher temperatures, but this was counteracted by variable recirculation flow and mechanical wall tapping. Different granule sizes could explain the difference in reactor sludge behavior. Granule size was observed during the experiment and larger granules were initially applied in reactor B by roughly 2 - 3 mm of diameter compared to 1 - 2 mm of diameter in reactor A, likely due to fractionation during transport and storage. A distinct decrease in the granule diameter was observed during operation of reactors, whereby the average granule size reduced from approximately 3 to 1 - 2 mm in reactor

B. In reactor A, granules became even smaller constituting fine particles by approximately 0.5 mm of granules size towards the end of the period. In reactor B, even though granules expanded several times, granules could be still retained and wash out was prevented. Wu et al. (2016) and Owusu-Agyeman et al. (2019) has observed large granules (3 - 3.5 mm) and claim higher mass transfer due to their internal structure, including big pore size, high porosity and short diffusion distance compared to medium and small granules. Small granules (<1 mm) appeared to be weaker and more easily washed-out from the system (Wu et al., 2016; Owusu-Agyeman et al., 2019). Moreover, Singh et al. (2019) investigated UASB reactor operation treating dairy wastewater at 20 °C and found that LCFA-containing feed stimulated granule flotation and wash out from the reactors due to LCFA-encapsulated granular sludge (Singh et al., 2019). This could also explain the frequent granule expansion in the system as parts of the wastewater inlet at IVAR Grødaland originates from a dairy and a slaughterhouse.

UASB reactor performance was analyzed and evaluated by investigating two main parameters: COD removal and methane production. Based on Figure 3, the rapid transient times at temperatures 25, 16, and 12 °C indicated the granules adapted quickly to decreased operating temperatures, adaptations that would not require community structure changes. The ability of UASB system to recover rapidly from temperature and loading shock perturbations, demonstrates the robustness of the system, which is an important consideration for pilot- and even full-scale applications. At lower temperatures (8.5, 5.5, and 2.5 °C), more extended periods were required to adapt and achieve new steady-states. Furthermore, during 8.5, 5.5, and 2.5 °C operation, lower inlet COD concentration at high OLRs affected the hydrodynamic condition by increasing the inlet flow rate to achieve the desired OLR, resulting in lower HRT in the system and reduced COD removal efficiency. Decreasing HRT leads to insufficient contact time of wastewater with the granules and less organic matter utilized (Zhang et

al., 2015). While the increasing OLR represents increasing biomass concentration and biomass growth in the reactor until it reached the maximum growth rate (μ_{\max}), according to Monod kinetic, which is associated with the increasing substrate concentration. This increasing substrate loading could also lead to a reduction of COD removal efficiency. Therefore, the effluent COD increased to a certain amount every first day after increase in OLR. Additionally, during acclimatization period, COD removal efficiency was affected by VFA accumulation and decreasing alkalinity which were also observed, especially when dropping the temperatures and applying higher OLRs ($>8.0 \text{ gCOD}\cdot\text{l}^{-1}\cdot\text{d}^{-1}$) (Figure S4), thus additional buffer (e.g., NaHCO_3) was needed to assure process stability. Then, the effluent COD and VFA accumulation started decreasing until the steady-state condition was achieved.

After achieving steady-state conditions, COD removal efficiencies in excess of 50% could be maintained at 25 - 12 °C for all operating OLRs, and at 8.5 °C up to OLR $8.0 \text{ gCOD}\cdot\text{l}^{-1}\cdot\text{d}^{-1}$ (Figure 4). Furthermore, at steady-state conditions, alkalinity and VFA variability were also balance in both reactors. Therefore, the addition of a buffer solution was not necessary. Gradual increments in OLRs and recirculation stabilized the UASB reactors. However, at low-temperatures ($<8.5 \text{ °C}$) and high OLRs above $12 \text{ gCOD}\cdot\text{l}^{-1}\cdot\text{d}^{-1}$, VFA accumulation and decreasing alkalinity in the reactors were observed more frequently (Figure S4), indicating the reactors to be close to become overloaded and the COD removal efficiencies decreased to below 30%. This is comparable to the result by Dague, Banik, and Ellis (1998), whereby lower temperatures resulted in reduced rates of substrate removal when treating synthetic wastewater at 5 - 25 °C (Dague, Banik, and Ellis, 1998). Similar findings have also been reported in the literature by Mahmoud et al. (2004) and Bandara et al. (2012) using UASB reactors treating real municipal wastewater at lower temperatures over a short term period (<400 days) and relatively low OLR $<3 \text{ gCOD}\cdot\text{l}^{-1}\cdot\text{d}^{-1}$. Using a single stage UASB, the COD

removal efficiencies were 44% at 15 °C (Mahmoud et al., 2004) and 40% during wintertime down to 6 °C (Bandara et al., 2012). However, our results were relatively lower than another long-term anaerobic granular reactor operation (1243 days) at 4 - 15 °C and OLR up to 10 gCOD·l⁻¹·d⁻¹ who demonstrated >80% COD removal efficiencies with VFA-based synthetic wastewater (McKeown et al., 2009). The distinctive results occurred due to the different substrates used. Compared to our UASB reactor substrate, VFA-based wastewater is more easily degradable than real municipal wastewater, indicating hydrolysis or fermentations could be rate-limiting. Petropoulos et al. (2017) investigated the intrinsic capacity of cold-adapted communities to treat domestic wastewater at 4, 8, and 15 °C in batch systems and showed hydrolysis/fermentation to be a limiting step at low-temperature and was twice as temperature sensitive as methanogenesis, Q₁₀ values were 4.62 and 1.57 respectively (Petropoulos et al., 2017).

UASB reactor performance may also be evaluated by methane production. At each temperature, methane production rates increased with the increasing OLR, proportional to the amount of organic matter removed in the UASB reactors. Despite significantly decreased methane productions were observed under low-temperatures (5.5 and 2.5 °C), at 25, 16, 12, and 8.5 °C, methane production rate was comparable in all OLRs, indicating that the reduction in operating temperature did not negatively affect methane production (Figure 6a and 6b). These findings are important for development of anaerobic municipal wastewater treatment at low-temperatures as it suggests that anaerobic granules are capable to adapt to low-temperatures and maintain system performances (COD removal and methane production) in a long-term operation.

Our results show the produced biogas contained an average methane fraction above 70% (v/v) (Figure 5), and more than 80% of COD removed was converted to methane (Figure 6c and 6d). The overall mean COD balance were above 90% in UASB reactors at all operating temperature and OLRs (Figure S2). Analytical uncertainty, gas leakages,

and the inaccuracy of the gas counter at low gas flow rates are possible explanations of the minor shortage. Henze et al. (2008) mentioned that fat or LCFA-containing substrates resulting in very high COD removal efficiencies, but low CH₄ production rates lead to considerable COD balance gaps (Henze et al., 2008). Singh et al. (2019; 2020) found this occurrence could be explained by lipid and/or LCFA accumulation in the granules which also associated with granules flotation and washed out. Another reason could also be the entrapment or accumulation of COD in the sludge blanket, not only lipid but also protein and/or other macromolecules (Zhang et al., 2018). Therefore, the COD balance gaps by around 3 - 10% in this study may be also explained by the high fat and protein containing substrate in wastewater. Another frequently cited cause for a COD gap at low-temperatures is a significant amount of dissolved methane at the effluent. We compensated the dissolved methane, which was estimated using Henry coefficients. However, Souza et al. (2011) and Wu et al. (2017) found that dissolved methane was oversaturated in the liquid phase of an anaerobic bioreactor effluent (saturation factor of 1.03–1.67), increasing with the increased methane solubility at decreasing temperatures.

Besides organic conversion and methane production, nutrient (N and P) availability in the anaerobic reactors was also important to assure bioreactor performance. The UASB reactors removed the mostly particulate nutrients. Particulate nutrients could be removed by UASB reactor by sedimentation and accumulation (Elmitwalli and Otterpohl, 2011). Some of the nutrients were consumed for the assimilation of microbial growth. Although the UASB reactor removed total nitrogen and phosphorous in the range of 10 - 33% and 4 - 20 %, respectively, the reactor had a limited removal of dissolved nutrients, especially ammonium (Figure S3). The ammonium removal has a negative reduction, which might be due to the ammonification during fermentation small organic molecules containing an amine group (such as, amino acids, amino sugars, urea, and nucleotides).

The stable UASB performance indicated long-term reactor operation at low-temperatures even at high OLRs may facilitate the development of well-balanced, stable community interactions in the granules. Hence, microbial community characterization of the low-temperature and loading gradients were investigated. The distribution of sequences at the species level within the Archaea domain is shown in Figure 7. Nine species of methanogens were observed with relative abundances of at least 97% of the archaeal community. The most predominant methanogen species in all granule samples were: the obligate acetoclastic methanogen *Methanothrix soehngenii* belongs to *Methanosarcinales* order which decarboxylates acetate (Huser, Wuhrmann, and Zehnder, 1982); the H₂-dependant methylotrophic methanogen *Methanomassiliicoccus luminyensi* belongs to *Methanomassiliicoccales* order which reduces the methyl-groups of methylated compounds to methane with H₂ as electron donor (Söllinger & Urich, 2019); and the two autotrophic hydrogen oxidizer *Methanocorpusculum aggregans* (heterotype *parvum*) and *Methanobacterium beijingense* belong to *Methanomicrobiales* and *Methanobacteriales* order, respectively, using hydrogen and carbon dioxide or formate as substrates (Ma et al., 2005; Oren, 2014). These four species made up more than 90% relative abundance in the archaeal communities regardless of operating temperatures and OLRs. However, shifts in the methanogen composition were observed with an increase in OLR and a decrease in temperature, suggesting shift in methanogenesis pathway (Figure 7b).

During operating temperature of 12 °C and low OLR, acetoclastic methanogens were relatively more abundant in both reactors and acetoclastic methanogens slightly increased at high OLR (Figure 4.6b). Similar observations were reported by Zhang et al., (2018) whereby acetoclastic *Methanosaetaceae* was abundant after 300 days of operation at 10 - 20 °C in a UASB reactor. By decreasing operating temperature to 8.5 °C, a significant methanogenic composition shifts were observed, especially at low to medium OLRs. Methylotrophic methanogens,

specifically *Methanomassiliicoccales*, became more dominant contributing to more than 70% relative abundance of the archaeal community. Interestingly, *Methanomassiliicoccales* is known as a methylotrophic methanogens lacking the Wood-Ljungdahl pathway and therefore cannot oxidize methyl-groups to CO₂ (Söllinger & Urich, 2019). Consequently, they are dependent on an external electron donor (i.e. H₂) and compete with autotrophic methanogens. Furthermore, Liu and Whitman. (2008) stated that H₂-dependant methylotrophic methanogenesis e.g., from methanol, is thermodynamically more favorable than acetoclastic methanogenesis under standard conditions (-113 kJ·mol⁻¹ vs. -33 kJ·mol⁻¹ respectively) (Liu and Whitman 2008). However, with the increased OLRs and decreased temperatures further down to 2.5 °C, the relative abundance of acetoclastic methanogen increased again to more than 70%. This has also been demonstrated by Nozhevnikova et al. (2007) reporting about 95% methane to originate from acetate at 5 °C. In this study, acetoclastic methanogens became increasingly dominant under low-temperature (2.5 °C), indicating acetoclastic growth and acetate to be the main precursor of methanogenesis at low-temperatures.

In many studies, hydrogenotrophic methanogens played an essential role in anaerobic treatment at low-temperatures (McKeown et al., 2009; Bandara et al., 2012; Smith, Skerlos, and Raskin, 2015; Petropoulos et al., 2017). However, our results showed the relative abundances of hydrogenotrophic methanogens were low and decreased with the decreasing temperatures by approximately 14%, 7.3%, 4.5% and 1.1% at 12, 8.5, 5.5, and 2.5 °C, respectively. Most probably, homoacetogenesis becomes the main fermentation reaction under this condition. An increased acetate production was also observed during UASB operation, especially at 2.5 °C (Figure S4). Furthermore, bacterial community analysis showed an increased relative abundances of genus *Acetoanaerobium* (homoacetogen) in UASB granules at the decreasing temperatures (Safitri, Kommedal, and Kaster, *in preparation*).

Homoacetogens convert H_2 and CO_2 to acetate outcompeting with hydrogenotrophic methanogens at low-temperatures and these microbes could also grow under both acidic and alkaline conditions (Kotsyurbenko et al., 2001; Nozhevnikova et al., 2007). Furthermore, Kotsyurbenko et al. (1996) showed that at 6 °C, homoacetogens grow two times faster and were less sensitive than hydrogenotrophic methanogens with 2.2 and 4.1 Q_{10} value, respectively (Kotsyurbenko et al., 1996).

Overall, our finding suggested temperature and organic loading did not only affect UASB bioprocess performances but also results in a change in the microbial community composition and the degradation pathway of organic matter. This successful operation at low-temperatures, along with microbial community confirmation, may select the prevalence of psychrotolerant methanogens throughout long-term UASB reactor operation, indicating the long-term adaptation of the microbial community in granulated biomass. Furthermore, our study demonstrates that these functionally important groups may be retained within the granular during long-term low-temperature operation, likely contributing to a stable UASB reactor operation.

Low-temperatures anaerobic bioreactor operation offers economic advantages, especially for some high latitude countries, due to reduce heating requirement and bioenergy production potential. Despite the stable and robust reactor performance of the UASB system for treating wastewater treatment at low-temperatures below 20 °C, a significant fraction of organic matter still remained in the effluent. Furthermore, the methane loss in the dissolved phase could also offset the positive effect of energy recovery from anaerobic wastewater treatment (Liu et al. 2014). Moreover, this study also demonstrated that the UASB system for treating municipal wastewater had limited application removing nutrient. In field application, a post-treatment requires to be considered to remove residual COD, methane and nutrient recovery. Comprehensive reviews on post-treatment technologies for anaerobic effluents for discharge and recycling wastewater have been done by several researchers

(Chernicharo, 2006; Mai, Kunacheva, and Stuckey, 2018). UASB system shows a viable secondary pre-treatment option unit process for sustainable wastewater treatment. However, the suitability of pre-treatment, post-treatment, and by-product treatment would influence anaerobic treatment's successfulness using UASB system treating municipal wastewater treatment at low-temperatures.

5. Conclusions

The conclusions were as following:

- The sustained UASB reactor performance was maintained and proven by COD removal efficiency, methane production and microbial community analysis. We demonstrated the feasibility of UASB system application at low-temperatures treating municipal wastewater.
- Stable COD removal efficiencies of 50 - 70 % was achieved down 8.5 °C up to 15.0 gCOD·l⁻¹·d⁻¹. Below 8.5 °C COD removal efficiencies and methane yields reduced, but significant methane formation was observed even at 2.5 °C at reduced loading (up to 5 gCOD·l⁻¹·d⁻¹). The overall COD balance closed at above 90% of the inlet COD at all operating temperatures and OLRs.
- Methanogen communities showed temperature and loading change effected the degradation pathway of organic matter with acetoclastic methanogen and H₂-dependent methylotrophic methanogens played significant roles.
- Methanogenic archaea communities proved the adaptation ability to very low-temperatures down to 2.5 °C regardless of the operating OLR.
- Further research will focus on treating real anaerobic wastewaters in a long-term pilot- or full-scale UASB system at

low-temperatures. Nutrient and dissolved methane recovery as UASB post-treatment unit process need also to be studied as a function of temperature.

References

- Aiyuk, Sunny, Joyce Amoako, Lutgarde Raskin, Adrianus van Haandel, and Willy Verstraete. 2004. "Removal of Carbon and Nutrients from Domestic Wastewater Using a Low Investment, Integrated Treatment Concept." *Water Research* 38 (13): 3031–42. <https://doi.org/10.1016/j.watres.2004.04.040>.
- Akila, G., and T.S. Chandra. 2007. "Performance of an UASB Reactor Treating Synthetic Wastewater at Low-Temperature Using Cold-Adapted Seed Slurry." *Process Biochemistry* 42 (3): 466–71. <https://doi.org/10.1016/j.procbio.2006.09.010>.
- Bandara, Wasala M.K.R.T.W., Tomonori Kindaichi, Hisashi Satoh, Manabu Sasakawa, Yoshihito Nakahara, Masahiro Takahashi, and Satoshi Okabe. 2012. "Anaerobic Treatment of Municipal Wastewater at Ambient Temperature: Analysis of Archaeal Community Structure and Recovery of Dissolved Methane." *Water Research* 46 (17): 5756–64. <https://doi.org/10.1016/j.watres.2012.07.061>.
- Bowen, Emma J., Jan Dolfing, Russell J. Davenport, Fiona L. Read, and Thomas P. Curtis. 2014. "Low-Temperature Limitation of Bioreactor Sludge in Anaerobic Treatment of Domestic Wastewater." *Water Science and Technology* 69 (5): 1004. <https://doi.org/10.2166/wst.2013.821>.
- Cardinali-Rezende, Juliana, Juliana C. Araújo, Paulo G. S. Almeida, Carlos A. L. Chernicharo, José L. Sanz, Edmar Chartone-Souza, and Andréa M. A. Nascimento. 2013. "Organic Loading Rate and Food-to-Microorganism Ratio Shape Prokaryotic Diversity in a Demo-Scale up-Flow Anaerobic Sludge Blanket Reactor Treating

- Domestic Wastewater.” *Antonie van Leeuwenhoek* 104 (6): 993–1003. <https://doi.org/10.1007/s10482-013-0018-y>.
- Chernicharo, C. A. L. 2006. “Post-Treatment Options for the Anaerobic Treatment of Domestic Wastewater.” *Reviews in Environmental Science and Bio/Technology* 5 (1): 73–92. <https://doi.org/10.1007/s11157-005-5683-5>.
- Collins, Gavin, Sharon McHugh, Sean Connaughton, Anne-Marie Enright, Aileen Kearney, Colm Scully, Thérèse Mahony, Paádhraig Madden, and Vincent O’Flaherty. 2006. “New Low-Temperature Applications of Anaerobic Wastewater Treatment.” *Journal of Environmental Science and Health, Part A* 41 (5): 881–95. <https://doi.org/10.1080/10934520600614504>.
- Dague, Richard R., Gouranga C. Banik, and Timothy G. Ellis. 1998. “Anaerobic Sequencing Batch Reactor Treatment of Dilute Wastewater at Psychrophilic Temperatures.” *Water Environment Research* 70 (2): 155–60.
- De Vrieze, Jo, Tom Hennebel, Nico Boon, and Willy Verstraete. 2012. “Methanosarcina: The Rediscovered Methanogen for Heavy Duty Biomethanation.” *Bioresource Technology* 112 (May): 1–9. <https://doi.org/10.1016/j.biortech.2012.02.079>.
- Earl, J., G. Hall, R. W. Pickup, D. A. Ritchie, and C. Edwards. 2003. “Analysis of Methanogen Diversity in a Hypereutrophic Lake Using PCR-RFLP Analysis of Mcr Sequences.” *Microbial Ecology* 46 (2): 270–78. <https://doi.org/10.1007/s00248-003-2003-x>.
- Elmitwalli, Tarek A., Kim L.T. Oahn, Grietje Zeeman, and Gatzte Lettinga. 2002. “Treatment of Domestic Sewage in a Two-Step Anaerobic Filter/Anaerobic Hybrid System at Low-temperature.” *Water Research* 36 (9): 2225–32. [https://doi.org/10.1016/S0043-1354\(01\)00438-9](https://doi.org/10.1016/S0043-1354(01)00438-9).
- Elmitwalli, Tarek, and Ralf Otterpohl. 2011. “Grey Water Treatment in Upflow Anaerobic Sludge Blanket (UASB) Reactor at Different

- Temperatures.” *Water Science and Technology* 64 (3): 610–17.
<https://doi.org/10.2166/wst.2011.616>.
- Großkopf Regine, Stubner Stephan, and Liesack Werner. 1998. “Novel Euryarchaeotal Lineages Detected on Rice Roots and in the Anoxic Bulk Soil of Flooded Rice Microcosms.” *Applied and Environmental Microbiology* 64 (12): 4983–89.
<https://doi.org/10.1128/AEM.64.12.4983-4989.1998>.
- Henze, M., M. C. M. van Loosdrecht, G.A. Ekama, and D. Brdjanovic. 2008. *Biological Wastewater Treatment: Principles, Modelling and Design*. IWA Publishing.
<https://doi.org/10.2166/9781780401867>.
- Høj, Lone, Rolf A Olsen, and Vigdis L Torsvik. 2008. “Effects of Temperature on the Diversity and Community Structure of Known Methanogenic Groups and Other Archaea in High Arctic Peat.” *The ISME Journal* 2 (1): 37–48.
<https://doi.org/10.1038/ismej.2007.84>.
- Huser, Beat A., Karl Wuhrmann, and Alexander J. B. Zehnder. 1982. “*Methanotherix soehngeni* Gen. Nov. Sp. Nov., a New Acetotrophic Non-Hydrogen-Oxidizing Methane Bacterium.” *Archives of Microbiology* 132 (1): 1–9.
<https://doi.org/10.1007/BF00690808>.
- Kettunen, R. H., and J. A. Rintala. 1997. “The Effect of Low-temperature (5–29 °C) and Adaptation on the Methanogenic Activity of Biomass.” *Applied Microbiology and Biotechnology* 48 (4): 570–76. <https://doi.org/10.1007/s002530051098>.
- Kettunen, Riitta H., and Jukka A. Rintala. 1998. “Performance of an On-Site UASB Reactor Treating Leachate at Low-temperature.” *Water Research* 32 (3): 537–46. [https://doi.org/10.1016/S0043-1354\(97\)00319-9](https://doi.org/10.1016/S0043-1354(97)00319-9).
- Koster, I. W., and G. Lettinga. 1985. “Application of the Upflow Anaerobic Sludge Bed (UASB) Process for Treatment of Complex Wastewaters at Low-temperatures.” *Biotechnology and*

Bioengineering 27 (10): 1411–17.
<https://doi.org/10.1002/bit.260271004>.

Kotsyurbenko, O. R., A. N. Nozhevnikova, T. I. Soloviova, and G. A. Zavarzin. 1996. “Methanogenesis at Low-temperatures by Microflora of Tundra Wetland Soil.” *Antonie van Leeuwenhoek* 69 (1): 75–86. <https://doi.org/10.1007/BF00641614>.

Kotsyurbenko, Oleg R., Michail V. Glagolev, Alla N. Nozhevnikova, and Ralf Conrad. 2001. “Competition between Homoacetogenic Bacteria and Methanogenic Archaea for Hydrogen at Low-temperature.” *FEMS Microbiology Ecology* 38 (2–3): 153–59. <https://doi.org/10.1111/j.1574-6941.2001.tb00893.x>.

Kwon, Min Jung, Ji Young Jung, Binu M. Tripathi, Mathias Göckede, Yoo Kyung Lee, and Mincheol Kim. 2019. “Dynamics of Microbial Communities and CO₂ and CH₄ Fluxes in the Tundra Ecosystems of the Changing Arctic.” *Journal of Microbiology* 57 (5): 325–36. <https://doi.org/10.1007/s12275-019-8661-2>.

Lettinga, G., J. B. van Lier, J. C.L. van Buuren, and G. Zeeman. 2001. “Sustainable Development in Pollution Control and the Role of Anaerobic Treatment.” *Water Science and Technology* 44 (6): 181–88. <https://doi.org/10.2166/wst.2001.0370>.

Lettinga, G., A. F. M. van Velsen, S. W. Hobma, W. de Zeeuw, and A. Klapwijk. 1980. “Use of the Upflow Sludge Blanket (USB) Reactor Concept for Biological Wastewater Treatment, Especially for Anaerobic Treatment.” *Biotechnology and Bioengineering* 22 (4): 699–734. <https://doi.org/10.1002/bit.260220402>.

Lettinga, Gatzke, Salih Rebac, and Grietje Zeeman. 2001. “Challenge of Psychrophilic Anaerobic Wastewater Treatment.” *Trends in Biotechnology* 19 (9): 363–70. [https://doi.org/10.1016/S0167-7799\(01\)01701-2](https://doi.org/10.1016/S0167-7799(01)01701-2).

Li, Weizhong, Limin Fu, Beifang Niu, Sitao Wu, and John Wooley. 2012. “Ultrafast Clustering Algorithms for Metagenomic

- Sequence Analysis.” *Briefings in Bioinformatics* 13 (6): 656–68.
<https://doi.org/10.1093/bib/bbs035>.
- Liu, Yuchen, and William B. Whitman. 2008. “Metabolic, Phylogenetic, and Ecological Diversity of the Methanogenic Archaea.” *Annals of the New York Academy of Sciences* 1125 (1): 171–89.
<https://doi.org/10.1196/annals.1419.019>.
- Liu, Ze-hua, Hua Yin, Zhi Dang, and Yu Liu. 2014. “Dissolved Methane: A Hurdle for Anaerobic Treatment of Municipal Wastewater.” *Environmental Science & Technology* 48 (2): 889–90.
<https://doi.org/10.1021/es405553j>.
- Ma, Kai, Xiaoli Liu, and Xiuzhu Dong. 2005. “Methanobacterium Beijingense Sp. Nov., a Novel Methanogen Isolated from Anaerobic Digesters.” *International Journal of Systematic and Evolutionary Microbiology*. Microbiology Society.
<https://doi.org/10.1099/ijs.0.63254-0>.
- Magoč, Tanja, and Steven L Salzberg. 2011. “FLASH: Fast Length Adjustment of Short Reads to Improve Genome Assemblies.” *Bioinformatics (Oxford, England)* 27 (21): 2957–63.
<https://doi.org/10.1093/bioinformatics/btr507>.
- Mahmoud, Nidal, Grietje Zeeman, Huub Gijzen, and Gatze Lettinga. 2004. “Anaerobic Sewage Treatment in a One-Stage UASB Reactor and a Combined UASB-Digester System.” *Water Research* 38 (9): 2348–58.
<https://doi.org/10.1016/j.watres.2004.01.041>.
- Mai, D. T., C. Kunacheva, and D. C. Stuckey. 2018. “A Review of Posttreatment Technologies for Anaerobic Effluents for Discharge and Recycling of Wastewater.” *Critical Reviews in Environmental Science and Technology* 48 (2): 167–209.
<https://doi.org/10.1080/10643389.2018.1443667>.
- McKeown, Rory M., Colm Scully, Thérèse Mahony, Gavin Collins, and Vincent O’Flaherty. 2009. “Long-Term (1243 Days), Low-Temperature (4–15°C), Anaerobic Biotreatment of Acidified

- Wastewaters: Bioprocess Performance and Physiological Characteristics.” *Water Research* 43 (6): 1611–20. <https://doi.org/10.1016/j.watres.2009.01.015>.
- McKeown, Rory, Colm Scully, Anne-Marie Enright, Fabio Chinalia, Changsoo Lee, Thérèse Mahony, Gavin Collins, and Vincent O’Flaherty. 2009. “Psychrophilic Methanogenic Community Development during Long-Term Cultivation of Anaerobic Granular Biofilms.” *The ISME Journal* 3 (11): 1231–42. <https://doi.org/10.1038/ismej.2009.67>.
- Moosbrugger, R. E., M. C. Wentzel, G. A. Ekama, and G. v. R. Marais. 1993. “A 5 PH Point Titration Method for Determining the Carbonate and SCFA Weak Acid/Bases in Anaerobic Systems.” *Water Science and Technology* 28 (2): 237–45. <https://doi.org/10.2166/wst.1993.0112>.
- Nordgård, Anna Synnøve Røstad, Wenche Hennie Bergland, Olav Vadstein, Vladimir Mironov, Rune Bakke, Kjetill Østgaard, and Ingrid Bakke. 2017. “Anaerobic Digestion of Pig Manure Supernatant at High Ammonia Concentrations Characterized by High Abundances of Methanosaeta and Non-Euryarchaeotal Archaea.” *Scientific Reports* 7 (1): 15077. <https://doi.org/10.1038/s41598-017-14527-1>.
- Nozhevnikova, Alla N., Valeria Nekrasova, Adrian Ammann, Alexander J.B. Zehnder, Bernhard Wehrli, and Christof Holliger. 2007. “Influence of Temperature and High Acetate Concentrations on Methanogenesis in Lake Sediment Slurries.” *FEMS Microbiology Ecology* 62 (3): 336–44. <https://doi.org/10.1111/j.1574-6941.2007.00389.x>.
- Oren, Aharon. 2014. “The Family Methanocorpusculaceae.” In *The Prokaryotes: Other Major Lineages of Bacteria and The Archaea*, edited by Eugene Rosenberg, Edward F. DeLong, Stephen Lory, Erko Stackebrandt, and Fabiano Thompson, 225–30. Berlin,

Heidelberg: Springer Berlin Heidelberg.
https://doi.org/10.1007/978-3-642-38954-2_314.

- Owusu-Agyeman, Isaac, Özge Eyice, Zeynep Cetecioglu, and Elzbieta Plaza. 2019. "The Study of Structure of Anaerobic Granules and Methane Producing Pathways of Pilot-Scale UASB Reactors Treating Municipal Wastewater under Sub-Mesophilic Conditions." *Bioresource Technology* 290 (October): 121733. <https://doi.org/10.1016/j.biortech.2019.121733>.
- Petropoulos, Evangelos, Jan Dolfing, Russell J. Davenport, Emma J. Bowen, and Thomas P. Curtis. 2017. "Developing Cold-Adapted Biomass for the Anaerobic Treatment of Domestic Wastewater at Low-temperatures (4, 8 and 15 °C) with Inocula from Cold Environments." *Water Research* 112 (April): 100–109. <https://doi.org/10.1016/j.watres.2016.12.009>.
- Petropoulos, Evangelos, Burhan Shamurad, Shamas Tabraiz, Yongjie Yu, Russell Davenport, Thomas P. Curtis, and Jan Dolfing. 2021. "Sewage Treatment at 4 °C in Anaerobic Upflow Reactors with and without a Membrane – Performance, Function and Microbial Diversity." *Environmental Science: Water Research & Technology* 7 (1): 156–71. <https://doi.org/10.1039/D0EW00753F>.
- Rebac, S., J.B. van Lier, P. Lens, A.J.M. Stams, F. Dekkers, K.Th.M. Swinkels, and G. Lettinga. 1999. *Psychrophilic Anaerobic Treatment of Low Strength Wastewaters*. Vol. 39. *Water Science and Technology*. [https://doi.org/10.1016/S0273-1223\(99\)00103-1](https://doi.org/10.1016/S0273-1223(99)00103-1).
- Rebac, Salih, Julia Ruskova, Sybren Gerbens, Jules B. van Lier, Alfons J.M. Stams, and Gatzke Lettinga. 1995. "High-Rate Anaerobic Treatment of Wastewater under Psychrophilic Conditions." *Journal of Fermentation and Bioengineering* 80 (5): 499–506. [https://doi.org/10.1016/0922-338X\(96\)80926-3](https://doi.org/10.1016/0922-338X(96)80926-3).
- Rosa, A.P., C.A.L. Chernicharo, L.C.S. Lobato, R.V. Silva, R.F. Padilha, and J.M. Borges. 2018. "Assessing the Potential of Renewable Energy Sources (Biogas and Sludge) in a Full-Scale UASB-Based

- Treatment Plant.” *SI: Waste Biomass to Biofuel* 124 (August): 21–26. <https://doi.org/10.1016/j.renene.2017.09.025>.
- Safitri, Anissa Sukma, Roald Kommedal, and Krista M. Kaster. n.d. “Microbial Community Dynamic in Long-Term UASB Reactor Operation Treating Municipal Wastewater at Low-temperatures.” In Preparation.
- Schellinkhout, A., and C. J. Collazos. 1992. “Full-Scale Application of the UASB Technology for Sewage Treatment.” *Water Science and Technology* 25 (7): 159–66. <https://doi.org/10.2166/wst.1992.0148>.
- Seghezzo, Lucas, Grietje Zeeman, Jules B. van Lier, H.V.M. Hamelers, and Gatze Lettinga. 1998. “A Review: The Anaerobic Treatment of Sewage in UASB and EGSB Reactors.” *Bioresource Technology* 65 (3): 175–90. [https://doi.org/10.1016/S0960-8524\(98\)00046-7](https://doi.org/10.1016/S0960-8524(98)00046-7).
- Show, Kuan-Yeow, Yuegen Yan, Haiyong Yao, Hui Guo, Ting Li, De-Yang Show, Jo-Shu Chang, and Duu-Jong Lee. 2020. “Anaerobic Granulation: A Review of Granulation Hypotheses, Bioreactor Designs and Emerging Green Applications.” *Bioresource Technology* 300 (March): 122751. <https://doi.org/10.1016/j.biortech.2020.122751>.
- Silva Martins, Alessandra da, Bernardo Ornelas Ferreira, Nirvana Cecília Ribeiro, Raiane Martins, Laura Rabelo Leite, Guilherme Oliveira, Luis Felipe Colturato, Carlos Augusto Chernicharo, and Juliana Calabria de Araujo. 2017. “Metagenomic Analysis and Performance of a Mesophilic Anaerobic Reactor Treating Food Waste at Various Load Rates.” *Environmental Technology* 38 (17): 2153–63. <https://doi.org/10.1080/09593330.2016.1247197>.
- Singh, Kripa Shankar, Hideki Harada, and T. Viraraghavan. 1996. “Low-Strength Wastewater Treatment by a UASB Reactor.” *Bioresource Technology* 55 (3): 187–94. [https://doi.org/10.1016/0960-8524\(96\)86817-9](https://doi.org/10.1016/0960-8524(96)86817-9).

- Singh, Suniti, B. Conall Holohan, Simon Mills, Juan Castilla-Archilla, Marika Kokko, Jukka Rintala, Piet N. L. Lens, Gavin Collins, and Vincent O’Flaherty. 2020. “Enhanced Methanization of Long-Chain Fatty Acid Wastewater at 20°C in the Novel Dynamic Sludge Chamber–Fixed Film Bioreactor.” *Frontiers in Energy Research* 8: 166. <https://doi.org/10.3389/fenrg.2020.00166>.
- Singh, Suniti, Johanna M. Rinta-Kanto, Riitta Kettunen, Henrik Tolvanen, Piet Lens, Gavin Collins, Marika Kokko, and Jukka Rintala. 2019. “Anaerobic Treatment of LCFA-Containing Synthetic Dairy Wastewater at 20 °C: Process Performance and Microbial Community Dynamics.” *Science of The Total Environment* 691 (November): 960–68. <https://doi.org/10.1016/j.scitotenv.2019.07.136>.
- Smith, A. L., S. J. Skerlos, and L. Raskin. 2015. “Anaerobic Membrane Bioreactor Treatment of Domestic Wastewater at Psychrophilic Temperatures Ranging from 15 °C to 3 °C.” *Environmental Science: Water Research & Technology* 1 (1): 56–64. <https://doi.org/10.1039/C4EW00070F>.
- Smith, Adam L., Steven J. Skerlos, and Lutgarde Raskin. 2012. “Psychrophilic Anaerobic Membrane Bioreactor Treatment of Domestic Wastewater.” *Water Research*. <https://doi.org/10.1016/j.watres.2012.12.028>.
- Söllinger, Andrea, and Tim Urich. 2019. “Methylotrophic Methanogens Everywhere — Physiology and Ecology of Novel Players in Global Methane Cycling.” *Biochemical Society Transactions* 47 (6): 1895–1907. <https://doi.org/10.1042/BST20180565>.
- Souza, C. L., C. A. L. Chernicharo, and S. F. Aquino. 2011. “Quantification of Dissolved Methane in UASB Reactors Treating Domestic Wastewater under Different Operating Conditions.” *Water Science and Technology* 64 (11): 2259–64. <https://doi.org/10.2166/wst.2011.695>.

- Varsadiya, Milan, Tim Urich, Gustaf Hugelius, and Jiří Bárta. 2021. "Microbiome Structure and Functional Potential in Permafrost Soils of the Western Canadian Arctic." *FEMS Microbiology Ecology*, no. fiab008 (January). <https://doi.org/10.1093/femsec/fiab008>.
- Wainaina, Steven, Mukesh Kumar Awasthi, Surendra Sarsaiya, Hongyu Chen, Ekta Singh, Aman Kumar, B. Ravindran, et al. 2020. "Resource Recovery and Circular Economy from Organic Solid Waste Using Aerobic and Anaerobic Digestion Technologies." *Bioresource Technology* 301 (April): 122778. <https://doi.org/10.1016/j.biortech.2020.122778>.
- Wilhelm, Emmerich., Rubin. Battino, and Robert J. Wilcock. 1977. "Low-Pressure Solubility of Gases in Liquid Water." *Chemical Reviews* 77 (2): 219–62. <https://doi.org/10.1021/cr60306a003>.
- Wu, Jing, Zohaib Ur Rehman Afridi, Zhi Ping Cao, Zhong Liang Zhang, Souhila Poncin, Huai Zhi Li, Jian E. Zuo, and Kai Jun Wang. 2016. "Size Effect of Anaerobic Granular Sludge on Biogas Production: A Micro Scale Study." *Bioresource Technology* 202 (February): 165–71. <https://doi.org/10.1016/j.biortech.2015.12.006>.
- Wu, Pei-Hsun, Kok Kwang Ng, Pui-Kwan Andy Hong, Ping-Yi Yang, and Cheng-Fang Lin. 2017. "Treatment of Low-Strength Wastewater at Mesophilic and Psychrophilic Conditions Using Immobilized Anaerobic Biomass." *Chemical Engineering Journal* 311 (March): 46–54. <https://doi.org/10.1016/j.cej.2016.11.077>.
- Yang, Sizhong, Susanne Liebner, Matthias Winkel, Mashal Alawi, Fabian Horn, Corina Dörfer, Julien Ollivier, et al. 2017. "In-Depth Analysis of Core Methanogenic Communities from High Elevation Permafrost-Affected Wetlands." *Soil Biology and Biochemistry* 111 (August): 66–77. <https://doi.org/10.1016/j.soilbio.2017.03.007>.
- Zhang, Lei, Jo de Vrieze, Tim L.G. Hendrickx, Wei Wei, Hardy Temmink, Huub Rijnaarts, and Grietje Zeeman. 2018. "Anaerobic

Treatment of Raw Domestic Wastewater in a UASB-Digester at 10 °C and Microbial Community Dynamics.” *Chemical Engineering Journal* 334 (February): 2088–97. <https://doi.org/10.1016/j.cej.2017.11.073>.

Zhang, Ying, Xin Wang, Miao Hu, and Pengfei Li. 2015. “Effect of Hydraulic Retention Time (HRT) on the Biodegradation of Trichloroethylene Wastewater and Anaerobic Bacterial Community in the UASB Reactor.” *Applied Microbiology and Biotechnology* 99 (4): 1977–87. <https://doi.org/10.1007/s00253-014-6096-6>.

Supplementary Document

1. Reactor configuration images

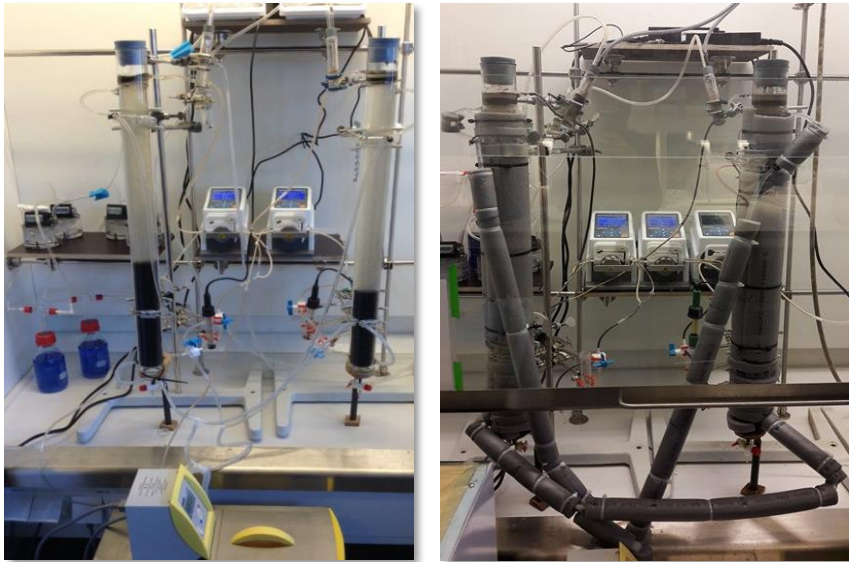


Figure S1 UASB reactor configuration images without and with insulation

2. COD Balance

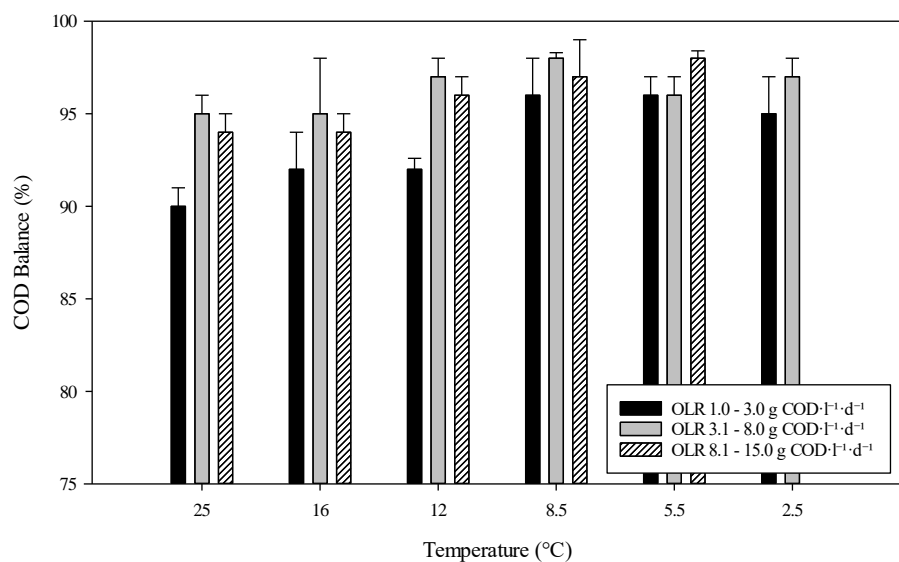


Figure S2 COD balance at steady-state conditions at different temperatures and OLRs. Error bars represent standard errors from measurements taken during steady-state conditions in reactor A and B. The student *t*-test revealed no significant difference ($p > 0.05$) between reactor A and B COD methane fraction.

3. Nutrient variability

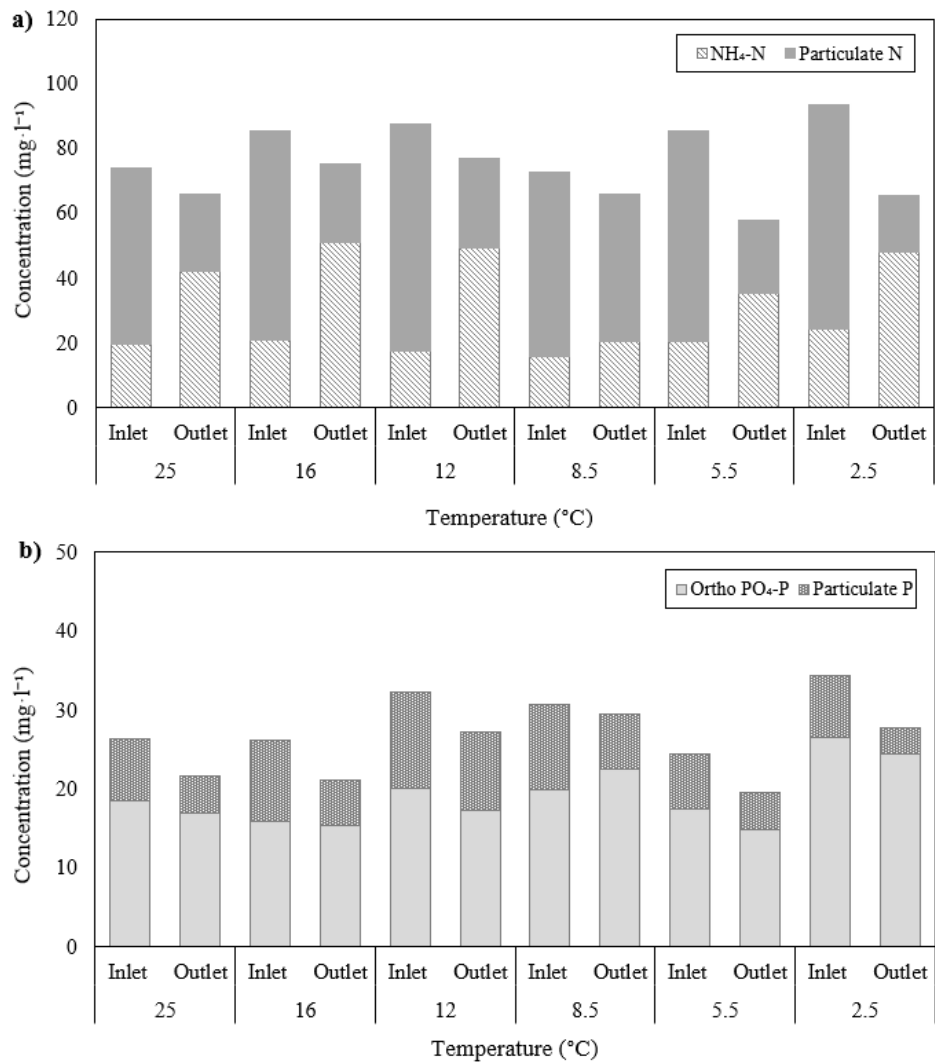


Figure S3. The average concentration of nutrients (N and P) treating municipal wastewater in the UASB reactors. The student t-test revealed no significant difference ($p > 0.05$) between reactor A and B nutrient concentration.

4. pH, VFA and alkalinity variability



Figure S4. pH, VFA and alkalinity variability profile in the UASB (reactor A and B). Solid (—) and dash dot (- · -) lines in the graph represent temperature and organic loading rate (OLR) change borders. Red arrows (↓) show when 1 g l⁻¹ NaHCO₃ was added occasionally to the feed wastewater.

Appendix 2 – Paper II

Microbial community development on psychrophilic granules during long-term UASB operation. Anissa Sukma Safitri, Krista M. Kaster, and Roald Kommedal. *In preparation manuscript.*

Microbial community development on psychrophilic granules during long-term UASB operation

Anissa Sukma Safitri, Krista M. Kaster, and Roald Kommedal*

Institute of Chemistry, Bioscience and Environmental Engineering,
University of Stavanger, 4036 Stavanger, Norway

*Corresponding Author. Email address: roald.kommedal@uis.no

Abstract

Microbial community characterization of the low-temperature and loading gradients in anaerobic granules were presented in this study. Granules were taken from UASB reactors at 12, 8.5, 5.5 and 2.5 °C which were operated continuously over 1025 days by applying a stepwise increase of organic loading rate (OLR) by intermittent increases to $15.2 \pm 0.2 \text{ gCOD} \cdot \text{l}^{-1} \cdot \text{d}^{-1}$. In this study, methanogen communities showed temperature and loading change effected the degradation pathway of organic matter with acetoclastic methanogen and H_2 -dependent methylotrophic methanogens played significant roles. At 2.5 °C, acetate might be the main precursor of methanogenesis. This successful operation at low-temperatures along with microbial community confirmation, the prevalence of psychrotolerant communities was observed throughout long-term UASB reactor operation, indicating the long-term adaptation of the microbial community in granulated biomass through changes in the community structure and low-temperature anaerobic treatment potential in pilot-and/or full-scale application for treating municipal wastewater.

Keywords: microbial community; anaerobic granules; acetoclastic methanogen; H_2 -dependent methylotrophic methanogens; UASB

1. Introduction

Anaerobic treatment of municipal wastewater is an established technology, the majority of full-scale applications have concentrated on high-rate anaerobic system such as UASB at mesophilic temperature ranges (Leitão et al., 2006). This was largely due to the belief that low-temperature or psychrophilic (<20 °C) anaerobic treatment was not viable because of lower substrate utilization rate, growth rate, methane production and wastewater hydrolysis. Anaerobic treatment at lower temperatures become more difficult when the substrate is low strength municipal wastewater. Low levels of substrate, poor substrate-biomass contact, low gas production and the need for excellent biomass retention are the main barriers for the anaerobic treatment of wastewater at ambient temperature in temperate climates (Lettinga et al., 2001). In addition, previous studies done by several researchers have shown a significant adverse effect on the metabolic activity of mesophilic methanogens with decreasing temperatures (Bowen et al. 2014; Kettunen and Rintala 1997; Koster and Lettinga 1985; Rebac et al. 1999; Rebac et al. 1995).

Despite the decreased activity of anaerobic microorganisms during anaerobic wastewater treatment at temperatures below 20 °C, Cavicchioli (2006) found that methanogens were the most abundant archaea in many samples from cold environments. Recently, it has been confirmed methanogen are abundant in extreme cold natural environments, such as, in lake sediment, high Arctic peat, permafrost, or tundra (Kwon et al., 2019; Varsadiya et al., 2021). This suggests that the growth and multiplication of methanogenic organisms at low-temperatures is common in nature. Furthermore, they reported that psychrophilic methanogens contribute significantly to organic biotransformation through methanogenesis under cold and anoxic conditions (Kwon et al., 2019; Varsadiya et al., 2021). There are three

main methanogenesis pathways: (1) CO₂-reducing (hydrogenotrophic methanogenesis), (2) acetoclastic methanogenesis, and (3) methylotrophic methanogenesis (Söllinger & Urich, 2019). Normally, acetoclastic methanogenesis is commonly reported as the dominant methanogenic pathway at a ratio of >67% (Conrad, 2020), as well as in low-temperature conditions (Kotsyurbenko et al. 1996; Fey, Claus, and Conrad 2004). In low-temperature conditions, homoacetogens have an important role in methanogenesis and are more competitive than hydrogenic methanogens (Pan et al., 2021). Homoacetogens convert H₂ and CO₂ to acetate outcompeting with hydrogenotrophic methanogens at low-temperatures and these microbes could also grow under both acidic and alkaline conditions (Kotsyurbenko et al. 2001; Nozhevnikova et al. 2007).

Few studies have investigated the microbial communities during anaerobic wastewater treatment at low-temperature down to 4 °C in anaerobic batch reactors treating real municipal wastewater (Dolejs et al., 2018; Petropoulos et al., 2017). In many studies, synthetic wastewater was also commonly used in different types of continuous anaerobic reactors and configurations at low-temperatures (Rebac et al., 1995; McKeown et al., 2009; Collins, Mahony, and O'Flaherty, 2006; Collins et al., 2006; Akila and Chandra, 2007; Wu et al., 2017; Zhang et al., 2012). Even though real wastewater treatment in continuous anaerobic reactors at low-temperature is well documented (Kettunen and Rintala, 1998; Elmitwalli et al., 2002; Mahmoud et al., 2004; Bandara et al., 2012; Smith, Skerlos, and Raskin, 2012; Zhang et al., 2018; Petropoulos et al., 2021), studies investigating the microbial communities of long term operating UASB reactor treating real municipal wastewater at low-temperatures below 10 °C in the combination with the effects of organic loading rate (OLR) are scarce.

We hypothesize the performance of anaerobic municipal wastewater treatment at low-temperature is affected by seasonal/archaeal community adaptations. Hence, the investigation of the microbial

communities during anaerobic municipal wastewater treatment at low-temperature is required. In our previous studies, we investigated long-term temperature effects (2.5, 5.5, 8.5, 12, 16, and 25 °C) on UASB reactor performance with increasing organic loading rates using real municipal wastewater over an experimental period of 1025 days (Safitri, Kaster, and Kommedal, *submitted*). In this study, MiSeq amplicon sequencing was conducted on the granule samples in order to monitor the microbial community development and the emergence of psychrophilic methanogens and/or bacteria during the UASB operation down to 2.5 °C. Furthermore, we discuss the effect of low-temperatures and organic loading in trophic structure changes and carbon flow.

2. Materials and Methods

2.1. Granule source

Granules were sampled from in-house designed laboratory-scale UASB reactors at 12, 8.5, 5.5 and 2.5 °C at different selected OLRs at each temperature, as shown in Table 1. UASB reactors were originally seeded with mesophilic granules inoculum which were kindly provided by the late Prof. Rune Bakke's laboratory, University of South-Eastern Norway (USN), Norway. Granules were made from diverse sources: (a) pulp and paper company treating cellulose and lignin-containing waste (Moss, Norway); (b) agriculture pilot-plant treating swine and cow manure supernatant (Skien, Norway); and (c) hydrocarbon oil-containing wastewater from Bamble Industrial Park (Telemark, Norway).

Table 1 Granule samples on microbial community analysis from the UASB system

Temperature (°C)	Reactor A			Reactor B		
	*OLR 3	OLR 8	OLR 15	OLR 3	OLR 8	OLR 15
12	-	√	√	-	√	√
8.5	√	√	√	√	√	√
5.5	√	-	√	√	-	√
2.5	-	-	-	√	-	-

*OLR in $\text{gCOD}\cdot\text{l}^{-1}\cdot\text{d}^{-1}$

2.2. UASB reactors set up and performances

Approximately 30 % v/v of granules inoculum were transferred to the UASB reactors which have a total volume of a 1000 ml. Two parallel in-house designed laboratory-scale UASB reactors (reactor A and B) were operated continuously, receiving primary treated municipal wastewater, from the Grødalund wastewater treatment plant (WWTP), Norway. Grødalund WWTP receives wastewater from several sources in Rogaland County area (Norway): (a) animal destruction in Biosirk Protein ($167 \text{ m}^3\cdot\text{d}^{-1}$); (b) municipal wastewater of approximately 3000 houses in Varhaug and food industry in Fjordland ($1910 \text{ m}^3\cdot\text{d}^{-1}$); (c) dairy industry and chicken slaughtering in Kviamarka ($3020 \text{ m}^3\cdot\text{d}^{-1}$); and (d) reject water from thickening and dewatering digested sludge in Grødalund biogas plant ($345 \text{ m}^3\cdot\text{d}^{-1}$). The dissolved COD concentrations of inlet wastewater during UASB reactor operation fluctuated in the range $439 - 1473 \text{ mgCOD}_{\text{dissolved}}\cdot\text{l}^{-1}$ with the mean concentration by $741\pm 7 \text{ mgCOD}_{\text{dissolved}}\cdot\text{l}^{-1}$ (\pm standard error). Wastewater samples were collected weekly and stored in the dark at $4 \text{ }^\circ\text{C}$ before use (average storage time 5 days).

Table 2 Operational characteristics and reactor performances during continuous UASB system operation

Day	Duration (days)	T ^a	OLR ^b	HRT ^c	COD ^d removal efficiency (%)	Methane fraction in biogas (%)	Methane yield ^e
0-107	107	25	1.0-15.0	1.1-16.7	60-72	87	0.9
108-243	136	16	1.0-15.0		60-72	86	0.93
244-411	168	12	1.0-15.0		51-65	81	0.91
412-642	231	8.5	1.0-15.0		39-57	80	0.88
641-841	199	5.5	3.0-15.0		25-50	77	0.91
842-1025	184	2.5	1.0-8.0		17-43	84	0.86

^aT : operating temperature (°C)
^bOLR : organic loading rate (gCOD·l⁻¹·d⁻¹)
^cHRT : hydraulic retention time (hour)
^dCOD : chemical oxygen demand
^eMethane yield : averaged number expressed as gCOD-CH₄/gCOD removed⁻¹

The UASB reactors were operated continuously increasing the organic loading rate (OLR) stepwise from approximately 1.3±0.1 to 15.2±0.2 gCOD_{dissolved}·l⁻¹·d⁻¹ (±standard error) following steady-state tests at decreasing temperatures (25, 16, 12, 8.5, 5.5 and 2.5 °C) throughout 1025 days operation. OLR was controlled by adjusting the inlet flow rate based on the dissolved COD concentration of inlet wastewater. UASB reactors were started-up at 25 °C with low OLR around 1.0 gCOD_{dissolved}·l⁻¹·d⁻¹ and increased gradually up to approximately 15 gCOD_{dissolved}·l⁻¹·d⁻¹. During operation, hydraulic retention rate (HRT) started at about 16.7 h then gradually decreased along with the increasing OLR, down to 1.1 h. The operating temperatures were then reduced to the next lower temperature experiments as follows; 16, 12, 8.5, 5.5 and finally 2.5 °C. Operational characteristics and reactor performances

during continuous UASB system operation is shown in Table 2. The gradual increment of OLR was used to ensure that granules would not wash out of the system while the microorganisms were acclimating to the higher loading. Severe deterioration of granules occurred in reactor A when applying OLR approximately $15 \text{ gCOD}\cdot\text{l}^{-1}\cdot\text{d}^{-1}$ at $5.5 \text{ }^\circ\text{C}$ and the reactor A stopped operating at day 738. A detailed description of the UASB reactor set up and operation are provided elsewhere (Safitri, Kaster, and Kommedal, *submitted*).

2.3. Microbial community analysis

Approximately 0.25 g (wet weight) of granule samples were obtained from the reactor during 12, 8.5, 5.5 and 2.5°C reactor operation carried out at different OLRs at each temperature (Table 2). DNA was extracted using a DNeasy PowerWater Kit (Qiagen, Germany) as described by the manufacturer. Samples were homogenized in PowerBead tubes using the FastPrep-24™ bead beater (MPBio, USA) for 60s prior to extraction. After extraction, DNA was checked via agarose gel electrophoresis. The DNA concentration was determined using the NanoVue™ Plus Spectrophotometer (GE Healthcare, USA) at absorbance 260 nm before sending samples for external sequencing (Macrogen Europe B.V., Netherlands). The averaged DNA concentration was approximately $100 \text{ ng}\cdot\mu\text{l}^{-1}$. The isolated DNA was stored at $-20 \text{ }^\circ\text{C}$ until further processing.

For polymerase chain reaction (PCR) amplification, the DNA was amplified using primers the v3–4 region of the 16S rRNA gene; B-341F ($5'\text{-CCTACGGGNGGCWGCAG}$) and B-805R ($5'\text{-GACTACNVGGGTATCTAAKCC}$) amplifying 465 base pairs (bp) for bacterial DNA, A-340F ($\text{CCCTAYGGGGYGCASCAG}$) and A-760R ($\text{GGACTACCSGGGTATCTAATCC}$) for archaeal DNA (Nordgård et al., 2017). Pair end sequencing was done by Macrogen Europe B.V, Netherlands, using the MiSeq™ platform. FLASH (fast length adjustment of short reads) software was used to assembly reading data by merging paired-end reads from next-generation sequencing

experiments (Magoč and Salzberg, 2011). CD-HIT-OTU was utilized to preprocess and cluster the data with a three-step clustering to identify operational taxonomic units (OTU) and rDnaTools (Li et al., 2012).

2.4. Statistical analysis

Statistical analyses, standard errors and student t-tests at 95% confidence were calculated and applied using Excel and SigmaPlot V14.0 for Windows (SyStat Inc., USA).

3. Results and Discussions

The feasibility of long-term anaerobic bioreactor operation using UASB system treating municipal wastewater has been demonstrated in psychrophilic condition down to 2.5 °C as shown in Table 2. The study has shown that efficient municipal wastewater treatment was achieved in long term UASB reactors operated at temperatures of 25 down to 12 °C and OLR up to $15.2 \pm 0.2 \text{ gCOD} \cdot \text{l}^{-1} \cdot \text{d}^{-1}$ (\pm standard error). Besides, the remarkable operation of the long-term treatment UASB reactors at 8.5, 5.5, 2.5 °C serves to confirm the feasibility of this treatment at low-temperatures and high organic loading, not only for degrading the organic carbon but also for a positive energy balance potential achieving sustainable wastewater treatment (Safitri, Kaster, and Kommedal, *submitted*). The stable UASB performance indicated long-term reactor operation at low-temperatures even at high OLRs may facilitate the development of well-balanced and stable community interactions in the granules. Hence, microbial community characterization of the low-temperature and loading gradients were presented in this study.

Microbial community analysis using MiSeq amplicon sequencing produced high quality data by on average more than 89% coverage, representing the percentage of sample sequences aligned to a deposited sequence in National Center for Biotechnology Information (NCBI) gen

bank. Based on sequencing data (weighted unifrac), the overall similarity of the communities between samples are shown in a split matrix (Supplementary Document Figure S1). Results showed that granule samples had no significant common features between the two samples within UASB granules; the similarity index was in the range 0.50 - 0.71. Figure 1 shows the bacterial and archaeal Shannon diversity fluctuated in different temperatures and OLR. For the archaeal communities, the Shannon index was reduced at lower temperatures (2.5 and 5.5 °C) indicative of a less diverse and specialized community. Higher OLR also resulted in a decrease of archaeal diversity. The lower community diversities probably resulted from long-term acclimation in higher concentrations of substrates that could be selective for specific microorganisms and caused a significant change in the microbial community in the reactor. However, there is no trend within bacterial community diversity. Based on statistical analysis (student t-test at 95% confidence level) the two reactors demonstrated no significant difference in terms of bacterial and archaeal community diversity at the different temperatures and loadings ($p > 0.05$). Furthermore, the relative abundance of archaeal communities increased along with the increasing OLR and decreasing temperature (Figure 2). At low-temperature and high OLR (5.5 °C and 15 gCOD·l⁻¹·d⁻¹) in reactor B, the archaeal community contributed to the highest percentage in the granule microbial community, 9.6%. At the lowest operating temperature (2.5 °C), it contributed to 8.5%.

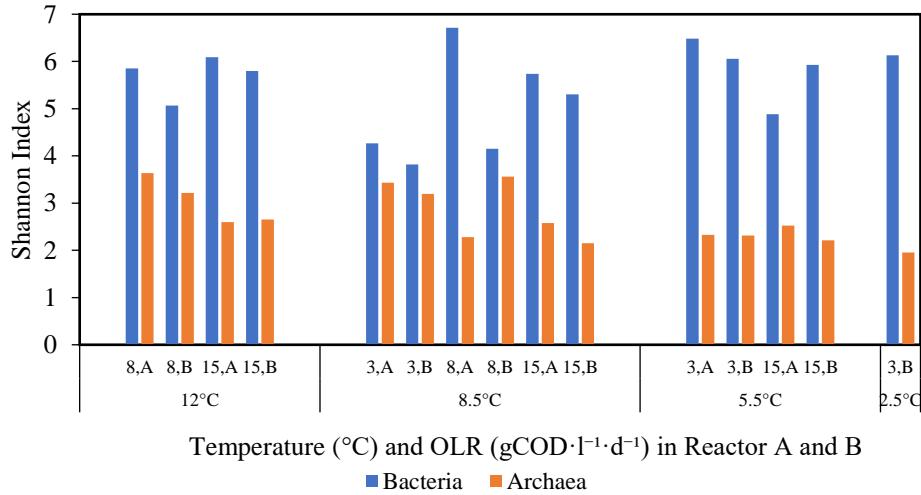


Figure 1 Bacterial and archaeal diversity statistics based on Shannon Index in UASB granules at different operating temperatures and OLRs. A and B on the x-axis represent two parallel reactors, A and B. Numbers beside A and B represent OLR in gCOD·l⁻¹·d⁻¹.

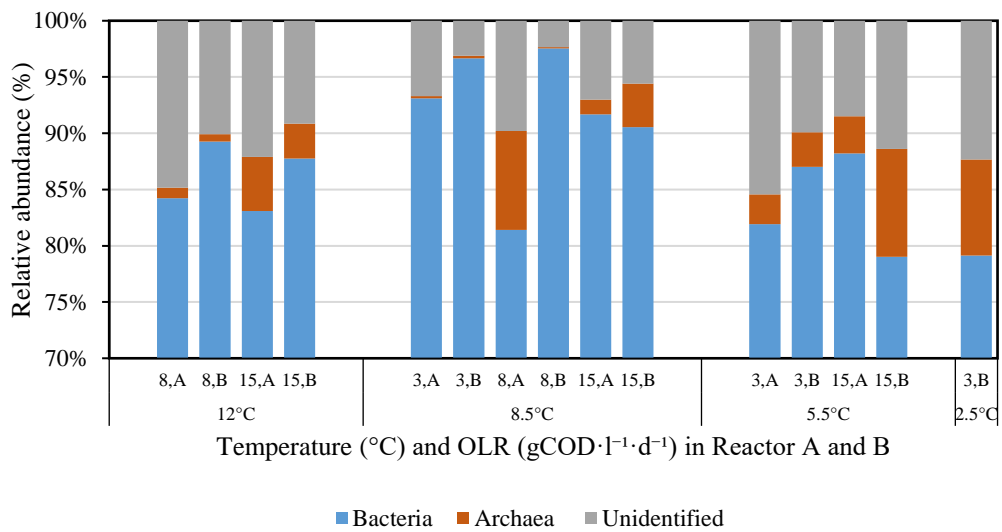


Figure 2 Relative abundances of microbial population structure in UASB granules at the kingdom level. A and B on the x-axis represent two parallel reactors, A and B. Numbers beside A and B represent OLR in gCOD·l⁻¹·d⁻¹.

3.1. Composition shift of bacterial community

Microbial community analysis resulted in an average of 257917 ± 26324 reads (\pm standard deviations) for the bacterial community, while 727217 ± 65465 reads were obtained for the archaeal community. Chlorobi, Bacteroidetes, Proteobacteria, and Firmicutes were identified as the four most dominant phyla within the bacterial community in granules. The most abundant bacterial species in granules are shown in Figure 4.5. Five dominant species were found in all granules these include, *Chlorobium limicola*, *Lentimicrobium saccharophilum*, *Hydrogenispora ethanolica*, *Anaerophaga thermohalophila*, and *Anaerocella delicata*. However, there was a dynamic in the bacterial community structure, with shifts at the bacterial species level following decreasing temperatures and increasing OLRs.

At 12 and 8.5 °C, the species *C. limicola* dominated the bacterial community by 38 - 46% relative abundance especially at low to medium OLR, 3 - 8 $\text{gCOD} \cdot \text{l}^{-1} \cdot \text{d}^{-1}$. However, it decreased remarkably to 2 - 20% relative abundance when applying higher OLR, 15 $\text{gCOD} \cdot \text{l}^{-1} \cdot \text{d}^{-1}$. On the contrary, *L. saccharophilum* contributions to the bacterial community increased along with the increasing OLR from were 3 - 10% to 12 - 28% in 3 - 8 $\text{gCOD} \cdot \text{l}^{-1} \cdot \text{d}^{-1}$ and 15 $\text{gCOD} \cdot \text{l}^{-1} \cdot \text{d}^{-1}$, respectively. A significant shift was observed on the predominant species when decreasing temperature to 5.5 and 2.5 °C in both reactors. The relative abundance of *L. saccharophilum* increased up to 10 - 28%, and the relative abundance of *C. limicola* decreased to less than 5%.

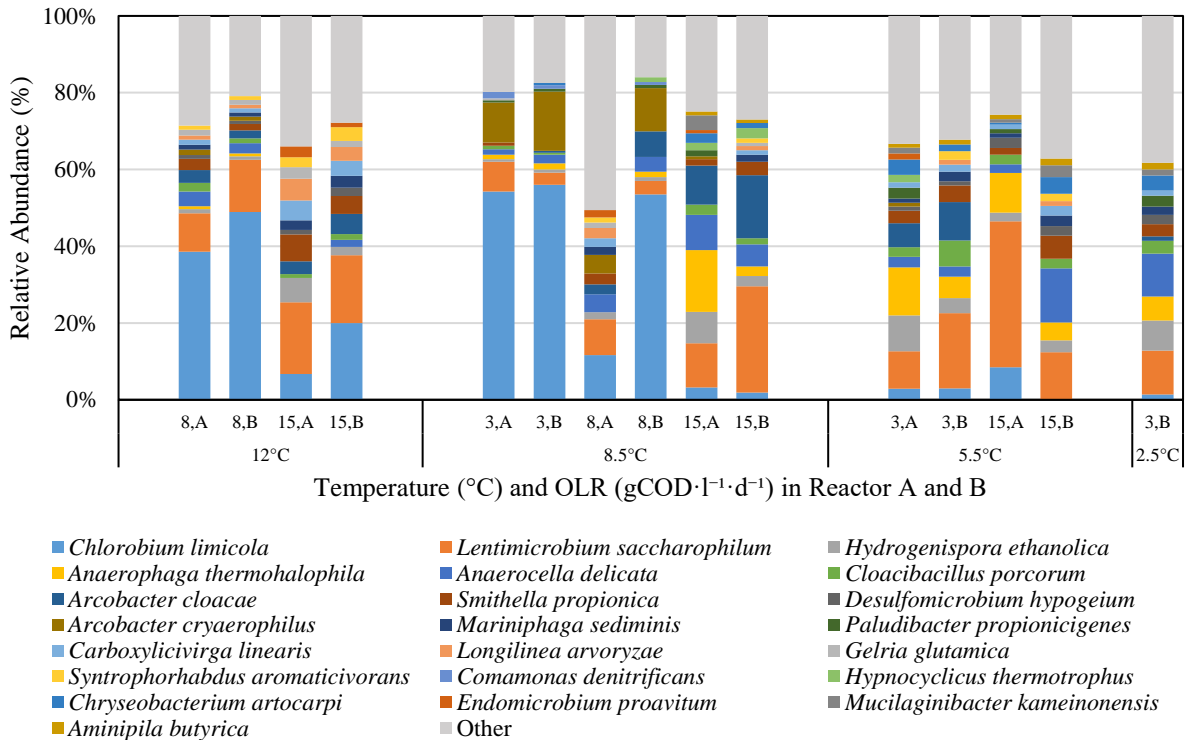


Figure 3 Relative abundances of microbial population structure in UASB granules at the bacterial species level at different operating temperatures and OLRs. A and B on the x-axis represents microbial population structure in two parallel reactors, A and B. Numbers beside A and B represent OLR in gCOD·l⁻¹·d⁻¹.

C. limicola is an auto- and mixotrophic, green phototrophic bacterium belonging to the *Chlorobiaceae* family. This species carry out anaerobic photosynthesis in which reduced sulfur compounds are used as electron donor to fix carbon dioxide (Verté et al., 2002), in particular sulfide ions (Henshaw et al., 1998). Cabral et al. (2020) and Aida et al. (2015) revealed the presence of green sulfur bacteria in UASB reactor system related to sulfide oxidation (Cabral et al., 2020) and low-temperature conditions (Aida et al., 2015). Their results showed that this group played a significant role in anaerobic sulfur oxidation in low-temperatures (10 - 26 °C) consortia (Aida et al., 2015). A significant decrement of *C.*

limicola abundance in this current study was observed when decreasing temperature to 5.5 and 2.5 °C. This coincided with the insulation of the reactors by opaque external foam covers at the end of the 8.5 °C experiment. Hence, their reduced abundance most likely resulted from lack of photons rather than reduced temperature. *L. saccharophilum* is a strictly anaerobic bacteria which belongs to the *Lentimicrobiaceae* family. It is a chemo-organotrophic fermenter which is widely found in the environment, and it is especially common in organic-rich anoxic ecosystems, such as animal gut and anaerobic waste/wastewater treatment systems. Their major fermentative products are acetate, malate, propionate, formate and hydrogen (Sun et al., 2016), filling the major niche of fermenters in the consortia of anaerobic organic carbon converters.

The mesophile *H. ethanolica* also emerged as a predominant community member at all operating conditions with relative abundance increasing with decreasing temperatures from approximately 1% (around 1000 OTU counts) at 12 °C to approximately 8% (around 5000 OTU counts) at 2.5 °C. As for the previously described specie, *L. saccharophilum*, *H. ethanolica* is commonly found in anaerobic wastewater systems as an ethanol-hydrogen-coproducing bacteria which co-culture with the hydrogenotrophic methanogens in syntrophic substrate utilization (Liu et al., 2014). Their major end-products of glucose fermentation are acetate, ethanol and hydrogen (Yang et al., 2016). Two other predominant species in the granule bacterial communities were *A. thermohalophila*, and *A. delicata* that appeared at 8.5, 5.5, and 2.5 °C. *A. thermohalophila* and *A. delicata* are strictly anaerobic bacteria and live where they may show both fermentative and acetogenic metabolism (Abe et al., 2012; Denger et al., 2002). *A. thermohalophila* is classified as a thermophilic bacteria and has not been reported to play a significant role at low-temperature conditions (Denger et al., 2002). Presence at low-temperatures might be due to novel biological capabilities (and re-classification) or an indication of psychrotolerance. As only a single

species is characterized among the *Anaerophaga*, by an isolated study from an anaerobic sludge, only putative conclusions to their role and growth are possible. *A. delicata* can grow down to 10 °C (Abe et al., 2012) and the relative abundances of *A. delicata* increased from 3% (approximately 1500 OTU counts) at 12 °C to 11% at 2.5 °C (approximately 7500 OTU counts). Eco-physiological studies by Abe et al. (2012) showed the species to be able to ferment some amino acids to acetate, butyrate and valerate, and a limited ability to reduce sulfate. The relative increase in abundance indicated psychrotolerant ecophysiology concurrent with reduced general diversity. In addition to the dominant and omnipresent species, several predominant species emerged at more obligate psychrophilic (5.5 and 2.5 °C) conditions and represented interesting and relevant ecological capabilities as suggested by the literature: *Paludibacter propionigenes*, *Chryseobacterium artocarpi*, *Mucilaginibacter kameinonensis*, and *Aminipila butyrlica* should be mentioned. *P. propionigenes* is a natural occurring mesophilic fermentative bacteria which utilized various sugars and produce propionate and acetate as major products (Kim et al., 2015; Ueki et al., 2006). *C. artocarpi* have been known as a psychrotolerant and halotolerant bacteria (Venil et al., 2014) and is known to produce mucoid colonies suggesting a role in granule formation. Likewise, *M. kameinonensis* are extracellular polymeric substances (EPS)-producing bacteria, including fatty acids containing EPS and could live in a wide range environment at 5 - 30 °C (Urai et al., 2008). *A. butyrlica* fermented amino acids as growth substrates and produced acetate and butyrate (Ueki et al., 2018).

Among the top predominant species identified from granule communities, three pathogenic species were identified: *Cloacibacillus porcorum* (0 - 7% relative abundance), *Arcobacter cryaerophilus* (0 - 15% relative abundance), and *Citrobacter gillenii* (0 - 1% relative abundance). *C. porcorum* can cause soft tissue infections, abscesses, blood, peritoneal fluid, and dental infections (Domingo et al., 2015;

Looft et al., 2013). *A. cryaerophilus* is a globally emerging foodborne pathogen which is a dominant member in wastewater causing diarrhea, mastitis and abortion in animals, and bacteremia, endocarditis, peritonitis, gastroenteritis and diarrhea in humans (Müller et al., 2020). Finally, *C. gillanii* is an opportunistic human pathogen that can lead to invasive diseases, including infections of the urinary tract and respiratory tract (Samonis et al., 2008). Based on this result, there was a slight increase of *C. porcorum* relative abundance with decreasing temperature from 1 - 2 % at 12 °C to 3 - 7% at 5.5 °C, suggesting of psychrotolerance. Significant increases of *A. cryaerophilus* relative abundance was observed from 1% at 12 °C to approximately 15% when applying 8.5 °C. However, they were only detected in traces below 0.01% relative abundance at 5.5 and 2.5 °C. There was no significant trend observed in *C. gillanii* relative abundance at the different temperatures and loadings.

The original wastewater showed a significant dissimilarity of the predominant bacterial species compared to granule samples. The wastewater was dominated by *Trichococcus paludicola* with 14767 OTUs count (31.2±0.08% relative abundance ± standard deviation), *Aliarcobacter cryaerophilus* with 4494 OTUs count (10.0±0.01%), and *Lactococcus raffinolactis* with 3954 OTUs count (8.4±0.08%). *T. paludicola* is psychrotolerant facultative anaerobes and alkaliphilic with optimum growth at pH 9.0 (Dai et al., 2018). *L. raffinolactis* is nonstarter lactic acid bacterium in a wide range of environments such as in the dairy wastewater (Meslier, Loux, and Renault, 2012). However, the OTUs count of these three species in the granules were insignificant (0 - 293 OTUs count). The inability to detect them in the granules suggests that this group were functionally lacked the ability to attach in granules biofilm and adapt to psychrophilic conditions. Detailed wastewater sequencing data of predominant species are presented in Supplementary Document (Figure S3).

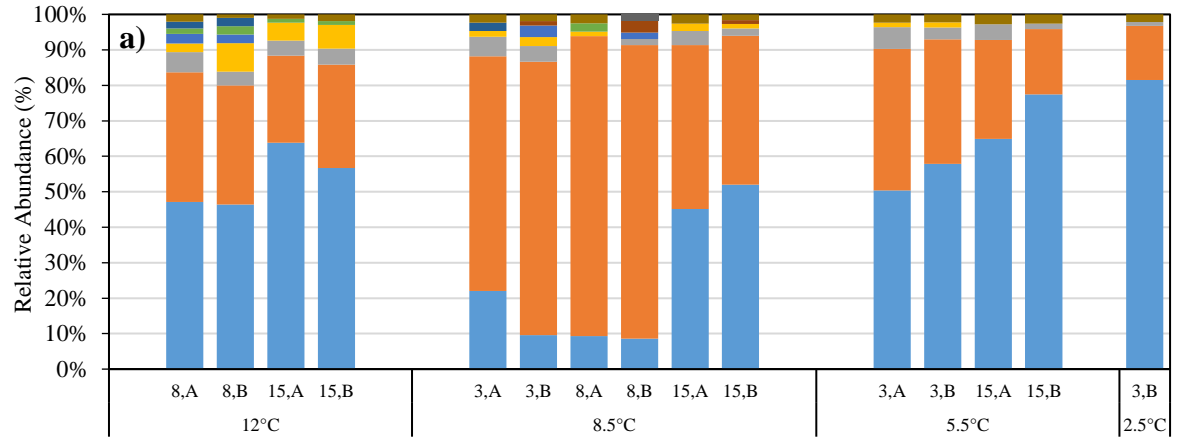
3.2. Composition shift of methanogenic archaeal community

Based on the results, we detected the presence of sequences belonging to the archaea kingdom in our samples. The relative abundances of the microbial population structure in granules at the predominant archaeal species level at different operating temperatures and OLRs are presented in Figure 4. The archaeal community structure was dynamic, with shifts at the methanogen species level following decreasing temperatures and increasing OLRs. Figure 4a shows predominant species in the archaeal community contributing to at least 97% relative abundance, and the insignificant abundance was accounted for less than 3%. The most predominant methanogen species in all granule samples were *Methanotheriix soehngeni*, *Methanomassiliicoccus luminyensis*, *Methanocorpusculum aggregans*, and *Methanobacterium beijingense* contributing to more than 90% relative abundance in the archaeal communities. Similar to the granule's sequences, the predominant species in the original wastewater are *M. luminyensis* (27 % relative abundance) and *M. soehngeni* (25 % relative abundance). Detailed predominant species in wastewater sequencing data are presented in Supplementary Document (Figure S3).

At 12 °C, *M. soehngeni* and *M. luminyensis* contributions in archaeal community were 46 - 64% and 29 - 47%, respectively. A significant shift was observed on predominant species when decreasing temperature to 8.5 °C in reactor A and B. At OLR 3 and 8 gCOD·l⁻¹·d⁻¹, the relative abundance of *M. luminyensis* increased up to 85%, and the relative abundance of *M. soehngeni* decreased down to less than 10%. However, after further decrement of the operating temperatures, *M. soehngeni* abundance gradually increased to more than 82% at 2.5 °C. The relative abundance of *M. aggregans*, and *M. beijingense* fluctuated regardless of operating temperatures and OLRs in the range 2 - 10%.

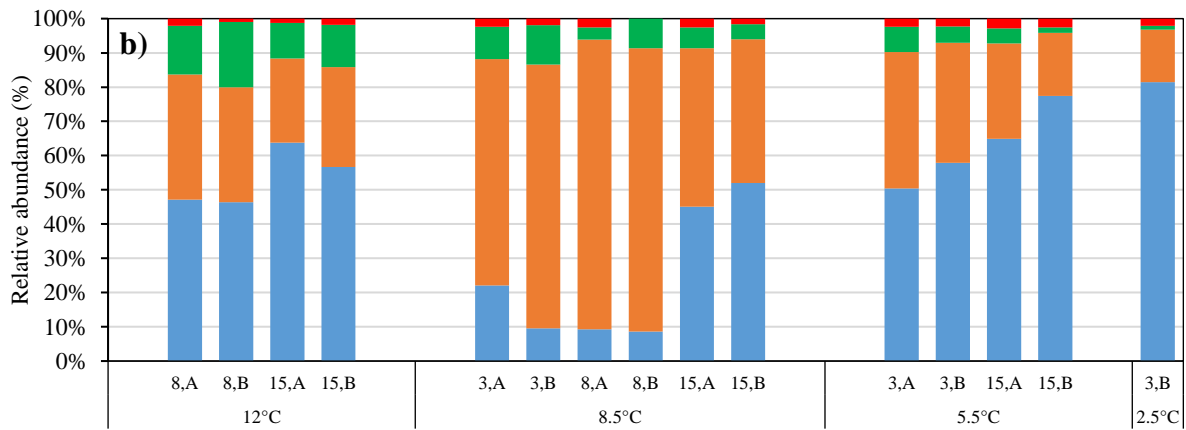
Based on methanogenesis pathway, our archaeal community could be divided into three methanogen groups, corresponding to archaeal

dominant species in Figure 4b. At 12 °C, acetoclastic methanogen contributions in archaeal community were 46 - 64% and 29 - 47%, respectively. A significant shift was observed upon temperature reduction to 8.5 °C in both reactors. At OLR 3 and 8 gCOD·l⁻¹·d⁻¹, the relative abundance of H₂-dependent methylotrophic methanogens increased up to 85%. However, after further decrement of the operating temperatures, acetoclastic methanogens abundance gradually increased to more than 82% at 2.5 °C. The relative abundance of hydrogenotrophic methanogen decreased in decreasing temperatures.



Temperature (°C) and OLR (gCOD·l⁻¹·d⁻¹) in Reactor A and B

- *Methanotherix soehngeni*
- *Methanomassiliicoccus luminyensis*
- *Methanocorpusculum aggregans*
- *Methanobacterium beijingense*
- *Methanoregula formicica*
- *Methanobacterium subterraneum*
- *Methanobrevibacter millerae*
- *Methanospirillum psychrodurum*
- *Methanosphaerula palustris*
- Insignificant abundance <3%



Temperature (°C) and OLR (gCOD·l⁻¹·d⁻¹) in Reactor A and B

- Acetoclastic methanogens
- Methylotrophic methanogens
- Hydrogenotrophic methanogens
- Insignificant abundance <3%

Figure 4 Relative abundances of microbial population structure in UASB granules at archaeal species level (a) and methanogen groups based on methanogenesis pathway (b) at different operating temperatures and OLRs. A and B on the x-axis represents microbial population structure in two parallel reactors, A and B. Numbers beside A and B represent OLR in gCOD·l⁻¹·d⁻¹.

The most predominant methanogen species in all granule samples were: the obligate acetoclastic methanogen *Methanothermobacter thermoautotrophicus* belongs to *Methanosarcinales* order which decarboxylates acetate (Huser, Wuhrmann, and Zehnder, 1982); the H₂-dependant methylotrophic methanogen *Methanomassiliicoccus luminyensis* belongs to *Methanomassiliicoccales* order which reduces the methyl-groups of methylated compounds to methane with H₂ as electron donor (Söllinger and Urich, 2019); and the two autotrophic hydrogen oxidizer *Methanocorpusculum aggregans* (heterotype *parvum*) and *Methanobacterium beijingense* belong to *Methanomicrobiales* and *Methanobacteriales* order, respectively, using hydrogen and carbon dioxide or formate as substrates (Ma, Liu, and Dong, 2005; Oren, 2014). These four species made up more than 90% relative abundance in the archaeal communities regardless of operating temperatures and OLRs. However, shifts in the methanogen composition were observed with an increase in OLR and a decrease in temperature, suggesting shift in methanogenesis pathway (Figure 4b).

During operating temperature of 12 °C and low OLR, acetoclastic methanogens were relatively more abundant in both reactors and acetoclastic methanogens slightly increased at high OLR (Figure 4.6b). Similar observations were reported by Zhang et al., (2018) whereby acetoclastic *Methanosaetaceae* was abundant after 300 days of operation at 10 - 20 °C in a UASB reactor. By decreasing operating temperature to 8.5 °C, a significant methanogenic composition shifts were observed, especially at low to medium OLRs. Methylotrophic methanogens, specifically *Methanomassiliicoccales*, became more dominant contributing to more than 70% relative abundance of the archaeal community. Interestingly, *Methanomassiliicoccales* is known as a methylotrophic methanogens lacking the Wood-Ljungdahl pathway and therefore cannot oxidize methyl-groups to CO₂ (Söllinger & Urich, 2019). Consequently, they are dependent on an external electron donor (i.e. H₂) and compete with autotrophic methanogens. Furthermore, Liu

and Whitman. (2008) stated that H₂-dependant methylotrophic methanogenesis e.g., from methanol, is thermodynamically more favorable than acetoclastic methanogenesis under standard conditions (-113 kJ·mol⁻¹ vs. -33 kJ·mol⁻¹ respectively) (Liu and Whitman 2008). However, with the increased OLRs and decreased temperatures further down to 2.5 °C, the relative abundance of acetoclastic methanogen increased again to more than 70%. This has also been demonstrated by Nozhevnikova et al. (2007) reporting about 95% methane to originate from acetate at 5 °C. In this study, acetoclastic methanogens became increasingly dominant under low-temperature (2.5 °C), indicating acetoclastic growth and acetate to be the main precursor of methanogenesis at low-temperatures.

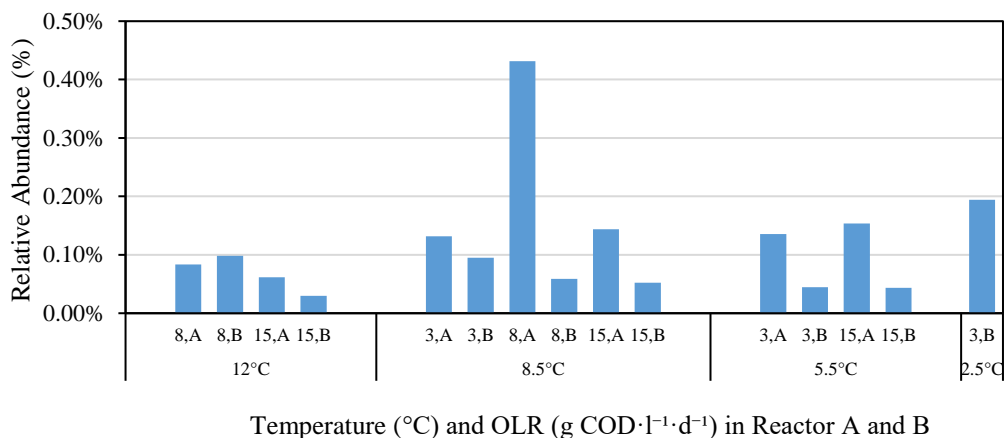


Figure 5 Relative abundances of genus *Acetoanaerobium* (*homoacetogen*) in UASB granules at different operating temperatures and OLRs. A and B on the x-axis represents microbial population structure in two parallel reactors, A and B. Numbers beside A and B represent OLR in gCOD·l⁻¹·d⁻¹.

In many studies, hydrogenotrophic methanogens played an essential role in anaerobic treatment at low-temperatures (McKeown et al., 2009; Bandara et al., 2012; Smith, Skerlos, and Raskin, 2015; Petropoulos et al., 2017). However, our results showed the relative abundances of hydrogenotrophic methanogens were low and decreased with the

decreasing temperatures by approximately 14%, 7.3%, 4.5% and 1.1% at 12, 8.5, 5.5, and 2.5 °C, respectively. Most probably, homoacetogenesis becomes the main fermentation reaction under this condition. An increased acetate production was also observed during UASB operation, especially at 2.5 °C (Safitri, Kaster, and Kommedal, *in preparation*). Furthermore, bacterial community analysis showed an increased relative abundances of genus *Acetoanaerobium* (homoacetogen) in UASB granules at the decreasing temperatures (Figure 5). Homoacetogens convert H₂ and CO₂ to acetate outcompeting with hydrogenotrophic methanogens at low-temperatures and these microbes could also grow under both acidic and alkaline conditions (Kotsyurbenko et al., 2001; Nozhevnikova et al., 2007). Furthermore, Kotsyurbenko et al. (1996) showed that at 6 °C, homoacetogens grow two times faster and were less sensitive than hydrogenotrophic methanogens with 2.2 and 4.1 Q₁₀ value, respectively (Kotsyurbenko et al., 1996).

Overall, our finding suggested temperature and organic loading did not only affect UASB bioprocess performances but also results in a change in the microbial community composition and the degradation pathway of organic matter. In Figure 6, anaerobic process pathway under psychrophilic conditions is suggested. Generally, this study presented that, under low-temperature conditions, acetoclastic methanogens emerged as an important role, and acetate was the main precursor of methanogenesis. This successful operation at low-temperatures along with microbial community confirmation, the prevalence of psychrotolerant communities was observed throughout long-term UASB reactor operation, indicating the long-term adaptation of the microbial community in granulated biomass through changes in the community structure. This study provides valuable evidence for the possibility of using anaerobic wastewater treatment at low-temperature and high loading by incorporating granulated biomass. However, the improvement in reactor design and the optimization of the operational

conditions are important in further research to aggregate more anaerobic microorganisms that are well adapted to low-temperature.

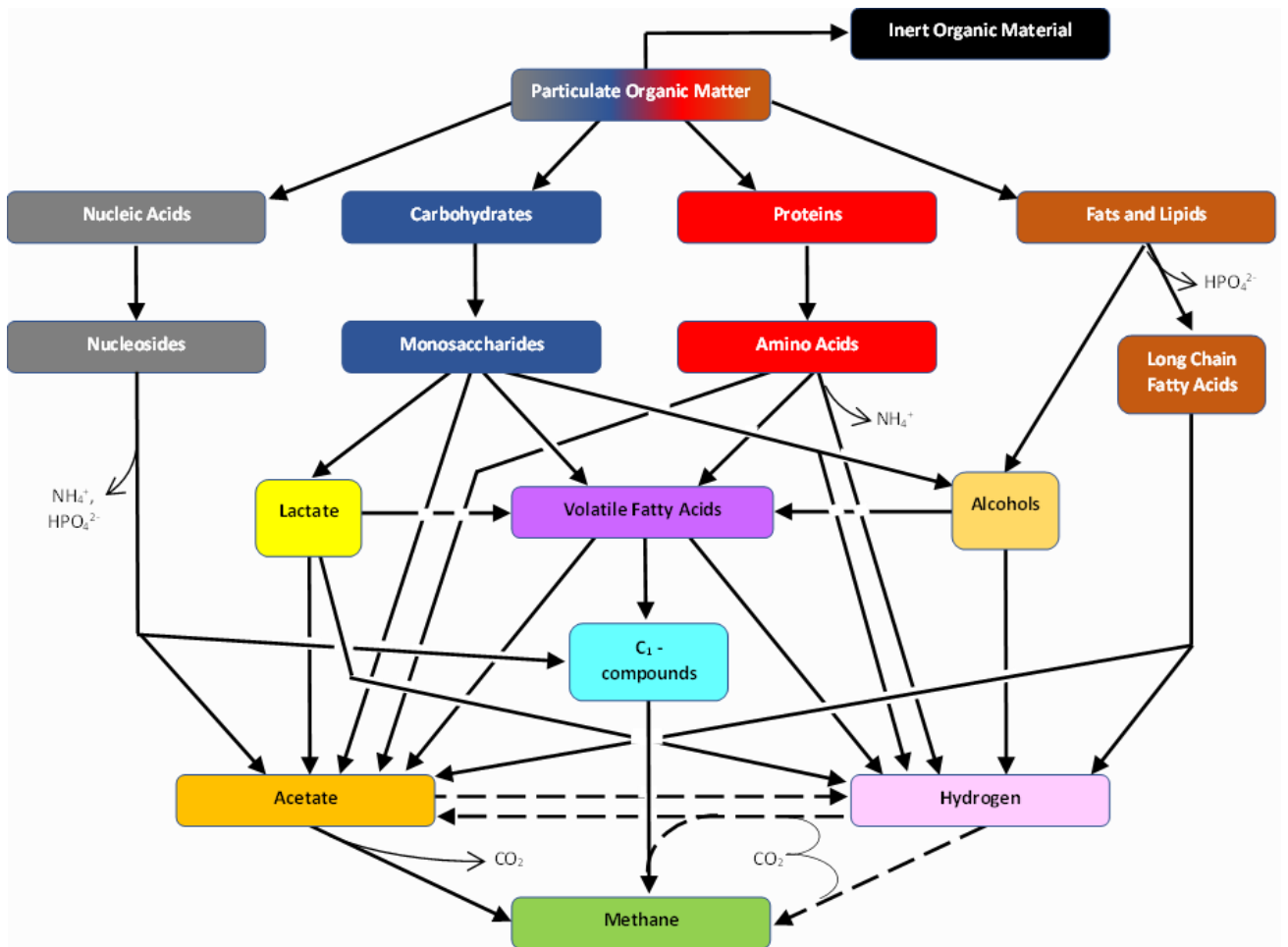


Figure 6 Anaerobic process pathway proposed under psychrophilic conditions. Dashed arrows represent the hydrogen producing and consuming pathways.

4. Conclusions

The conclusions were as following:

- Long-term operation under low-temperature conditions can then lead to the selection of a less dynamic cold-adapted methanogenic consortium, including psychrophilic bacteria and methanogens.
- Temperature affected the reactor performances and the structure of the microbial community.
- Methanogenic archaea communities proved the adaptation ability to very low-temperatures down to 2.5 °C regardless of the operating OLR; psychrotolerant communities.
- Acetoclastic methanogens can become important members of the methanogenic community at temperature 12, 5.5 and 2.5 °C. While at 8.5 °C, homoacetogens and methylotrophic methanogens emerge as significant roles in trophic change and carbon flow.

References

- Abe, Kunihiro, Atsuko Ueki, Yoshimi Ohtaki, Nobuo Kaku, Kazuya Watanabe, and Katsuji Ueki. 2012. "Anaerocella Delicata Gen. Nov., Sp. Nov., a Strictly Anaerobic Bacterium in the Phylum Bacteroidetes Isolated from a Methanogenic Reactor of Cattle Farms." *The Journal of General and Applied Microbiology* 58 (6): 405–12. <https://doi.org/10.2323/jgam.58.405>.
- Aida, Azrina A, Kyohei Kuroda, Masamitsu Yamamoto, Akinobu Nakamura, Masashi Hatamoto, and Takashi Yamaguchi. 2015. "Diversity Profile of Microbes Associated with Anaerobic Sulfur Oxidation in an Upflow Anaerobic Sludge Blanket Reactor Treating Municipal Sewage." *Microbes and Environments* 30 (2): 157–63. <https://doi.org/10.1264/jsme2.ME14105>.

- Akila, G., and T.S. Chandra. 2007. "Performance of an UASB Reactor Treating Synthetic Wastewater at Low-Temperature Using Cold-Adapted Seed Slurry." *Process Biochemistry* 42 (3): 466–71. <https://doi.org/10.1016/j.procbio.2006.09.010>.
- Bandara, Wasala M.K.R.T.W., Tomonori Kindaichi, Hisashi Satoh, Manabu Sasakawa, Yoshihito Nakahara, Masahiro Takahashi, and Satoshi Okabe. 2012. "Anaerobic Treatment of Municipal Wastewater at Ambient Temperature: Analysis of Archaeal Community Structure and Recovery of Dissolved Methane." *Water Research* 46 (17): 5756–64. <https://doi.org/10.1016/j.watres.2012.07.061>.
- Bowen, Emma J., Jan Dolfing, Russell J. Davenport, Fiona L. Read, and Thomas P. Curtis. 2014. "Low-Temperature Limitation of Bioreactor Sludge in Anaerobic Treatment of Domestic Wastewater." *Water Science and Technology* 69 (5): 1004. <https://doi.org/10.2166/wst.2013.821>.
- Cabral, C. S., A. L. Sanson, R. J. C. F. Afonso, C. A. L. Chernicharo, and J. C. Araújo. 2020. "Impact of Microaeration Bioreactor on Dissolved Sulfide and Methane Removal from Real UASB Effluent for Sewage Treatment." *Water Science and Technology* 81 (9): 1951–60. <https://doi.org/10.2166/wst.2020.250>.
- Cavicchioli, Ricardo. 2006. "Cold-Adapted Archaea." *Nature Reviews Microbiology* 4 (April): 331.
- Collins, Gavin, Thérèse Mahony, and Vincent O’Flaherty. 2006. "Stability and Reproducibility of Low-Temperature Anaerobic Biological Wastewater Treatment." *FEMS Microbiology Ecology* 55 (3): 449–58. <https://doi.org/10.1111/j.1574-6941.2005.00034.x>.
- Collins, Gavin, Sharon McHugh, Sean Connaughton, Anne-Marie Enright, Aileen Kearney, Colm Scully, Thérèse Mahony, Paádhraig Madden, and Vincent O’Flaherty. 2006. "New Low-Temperature Applications of Anaerobic Wastewater Treatment."

- Journal of Environmental Science and Health, Part A 41 (5): 881–95. <https://doi.org/10.1080/10934520600614504>.
- Conrad, Ralf. 2020. “Importance of Hydrogenotrophic, Aceticlastic and Methylotrophic Methanogenesis for Methane Production in Terrestrial, Aquatic and Other Anoxic Environments: A Mini Review.” *Pedosphere* 30 (1): 25–39. [https://doi.org/10.1016/S1002-0160\(18\)60052-9](https://doi.org/10.1016/S1002-0160(18)60052-9).
- Dai, Yu-Mei, Ling-Li Zhang, Yan Li, Yu-Qian Li, Xiao-Hui Deng, Ting-Ting Wang, Feng Yang, et al. 2018. “Characterization of *Trichococcus Paludicola* Sp. Nov. and *Trichococcus Alkaliphilus* Sp. Nov., Isolated from a High-Elevation Wetland, by Phenotypic and Genomic Analyses.” *International Journal of Systematic and Evolutionary Microbiology*. Microbiology Society. <https://doi.org/10.1099/ijsem.0.002464>.
- Denger, Karin, Rolf Warthmann, Wolfgang Ludwig, and Bernhard Schink. 2002. “*Anaerophaga Thermohalophila* Gen. Nov., Sp. Nov., a Moderately Thermohalophilic, Strictly Anaerobic Fermentative Bacterium.” *International Journal of Systematic and Evolutionary Microbiology* 52 (1): 173–78. <https://doi.org/10.1099/00207713-52-1-173>.
- Dolejs, Petr, Ghinwa El Tayar, Dana Vejmelkova, Martin Pecenka, Martina Polaskova, and Jan Bartacek. 2018. “Psychrophilic Anaerobic Treatment of Sewage: Biomethane Potential, Kinetics and Importance of Inoculum Selection.” *Journal of Cleaner Production* 199 (October): 93–100. <https://doi.org/10.1016/j.jclepro.2018.07.134>.
- Domingo M.-C., Yansouni C., Gaudreau C., Lamothe F., Lévesque S., Tremblay C., Garceau R., and Richter S. S. 2015. “*Cloacibacillus* Sp., a Potential Human Pathogen Associated with Bacteremia in Quebec and New Brunswick.” *Journal of Clinical Microbiology* 53 (10): 3380–83. <https://doi.org/10.1128/JCM.01137-15>.

- Earl, J., G. Hall, R. W. Pickup, D. A. Ritchie, and C. Edwards. 2003. "Analysis of Methanogen Diversity in a Hypereutrophic Lake Using PCR-RFLP Analysis of *Mcr* Sequences." *Microbial Ecology* 46 (2): 270–78. <https://doi.org/10.1007/s00248-003-2003-x>.
- Elmitwalli, Tarek A., Kim L.T. Oahn, Grietje Zeeman, and Gatzke Lettinga. 2002. "Treatment of Domestic Sewage in a Two-Step Anaerobic Filter/Anaerobic Hybrid System at Low-temperature." *Water Research* 36 (9): 2225–32. [https://doi.org/10.1016/S0043-1354\(01\)00438-9](https://doi.org/10.1016/S0043-1354(01)00438-9).
- Fey, Axel, Peter Claus, and Ralf Conrad. 2004. "Temporal Change of ¹³C-Isotope Signatures and Methanogenic Pathways in Rice Field Soil Incubated Anoxically at Different Temperatures." *Geochimica et Cosmochimica Acta* 68 (2): 293–306. [https://doi.org/10.1016/S0016-7037\(03\)00426-5](https://doi.org/10.1016/S0016-7037(03)00426-5).
- Großkopf Regine, Stubner Stephan, and Liesack Werner. 1998. "Novel Euryarchaeotal Lineages Detected on Rice Roots and in the Anoxic Bulk Soil of Flooded Rice Microcosms." *Applied and Environmental Microbiology* 64 (12): 4983–89. <https://doi.org/10.1128/AEM.64.12.4983-4989.1998>.
- Henshaw, Paul F., J.K. Bewtra, and N. Biswas. 1998. "Hydrogen Sulphide Conversion to Elemental Sulphur in a Suspended-Growth Continuous Stirred Tank Reactor Using *Chlorobium limicola*." *Water Research* 32 (6): 1769–78. [https://doi.org/10.1016/S0043-1354\(97\)00393-X](https://doi.org/10.1016/S0043-1354(97)00393-X).
- Huser, Beat A., Karl Wuhrmann, and Alexander J. B. Zehnder. 1982. "Methanotrix Soehngeni Gen. Nov. Sp. Nov., a New Acetotrophic Non-Hydrogen-Oxidizing Methane Bacterium." *Archives of Microbiology* 132 (1): 1–9. <https://doi.org/10.1007/BF00690808>.
- Kettunen, R. H., and J. A. Rintala. 1997. "The Effect of Low-temperature (5–29 °C) and Adaptation on the Methanogenic Activity of

- Biomass.” *Applied Microbiology and Biotechnology* 48 (4): 570–76. <https://doi.org/10.1007/s002530051098>.
- Kettunen, Riitta H., and Jukka A. Rintala. 1998. “Performance of an On-Site UASB Reactor Treating Leachate at Low-temperature.” *Water Research* 32 (3): 537–46. [https://doi.org/10.1016/S0043-1354\(97\)00319-9](https://doi.org/10.1016/S0043-1354(97)00319-9).
- Kim, Woong, Seung Gu Shin, Gyuseong Han, Kyungjin Cho, and Seokhwan Hwang. 2015. “Structures of Microbial Communities Found in Anaerobic Batch Runs That Produce Methane from Propionic Acid—Seeded from Full-Scale Anaerobic Digesters above a Certain Threshold.” *Journal of Biotechnology* 214 (November): 192–98. <https://doi.org/10.1016/j.jbiotec.2015.09.040>.
- Koster, I. W., and G. Lettinga. 1985. “Application of the Upflow Anaerobic Sludge Bed (UASB) Process for Treatment of Complex Wastewaters at Low-temperatures.” *Biotechnology and Bioengineering* 27 (10): 1411–17. <https://doi.org/10.1002/bit.260271004>.
- Kotsyurbenko, O. R., A. N. Nozhevnikova, T. I. Soloviova, and G. A. Zavarzin. 1996. “Methanogenesis at Low-temperatures by Microflora of Tundra Wetland Soil.” *Antonie van Leeuwenhoek* 69 (1): 75–86. <https://doi.org/10.1007/BF00641614>.
- Kotsyurbenko, Oleg R., Michail V. Glagolev, Alla N. Nozhevnikova, and Ralf Conrad. 2001. “Competition between Homoacetogenic Bacteria and Methanogenic Archaea for Hydrogen at Low-temperature.” *FEMS Microbiology Ecology* 38 (2–3): 153–59. <https://doi.org/10.1111/j.1574-6941.2001.tb00893.x>.
- Kwon, Min Jung, Ji Young Jung, Binu M. Tripathi, Mathias Göckede, Yoo Kyung Lee, and Mincheol Kim. 2019. “Dynamics of Microbial Communities and CO₂ and CH₄ Fluxes in the Tundra Ecosystems of the Changing Arctic.” *Journal of Microbiology* 57 (5): 325–36. <https://doi.org/10.1007/s12275-019-8661-2>.

- Leitão, Renato Carrhá, Adrianus Cornelius van Haandel, Grietje Zeeman, and Gatze Lettinga. 2006. “The Effects of Operational and Environmental Variations on Anaerobic Wastewater Treatment Systems: A Review.” *Bioresource Technology* 97 (9): 1105–18. <https://doi.org/10.1016/j.biortech.2004.12.007>.
- Lettinga, Gatze, Salih Rebac, and Grietje Zeeman. 2001. “Challenge of Psychrophilic Anaerobic Wastewater Treatment.” *Trends in Biotechnology* 19 (9): 363–70. [https://doi.org/10.1016/S0167-7799\(01\)01701-2](https://doi.org/10.1016/S0167-7799(01)01701-2).
- Li, Weizhong, Limin Fu, Beifang Niu, Sitao Wu, and John Wooley. 2012. “Ultrafast Clustering Algorithms for Metagenomic Sequence Analysis.” *Briefings in Bioinformatics* 13 (6): 656–68. <https://doi.org/10.1093/bib/bbs035>.
- Liu, Yi, Jiang-Tao Qiao, Xian-Zheng Yuan, Rong-Bo Guo, and Yan-Ling Qiu. 2014. “Hydrogenispora Ethanolica Gen. Nov., Sp. Nov., an Anaerobic Carbohydrate-Fermenting Bacterium from Anaerobic Sludge.” *International Journal of Systematic and Evolutionary Microbiology* 64 (5): 1756–62. <https://doi.org/10.1099/ijs.0.060186-0>.
- Liu, Yuchen, and William B. Whitman. 2008. “Metabolic, Phylogenetic, and Ecological Diversity of the Methanogenic Archaea.” *Annals of the New York Academy of Sciences* 1125 (1): 171–89. <https://doi.org/10.1196/annals.1419.019>.
- Looft, T., U. Y. Levine, and T. B. Stanton. 2013. “Cloacibacillus Porcorum Sp. Nov., a Mucin-Degrading Bacterium from the Swine Intestinal Tract and Emended Description of the Genus Cloacibacillus.” *International Journal of Systematic and Evolutionary Microbiology* 63 (6): 1960–66. <https://doi.org/10.1099/ijs.0.044719-0>.
- Ma, Kai, Xiaoli Liu, and Xiuzhu Dong. 2005. “Methanobacterium Beijingense Sp. Nov., a Novel Methanogen Isolated from Anaerobic Digesters.” *International Journal of Systematic and*

- Evolutionary Microbiology. Microbiology Society.
<https://doi.org/10.1099/ijs.0.63254-0>.
- Magoč, Tanja, and Steven L Salzberg. 2011. “FLASH: Fast Length Adjustment of Short Reads to Improve Genome Assemblies.” *Bioinformatics* (Oxford, England) 27 (21): 2957–63.
<https://doi.org/10.1093/bioinformatics/btr507>.
- Mahmoud, Nidal, Grietje Zeeman, Huub Gijzen, and Gatze Lettinga. 2004. “Anaerobic Sewage Treatment in a One-Stage UASB Reactor and a Combined UASB-Digester System.” *Water Research* 38 (9): 2348–58.
<https://doi.org/10.1016/j.watres.2004.01.041>.
- McKeown, Rory M., Colm Scully, Thérèse Mahony, Gavin Collins, and Vincent O’Flaherty. 2009. “Long-Term (1243 Days), Low-Temperature (4–15°C), Anaerobic Biotreatment of Acidified Wastewaters: Bioprocess Performance and Physiological Characteristics.” *Water Research* 43 (6): 1611–20.
<https://doi.org/10.1016/j.watres.2009.01.015>.
- McKeown, Rory, Colm Scully, Anne-Marie Enright, Fabio Chinalia, Changsoo Lee, Thérèse Mahony, Gavin Collins, and Vincent O’Flaherty. 2009. “Psychrophilic Methanogenic Community Development during Long-Term Cultivation of Anaerobic Granular Biofilms.” *The ISME Journal* 3 (11): 1231–42.
<https://doi.org/10.1038/ismej.2009.67>.
- Meslier, Victoria, Valentin Loux, and Pierre Renault. 2012. “Genome Sequence of *Lactococcus Raffinolactis* Strain 4877, Isolated from Natural Dairy Starter Culture.” *Journal of Bacteriology* 194 (22): 6364–6364. <https://doi.org/10.1128/JB.01697-12>.
- Müller, Eva, Helmut Hotzel, Christine Ahlers, Ingrid Hänel, Herbert Tomaso, and Mostafa Y. Abdel-Glil. 2020. “Genomic Analysis and Antimicrobial Resistance of *Aliarcobacter Cryaerophilus* Strains From German Water Poultry.” *Frontiers in Microbiology* 11: 1549. <https://doi.org/10.3389/fmicb.2020.01549>.

- Nordgård, Anna Synnøve Røstad, Wenche Hennie Bergland, Olav Vadstein, Vladimir Mironov, Rune Bakke, Kjetill Østgaard, and Ingrid Bakke. 2017. “Anaerobic Digestion of Pig Manure Supernatant at High Ammonia Concentrations Characterized by High Abundances of Methanosaeta and Non-Euryarchaeotal Archaea.” *Scientific Reports* 7 (1): 15077. <https://doi.org/10.1038/s41598-017-14527-1>.
- Nozhevnikova, Alla N., Valeria Nekrasova, Adrian Ammann, Alexander J.B. Zehnder, Bernhard Wehrli, and Christof Holliger. 2007. “Influence of Temperature and High Acetate Concentrations on Methanogenesis in Lake Sediment Slurries.” *FEMS Microbiology Ecology* 62 (3): 336–44. <https://doi.org/10.1111/j.1574-6941.2007.00389.x>.
- Oren, Aharon. 2014. “The Family Methanocorpusculaceae.” In *The Prokaryotes: Other Major Lineages of Bacteria and The Archaea*, edited by Eugene Rosenberg, Edward F. DeLong, Stephen Lory, Erko Stackebrandt, and Fabiano Thompson, 225–30. Berlin, Heidelberg: Springer Berlin Heidelberg. https://doi.org/10.1007/978-3-642-38954-2_314.
- Pan, Xiaofang, Lixin Zhao, Chunxing Li, Irimi Angelidaki, Nan Lv, Jing Ning, Guanqing Cai, and Gefu Zhu. 2021. “Deep Insights into the Network of Acetate Metabolism in Anaerobic Digestion: Focusing on Syntrophic Acetate Oxidation and Homoacetogenesis.” *Water Research* 190 (February): 116774. <https://doi.org/10.1016/j.watres.2020.116774>.
- Petropoulos, Evangelos, Jan Dolfing, Russell J. Davenport, Emma J. Bowen, and Thomas P. Curtis. 2017. “Developing Cold-Adapted Biomass for the Anaerobic Treatment of Domestic Wastewater at Low-temperatures (4, 8 and 15 °C) with Inocula from Cold Environments.” *Water Research* 112 (April): 100–109. <https://doi.org/10.1016/j.watres.2016.12.009>.

- Petropoulos, Evangelos, Burhan Shamurad, Shamas Tabraiz, Yongjie Yu, Russell Davenport, Thomas P. Curtis, and Jan Dolfing. 2021. "Sewage Treatment at 4 °C in Anaerobic Upflow Reactors with and without a Membrane – Performance, Function and Microbial Diversity." *Environmental Science: Water Research & Technology* 7 (1): 156–71. <https://doi.org/10.1039/D0EW00753F>.
- Rebac, S., J.B. van Lier, P. Lens, A.J.M. Stams, F. Dekkers, K.Th.M. Swinkels, and G. Lettinga. 1999. Psychrophilic Anaerobic Treatment of Low Strength Wastewaters. Vol. 39. *Water Science and Technology*. [https://doi.org/10.1016/S0273-1223\(99\)00103-1](https://doi.org/10.1016/S0273-1223(99)00103-1).
- Rebac, Salih, Julia Ruskova, Sybren Gerbens, Jules B. van Lier, Alfons J.M. Stams, and Gatzke Lettinga. 1995. "High-Rate Anaerobic Treatment of Wastewater under Psychrophilic Conditions." *Journal of Fermentation and Bioengineering* 80 (5): 499–506. [https://doi.org/10.1016/0922-338X\(96\)80926-3](https://doi.org/10.1016/0922-338X(96)80926-3).
- Safitri, Anissa Sukma, Krista M. Kaster, and Roald Kommedal. n.d. "Effect of Low-temperature and Municipal Wastewater Organic Loading on UASB System Performance." *In Preparation*.
- Samonis, G., D. E. Karageorgopoulos, D. P. Kofteridis, D. K. Matthaïou, V. Sidiropoulou, S. Maraki, and M. E. Falagas. 2008. "Citrobacter Infections in a General Hospital: Characteristics and Outcomes." *European Journal of Clinical Microbiology & Infectious Diseases* 28 (1): 61. <https://doi.org/10.1007/s10096-008-0598-z>.
- Smith, A. L., S. J. Skerlos, and L. Raskin. 2015. "Anaerobic Membrane Bioreactor Treatment of Domestic Wastewater at Psychrophilic Temperatures Ranging from 15 °C to 3 °C." *Environmental Science: Water Research & Technology* 1 (1): 56–64. <https://doi.org/10.1039/C4EW00070F>.
- Smith, Adam L., Steven J. Skerlos, and Lutgarde Raskin. 2012. "Psychrophilic Anaerobic Membrane Bioreactor Treatment of Domestic Wastewater." *Water Research*. <https://doi.org/10.1016/j.watres.2012.12.028>.

- Söllinger, Andrea, and Tim Urich. 2019. "Methylotrophic Methanogens Everywhere — Physiology and Ecology of Novel Players in Global Methane Cycling." *Biochemical Society Transactions* 47 (6): 1895–1907. <https://doi.org/10.1042/BST20180565>.
- Sun, Liwei, Mayu Toyonaga, Akiko Ohashi, Dieter M. Turlousse, Norihisa Matsuura, Xian-Ying Meng, Hideyuki Tamaki, et al. 2016. "Lentimicrobium Saccharophilum Gen. Nov., Sp. Nov., a Strictly Anaerobic Bacterium Representing a New Family in the Phylum Bacteroidetes, and Proposal of Lentimicrobiaceae Fam. Nov." *International Journal of Systematic and Evolutionary Microbiology* 66 (7): 2635–42. <https://doi.org/10.1099/ijsem.0.001103>.
- Ueki, Atsuko, Hiroshi Akasaka, Daisuke Suzuki, and Katsuji Ueki. 2006. "Paludibacter Propionicigenes Gen. Nov., Sp. Nov., a Novel Strictly Anaerobic, Gram-Negative, Propionate-Producing Bacterium Isolated from Plant Residue in Irrigated Rice-Field Soil in Japan." *International Journal of Systematic and Evolutionary Microbiology*. Microbiology Society. <https://doi.org/10.1099/ijs.0.63896-0>.
- Ueki, Atsuko, Kazushi Goto, Nobuo Kaku, and Katsuji Ueki. 2018. "Aminipila Butyricea Gen. Nov., Sp. Nov., a Strictly Anaerobic, Arginine-Decomposing Bacterium Isolated from a Methanogenic Reactor of Cattle Waste." *International Journal of Systematic and Evolutionary Microbiology*. Microbiology Society. <https://doi.org/10.1099/ijsem.0.002534>.
- Urai, Makoto, Tomoko Aizawa, Yasuyoshi Nakagawa, Mutsuyasu Nakajima, and Michio Sunairi. 2008. "Mucilaginibacter Kameinonensis Sp., Nov., Isolated from Garden Soil." *International Journal of Systematic and Evolutionary Microbiology*. Microbiology Society. <https://doi.org/10.1099/ijs.0.65777-0>.

- Varsadiya, Milan, Tim Urich, Gustaf Hugelius, and Jiří Bárta. 2021. "Microbiome Structure and Functional Potential in Permafrost Soils of the Western Canadian Arctic." *FEMS Microbiology Ecology*, no. fiab008 (January). <https://doi.org/10.1093/femsec/fiab008>.
- Venil, Chidambaram Kulandaisamy, Nordiana Nordin, Zainul Akmar Zakaria, and Wan Azlina Ahmad. 2014. "Chryseobacterium Artocarpi Sp. Nov., Isolated from the Rhizosphere Soil of Artocarpus Integer." *International Journal of Systematic and Evolutionary Microbiology*. Microbiology Society. <https://doi.org/10.1099/ijs.0.063594-0>.
- Verté, F., V. Kostanjevecki, L. de Smet, T. E. Meyer, M. A. Cusanovich, and J. J. van Beeumen. 2002. "Identification of a Thiosulfate Utilization Gene Cluster from the Green Phototrophic Bacterium *Chlorobium limicola*." *Biochemistry* 41 (9): 2932–45. <https://doi.org/10.1021/bi011404m>.
- Wu, Pei-Hsun, Kok Kwang Ng, Pui-Kwan Andy Hong, Ping-Yi Yang, and Cheng-Fang Lin. 2017. "Treatment of Low-Strength Wastewater at Mesophilic and Psychrophilic Conditions Using Immobilized Anaerobic Biomass." *Chemical Engineering Journal* 311 (March): 46–54. <https://doi.org/10.1016/j.cej.2016.11.077>.
- Yang, Sizhong, Susanne Liebner, Matthias Winkel, Mashal Alawi, Fabian Horn, Corina Dörfer, Julien Ollivier, et al. 2017. "In-Depth Analysis of Core Methanogenic Communities from High Elevation Permafrost-Affected Wetlands." *Soil Biology and Biochemistry* 111 (August): 66–77. <https://doi.org/10.1016/j.soilbio.2017.03.007>.
- Yang, Zhiman, Rongbo Guo, Xiaoshuang Shi, Shuai He, Lin Wang, Meng Dai, Yanling Qiu, and Xiaoxiao Dang. 2016. "Bioaugmentation of *Hydrogenispora ethanolica* LX-B Affects Hydrogen Production through Altering Indigenous Bacterial

Community Structure.” *Bioresource Technology* 211 (July): 319–26. <https://doi.org/10.1016/j.biortech.2016.03.097>.

Zhang, Dongdong, Wanbin Zhu, Can Tang, Yali Suo, Lijuan Gao, Xufeng Yuan, Xiaofen Wang, and Zongjun Cui. 2012. “Bioreactor Performance and Methanogenic Population Dynamics in a Low-Temperature (5–18°C) Anaerobic Fixed-Bed Reactor.” *Bioresource Technology* 104 (January): 136–43. <https://doi.org/10.1016/j.biortech.2011.10.086>.

Zhang, Lei, Jo de Vrieze, Tim L.G. Hendrickx, Wei Wei, Hardy Temmink, Huub Rijnaarts, and Grietje Zeeman. 2018. “Anaerobic Treatment of Raw Domestic Wastewater in a UASB-Digester at 10 °C and Microbial Community Dynamics.” *Chemical Engineering Journal* 334 (February): 2088–97. <https://doi.org/10.1016/j.cej.2017.11.073>.

Supplementary Document

1. Similarity matrices for OTUs (Weighted UniFrac)

Table S1 Similarity matrices for OTUs (Weighted UniFrac) in granule samples in UASB reactor A and B

Reactor	Reactor	A	B	A	B	A	B	A	B	A	B	A	B	A	B	B
	T (°C)	12	12	12	12	8.5	8.5	8.5	8.5	8.5	8.5	5.5	5.5	5.5	5.5	5.5
	OLR (gCOD·l ⁻¹ ·d ⁻¹)	8	8	15	15	3	3	8	8	15	15	3	3	15	15	3
A	12°C; 8	1.00	0.69	0.67	0.66	0.63	0.61	0.64	0.53	0.56	0.57	0.58	0.59	0.55	0.57	0.55
B	12°C; 8	0.69	1.00	0.66	0.66	0.65	0.63	0.63	0.57	0.58	0.59	0.59	0.60	0.56	0.58	0.55
A	12°C; 15	0.67	0.66	1.00	0.68	0.62	0.59	0.66	0.53	0.58	0.61	0.59	0.63	0.57	0.61	0.56
B	12°C; 15	0.66	0.66	0.68	1.00	0.61	0.59	0.64	0.52	0.56	0.60	0.57	0.61	0.55	0.59	0.55
A	8.5°C; 3	0.63	0.65	0.62	0.61	1.00	0.67	0.60	0.63	0.56	0.57	0.57	0.58	0.56	0.55	0.55
B	8.5°C; 3	0.61	0.63	0.59	0.59	0.67	1.00	0.59	0.64	0.58	0.57	0.58	0.59	0.56	0.55	0.55
A	8.5°C; 8	0.64	0.63	0.66	0.64	0.60	0.59	1.00	0.53	0.58	0.62	0.59	0.62	0.56	0.59	0.55
B	8.5°C; 8	0.53	0.57	0.53	0.52	0.63	0.64	0.53	1.00	0.56	0.54	0.55	0.55	0.55	0.50	0.53
A	8.5°C; 15	0.56	0.58	0.58	0.56	0.56	0.58	0.58	0.56	1.00	0.64	0.64	0.64	0.60	0.58	0.60
B	8.5°C; 15	0.57	0.59	0.61	0.60	0.57	0.57	0.62	0.54	0.64	1.00	0.63	0.67	0.59	0.63	0.59
A	5.5°C; 3	0.58	0.59	0.59	0.57	0.57	0.58	0.59	0.55	0.64	0.63	1.00	0.71	0.63	0.62	0.61
B	5.5°C; 3	0.59	0.60	0.63	0.61	0.58	0.59	0.62	0.55	0.64	0.67	0.71	1.00	0.63	0.67	0.64
A	5.5°C; 15	0.55	0.56	0.57	0.55	0.56	0.56	0.56	0.55	0.60	0.59	0.63	0.63	1.00	0.62	0.63

B	5.5°C; 15	0.57	0.58	0.61	0.59	0.55	0.55	0.59	0.50	0.58	0.63	0.62	0.67	0.62	1.00	0.64
B	5.5°C; 3	0.55	0.55	0.56	0.55	0.55	0.55	0.55	0.53	0.60	0.59	0.61	0.64	0.63	0.64	1.00

2. UPGMA tree

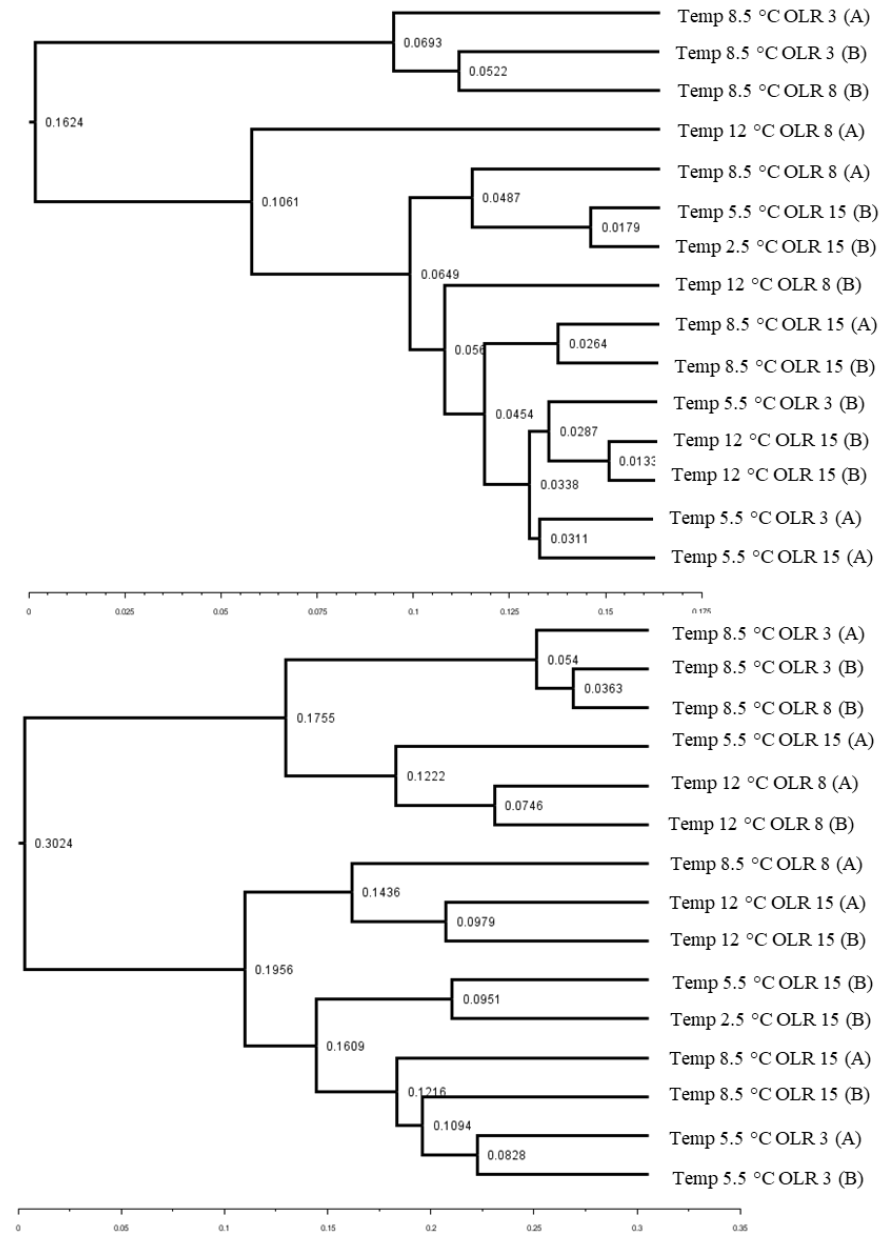


Figure S2 UPGMA tree bacterial (top) and archaeal (bottom) community in granule samples in UASB reactor A and B

3. Wastewater sequencing data

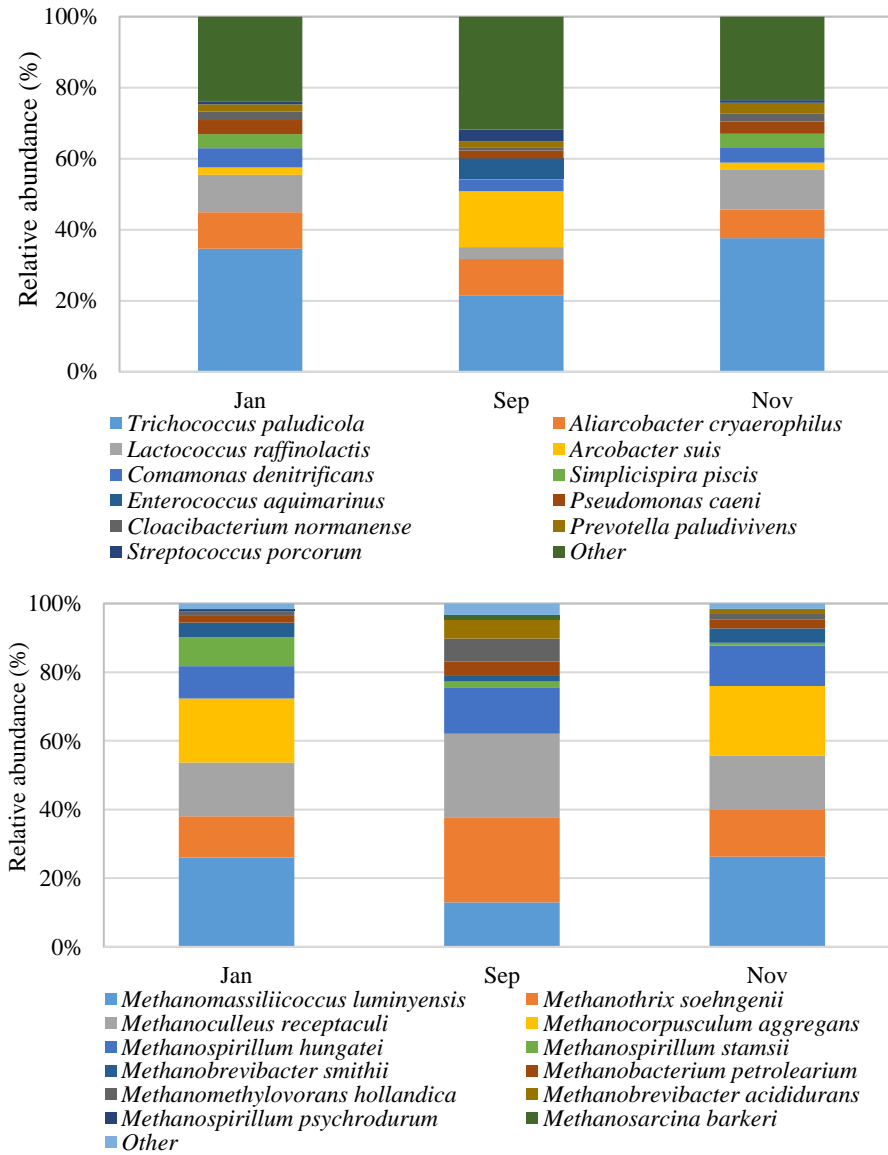


Figure S3 Relative abundances of pre-dominant bacterial (top) and archaeal (bottom) population at species level in Grødaland wastewater at three different time points (January, September, and November).

Appendix 3 – Paper III

Engineered methanotrophic syntrophy in photogranule communities removes dissolved methane. Anissa Sukma Safitri, Jérôme Hamelin, Roald Kommedal, and Kim Milferstedt. Published in Water Research X journal, <https://doi.org/10.1016/j.wroa.2021.100106>.

Engineered methanotrophic syntrophy in photogranule communities removes dissolved methane

Anissa Sukma Safitri^a, Jérôme Hamelin^b, Roald Kommedal^a, and Kim Milferstedt^{b*}

^aDepartment of Chemistry, Bioscience and Environmental Engineering, University of Stavanger, 4036 Stavanger, Norway

^bINRAE, Univ Montpellier, LBE, 102 Avenue des Etangs, 11100, Narbonne, France

*Corresponding author. Email address: kim.milferstedt@inrae.fr

Abstract

The anaerobic treatment of wastewater leads to the loss of dissolved methane in the effluent of the treatment plant, especially when operated at low-temperatures. The emission of this greenhouse gas may reduce or even offset the environmental gain from energy recovery through anaerobic treatment. We demonstrate here the removal and elimination of these comparably small methane concentrations using an ecologically engineered methanotrophic community harbored in oxygenic photogranules. We constructed a syntrophy between methanotrophs enriched from activated sludge and cyanobacteria residing in photogranules and maintained it over a two-month period in a continuously operated reactor. The novel community removed dissolved methane during stable reactor operation by on average $84.8 \pm 7.4\%$ (\pm standard deviation) with an average effluent concentration of dissolved methane of $4.9 \pm 3.7 \text{ mg CH}_4 \cdot \text{l}^{-1}$. The average methane removal rate was $26 \text{ mg CH}_4 \cdot \text{l}^{-1} \cdot \text{d}^{-1}$, with an observed combined biomass yield of $2.4 \text{ g VSS} \cdot \text{g CH}_4^{-1}$. The overall COD balance closed at around 91%. Small photogranules removed methane more efficiently than larger

photogranule, likely because of a more favorable surface to volume ratio of the biomass. MiSeq amplicon sequencing of 16S and 23S rRNA revealed a potential syntrophic chain between methanotrophs, non-methanotrophic methylotrophs and filamentous cyanobacteria. The community composition between individual photogranules varied considerably, suggesting cross-feeding between photogranules of different community composition. Methanotrophic photogranules may be a viable option for dissolved methane removal as anaerobic effluent post-treatment.

Keywords:

Dissolved methane; interactions; bioaugmentation; ecological engineering; effluent polishing; anaerobic digestion

1. Introduction

The use of anaerobic granulated biomass for biological wastewater treatment was introduced about 40 years ago (Lettinga et al., 1980), and is now regarded an adequate methodology for municipal wastewater treatment (Seghezzi et al., 1998) and energy recovery (Gao et al., 2014). The development of anaerobic wastewater treatment since the end of the 1990s has been considered a more sustainable alternative to traditional aerobic processes, especially for high strength wastewater. Its primary purpose is the conversion of organic matter to methane as a renewable form of energy (Vandevivere, 1999; Verstraete et al., 1996).

An often-overlooked drawback of anaerobic wastewater treatment is the loss of dissolved methane as not all of it partitions to the gas phase inside the digesters. Estimations of the loss of dissolved methane from anaerobic wastewater treatment are typically calculated from methane concentrations in the gaseous headspace using Henry's Law, i.e., under equilibrium conditions (Lobato et al., 2012). This idealized case does not

always reflect the actual measured values of anaerobic treatment liquid effluent as mass-transfer limitations can lead to supersaturation of methane. In this case, an assumed equilibrium with headspace concentrations will thus underestimate the dissolved methane content. Souza et al. (2011) and Wu et al. (2017) found that dissolved methane was supersaturated in the liquid phase of an anaerobic bioreactor effluent (saturation factor of 1.03 - 1.67), increasing with the increased methane solubility at decreasing temperatures. Even at equilibrium, considerable amounts of methane are lost with the liquid effluent, especially when treating wastewater at low-temperatures and/or in high-flow through situations (low hydraulic retention time) (Brandt et al., 2019). Once the effluent is discharged and exposed to ambient methane partial pressures, methane degasses into the atmosphere.

Theoretically, 0.38 liters of methane are produced per gram of chemical oxygen demand (COD) removed from the anaerobic wastewater treatment at standard ambient condition (25 °C, 1 atm) (Tchobanoglous et al., 2003). By assuming 80% COD removal efficiency for a typical high-strength municipal wastewaters with an average soluble COD concentration of 450 g·m⁻³ (Henze et al., 2008), 137 l CH₄·m⁻³ is produced, equivalent to 89.7 g CH₄·m⁻³. At a methane solubility of approximately 20 g·m⁻³ at 25 °C (Liu et al., 2014), approximately 22% of all produced methane would be in its dissolved form and likely leave the digester. At most about 107 l CH₄·m⁻³ could be used for combustion, saving fossil CO₂ emissions of 107 l CO₂·m⁻³. Degassing of the dissolved methane to the atmosphere, however, would contribute approximately 500 g CO₂ equiv·m⁻³, equivalent to 278 l CO₂·m⁻³. Therefore, the greenhouse gas contribution in this example is about 2.5 times greater than the positive effects from generating a renewable energy (see Supplemental Materials). This methane loss is significantly reducing and, as in the given example, even offsetting the positive effect of energy recovery from anaerobic wastewater treatment. Therefore, a post-treatment process is required to remove dissolved methane, reducing the

environmental impact of anaerobic wastewater treatment. Several methods have been proposed for removing or recovering dissolved methane from anaerobic effluents. These include air stripping oxidation (Hatamoto et al., 2010; Matsuura et al., 2015) and degassing membrane-based recovery (Bandara et al., 2011; Cookney et al., 2016).

Dissolved methane can be biologically oxidized by methanotrophs. Methanotrophs are part of a larger group of bacteria called methylotrophs that typically utilize single-carbon compounds like methane, methanol, formic acid or even formaldehyde as carbon and energy source (Chistoserdova et al., 2009). Methanotrophs may fully oxidize methane to CO₂ or partially to molecules like methanol. Molecular oxygen is required for the conversion. Through the coupled activities of eukaryotic algae or photosynthetic bacteria and methanotrophs in syntrophic bioaggregates, oxygen may be provided by direct, or at least local transfer. The produced oxygen is then immediately utilized by the methanotrophs to convert organic matter to CO₂ which is in turn used by phototrophs for autotrophic CO₂ fixation. These interactions are found in natural systems, for example, at the chemocline between anaerobic and aerobic water layers in freshwater lakes (Milucka et al., 2015), and are also utilized in engineered systems, e.g., by van der Ha et al. (2012) for the production of lipids or polyhydroxy butyrate using co-cultured eukaryotic algae and methanotrophs. Rasoulie et al. (2018) also investigated a co-culture of green microalgae and methanotrophs for removing methane and recovering nutrients. They used industrial wastewater as media and synthetic biogas as methane source. In both studies, the authors used pure cultures of methanotrophs and microalgae (Rasouli et al., 2018; van der Ha et al., 2012). In nature, methanotrophs often co-occur with non-methanotrophic methylotrophs that feed on partially oxidized methane intermediates like methanol (Takeuchi et al., 2019; Yu et al., 2017). These more complex interactions are also relevant in our study using an environmental enrichment as basis for the construction of a new syntrophy.

In contrast to studies using suspended phototrophic-methanotrophic consortia, we present here an aggregated biomass in the form of photogranules for the aeration-free removal of dissolved methane. The conversion relies on syntrophic interactions between phototrophic cyanobacteria and methanotrophic bacteria aggregated in oxygenic photogranules. Aggregation is particularly important in the bioprocesses as it allows efficient and fast removal of the biomass from the treated water and efficient intra-aggregate oxygen transfer. We established the presence of methanotrophic bacteria in the photogranule aggregates and propagated the newly developed syntrophy in an open community, challenged by invading microbes. The syntrophy was ecologically engineered from an enrichment culture of methanotrophs from activated sludge and oxygenic photogranules converting synthetic wastewater, as described in Milferstedt et al. (2017). We discuss community assembly in the light of performance characteristics of a continuously operated reactor system for the removal of dissolved methane.

2. Materials and Methods

2.1. Media composition

The media composition for the batch experiments (i.e., enrichment and size specific analysis) and for the continuously operated reactor were identical, a modified nitrate mineral salt (NMS) solution (Whittenbury et al., 1970). The nutrient content of the NMS media was modified by increasing the phosphate concentration and replacing nitrate with ammonium as nitrogen sources to mimic effluents from anaerobic processes. The media was prepared and diluted with tap water which naturally containing approximately 4 mM as bicarbonate (HCO_3^-). The final concentrations in the feed were as following: 150 $\text{mg}\cdot\text{l}^{-1}$ of NH_4Cl , 20 $\text{mg}\cdot\text{l}^{-1}$ of $\text{MgSO}_4\cdot 7\text{H}_2\text{O}$, 4 $\text{mg}\cdot\text{l}^{-1}$ of $\text{CaCl}_2\cdot 6\text{H}_2\text{O}$, 5.44 $\text{mg}\cdot\text{l}^{-1}$ of KH_2PO_4 , 12.2 $\text{mg}\cdot\text{l}^{-1}$ of K_2HPO_4 , 5 $\text{mg}\cdot\text{l}^{-1}$ of FeCl_3 , 20 $\text{mg}\cdot\text{l}^{-1}$ of disodium EDTA, 0.03 $\text{ml}\cdot\text{l}^{-1}$ of HCl . From a stock solution, we added 1 $\text{ml}\cdot\text{l}^{-1}$ of

trace elements resulting in concentrations of 10 mg·l⁻¹ of disodium EDTA, 0.2 mg·l⁻¹ of ZnSO₄·7H₂O, 0.06 mg·l⁻¹ of MnCl₂·4H₂O, 0.6 mg·l⁻¹ of H₃BO₃, 0.06 mg·l⁻¹ of Na₂MoO₄·2H₂O, 4 mg·l⁻¹ of FeSO₄·7H₂O, 0.04 mg·l⁻¹ of NiCl₂·6H₂O, 0.4 mg·l⁻¹ of CoCl₂·6H₂O, and 0.02 mg·l⁻¹ of CuSO₄·5H₂O.

2.2. Methanotrophic enrichment

Methanotrophs were enriched under batch conditions from municipal activated sludge from the wastewater treatment plant in Narbonne, France. We used 160 ml serum bottles with 50 ml as liquid volume of the media. To the media, 10 ml of inoculum were added so that a 100 ml gaseous headspace remained. Replicated enrichments (4-10 replicates) were incubated either with or without mixing using magnetic stirring. We also enriched the activated sludge mixed with fresh oxygenic photogranules, and oxygenic photogranules only without mixing.

For all enrichments, the serum bottles were sealed with rubber stoppers and capped using aluminum crimp caps. The headspace gas was mixed prior to the gas injection by combining 30 vol % CH₄ and 70 vol-% O₂. During the injection, a pressure of 1.49±0.05 bar (±standard deviation) was achieved in the serum bottle headspace. The pressure was manually confirmed using a handheld manometer (Keller Leo 2, Switzerland). We used purified methane for feeding from biogas produced in two laboratory-scale anaerobic digesters. This was done using a CO₂-absorbing bubble column containing NaOH at 3 M. The final methane concentration was on average 98.1±2.3% (±standard deviation). Pure oxygen was used.

The serum bottles were incubated at room temperature. Using a serological pipette, a volume of 20 ml of the methanotroph enrichment culture was transferred every five to seven days into a new serum bottle containing 40 ml of fresh media. After each transfer, the headspace was renewed with a fresh CH₄ and O₂ mixture (30%/70%) at approximately 1.5 bar. After a third transfer, i.e., after about 21 days, we observed

decreasing oxygen and methane concentrations in the headspace of several bottles. From that point on, in all bottles, a mix of methane and oxygen (30%/70%) was added on a daily basis. After the fourth transfer, we harvested the enriched suspended methanotrophic cultures and transferred them to five new serum bottles with fresh media and approximately ten oxygenic photogranules, each, with an approximate average diameter of 1-2 mm. The untreated, fresh oxygenic photogranules were obtained from a continuously operated reactor. To the methanotroph enrichment and oxygenic photogranules, we added 100% methane in the headspace, assuming that oxygen would be provided by photosynthesis. Bottles were incubated on a shaker that was equipped with fluorescent light bulbs providing photoactive radiation (PAR) at approximately $58 \mu\text{mol}\cdot\text{m}^{-2}\cdot\text{s}^{-1}$. PAR was measured at the outside of the flasks using a light meter LI-250A (LI-COR, USA). After one week, the active methanotrophic photogranules were separated from the suspended biomass and rinsed. Photogranules were rinsed using deionized water before the final transfer into the continuous reactor to avoid suspended and loosely attached biomass. Only the solid photogranule biomass was used to inoculate the continuous reactor.

2.3. Set-up and operation of continuous reactor

Approximately 60 active methanotrophic photogranules were transferred to an air-tight glass vessel with 1.8 l of liquid volume, operated as a continuously stirred tank reactor. Figure 1 shows a schematic view of the reactor set-up. We used overhead mixing as this type of agitation does not impact photogranules stability. The use of magnetic stir bar resulted in gradually crushing photogranules (Milferstedt et al., 2017). We used an air-tight overhead magnetic stirrer head of the g-mrk ptfe type with a ground joint (Bola Bohlender GmbH, Germany), connected to an overhead motor using a polyoxymethylene globe stirrer coupling (Bola Bohlender GmbH, Germany). The coupling compensates potential misalignment between the overhead motor and the magnetic stirrer head.

The reactor vessel was a borosilicate glass beaker with a glass flat flange lid containing one central and three angled ground necks.

Mixing was provided by a stainless-steel impeller operated at 100 rpm during the first 30 days of reactor operation, increased to 125-128 rpm on day 31 for the remainder of the experiment. Light was provided using standard $60 \times 60 \text{ cm}^2$ LED panels emitting warm white at 4000K. A light intensity of approximately $45 \mu\text{mol}\cdot\text{m}^{-2}\cdot\text{s}^{-1}$ PAR was measured at the outside of the vertical reactor surface. The reactor was operated at an average room temperature of $23.2 \pm 1.0 \text{ }^\circ\text{C}$ (\pm standard deviation) without active temperature control. The dissolved oxygen concentration in the reactor fluctuated with an average $1.8 \pm 3.2 \text{ mg}\cdot\text{l}^{-1}$. High oxygen concentrations were observed to be a consequence of membrane fouling of the electrode membrane. The average pH in the reactor was 7.0 ± 0.2 .

Initially, all headspace compartments and the experimental set-up (e.g., tubings and fittings) were flushed with nitrogen and methane (92/8 vol/vol) before the start of operation. As the supply of biogenic purified methane was limited, pure nitrogen (100%) was used for flushing the headspace during routine reactor operation, e.g., after manual interventions for cleaning and biomass removal. After start-up, methane-saturated feed was continuously pumped into the reactor. The reactor was operated at a hydraulic retention time of 12 h. The media contained on average $17.6 \pm 2.2 \text{ mg CH}_4\cdot\text{l}^{-1}$ (\pm standard deviation) and the volumetric organic loading rate was approximately $35.1 \pm 4.5 \text{ mg CH}_4\cdot\text{l}^{-1}\cdot\text{d}^{-1}$.

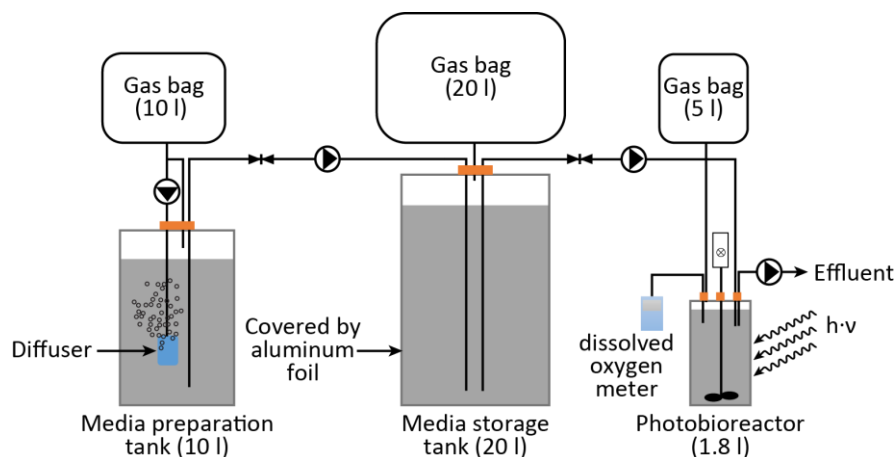


Figure 1 Presentation of the continuous reactor set-up. The gas bag connected to the media preparation tank was used as methane reservoir during the preparation of methane-saturated batches of media. The finished media batches were transferred to the media storage tank, from where it was continuously pumped into the reactor. The gas bag connected to media storage equilibrated pressure changes resulting from filling and emptying the tank. The gas bag connected to the reactor equilibrated potential pressure changes in the reactor.

2.4. Media preparation

As mentioned in Chapter 2.1, the initial media composition for the continuously operated reactor was identical with the batch experiments. Media was prepared in an O₂- and CO₂-free closed atmosphere obtained by initially sparging the preparation system with nitrogen gas for approximately 15 min until the dissolved oxygen concentration measured with a handheld oxygen meter (Multi 3620 IDS, WTW, Germany) was below the detection limit. This precaution was taken to limit the supply with externally provided CO₂ and oxygen, so that growth of methanotrophs and phototrophs in the reactor could be linked to their respective metabolic activities. Then, the media was saturated with purified methane by recirculating methane through the solution using a diaphragm pump and porous diffusers. This step took around six hours. The media was then transferred using gas-tight tubing and a peristaltic pump into the 20 l media storage tank. A capacity of 20 l ensured

autonomy for a 72 h period. Media preparation and media storage were physically separated in two bottles to assure continuous feeding during media preparation. One batch of methane saturated media had a maximum volume of 10 l, limited by laboratory safety consideration. The long preparation was mostly due to slow gas transfer from the methane atmosphere to the aqueous phase.

2.5. Photogranule size analysis

We quantified the total number of all photogranules in the reactor and their size distribution based on equivalent diameters. For this, we temporarily placed the entire content of the reactor on a custom-built square tray with a transparent glass bottom ($17.7 \times 17.6 \text{ cm}^2$) that was then placed on the glass surface of a desktop scanner (Canon LiDE 220, Japan). An image of the photogranules through the bottom of the tray was acquired with the dimensions of 5583×5556 pixels and saved as a non-compressed 8-bit gray-level tagged image format (tif) file. Care was taken to avoid overlap or contact between individual photogranules as this would have made the subsequent image analysis more complicated. With increasing numbers of photogranules in the reactor, photogranules were partitioned into several batches and multiple images were acquired. Using a custom-made script in ImageJ (Schneider et al., 2012), we then used the maximum entropy thresholding algorithm to differentiate photogranules from the background. Using the MorphoLibj plugin (Legland et al., 2016), noise was removed on the images by applying the morphological operation “opening” with a radius of 1. White pixels within apparent particles on the images were filled using the “fill holes” command. Particles in contact with the image boundaries were removed using the “kill borders” command to avoid counting particles that were not entirely visible on the images. The area of each detected object was then quantified and translated into the equivalent diameter of an assumed perfect circle with the same area.

2.6. Analytical methods

Gaseous samples were withdrawn from the headspace of enrichment cultures and the reactor using gas-tight syringes (SGE-Europe). Subsequently, samples were analyzed using gas chromatography (Perkin Elmer GC580, USA) for determination the concentration of CH₄, N₂, CO₂ and O₂. The GC was equipped with a thermal conductivity detector (RT-MSieve 5A column, 0.32 mm diameter, 30 m length and 30 μm film). Helium was used as the carrier gas at a flow rate of 35.4 ml·min⁻¹. The oven temperature was 60 °C. Dissolved methane was determined by converting the dissolved COD measurement by multiplying with the specific COD equivalent of methane: 4 g COD·g CH₄⁻¹. Total and dissolved COD were determined daily using standard COD test kits with a detection range of 0-150 mg·l⁻¹ (Aqualytic, Germany). The influent and effluent samples were withdrawn using a 5 ml syringe containing no gas phases. The samples were immediately and directly filtered through a 0.45 μm PTFE hydrophilic membrane syringe filter into a COD test kit and sealed immediately. Speedy sample handling and processing ensured reliable measurements of dissolved methane. Total COD measurement was conducted without filtering the sample. We compensated for any background COD by measuring blank COD concentrations in the ready-made media before methane equilibration, and then subtract that from all consecutive COD measurements made at the reactor inlet and outlet. COD compensation was done to account for any compounds in the media with a potential contribution to COD, notably EDTA. Total suspended solid (TSS) was measured following standard methods 2540D after the filtered samples (Pre-weighted Glass Fiber Filter, pore size 0.45 μm, diameter 47 mm, 934-AH RTU, Whatman, UK) dried at 105 °C for 1 h (Rice et al., 2013). Samples were taken in duplicates for each gas, COD and TSS measurement.

2.7. Observed biomass yield

The overall observed biomass yield was determined based on the ratio of cumulative generated biomass (g TSS) per cumulative consumed substrate (g CH₄). Assuming 15% inorganic biomass fraction, the cumulative generated biomass in the unit of g TSS is converted to the unit of g VSS. The consumed substrate (g CH₄) was measured daily as COD removed by the system. The cumulative generated biomass consists of the accumulated biomass in the system, cumulative biomass wastage, and biomass effluent. The accumulated biomass and biomass wastage were measured weekly while doing cleaning and maintenance. In addition, the suspended biomass in the effluent was measured daily. We calculated the specific COD of TSS using linear-regression analysis (Chon et al., 2011).

2.8. Dependence of methanotrophic activity on photogranules size

When assuming phototropic methane conversion to be a surface-depending process, photogranule size may influence the specific phototropic and methanotrophic activities by affecting surface to volume ratios and diffusional lengths. We analyzed the specific metabolic activity in batch experiments in serum bottles under the same conditions as during the enrichment experiments. We prepared a serum bottle per size class containing on average six similar-sized photogranules. Photogranules were sampled during stable reactor performance on day 29, 57, 72, 79, 86, and 97. For each test, three size classes, 1.0 – 2.2 mm, 2.3 – 3.7 mm, and 3.8 – 5.5 mm, were defined.

2.9. Microbial analysis

Photogranules were sampled for community analysis (1) before contact with methanotrophic enrichments (samples named ‘background’), (2) after incubation with methanotrophic enrichments (samples named ‘inoculum’) and (3) during continuous operation of the reactor (samples named ‘continuous reactor operation’). Sampled photogranules were

stored at $-20\text{ }^{\circ}\text{C}$ for subsequent DNA extraction. DNA was extracted using the DNeasy PowerWater Kit (Qiagen, Germany), according to the manufacturer's instructions. The genomic DNA was used in two independent MiSeq sequencing reactions for 16S rRNA amplicons and 23S rRNA amplicons.

The 16S rRNA amplicons were generated using the primer pair 515F (5'-GTGYCAGCMGCCGCGTA-3') and 928R (5'-CCCGYCAATTCMTTTRAGT-3') (Wang & Qian, 2009) plus their respective linkers. The primers target the V4-V5 hypervariable regions of the 16S rRNA gene. They amplify most of the bacterial and archaeal known diversity. The PCR mixtures (50 μl) contained 0.5 U of MTP™ Taq DNA Polymerase (Sigma-Aldrich, Germany) with its corresponding buffer, 200 mM of each dNTP, 0.5 mM of each primer, and 10 ng of genomic DNA. Reactions were performed in a Mastercycler thermal cycler (Eppendorf, Germany) as follows: $95\text{ }^{\circ}\text{C}$ for 2 min, followed by 30 cycles of $95\text{ }^{\circ}\text{C}$ for 1 min, $65\text{ }^{\circ}\text{C}$ for 1 min, and $72\text{ }^{\circ}\text{C}$ for 1 min, with a final extension at $72\text{ }^{\circ}\text{C}$ for 10 min.

The 23S rRNA amplicons were generated using the primers pair p23SrV_f1 (5'-GGACAGAAAGACCCTATGAA-3') and p23SrV_r1 (5'-TCAGCCTGTTATCCCTAGAG-3') (Sherwood & Presting, 2007) plus their respective linkers. This primer pair targets a region in the 23S rRNA of cyanobacteria and plastids in algae. The 50 μl PCR mixtures contained 0.5 U of MTP™ Taq DNA Polymerase (Sigma-Aldrich, Germany) with its corresponding buffer, 200 mM of each dNTP, 0.3 mM of each primer, and 10 ng of genomic DNA. Reactions were performed in a Mastercycler thermal cycler (Eppendorf, Germany) as follows: $94\text{ }^{\circ}\text{C}$ for 2 min, followed by 30 cycles of $94\text{ }^{\circ}\text{C}$ for 20 s, $59\text{ }^{\circ}\text{C}$ for 30 s, and $72\text{ }^{\circ}\text{C}$ for 30 s, with a final extension at $72\text{ }^{\circ}\text{C}$ for 10 min. The respective lengths of the PCR products were quality-checked using a Bioanalyzer 2100 (Agilent, USA).

In a second PCR of 12 cycles, an index sequence was added, and the resulting PCR products were purified and loaded onto the Illumina MiSeq cartridge according to the manufacturer's instructions for sequencing of paired 300 bp reads (v3 chemistry). Library preparation and sequencing was done at the GeT PlaGe Sequencing Center of the Genotoul Lifescience Network in Toulouse, France (<https://get.genotoul.fr/>). The datasets for this study can be found in the NCBI Sequence Read Archive (SRA) database as Bioproject PRJNA686893.

Sequences were dereplicated, quality checked, chimera checked and affiliated with a taxonomic description using Mothur version 1.42.3 (Schloss et al., 2009). Sequence treatment included preclustering at four differences in nucleotides over the length of the amplicon and chimera checking using uchime (Edgar et al., 2011). We removed all sequences that appeared less than three times in the entire dataset. The databases SILVA (Quast et al., 2013) 132 SSU (16S rRNA) and 132 LSUref (23S rRNA) were used for alignment and as taxonomic outline.

Cleaned up and taxonomically affiliated sequence data was written into a biom file and was subsequently merged with the environmental data and analyzed in R version 4.0.3 (R Core Team, 2020) using the R packages phyloseq (McMurdie & Holmes, 2013) and tidyverse (Wickham et al., 2019). For the 16S rRNA amplicons, we removed the sequences affiliated with cyanobacteria using subset_sample command in phyloseq with the argument `!(Phylum == "Cyanobacteria")`. For the 23S data, we separated the chloroplast sequences from cyanobacteria using the same command with the argument `(Phylum == "Cyanobacteria" & !(Order == "Chloroplast"))`.

On average, the 16S rRNA amplicons contained 50600 ± 7300 (\pm standard deviation) bacterial sequences per sample, of which on average 17100 ± 7500 were not cyanobacteria. Even though the 16S rRNA reverse primer supposedly excludes cyanobacterial sequences (Hodkinson &

Lutzoni, 2009), we nevertheless find them in high abundance, likely because of the overwhelming presence of cyanobacteria in the systems, with the exception of the activated sludge sample that only contained four sequences affiliated with phototrophs in the 16S amplicon. On average, the 23S rRNA amplicons contained 51700 ± 6700 sequences per sample, of which on average 1800 ± 1600 or $3.5 \pm 3.0\%$ were eukaryotic microalgae. The counts disregard the activated sludge sample that only contained 370 sequences affiliated with cyanobacteria in the 23S amplicon, however, in which we detected the highest absolute and relative counts of microalgae in this study.

Based on taxonomic outlines offered by the SILVA 132 SSU and LSU databases, we considered the following taxa detected in our amplicons as putative methanotrophic: the families Methylococcaceae (containing the genus *Methyloparacoccus*), Methylomonaceae (containing the genera *Methylomonas*, *Methylobacter*, *Methylomicrobium*, and *Methylosarcina*), and Beijerinckiaceae (containing *Methylocystis* and *Methylobacterium*). We considered as non-methanotrophic methylotrophs the genus *Methyloversatilis* of the family Rhodocyclaceae and the family Methylophilaceae (containing the genera *Methylophilus* and *Methylobacillus*).

3. Results and Discussions

3.1. Successful establishment of a syntrophic, methane-degrading community

Methanotrophs were enriched from activated sludge in gas-tight, stoppered serum bottles with a mixture of oxygen and methane in the headspace. We tested enrichments with and without mixing by magnetic stirring. After four transfers every five days into fresh media, all enrichments that were mixed during incubation removed methane and produced carbon dioxide according to the methane oxidation

stoichiometry, closing the mass balance by more than 80%. We detected methane removal in approximately half of statically incubated cultures (i.e., without mixing). Mixing increases methane transfer across the gas-liquid interface, leading to more successful incubations. The enrichments from unstirred oxygenic photogranules mixed with activated sludge removed methane. However, unstirred and stirred activated sludge enrichments removed methane twice and four times faster, respectively. Fresh photogranules did not exhibit a measurable methanotrophic activity.

We detected methane removal after adding 100% methane without externally provided oxygen to a mixture of fresh, non-methanotrophic photogranules and methanotrophic enrichments from activated sludge. Also, the production of oxygen and CO₂ was measured. This observation demonstrated the onset of engineered syntrophic interactions between methanotrophs and oxygenic photogranules. We were thus able to introduce a novel function into an existing, granulated microbial ecosystem, laying the basis for a potential future application in biotechnology in which biomass harvesting is feasible.

3.2. Continuous reactor performance for removing dissolved methane

The ecologically engineered methane-converting photogranules were then used as inoculum for the continuously operated reactor. Figure 2 shows the dissolved COD removal efficiency as proxy for methane removal as well as effluent total suspended solids (TSS) over time. Dissolved methane removal efficiencies fluctuated over the first week of operation. Effluent concentrations stabilized over the following two weeks and the methane removal efficiency steadily increased. On day 16, biofilm on reactor surfaces and equipment was removed, resulting in a 5% decrease in methane removal. The rather moderate decrement indicates that the vast majority of methane oxidation was situated in photogranular biomass and not in the biofilm formed on the reactor

surfaces. Approximately $10 \text{ mg TSS}\cdot\text{l}^{-1}$ of suspended solids were washed out from the reactor. Photogranules became increasingly more filamentous at this time (Figure 3a, middle). The change of photogranule morphology could have been influenced by the increase in biomass concentration and a local decrease in light availability in the reactor. The cyanobacteria might try to increase their surface area by forming filamentous outgrowth and therefore exposure to light (Biddanda et al., 2015).

After about three weeks of operation, effluent TSS increased due to the detachment of filaments from the photogranules. Application of higher mixing intensity on day 31 from 100 rpm to 125-128 rpm resulted in an increase in methane removal efficiency, now exceeding 90%. Mixing serves the purposes of minimizing the laminar boundary layer around the photogranules and keeping the photogranules in suspension (Beun et al., 2000; Liu et al., 2003). We also changed mixing to increase detachment of filaments from the photogranule surfaces. This approach worked, resulting in temporarily increased effluent suspended solid concentrations from the reactor (Figure 2, days 31 to 40) and less filamentous photogranules. However, the sudden detachment became problematic for reactor operation at day 40 when the effluent clogged, turning operation into safety mode for two days, i.e., without water in and outflow. The reactor was operational again after cleaning and wasting some photogranules at day 43.

On day 43, biomass was purposely wasted to obtain approximately $1.5 \text{ g TSS}\cdot\text{l}^{-1}$. Introduction of a weekly cleaning and biomass wasting protocol, by removing approximately $0.5\text{-}0.7 \text{ g TSS}\cdot\text{l}^{-1}$, prevented further clogging and maintained a balanced biomass concentration in the reactor of approximately $1.2 \text{ g TSS}\cdot\text{l}^{-1}$. This weekly biomass removal represented about one third to half of the biomass in the reactor. The removal of granular biomass on day 43 caused a drop in methane removal efficiency from about 90% to 60%. The removal efficiency reached on average $84.8\pm 7.4\%$ (\pm standard deviation) between day 54-93. On day 94, a

decreased methane removal efficiency was observed due to accidental wasting of a large numbers of photogranules. However, performance recovered over the next week to above 80%. The average effluent concentration of dissolved methane and the averaged methane removal rate during reactor operation was $4.9 \pm 3.7 \text{ mg CH}_4 \cdot \text{l}^{-1}$ and $26.3 \pm 2.6 \text{ mg CH}_4 \cdot \text{l}^{-1} \cdot \text{d}^{-1}$, respectively. In van der Ha et al. (2011), an overall methane oxidation rate was reported to be $171 \text{ mg CH}_4 \cdot \text{l}^{-1} \text{ liquid phase} \cdot \text{d}^{-1}$ which appears to be 6.6 times higher than in our experiments. A major factor leading to a higher removal rate is the organic loading. In van der Ha et al. (2011), 235 ml of CH_4 were added over 72 hours, which corresponds to approximately $258 \text{ mg CH}_4 \cdot \text{l}^{-1} \cdot \text{d}^{-1}$ at 22°C . Our OLR of $35.1 \pm 4.5 \text{ mg CH}_4 \cdot \text{l}^{-1} \cdot \text{d}^{-1}$ was thus, 7.3 times lower. It is important to note that the rates are not immediately comparable as van der Ha et al. (2011) worked in a batch system over 90 h, while our results are obtained in a CSTR with an HRT of 12 h.

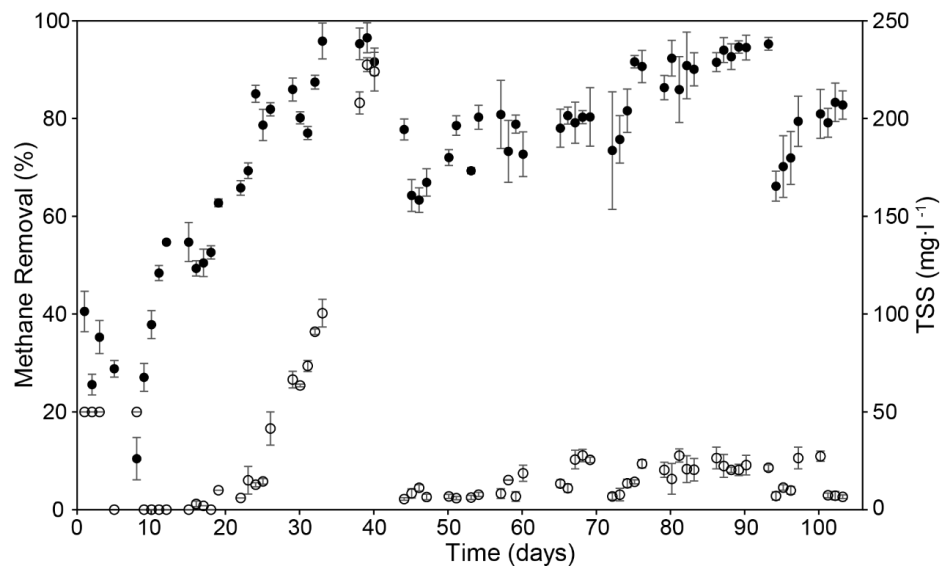


Figure 2 Removal efficiency of dissolved methane (filled circles) and concentrations of total suspended solids in the effluent (TSS, open circles) during continuous reactor operation. Mixing speed was increased on day 31. On day 40, the reactor effluent clogged. Severe biomass washout occurred on days 43 (deliberate) and 94 (accidental).

The observed overall biomass yield was $0.7 \text{ g TSS} \cdot \text{g COD}^{-1}$, equivalent to $0.6 \text{ g VSS} \cdot \text{g COD}^{-1}$ (assuming 15 % inorganic biomass fraction). Per mass substrate (CH_4) this is equivalent to $2.4 \text{ g VSS} \cdot \text{g CH}_4^{-1}$. The observed yield represents the combination of cellular yield from methanotrophic and cyanobacterial growth. Literature values of methanotrophic yields relevant for our study have been reported by Leak & Dalton (1986) and Arcangeli & Arvin, (1999). By theoretical analysis and experimental observations on suspended *Methylococcus capsulatus*, Leak & Dalton (1986) reported cellular yield of $0.6\text{-}0.7 \text{ g VSS} \cdot \text{g CH}_4^{-1}$ on cultivation conditions similar to this study. Arcangeli & Arvin (1999) studied a methanotrophic biofilm enriched from landfill soil and estimated the dry weight yield to be $0.56 \text{ g VSS} \cdot \text{g CH}_4^{-1}$. As conditions and growth technique, granular aggregation is similar to biofilms, and our media ($0.02 \text{ mg} \cdot \text{l}^{-1}$ of $\text{CuSO}_4 \cdot 5\text{H}_2\text{O}$) was comparable to the Cu limited experiment of Leak and Dalton (1986), we estimate methanotrophic yields to be in the order of $0.5\text{-}0.6 \text{ g VSS} \cdot \text{g CH}_4^{-1}$, which leaves the remaining observed $1.8 \text{ g VSS} \cdot \text{g CH}_4^{-1}$ to be the autotrophic contribution. Assuming all CO_2 from the mineralization of methane to be assimilated by the phototrophic bacteria, a combined methanotrophic and phototrophic yield of $1.54 \text{ g VSS} \cdot \text{g CH}_4^{-1}$ would be theoretically possible. The observed combined yield ($2.4 \text{ g VSS} \cdot \text{g CH}_4^{-1}$) therefore indicates an additional autotrophic growth contribution of $0.9 \text{ g VSS} \cdot \text{g CH}_4^{-1}$ probably originating from the inlet bicarbonate. High biomass yields in this system highlight the potential for the recovery of chemical energy or the methane-based biorefinery using photogranules. The overall COD balance closed at 91% of the inlet COD. The unaccounted 9% COD could be explained the reactor system still not completely at steady-state (positive bioaccumulation), and by the negative COD contribution by phototrophically produced oxygen consumed by the methanotrophs during methane mineralization.

We can rule out leakages in the system and therefore potential methane loss or oxygen and CO_2 entering the system. The tightness of the reactor

system was verified by frequently checking the gas composition in the headspace of the reactor using gas chromatography. The results showed that in the headspace, the dominant gas were nitrogen, oxygen, and methane by $89.3\pm 3.3\%$, $4.4\pm 2.6\%$, and $4.9\pm 2.3\%$ (v/v) (\pm standard deviation), respectively. The high presence of nitrogen gas resulted from the regular flushing of the headspace with nitrogen during reactor cleaning and maintenance. Only at most traces of CO_2 were detected in the gas phase at $0.01\pm 0.02\%$ (v/v).

Cyanobacteria can use CO_2 , HCO_3^- and possibly also CO_3^{2-} as carbon source (Schneider & Campion-Alsumard, 1999). In our study, methane was not the sole carbon sources, but HCO_3^- was contained as hardness in the tap water we used for media preparation. Based on the growth stoichiometry for methane oxidation coupled to photosynthesis, the theoretically produced oxygen from CO_2 assimilation during photosynthesis only provides roughly 20% of the oxygen needed for complete methane oxidation. The presence of HCO_3^- to the media would enhance the methane removal efficiency due to higher oxygen availability from bicarbonate photosynthesis. The 4 mM HCO_3^- contained in the tap water could theoretically supply an additional 2.58 mM O_2 , or an equivalent COD of $82 \text{ mg}\cdot\text{l}^{-1}$, upon autotrophic growth. Hence, methane oxidation is not stoichiometric oxygen limited by cyanobacterial growth. Similar findings were reported in the literature where in the absence of external oxygen supply, microalgal photosynthesis was not sufficient for methane oxidation (Bahr et al., 2011). Only when bicarbonate was introduced, the methane removal efficiency increased.

We suggest that the elevated methane removal in the absence of any external oxygen supply can only be explained by in-situ oxygen production and immediate uptake by methanotrophs. Our results therefore demonstrate the establishment of syntrophic interactions between phototrophs and methanotrophs. This syntrophy was stably maintained over seven weeks during continuous reactor operation.

3.3. Photogranule development in continuously operated reactor

During continuous reactor operation, new photogranules rapidly formed (Figure 3). After 16 days of continuous operation, the photogranules became dark green, roughly spherical, and filamentous (Figure 3). The presence of filamentous cyanobacteria was confirmed by white-light and fluorescence microscopy. Development of the filamentous morphology likely caused the increase in suspended solids in the reactor effluent (Figure 2). We successfully generated a less filamentous photogranule phenotype by increasing mixing from 100 rpm to 125-128 rpm starting on day 31. Immediately after the increase, the photogranules lost substantial amounts of filaments. Whitish areas on the photogranules surface became visible (Figure 3b, middle).

Using image analysis, we determined the number and the size of photogranules in the reactor. Over the first four weeks, the number of photogranules increased from initially 60 with an approximated total surface area of 0.08 cm² (day 0), to 888 and a total surface area of 240 cm² on day 16, and to about 2000 with a total surface area of 551 cm² on day 29 (Figure 4). After the major wasting and cleaning event on day 43, the number and surface area of photogranules decreased to 613 and 77.3 cm², respectively. However, the biomass concentration increased in the following days and reached more than 3500 photogranules and 1105 cm² of surface area on day 79 (Figure 4).

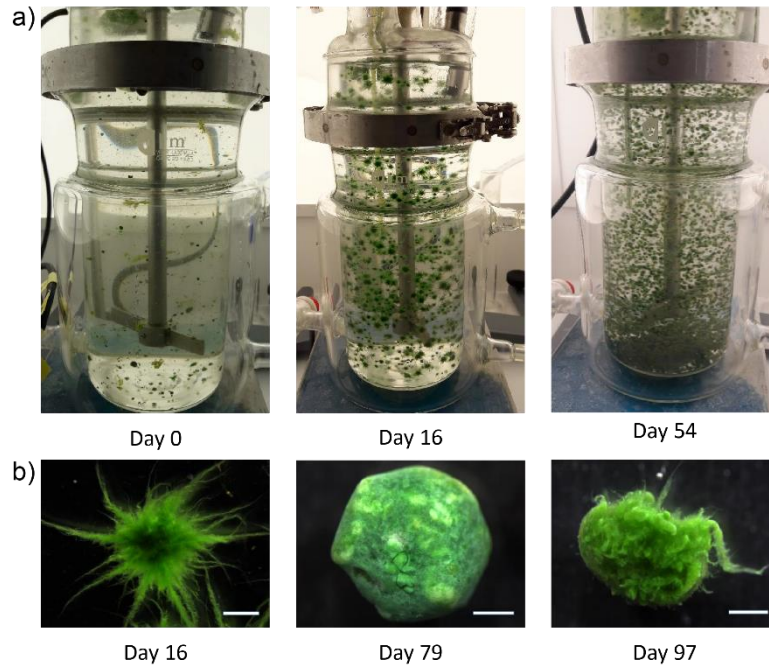


Figure 3 Photogranule development on macro and micro-scale. a) Full views of the reactor vessel. b) Examples of typical photogranule morphologies during continuous operation. Images were taken using white-light stereomicroscopy (scale bar for all images is 1 mm).

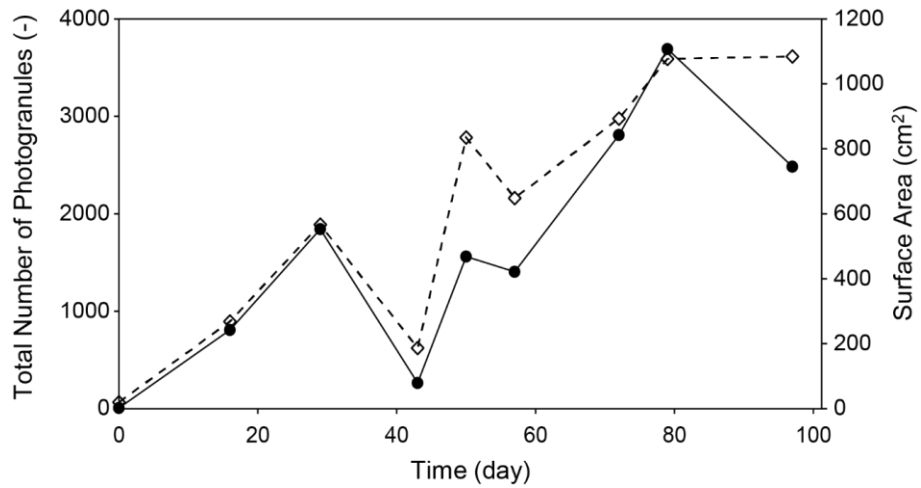


Figure 4 The total number (empty diamonds) and surface area of photogranules (filled circles) in the reactor during continuous operation.

The range of biomass diameters on day 16 was between 1 and 7 mm, with an average of 2.6 ± 1.3 mm (\pm standard deviation). On day 43, because of increasing shear, the predominant diameter of photogranules was less than 2 mm. The largest size of photogranules in the reactor was approximately 7.5 mm. This size is larger than the typical size of aerobic granular sludge with sizes in the range of 4 to 6 mm (Beun et al., 2000; Morgenroth et al., 1997). However, towards the end of reactor operation, more than 90% of the photogranules were between 1 and 3 mm with an average diameter of 2.6 ± 1.0 mm. This value is greater than the size of photogranules (≤ 2 mm in diameter) reported from previous photogranule reactor studies (Abouhend et al., 2018; Liu et al., 2017).

3.4. Size specific analysis of methanotrophic activity

Photogranule size may influence the specific phototrophic and methanotrophic activities as we assume phototrophic methane conversion to be a surface-depending process. Photogranule size affects the surface to volume ratios and diffusional lengths. We analyzed the specific metabolic activity in batch experiments for sets of on average six similar-sized photogranules in size classes between 1.3 and 5.5 mm in average diameter (Figure 5). Photogranules were sampled during stable reactor performance. Photogranules with diameters of approximately 1-2 mm gave the highest surface-specific methane removal rate of 0.53 ± 0.02 mg $\text{CH}_4 \cdot \text{d}^{-1} \cdot \text{mm}^{-2}$ (\pm standard deviation). The methane removal rate per photogranule surface area decreased with increasing diameter (Figure 5a). The relation with the surface to volume ratio is presented in Figure 5b. An elevated surface to volume ratio is beneficial for methane removal. From a conversion perspective, it is favorable to engineer a size distribution within the reactor of minimal photogranule diameter. The surface dependent character of photogranule metabolism was also shown in a recent study by Abouhend et al. (2020) in which oxygenic photogranules of 0.5–1.7 mm in diameter showed the highest oxygen production rate compared to bigger photogranules (Abouhend et al., 2020). Higher oxygen production rates influence the

treatment potential of the biomass, in this case dissolved methane removal, due to higher oxygen availability from photosynthesis as electron acceptor. Bigger photogranules may also become less active because they lose their cyanobacteria from the core as the photo-layer appear to be limited to depth of about 700 μm (Milferstedt et al., 2017).

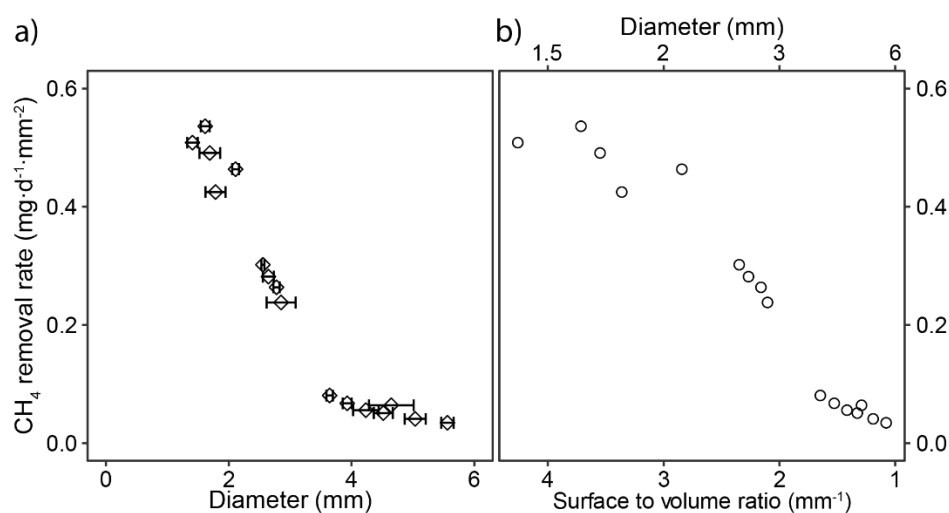


Figure 5 Surface specific methane removal rates for individual photogranule sizes. Rates are plotted by (a) the average diameter of the photogranule batch, and (b) by the surface to volume ratio, derived from the average diameters of the tested photogranules. Each point represents an independent batch experiment conducted with on average six similar-sized photogranules.

3.5. Community analysis related to methane removal performances

Using MiSeq amplicon sequencing, we analyzed the microbial communities in various photogranules sampled from the sequencing batch reactor, as well as the enriched inoculum and background material before the enrichment. We detected the presence of sequences belonging to methylotrophic bacteria in our samples (Figure 6a). The detected methylotrophs predominantly belong to methanotrophic bacteria, a subgroup of the methylotrophs, able to directly use methane as carbon and energy source. A frequent intermediate or even final product of methanotrophs is methanol (Kalyuzhnaya & Xing, 2018). Also, non-

methanotrophic methylotrophs were detected in elevated abundances (Figure 6a), notably of the family *Methylophilaceae*, often involved in methanol conversion (Yu et al., 2017). These groups of bacteria may participate in a communal metabolism of methane (Beck et al., 2013; Oshkin et al., 2015).

In the background material before the enrichment process, only in raw activated sludge, we detected sequences of one methanotrophic type in the 16S rRNA amplicons at a relative abundance of 0.02% of all bacterial sequences (excluding cyanobacteria). This sequence type was unique to the activated sludge sample and undetected in the inoculum and during reactor operation. In oxygenic photogranules, no sequences affiliated with known methanotrophic bacteria were detected (Figure 6a, “background”). The activated sludge and oxygenic photogranules used as starting material in this study contained fewer sequences of methanotrophic bacteria than previous observations (Milferstedt et al., 2017). Non-methanotrophic methylotrophs were undetectable in background activated sludge and oxygenic photogranules.

The enrichment process had a profound impact on the microbial community as at the end of it, 18.5±6.0% (±standard deviation) of all non-cyanobacterial bacterial 16S rRNA sequences were affiliated with known methylotrophic bacterial genera (Figure 6a, “inoculum”). Of this methylotrophic fraction, 74.1±4.8% were known methanotrophs, notably of the family of *Beijerinckiaceae*. These bacteria are Alphaproteobacteria, frequently described as type II methanotrophs. Across all samples containing sequences of methanotrophic *Beijerinckiaceae*, 98.5±4.5% were of the genus *Methylocystis*. *Methylocystis* are often considered versatile in their oxygen and methane requirements (Knief, 2015) allowing them to thrive in ecosystems with a varying methane supply (Knief, 2015). This survival strategy is believed to be linked to the presence of two variants of particulate methane monooxygenase A (PmoA) (Knief, 2015), the key enzyme in methane oxidation, converting methane to the intermediate methanol.

One of them is especially adapted to low methane to oxygen ratios in the feed, as likely encountered during batch feeding cycles in the enrichment process. The batch supply of methane and oxygen may thus be a key environmental factor favoring growth of these methanotrophs whereas the continuous exposure to methane at low concentrations as in the continuously fed reactor may promote others.

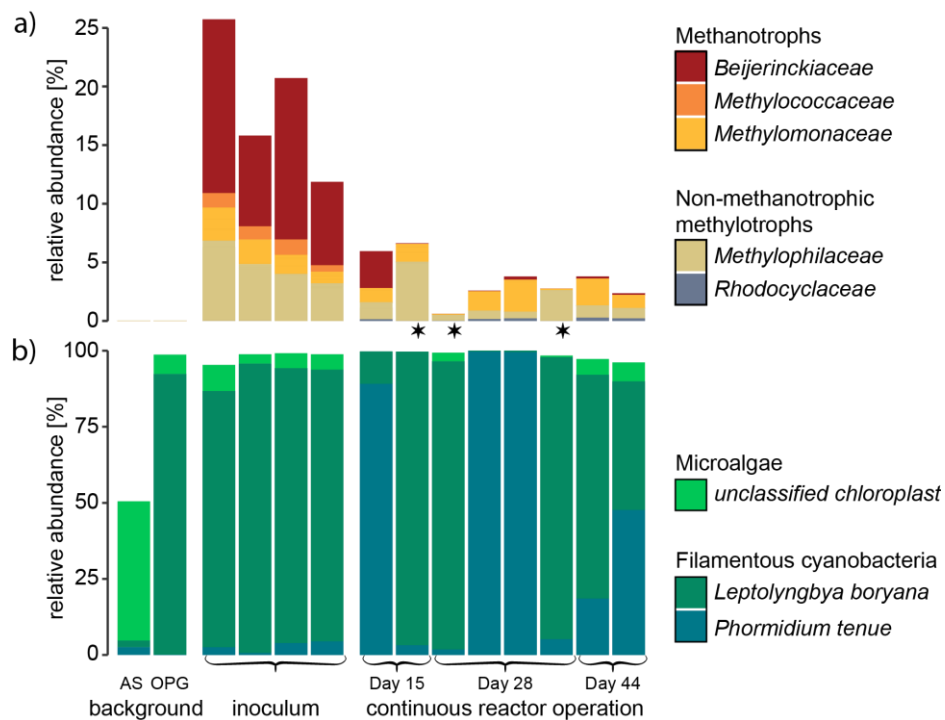


Figure 6 Relative abundances of methylotrophic and phototrophic taxa in photogranules and background material. The background material before the enrichment is the original activated sludge (AS), and an oxygenic photogranules (OPG). The inoculum after the enrichment process is represented by four photogranules. In total eight photogranule communities during continuous reactor operation are shown for days 15, 28 and 44. a) Putative methylotrophic bacteria (*Silva* SSU 132) among the non-phototrophic bacteria, i.e., excluding cyanobacteria, in the 16S rRNA amplicons. The three samples with asterisks mark photogranules in which methanotrophs are present in low abundances compared to non-methanotrophic methylotrophs. b) Major (>5% total abundance) cyanobacterial and chloroplast OTUs (*Silva* LSU 132) among the phototrophic taxa of the 23S rRNA amplicons.

Also present at the end of the enrichment, however, at notably lower abundances of $21.6 \pm 5.5\%$ (\pm standard deviation) of all methanotrophic bacteria, were members of the families of *Methylococcaceae* and *Methylomonaceae*. These subdominant families belong to the Gammaproteobacteria, also known as type I methanotrophs. Traditionally, the distinction in type I and type II methanotrophs allowed the differentiation of mutually exclusive physiological traits. Over the last years, however, it was realized that the distribution of these traits was less exclusive, and the distinction has become less meaningful (Dedysh & Knief, 2018).

During photoreactor operation, the overall relative abundance of methylotrophs dropped from 18.5% in the inoculum to, on average, $3.5 \pm 2.0\%$ (\pm standard deviation), of which roughly half of all sequences were known methanotrophs ($1.8 \pm 1.4\%$). Most analyzed photogranules had an approximate diameter of 2 mm and thus a comparable biovolume, with the exception of the third and fourth samples on day 28 that had a diameter of 5 mm. Assuming an approximately constant microbial community size for equally sized photogranules, the observed relative changes in the microbial community are likely translated into an absolute decrease in abundance per photogranule. Most of this loss is attributed to a significant decrease in the methanotroph *Methylocystis* of the *Beijerinckiaceae* (t-test, p-value=0.006). Also, the abundance of the other two methanotrophic families *Methylococcaceae* and *Methylomonaceae* decreased significantly (t-test, p-value=0.02) dropping from, on average, $2.9 \pm 1.0\%$ to $1.3 \pm 0.9\%$. After the disappearance of the *Methylocystis*, these two families presented the majority of methanotroph-affiliated sequences during reactor operation ($87.2 \pm 24.2\%$, Figure 6 “continuous reactor operation”). Two photogranules, sampled at day 28, only contained about 0.1% of methanotrophic sequences, more than ten times fewer than the other samples taken during reactor operation. The overall loss of methanotrophs may be explained by a reduced substrate availability per

photogranule during reactor operation with the increasing number of photogranules in the system. The comparably low number of methanotrophs may thus be a steady-state concentration adapted to the prevailing environmental conditions. Even though the drop in methanotrophs is significant, the abundance of methylotrophic bacteria, including methanotrophs remains about 100 times above the background levels before the enrichment. We note that the overall methanotrophic performance of the reactor system was maintained even at comparably low sequence abundances of $1.8 \pm 1.4\%$ of methanotrophs.

We systematically detected sequences of non-methanotrophic methylotrophs in our amplicons, notably of the family *Methylophilaceae*. Their sequences represented on average $4.7 \pm 1.6\%$ (\pm standard deviation) in the inoculum, and $1.7 \pm 1.5\%$ during reactor operation. In natural systems like sediments, these organisms are frequently found to respire methanol produced by methanotrophic bacteria (Yu et al., 2017). Yu et al. (2017) even suggested that among non-methanotrophic methylotrophs and methanotrophs, specific non-random pairings exist that seem to possess an environmental advantage over others. We did not detect specific pairings in our data, but the abundances of *Methylophilaceae* sequences appears to be roughly one third of the counts of known methanotrophic sequences in photogranules (linear regression through origin with slope of 0.345 and adj- r^2 of 0.74) (Figure 7). The constant ratio in abundance between two distinct phylogenetic groups hints towards a stoichiometric relationship between the implied organisms, possibly through metabolite dependencies. In Figure 7, notable exceptions to an otherwise strong linear relationship are two for the three samples marked with an asterisk in Figure 6. In these samples, methanotrophs are only present at a comparably low number. The exceptions indicate that metabolic heterogeneity between photogranules existed in our reactor, with the coexistence of putatively methanotrophic and non-methanotrophic photogranules. The non-methanotrophic photogranules may consume substrates provided by

other methanotrophic photogranules. These substrates could be for example methanol. A complete CH₄ to CO₂ conversion chain may therefore not be required to be present within each photogranule, but the entire population of photogranules participates in the methane conversion, cross-feeding beyond the boundaries of individual photogranules.

The enrichment process and the consequent transfer into the continuously operated reactor also shaped the non-methylotrophic and non-phototrophic bacteria in the community. During the enrichment, *Sphingomonadaceae* were enriched and reach abundances in the non-phototrophic 16S rRNA amplicons of more than 45% in one photogranule. This organism was affiliated with *Porphyrobacter*, an organism believed to be involved in the recycling of organic matter. During reactor operation this organism became less abundant in most cases while other recyclers increased in abundance, notably *Chitinophagaceae*. Some of the detected organisms are facultative anaerobes, suggesting that there are anaerobic microhabitats within the photogranules. No apparent correlation with the dynamics that we observed for the methylotrophs were detected. A graphical representation of the dominating families of non-methylotrophic and non-phototrophic bacteria is given in Figure S1. We were unable to detect sequences of nitrifiers in photogranules. Ammonium is therefore likely directly assimilated by the growing biomass. Archaea were only detected in traces in the activated sludge sample before enrichment and otherwise absent in the amplicons.

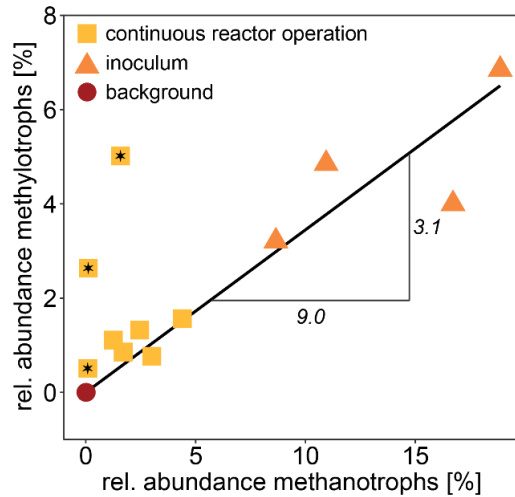


Figure 7 Ratio of non-methanotrophic methylotrophs vs. methanotrophs sequence types in the 16S rRNA amplicons.

The postulated trophic chain between the different methylotrophs in photogranules is coupled to the oxygen production by phototrophs, notably cyanobacteria. We analyzed in 23S rRNA amplicons the presence and abundance of cyanobacteria and microalgae. As expected, the total abundance of phototroph sequences in the background activated sludge sample was low compared to photogranule amplicons. Only 370 cyanobacterial sequences were found in activated sludge, whereas the mean cyanobacteria count in photogranules was 49900 ± 6700 (\pm standard deviation). Microalgal sequences represented the biggest part of the phototrophic population in activated sludge (93%). In photogranules, microalgal sequences were significantly less abundant, accounting for on average $3.5 \pm 3.0\%$. The microalgal population in photogranules was dominated by one single taxonomically unclassified sequence type with a sequence identity over the entire amplicon of approximately 95% to various microalgae genera. This sequence type made up on average $83 \pm 26\%$ (median 96%) of the microalgae we found in photogranules. In the activated sludge sample, this particular sequence type was virtually absent (1.2%) in a more diverse microalgal population. It appears that

this microalgae may be a member specific to the photogranule community, albeit low in abundance compared to cyanobacteria. In the background photogranule and the inocula at the end of the enrichment, three sequence types dominated the cyanobacterial counts were detected, two of which are affiliated with *Leptolyngbya boryana* and one with *Phormidium tenue*. These organisms are filamentous, motile cyanobacteria, as often found to constitute the phototrophic biomass of photogranules (Milferstedt et al., 2017). After the enrichment, $90.0\pm 4.3\%$ of all phototrophic sequences were related to *Leptolyngbya* and $2.9\pm 1.7\%$ to *Phormidium*. During reactor operation, the distribution of the two cyanobacterial types was close to binary in the different photogranules, where either one of the two dominated the photogranule community, as indicated by the high standard deviations around their mean abundances ($52\pm 43\%$ *Leptolyngbya* and $46\pm 44\%$ *Phormidium*). A heterogeneous cyanobacterial composition between individual photogranules within the same reactor was observed not unlike our observations for methanotrophic bacteria. When assuming that the two cyanobacteria perform the same ecosystem function, dominance of one over the other may be the result of a random event at the “birth” of the photogranule, e.g., a photogranule developing from a detached *Leptolyngbya*-dominated aggregate that develops into a *Leptolyngbya*-dominated photogranule.

Likewise, it may be possible that the dominance of either *Leptolyngbya* or *Phormidium* results from preferential interactions with other microbes, for example methanotrophs. Curiously, the samples that contain the lowest numbers of methanotrophs (marked with asterisk in Figure 6a) coincide with the photogranules in which the phototrophic community is dominated by *Leptolyngbya*-like sequences. Potential preferential pairing between microorganisms, as considered in this study within the methylotrophs, may need to be considered at larger phylogenetic scales than uniquely between methylotrophs. The differences between microbial communities of individual photogranules

from the same environment emphasize the need to study these systems at the scale of individual photogranules, for example when formulating the conversion process in a mathematical model.

4. Conclusions

- A methanotrophic-cyanobacterial syntrophy was established in the chassis of existing oxygenic photogranules. This syntrophy was maintained and propagated in a continuously operated reactor, proven by biomass growth and the removal of dissolved methane. We thus demonstrated the feasibility to ecologically engineer a novel photogranule community as potential biocatalyst for dissolved methane removal from anaerobic effluents.
- Photogranule morphology could be controlled in part by adapting hydrodynamic shear in the system, demonstrating that morphology not only depended on the developmental state of the photogranules.
- The established open community not only contained methanotrophic bacteria and phototrophs, but also non-methanotrophic methylotrophs, likely responsible for methanol conversion. Possibly, methanotrophs only incompletely oxidized methane to methanol, enabling the development of a methanol-degrading community, equally fueled by phototrophically generated oxygen.
- Community composition may differ considerably between photogranules, hinting towards cross-feeding between individuals of the photogranule population. This variability needs to be considered in experimental and modelling studies.
- The presence of non-methanotrophic methylotrophs is not problematic if the biotechnological aim was the removal of dissolved methane as post-treatment of anaerobic effluent. If simultaneous molecule recovery was the intention, e.g., methanol

production, more specific ways for controlling the activity of the open microbial community would be needed.

- Further research will focus on the treatment of real anaerobic wastewaters effluent in a long-term continuous mode. Nutrient recovery and an increased loading rate need to be studied as a function of temperature. Photogranules may be suitable to remove methane after psychrophilic anaerobic wastewater treatment with increased methane solubility and decreased biological kinetics.

References

- Abouhend, A. S., McNair, A., Kuo-Dahab, W. C., Watt, C., Butler, C. S., Milferstedt, K., Hamelin, J., Seo, J., Gikonyo, G. J., El-Moselhy, K. M., & Park, C. (2018). The oxygenic photogranule process for aeration-free wastewater treatment. *Environmental Science & Technology*, *52*(6), 3503–3511. <https://doi.org/10.1021/acs.est.8b00403>
- Abouhend, A. S., Milferstedt, K., Hamelin, J., Ansari, A. A., Butler, C., Carbajal-González, B. I., & Park, C. (2020). Growth progression of oxygenic photogranules and its impact on bioactivity for aeration-free wastewater treatment. *Environmental Science & Technology*, *54*(1), 486–496. <https://doi.org/10.1021/acs.est.9b04745>
- Arcangeli, J.-P., & Arvin, E. (1999). Modelling the growth of a methanotrophic biofilm: Estimation of parameters and variability. *Biodegradation*, *10*(3), 177–191. <https://doi.org/10.1023/A:1008317906069>
- Bahr, M., Stams, A. J. M., de la Rosa, F., García-Encina, P. A., & Muñoz, R. (2011). Assessing the influence of the carbon oxidation-reduction state on organic pollutant biodegradation in algal–bacterial photobioreactors. *Applied Microbiology and*

- Biotechnology*, 90(4), 1527–1536.
<https://doi.org/10.1007/s00253-011-3204-8>
- Bandara, W. M. K. R. T. W., Satoh, H., Sasakawa, M., Nakahara, Y., Takahashi, M., & Okabe, S. (2011). Removal of residual dissolved methane gas in an upflow anaerobic sludge blanket reactor treating low-strength wastewater at low-temperature with degassing membrane. *Water Research*, 45(11), 3533–3540. <https://doi.org/10.1016/j.watres.2011.04.030>
- Beck, D. A. C., Kalyuzhnaya, M. G., Malfatti, S., Tringe, S. G., Glavina Del Rio, T., Ivanova, N., Lidstrom, M. E., & Chistoserdova, L. (2013). A metagenomic insight into freshwater methane-utilizing communities and evidence for cooperation between the Methylococcaceae and the Methylophilaceae. *PeerJ*, 1, e23–e23. PubMed. <https://doi.org/10.7717/peerj.23>
- Beun, J. J., van Loosdrecht, M. C., & Heijnen, J. J. (2000). Aerobic granulation. *Water Science and Technology*, 41(4–5), 41–48. <https://doi.org/10.2166/wst.2000.0423>
- Biddanda, B., McMillan, A., Long, S., Snider, M., & Weinke, A. (2015). Seeking sunlight: Rapid phototactic motility of filamentous mat-forming cyanobacteria optimize photosynthesis and enhance carbon burial in Lake Huron’s submerged sinkholes. *Frontiers in Microbiology*, 6, 930. <https://doi.org/10.3389/fmicb.2015.00930>
- Brandt, E. M. F., Noyola, A., & McAdam, E. J. (2019). Control of diffuse emissions in UASB reactors treating sewage. In C. A. de Lemos Chernicharo & T. Bressani-Ribeiro (Eds.), *Anaerobic Reactors for Sewage Treatment: Design, Construction and Operation* (p. 0). IWA Publishing. https://doi.org/10.2166/9781780409238_0237
- Chistoserdova, L., Kalyuzhnaya, M. G., & Lidstrom, M. E. (2009). The expanding world of methylotrophic metabolism. *Annual Review of Microbiology*, 63(1), 477–499. <https://doi.org/10.1146/annurev.micro.091208.073600>

- Chon, D.-H., Rome, M., Kim, Y. M., Park, K. Y., & Park, C. (2011). Investigation of the sludge reduction mechanism in the anaerobic side-stream reactor process using several control biological wastewater treatment processes. *Water Research*, *45*(18), 6021–6029. <https://doi.org/10.1016/j.watres.2011.08.051>
- Cookney, J., Mcleod, A., Mathioudakis, V., Ncube, P., Soares, A., Jefferson, B., & McAdam, E. J. (2016). Dissolved methane recovery from anaerobic effluents using hollow fibre membrane contactors. *Journal of Membrane Science*, *502*, 141–150. <https://doi.org/10.1016/j.memsci.2015.12.037>
- Dedysh, S. N., & Knief, C. (2018). Diversity and phylogeny of described aerobic methanotrophs. In M. G. Kalyuzhnaya & X.-H. Xing (Eds.), *Methane biocatalysis: Paving the way to sustainability* (pp. 17–42). Springer International Publishing. https://doi.org/10.1007/978-3-319-74866-5_2
- Edgar, R. C., Haas, B. J., Clemente, J. C., Quince, C., & Knight, R. (2011). UCHIME improves sensitivity and speed of chimera detection. *Bioinformatics*, *27*(16), 2194–2200. <https://doi.org/10.1093/bioinformatics/btr381>
- Gao, H., Scherson, Y. D., & Wells, G. F. (2014). Towards energy neutral wastewater treatment: Methodology and state of the art. *Environmental Science: Processes & Impacts*, *16*(6), 1223–1246. <https://doi.org/10.1039/C4EM00069B>
- Hatamoto, M., Yamamoto, H., Kindaichi, T., Ozaki, N., & Ohashi, A. (2010). Biological oxidation of dissolved methane in effluents from anaerobic reactors using a down-flow hanging sponge reactor. *Water Research*, *44*(5), 1409–1418. <https://doi.org/10.1016/j.watres.2009.11.021>
- Henze, M., van Loosdrecht, M. C. M., Ekama, G. A., & Brdjanovic, D. (2008). *Biological Wastewater Treatment: Principles, Modelling and Design*. IWA Publishing. <https://doi.org/10.2166/9781780401867>

- Hodkinson, B. P., & Lutzoni, F. (2009). A microbiotic survey of lichen-associated bacteria reveals a new lineage from the Rhizobiales. *Symbiosis*, 49(3), 163–180. <https://doi.org/10.1007/s13199-009-0049-3>
- Kalyuzhnaya, M., & Xing, X.-H. (2018). *Methane biocatalysis: Paving the way to sustainability*. Springer. <https://www.springer.com/gp/book/9783319748658>
- Knief, C. (2015). Diversity and habitat preferences of cultivated and uncultivated aerobic methanotrophic bacteria evaluated based on pmoA as molecular marker. *Frontiers in Microbiology*, 6, 1346. <https://doi.org/10.3389/fmicb.2015.01346>
- Leak, D. J., & Dalton, H. (1986). Growth yields of methanotrophs. *Applied Microbiology and Biotechnology*, 23(6), 470–476. <https://doi.org/10.1007/BF02346062>
- Legland, D., Arganda-Carreras, I., & Andrey, P. (2016). MorphoLibJ: integrated library and plugins for mathematical morphology with ImageJ. *Bioinformatics (Oxford, England)*, 32(22), 3532–3534. <https://doi.org/10.1093/bioinformatics/btw413>
- Lettinga, G., van Velsen, A. F. M., Hobma, S. W., de Zeeuw, W., & Klapwijk, A. (1980). Use of the upflow sludge blanket (USB) reactor concept for biological wastewater treatment, especially for anaerobic treatment. *Biotechnology and Bioengineering*, 22(4), 699–734. <https://doi.org/10.1002/bit.260220402>
- Liu, L., Fan, H., Liu, Y., Liu, C., & Huang, X. (2017). Development of algae-bacteria granular consortia in photo-sequencing batch reactor. *Bioresource Technology*, 232, 64–71. <https://doi.org/10.1016/j.biortech.2017.02.025>
- Liu, Y., Xu, H.-L., Yang, S.-F., & Tay, J.-H. (2003). Mechanisms and models for anaerobic granulation in upflow anaerobic sludge blanket reactor. *Water Research*, 37(3), 661–673. [https://doi.org/10.1016/S0043-1354\(02\)00351-2](https://doi.org/10.1016/S0043-1354(02)00351-2)

- Liu, Z., Yin, H., Dang, Z., & Liu, Y. (2014). Dissolved methane: A hurdle for anaerobic treatment of municipal wastewater. *Environmental Science & Technology*, *48*(2), 889–890. <https://doi.org/10.1021/es405553j>
- Lobato, L. C. S., Chernicharo, C. A. L., & Souza, C. L. (2012). Estimates of methane loss and energy recovery potential in anaerobic reactors treating domestic wastewater. *Water Science and Technology*, *66*(12), 2745–2753. <https://doi.org/10.2166/wst.2012.514>
- Matsuura, N., Hatamoto, M., Sumino, H., Syutsubo, K., Yamaguchi, T., & Ohashi, A. (2015). Recovery and biological oxidation of dissolved methane in effluent from UASB treatment of municipal sewage using a two-stage closed downflow hanging sponge system. *Journal of Environmental Management*, *151*, 200–209. <https://doi.org/10.1016/j.jenvman.2014.12.026>
- McMurdie, P. J., & Holmes, S. (2013). phyloseq: An R package for reproducible interactive analysis and graphics of microbiome census data. *PLOS ONE*, *8*(4), e61217. <https://doi.org/10.1371/journal.pone.0061217>
- Milferstedt, K., Kuo-Dahab, W. C., Butler, C. S., Hamelin, J., Abouhend, A. S., Stauch-White, K., McNair, A., Watt, C., Carbajal-González, B. I., Dolan, S., & Park, C. (2017). The importance of filamentous cyanobacteria in the development of oxygenic photogranules. *Scientific Reports*, *7*(1), 17944. <https://doi.org/10.1038/s41598-017-16614-9>
- Milucka, J., Kirf, M., Lu, L., Krupke, A., Lam, P., Littmann, S., Kuypers, M. M., & Schubert, C. J. (2015). Methane oxidation coupled to oxygenic photosynthesis in anoxic waters. *The ISME Journal*, *9*, 1991.
- Morgenroth, E., Sherden, T., van Loosdrecht, M. C. M., Heijnen, J. J., & Wilderer, P. A. (1997). Aerobic granular sludge in a sequencing

- batch reactor. *Water Research*, *31*(12), 3191–3194. [https://doi.org/10.1016/S0043-1354\(97\)00216-9](https://doi.org/10.1016/S0043-1354(97)00216-9)
- Oshkin, I. Y., Beck, D. A., Lamb, A. E., Tchesnokova, V., Benuska, G., McTaggart, T. L., Kalyuzhnaya, M. G., Dedysh, S. N., Lidstrom, M. E., & Chistoserdova, L. (2015). Methane-fed microbial microcosms show differential community dynamics and pinpoint taxa involved in communal response. *The ISME Journal*, *9*(5), 1119–1129. <https://doi.org/10.1038/ismej.2014.203>
- Quast, C., Pruesse, E., Yilmaz, P., Gerken, J., Schweer, T., Yarza, P., Peplies, J., & Glöckner, F. O. (2013). The SILVA ribosomal RNA gene database project: Improved data processing and web-based tools. *Nucleic Acids Research*, *41*(D1), D590–D596. <https://doi.org/10.1093/nar/gks1219>
- R Core Team. (2020). R: A language and environment for statistical computing. R Foundation for Statistical Computing. Vienna, Austria. <http://www.r-project.org/index.html>
- Rasouli, Z., Valverde-Pérez, B., D'Este, M., de Francisci, D., & Angelidaki, I. (2018). Nutrient recovery from industrial wastewater as single cell protein by a co-culture of green microalgae and methanotrophs. *Biochemical Engineering Journal*, *134*, 129–135. <https://doi.org/10.1016/j.bej.2018.03.010>
- Rice, E. W., Baird, R. B., Eaton, A. D., & Clesceri, L. S. (2013). *Standard methods for the examination of water and wastewater, 20th edn.* (23rd ed.). APHA, AWWA, WEF.
- Schloss, P. D., Westcott, S. L., Ryabin, T., Hall, J. R., Hartmann, M., Hollister, E. B., Lesniewski, R. A., Oakley, B. B., Parks, D. H., Robinson, C. J., Sahl, J. W., Stres, B., Thallinger, G. G., van Horn, D. J., & Weber, C. F. (2009). Introducing mothur: Open-source, platform-independent, community-supported software for describing and comparing microbial communities. *Applied*

- and Environmental Microbiology*, 75(23), 7537.
<https://doi.org/10.1128/AEM.01541-09>
- Schneider, C. A., Rasband, W. S., & Eliceiri, K. W. (2012). NIH Image to ImageJ: 25 years of image analysis. *Nature Methods*, 9(7), 671–675. <https://doi.org/10.1038/nmeth.2089>
- Schneider, J., & Campion-Alsumard, T. L. (1999). Construction and destruction of carbonates by marine and freshwater cyanobacteria. *European Journal of Phycology*, 34(4), 417–426. <https://doi.org/10.1080/09670269910001736472>
- Seghezzo, L., Zeeman, G., van Lier, J. B., Hamelers, H. V. M., & Lettinga, G. (1998). A review: The anaerobic treatment of sewage in UASB and EGSB reactors. *Bioresource Technology*, 65(3), 175–190. [https://doi.org/10.1016/S0960-8524\(98\)00046-7](https://doi.org/10.1016/S0960-8524(98)00046-7)
- Sherwood, A. R., & Presting, G. G. (2007). Universal primers amplify a 23 rDNA plastid marker in eukaryotic algae and cyanobacteria. *Journal of Phycology*, 43(3), 605–608. <https://doi.org/10.1111/j.1529-8817.2007.00341.x>
- Souza, C. L., Chernicharo, C. A. L., & Aquino, S. F. (2011). Quantification of dissolved methane in UASB reactors treating domestic wastewater under different operating conditions. *Water Science and Technology*, 64(11), 2259–2264. <https://doi.org/10.2166/wst.2011.695>
- Takeuchi, M., Ozaki, H., Hiraoka, S., Kamagata, Y., Sakata, S., Yoshioka, H., & Iwasaki, W. (2019). Possible cross-feeding pathway of facultative methylotroph *Methyloceanibacter caenitepidi* Gela4 on methanotroph *Methylocaldum marinum* S8. *PloS One*, 14(3), e0213535–e0213535. PubMed. <https://doi.org/10.1371/journal.pone.0213535>
- Tchobanoglous, G., Burton, F. L., Stensel, H. D., Metcalf, & Eddy. (2003). *Wastewater engineering: Treatment and reuse* (4th ed.

revised by George Tchobanoglous, Franklin L. Burton, H. David Stensel.). McGraw-Hill.

- van der Ha, D., Nachtergaele, L., Kerckhof, F.-M., Rameiyanti, D., Bossier, P., Verstraete, W., & Boon, N. (2012). Conversion of biogas to bioproducts by algae and methane oxidizing bacteria. *Environmental Science & Technology*, *46*(24), 13425–13431. <https://doi.org/10.1021/es303929s>
- Vandevivere, P. (1999). New and broader applications of anaerobic digestion. *Critical Reviews in Environmental Science and Technology*, *29*(2), 151–173. <https://doi.org/10.1080/10643389991259191>
- Verstraete, W., Beer, D., Pena, M., Lettinga, G., & Lens, P. (1996). Anaerobic bioprocessing of organic wastes. *World Journal of Microbiology and Biotechnology*, *12*(3), 221–238. <https://doi.org/10.1007/BF00360919>
- Wang, Y., & Qian, P.-Y. (2009). Conservative fragments in bacterial 16S rRNA genes and primer design for 16S ribosomal DNA amplicons in metagenomic studies. *PLOS ONE*, *4*(10), e7401. <https://doi.org/10.1371/journal.pone.0007401>
- Wickham, H., Averick, M., Bryan, J., Chang, W., McGowan, L. D., François, R., Grolemond, G., Hayes, A., Henry, L., Hester, J., Kuhn, M., Pedersen, T. L., Miller, E., Bache, S. M., Müller, K., Ooms, J., Robinson, D., Seidel, D. P., Spinu, V., Takahashi, K., Vaughan, D., Wilke, C., Woo, K., & Yutani, H. (2019). Welcome to the Tidyverse. *Journal of Open Source Software*, *4*(43), 1686. <https://doi.org/10.21105/joss.01686>
- Wu, P.-H., Ng, K. K., Hong, P.-K. A., Yang, P.-Y., & Lin, C.-F. (2017). Treatment of low-strength wastewater at mesophilic and psychrophilic conditions using immobilized anaerobic biomass. *Chemical Engineering Journal*, *311*, 46–54. <https://doi.org/10.1016/j.cej.2016.11.077>

Yu, Z., Beck, D. A. C., & Chistoserdova, L. (2017). Natural selection in synthetic communities highlights the roles of *Methylococcaceae* and *Methylophilaceae* and suggests differential roles for alternative methanol dehydrogenases in methane consumption. *Frontiers in Microbiology*, 8, 2392. <https://doi.org/10.3389/fmicb.2017.02392>

Supplementary materials

1. Detailed calculation for methane loss estimation from wastewater treatment (Introduction):

- Theoretical methane production yield (Y) at standard ambient condition (25 °C (298 K), 1 atm) is 0.38 l CH₄/g COD (Tchobanoglous et al., 2003).
- Typical average soluble COD (sCOD) of high strength municipal wastewaters concentration is 450 g COD/m³ (Henze et al., 2008).
- Methane removal efficiency is assumed by 80%.
- Methane produced (per wastewater volume specific):

$$\begin{aligned} CH_{4,produced} &= 80\% \cdot Y \cdot sCOD \\ &= 80\% \cdot 0.38 \frac{\text{l CH}_4}{\text{g COD}} \cdot 450 \frac{\text{g COD}}{\text{m}^3} = 137 \frac{\text{l CH}_4}{\text{m}^3} \end{aligned}$$

By using the ideal gas law, volume of methane produced could be converted to mass.

$$P \cdot V = n \cdot R \cdot T = \frac{m}{M} \cdot R \cdot T$$

where M is the molecular weight of methane (16 g/mol), and R is universal gas constant. The value of R depends on the units involved, here, R is 0.082 L·atm/(mol·K).

$$m = \frac{P \cdot V \cdot M}{R \cdot T} = \frac{1 \text{ atm} \cdot 137 \frac{\text{l CH}_4}{\text{m}^3} \cdot 16 \frac{\text{g CH}_4}{\text{mol}}}{0.082 \frac{\text{l CH}_4 \cdot \text{atm}}{\text{mol} \cdot \text{K}} \cdot 298 \text{ K}} = 89.7 \frac{\text{g CH}_4}{\text{m}^3}$$

- The solubility of methane at 25 °C is approximately 20 g/m³ (Liu et al., 2014).

$$\begin{aligned} \text{Methane proportion in liquid effluent} &= \frac{20}{89.7} \cdot 100\% \\ &= 22\% \end{aligned}$$

- Methane recovery is then 78% relative to total methane produced in the system, equivalent to 107 l CH₄/m³ which could be used for combustion, saving fossil CO₂ emissions of 107 l CO₂/m³.
- The greenhouse gas produced as CO_{2,eq} due to dissolved methane loss:

$$GHG_{\text{CO}_2,\text{eq}} = 20 \frac{\text{g CH}_4}{\text{m}^3} \cdot 25 \frac{\text{g CO}_{2,\text{eq}}}{\text{g CH}_4} = 500 \frac{\text{g CO}_{2,\text{eq}}}{\text{m}^3}$$

By using the same gas ideal law, GHG produced as CO_{2,eq} volume due to dissolved methane loss to the atmosphere is 278 l CO₂/m³.

- The greenhouse gas contribution in this example is about 2.5 times greater than the positive effects from generating a renewable energy.

$$\text{Off - set} = \frac{GHG_{\text{produced}}_{\text{CO}_2,\text{eq}}}{GHG_{\text{saved}}_{\text{CO}_2,\text{eq}}} = \frac{278 \frac{\text{l CO}_2}{\text{m}^3}}{107 \frac{\text{l CO}_2}{\text{m}^3}} = 2.5$$

2. Relative abundance of non-methylotrophic and non-phototrophic bacteria in photogranules in the 16S rRNA amplicons:

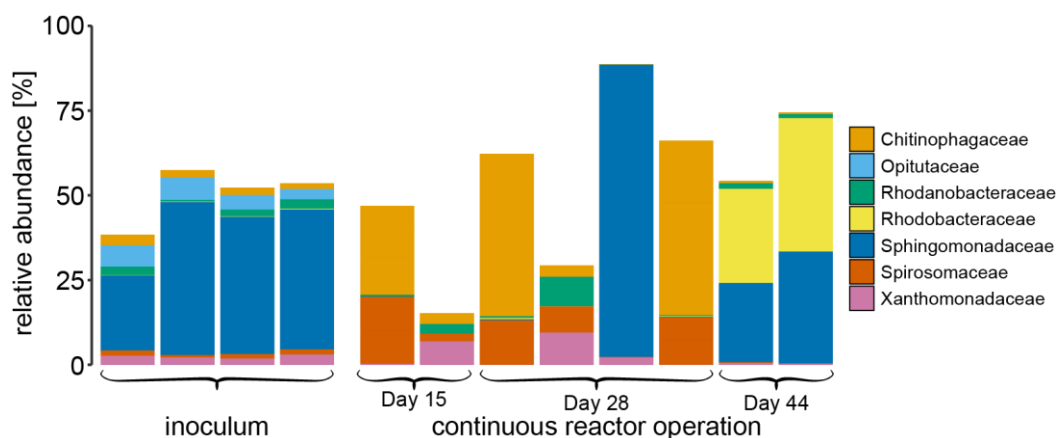


Figure S1: Relative abundances of non-methylotrophic and non-phototrophic bacteria in photogranules in the 16S rRNA amplicons. The inoculum after the enrichment process is represented by four photogranules. In total eight photogranule communities during continuous reactor operation are shown for days 15, 28 and 44.

References

- Henze, M., van Loosdrecht, M. C. M., Ekama, G. A., & Brdjanovic, D. (2008). *Biological Wastewater Treatment: Principles, Modelling and Design*. IWA Publishing. <https://doi.org/10.2166/9781780401867>
- Liu, Z., Yin, H., Dang, Z., & Liu, Y. (2014). Dissolved methane: A hurdle for anaerobic treatment of municipal wastewater. *Environmental Science & Technology*, 48(2), 889–890. <https://doi.org/10.1021/es405553j>
- Tchobanoglous, G., Burton, F. L., Stensel, H. D., Metcalf, & Eddy. (2003). *Wastewater engineering: Treatment and reuse* (4th ed.

revised by George Tchobanoglous, Franklin L. Burton, H. David Stensel.). McGraw-Hill.

Appendix 4 – Microalgal-based treatment for secondary wastewater effluent

Microalgal-based treatment for secondary wastewater effluent

A. MWC+Se and L1 media recipes:

Stock solutions and trace element solutions of MWC+Se media were prepared according to the recipe by Guillard & Lorenzen (1972), as presented in Table 1. The pH value in the stock solution was adjusted to 4-4.5 to retain solubility of the metals. Vitamin primary stock solutions were prepared according to Table 1. For the vitamin B₁₂ and Biotin stock solution approximately 11% water (0.89 ml of deionized water added for each 1 mg B₁₂) and 4% water (9.6 ml of deionized water added for each 1 mg Biotin) were added for crystallization, respectively. The vitamin stock solutions were covered and stored in freezer until use.

Table 1 Concentration of compounds used in preparation of stock solutions, trace element solutions and vitamin primary stock solutions of MWC+Se media

Stock Solutions	
Compound	Quantity
CaCl ₂ ·2H ₂ O	36.80 g·l ⁻¹
MgSO ₄ ·7H ₂ O	37.00 g·l ⁻¹
NaHCO ₃	12.60 g·l ⁻¹
K ₂ HPO ₄ ·3H ₂ O	11.40 g·l ⁻¹
NaNO ₃	85.00 g·l ⁻¹
Na ₂ O ₃ Si·9H ₂ O	28.40 g·l ⁻¹
Trace Element Solution	
Compound	Quantity
C ₁₀ H ₁₄ N ₂ Na ₂ O ₈ ·2H ₂ O	4.36 g·l ⁻¹
FeCl ₃ ·6H ₂ O	3.15 g·l ⁻¹
MnCl ₂ ·4H ₂ O	0.18 g
H ₃ BO ₃	1.00 g·l ⁻¹
1% CuSO ₄ ·4H ₂ O	1 ml·l ⁻¹
2.2 % ZnSO ₄ ·7H ₂ O	1 ml·l ⁻¹
1% COCl ₂ ·6H ₂ O	1 ml·l ⁻¹
0.6% Na ₂ MoO ₄ ·2H ₂ O	1 ml·l ⁻¹
Vitamin primary stock solution	

Compound	Quantity
Biotin	0.1 g·l ⁻¹
Cyanocobalamin (B ₁₂)	1 g·l ⁻¹

Stock solution for major elements, primary stock solutions and vitamin mix of L1 media were prepared according to recipe (Davis et al., 2015) as presented in Table 2.

Table 2 Concentration of compounds used in preparation of stock solutions, trace element solutions and vitamin stock solutions of L1

Stock solution for major elements	
Compound	Quantity
NaNO ₃	75 g·l ⁻¹
NaH ₂ PO ₄ ·H ₂ O	5 g·l ⁻¹
Primary trace elements stock solutions	
Compound	Quantity
CuSO ₄ ·5H ₂ O	2.45 g·l ⁻¹
Na ₂ MoO ₄ ·2H ₂ O	19.9 g·l ⁻¹
ZnSO ₄ ·7H ₂ O	22 g·l ⁻¹
CoCl ₂ ·6H ₂ O	10 g·l ⁻¹
MnCl ₂ ·4 H ₂ O	180 g·l ⁻¹
H ₂ SeO ₃	1.3 g·l ⁻¹
NiSO ₄ ·6H ₂ O	2.7 g·l ⁻¹
Na ₃ VO ₄	1.84 g·l ⁻¹
K ₂ CrO ₄	1.94 g·l ⁻¹
Vitamin stock solution	
Compound	Quantity
Biotin	0.0005 g
Thiamine HCl (B ₁)	0.1 g
Cyanocobalamin (B ₁₂)	0.0005 g

For the trace metal working stock solution, 4.36 g C₁₀H₁₄N₂Na₂O₈·2H₂O and 3.15 g FeCl₃·6H₂O were added to a 1000 ml volumetric flask, along with 0.25 ml of CuSO₄·5H₂O, 3 ml of Na₂MoO₄·2H₂O, and 1 ml of ZnSO₄·7H₂O, CoCl₂·6H₂O, MnCl₂·4H₂O, H₂SeO₃, NiSO₄·6H₂O, Na₃VO₄ and K₂CrO₄. Deionized water was filled to 1000 ml. For the final

preparation of L1 media 1 ml NaNO₃, 1 ml NaH₂PO₄·2H₂O, 1 ml of trace elements working stock solution and 1 ml of vitamin mix stock solution, as described in Table 2, were added to a 1000 ml volumetric flask. Filtered seawater was filled up to 1000 ml and pH was adjusted to 8.0±0.2 before autoclaving (Laboratory Autoclave MLS-3781L, Panasonic, Japan). Seawater was collected at NORCE research station at Mekjarvik from a marine pipeline drawing water from the Byfjorden (North: 58°57'48" East: 5°43'8") at 80 m depth (Randaberg, Norway).

B. Microalgal pre-culturing (pre-growth)

Microalgal pre-culturing was conducted to prepare the microalgal culture for testing quantification methods and strain screening. The inoculation of microalgal cultures into the media was done aseptically in a laminar flow hood (LabGard NU-540 Class II Type A2 Biosafety Cabinet, Nuair, USA) using sterile techniques. All equipment was autoclaved before use (MLS-3781L, Panasonic, Japan). Two ml of each of the suspended freshwater microalgae were transferred to 250 ml Erlenmeyer flasks containing 100 ml autoclaved MWC+Se media. An aliquot of *M. Salina* was transferred to 100 ml marine media L1 using a sterilized loop. Each strain was prepared in four replicates. The flasks were incubated at 18 °C, 80 - 90 rpm and photosynthetic LED light of 80 μmol·m⁻²·s⁻¹ with a light/dark regime of 16/8 hours (Innova S44i Eppendorf, Germany). When microalgal cultures were in the late logarithmic phase, they were sub-cultured for maintenance. The microalgal cultures were regularly examined and microscopically checked for contamination and cell viability (normal phase 40x Olympus BX61, Japan). The cultures were shaken once a day to avoid self-shading and ensure gas transfer.

C. Continuous PBR experiment results

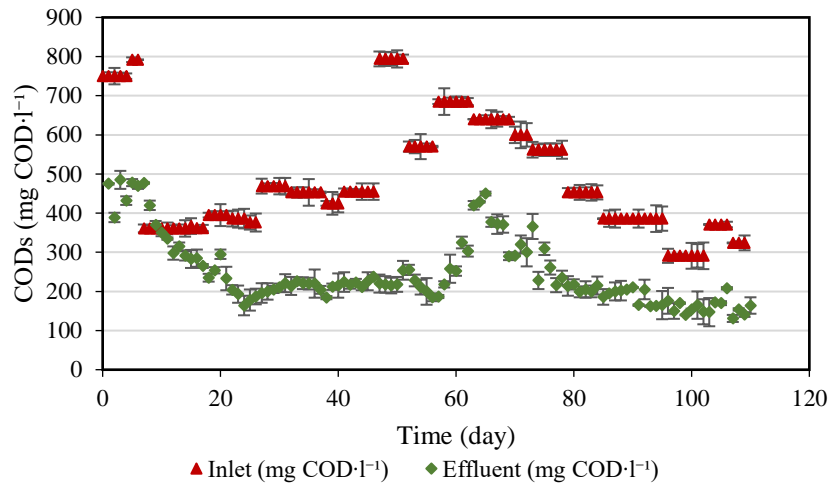


Figure 1 Dissolved COD concentration profiles at the inlet and effluent of the PBR throughout 109 days continuous operation. Error bars represent standard deviations from triplicate samples from PBR ($n=3$).

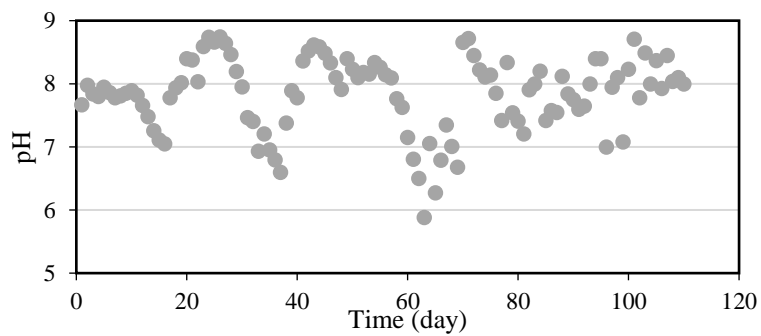


Figure 2 pH profiles inside PBR throughout 109 days continuous PBR operation.

D. Statistical analysis and microplate calibration results

Based on the statistical analysis, the t-test revealed no significant difference ($p>0.05$) between the direct counting and flow cytometry enumeration (Table 3).

Table 3 P-value of 95 percent two-tailed confidence analysis, t-test, of direct counting and flow cytometry cell quantification from four replications of four different concentrations

Method	Two-tailed p-value (t-test)			
	1	2	3	4
Direct counting	0.13	0.87	0.38	0.91
Flow cytometry				

Figure 1 presents the calibration curve of fluorescence signal microplate cell quantification using direct counting ($R^2=0.98$) and flow cytometry ($R^2=0.99$). These statistic values indicated both methods gave more than 95% of the linear regression could fit the plotted data points. When applying direct cell counting, the method will simultaneously provide information about if any contamination and viability of the cells while counting. The method is also simple and low-cost. However, direct counting is time-consuming. Furthermore, the standard errors of direct counting measurements gave higher values compared to flow cytometry method, as shown in Table 4. Therefore, flow cytometry method was used to calibrate microplate reader quantification during kinetic of nutrient-limited *C. sorokiniana* growth analysis, as shown in Equation 1.

Table 4 Cell quantification using direct counting and flow cytometry methods from four replications of four different concentrations (mean±standard error)

Method	Cell concentration (cell·ml ⁻¹)			
	1	2	3	4
Direct counting	138±1.5	553±3.0	1521±24.0	2688±12.5
Flow cytometry	135±0.4	553±0.3	1546±1.3	2686±0.9

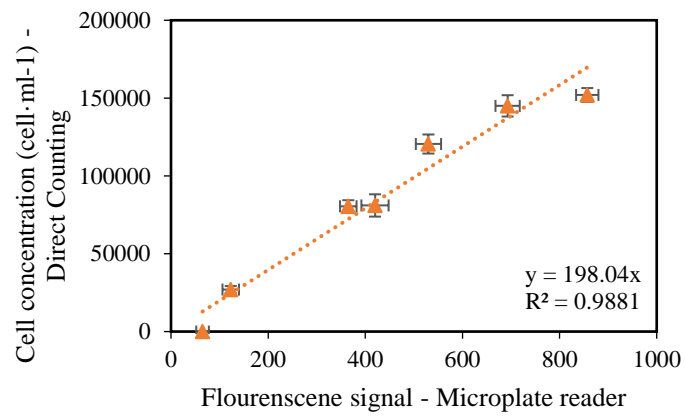
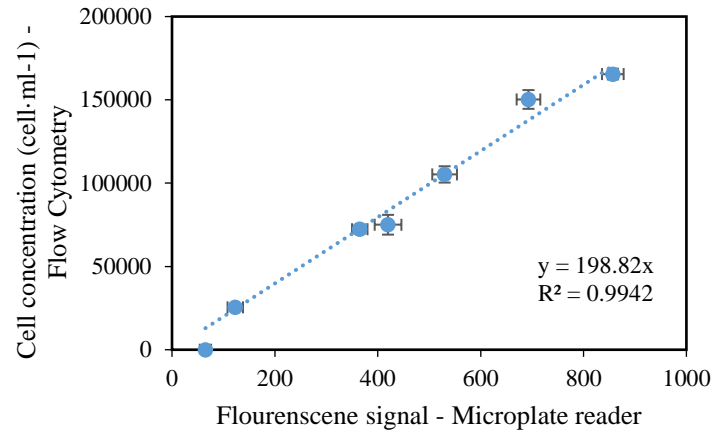


Figure 4 Calibration curve of microplate fluorescence signal using flow cytometry method (blue circle) and direct counting method (orange triangle)

Cell concentration ($\text{cell} \cdot \text{ml}^{-1}$) = $198.84 \times$ (fluorescence signal read) Equation 1

Appendix 5 – Pathogen analysis method

Pathogen analysis methods

A. Media preparation

Media plates were prepared for the viable count method. The agar used and the preparation methods are described below.

- Chromogenic coliform selective agar

Chromogenic agar is the selective media for detection of total coliforms which also helps in identification of *E. coli* (International Organization for Standardization, 2016). During the media preparation, 30 g of the media powder (Oxoid™, Thermo Fisher Scientific, USA) was dissolved in 1000 ml distilled water which was then allowed to boil until all particulates completely dissolved. The pH was then measured, and adjusted to 6.8 ± 0.2 at 25 °C. The media was then poured into the plates and after cooling stored at 4 °C.

- Slanetz-Bartley agar

Slanetz-Bartley agar is a media used for selective enumeration of *Enterococci* (Slanetz L. W. & Bartley Clara H., 1957). The agar manufacturer was Sigma-Aldrich, Germany. The media was prepared by dissolving 42 g of the media powder in 1000 ml of distilled water which was then heated until dissolve completely. The final pH was adjusted to 7.2 ± 0.2 at 25 °C. The agar was then kept in a fridge at 4 °C after cooling and solidifying.

- Bile Esculin agar

Bile Esculin agar is a selective media for *Enterococcus* and was used as confirmatory test of Slanetz-Bartley agar. It was also manufactured by Sigma-Aldrich, Germany. Preparation of the media was done by dissolving 56.65 g of media powder in 1000 ml of distilled water. It was then stirred to dissolve and was autoclaved at 121 °C for 15 min. The

final pH was adjusted to 7.1 ± 0.2 at $25\text{ }^{\circ}\text{C}$. The media was allowed to cool and then was poured in the media plates. It was then kept in fridge at $4\text{ }^{\circ}\text{C}$.

- Plate count agar

This media was used for the enumeration of total heterotroph bacteria in the wastewater sample (International Organization for Standardization, 1999). The media was prepared by dissolving 24 g Oxoid™ media powder (Thermo Fisher Scientific, USA) in 1000 ml distilled water. The suspension was heated and stirred to dissolve particulates completely. Dissolved media was thereafter sterilized by autoclavation at $121\text{ }^{\circ}\text{C}$ for 15 min. The final pH was adjusted to 7.2 ± 0.2 at $25\text{ }^{\circ}\text{C}$. Since the media was to be used for pour-plate count, it was transferred into smaller glass bottles and kept at $4\text{ }^{\circ}\text{C}$.

B. Viable plate count

Samples were collected from the in- and outlet of the UASB reactor and from the membrane permeate. Bacterial enumeration tests were conducted immediately upon sampling. The serial dilution technique was used for the cell culture using phosphate-buffered saline (PBS) at final concentrations: $8\text{ g}\cdot\text{l}^{-1}$ of NaCl, $0.2\text{ g}\cdot\text{l}^{-1}$ of KCl, $0.24\text{ g}\cdot\text{l}^{-1}$ of KH_2PO_4 , and $1.44\text{ g}\cdot\text{l}^{-1}$ of Na_2HPO_4 . pH was adjusted to 7.4 with HCl. The solution was then dispensed into aliquots and sterilized by autoclaving for 20 min at $121\text{ }^{\circ}\text{C}$.

The dilution factors started from 10^0 to 10^8 . A volume of 0.1 ml of the original sample was added to the first tube labelled 10^{-1} . 0.1 ml of each dilution was spread evenly spread onto the media plates in triplicates. The pour plate method was used in the case of the plate count agar media. 1 ml of the sample was transferred and poured with the agar and thoroughly mixed.

The chromogenic agar media plates were incubated at 36 °C for 24 hours before the colony count. The positive colonies were brownish color for coliform and green colonies for *E. coli*. The plate count media was incubated at 22 °C for 62 hours before the colony counting. Bacterial growth was observed as white color colonies.

The Slanetz-Bartley agar media was incubated at 36 °C for 48 hours. At the time of the colony count, *Enterococci* colony was dark brownish in color over the reddish media. For the confirmation of *Enterococci*, the colony grown in Slanetz-Bartley agar media was streaked in the Bile Esculin agar media. *E. coli* was used for negative confirmation. They were incubated for 24 hours at 44 °C. The positive result showed dark brown color colonies in the Bile-Esculin agar plates.

*Appendix 6 – Anaerobic granulated biofilm system model
for municipal wastewater treatment*

Anaerobic granulated biofilm system model for municipal wastewater treatment

A. Biological conversion processes

The stoichiometric matrix, composition matrix and kinetic expressions are summarized in Tables 1 and 2. Tables 3, 4 and 5 list the corresponding stoichiometric, kinetic, and physico-chemical parameters, respectively. pH inhibition (I_{pH}) was described the same as in ADM1:

$$I_{pH} = e^{-3 \cdot \left(\frac{pH - pH_{UL}}{pH_{UL} - pH_{LL}} \right)^2}$$

where pH is the actual value in UASB reactor, pH_{UL} is the pH value with no inhibition and pH_{LL} is the pH value with full inhibition.

Nitrogen inhibition ($I_{N,limit}$) was also described analogously to ADM1, with a lower limit of 10^{-6} to avoid numerical problems when nitrogen is limiting. (Batstone et al., 2002):

$$I_{N,limit} = \frac{S_{TIN}}{K_{s,IN} + S_{TIN}} \quad \text{for } S_{TIN} \geq K_{s,IN}$$

$$I_{N,limit} = 10^{-6} \quad \text{for } S_{TIN} < K_{s,IN}$$

where S_{TIN} is the concentration of inorganic nitrogen and $K_{s,IN}$ is the inorganic nitrogen concentration at which the growth ceases, 0.0001 M (Batstone et al., 2004).

Table 1 Stoichiometric, composition, and kinetic matrix part 1: soluble components, based on ADM1 (Batstone, 2006; Batstone et al., 2002)

Component →	i	1	2	3	4	5	6	7	8	9	10	11	12	Rate (ρ_j , kg COD·m ⁻³ ·d ⁻¹)
j	Process ↓	S _{va}	S _{aa}	S _{fa}	S _{va}	S _{bu}	S _{pro}	S _{ac}	S _{h2}	S _{ch4}	S _{ic}	S _{in}	S _i	
1	Disintegration												$f_{SI,xc}$	$k_{dis}X_c$
2	Hydrolysis of carbohydrates	1												$k_{hyd, ch}X_{ch}$
3	Hydrolysis of proteins		1											$k_{hyd, pr}X_{pr}$
4	Hydrolysis of lipids	$1 - f_{fa,li}$		$f_{fa,li}$										$k_{hyd, li}X_{li}$
5	Uptake of sugars	-1				$(1 - Y_{su})f_{bu,su}$	$(1 - Y_{su})f_{pro,su}$	$(1 - Y_{su})f_{ac,su}$	$(1 - Y_{su})f_{h2,su}$		$-\sum_{i=1-9,11-24} C_i v_{i,5}$	$-(Y_{su})N_{bac}$		$k_{m,su} \frac{S_{su}}{K_S + S} X_{su} I_1$
6	Uptake of amino acids		-1		$(1 - Y_{aa})f_{va,aa}$	$(1 - Y_{aa})f_{bu,aa}$	$(1 - Y_{aa})f_{pro,aa}$	$(1 - Y_{aa})f_{ac,aa}$	$(1 - Y_{aa})f_{h2,aa}$		$-\sum_{i=1-9,11-24} C_i v_{i,6}$	$N_{aa} - (Y_{aa})N_{bac}$		$k_{m,aa} \frac{S_{aa}}{K_S + S_{aa}} X_{aa} I_1$
7	Uptake of LCFA			-1				$(1 - Y_{fa})0.7$	$(1 - Y_{fa})0.3$				$-(Y_{fa})N_{bac}$	$k_{m,fa} \frac{S_{fa}}{K_S + S_{fa}} X_{fa} I_2$
8	Uptake of valerate				-1		$(1 - Y_{c4})0.54$	$(1 - Y_{c4})0.31$	$(1 - Y_{c4})0.15$				$-(Y_{c4})N_{bac}$	$k_{m,c4} \frac{S_{va}}{K_S + S_{va}} X_{c4} \frac{1}{1 + S_{bu}/S_{va}} I_2$
9	Uptake of butyrate					-1		$(1 - Y_{c4})0.8$	$(1 - Y_{c4})0.2$				$-(Y_{c4})N_{bac}$	$k_{m,c4} \frac{S_{bu}}{K_S + S_{bu}} X_{c4} \frac{1}{1 + S_{va}/S_{bu}} I_2$
10	Uptake of propionate						-1	$(1 - Y_{pro})0.57$	$(1 - Y_{pro})0.43$		$-\sum_{i=1-9,11-24} C_i v_{i,10}$	$-(Y_{pro})N_{bac}$		$k_{m,pro} \frac{S_{pro}}{K_S + S_{pro}} X_{pro} I_2$
11	Uptake of acetate							-1		$(1 - Y_{ac})$	$-\sum_{i=1-9,11-24} C_i v_{i,11}$	$-(Y_{ac})N_{bac}$		$k_{m,ac} \frac{S_{ac}}{K_S + S_{ac}} X_{ac} I_3$
12	Uptake of hydrogen								-1	$(1 - Y_{h2})$	$-\sum_{i=1-9,11-24} C_i v_{i,12}$	$-(Y_{h2})N_{bac}$		$k_{m,h2} \frac{S_{h2}}{K_S + S_{h2}} X_{h2} I_1$
13	Decay of X _{su}													$k_{dec, Xsu} X_{su}$
14	Decay of X _{aa}													$k_{dec, aa} X_{aa}$
15	Decay of X _{fa}													$k_{dec, Xfa} X_{fa}$
16	Decay of X _{c4}													$k_{dec, Xc4} X_{c4}$
17	Decay of X _{pro}													$k_{dec, Xpro} X_{pro}$
18	Decay of X _{ac}													$k_{dec, Xac} X_{ac}$
19	Decay of X _{h2}													$k_{dec, Xh2} X_{h2}$
		Monosaccharides (kg COD·m ⁻³)	Amino acids (kg COD·m ⁻³)	Long chain fatty acids (kg COD·m ⁻³)	Total valerate (kg COD·m ⁻³)	Total butyrate (kg COD·m ⁻³)	Total propionate (kg COD·m ⁻³)	Total acetate (kg COD·m ⁻³)	Hydrogen gas (kg COD·m ⁻³)	Methane gas (kg COD·m ⁻³)	Inorganic carbon (kmole C·m ⁻³)	Inorganic carbon (kmole N·m ⁻³)	Soluble inerts (kg COD·m ⁻³)	Inhibitor factors: $I_1 = I_{pH} I_{N,lim}$ $I_2 = I_{pH} I_{N,lim} I_{h2}$ $I_3 = I_{pH} I_{N,lim} I_{NH3, Xac}$

Table 2 Stoichiometric, composition, and kinetic matrix part 2: particulate components, based on ADMI (Batstone, 2006; Batstone et al., 2002)

Component →		i	13	14	15	16	17	18	19	20	21	22	23	24	Rate (ρ_j , kg COD·m ⁻³ ·d ⁻¹)
j	Process ↓	X _c	X _{cb}	X _{pr}	X _{li}	X _{su}	X _{aa}	X _{fa}	X _{c4}	X _{pro}	X _{ac}	X _{h2}	X _i		
1	Disintegration	-1	$f_{ch,Xc}$	$f_{pr,Xc}$	$f_{li,Xc}$									$f_{xl,Xc}$	$k_{dis}X_c$
2	Hydrolysis of carbohydrates		-1												$k_{hyd,cb}X_{ch}$
3	Hydrolysis of proteins			-1											$k_{hyd,pr}X_{pr}$
4	Hydrolysis of lipids				-1										$k_{hyd,li}X_{li}$
5	Uptake of sugars					Y_{su}									$k_{m,su} \frac{S_{su}}{K_S + S_{su}} X_{su} I_1$
6	Uptake of amino acids						Y_{aa}								$k_{m,aa} \frac{S_{aa}}{K_S + S_{aa}} X_{aa} I_1$
7	Uptake of LCFA							Y_{fa}							$k_{m,fa} \frac{S_{fa}}{K_S + S_{fa}} X_{fa} I_2$
8	Uptake of valerate								Y_{c4}						$k_{m,c4} \frac{S_{va}}{K_S + S_{va}} X_{c4} \frac{1}{1 + S_{bu}/S_{va}} I_2$
9	Uptake of butyrate								Y_{c4}						$k_{m,c4} \frac{S_{bu}}{K_S + S_{bu}} X_{c4} \frac{1}{1 + S_{va}/S_{bu}} I_2$
10	Uptake of propionate									Y_{pro}					$k_{m,pro} \frac{S_{pro}}{K_S + S_{pro}} X_{pro} I_2$
11	Uptake of acetate										Y_{ac}				$k_{m,ac} \frac{S_{ac}}{K_S + S_{ac}} X_{ac} I_3$
12	Uptake of hydrogen											Y_{h2}			$k_{m,h2} \frac{S_{h2}}{K_S + S_{h2}} X_{h2} I_1$
13	Decay of X _{su}	1				-1									$k_{dec, Xsu} X_{su}$
14	Decay of X _{aa}	1					-1								$k_{dec, aa} X_{aa}$
15	Decay of X _{fa}	1						-1							$k_{dec, Xfa} X_{fa}$
16	Decay of X _{c4}	1							-1						$k_{dec, Xc4} X_{c4}$
17	Decay of X _{pro}	1								-1					$k_{dec, Xpro} X_{pro}$
18	Decay of X _{ac}	1									-1				$k_{dec, Xac} X_{ac}$
19	Decay of X _{h2}	1										-1			$k_{dec, Xh2} X_{h2}$
		Composites (kg COD·m ⁻³)	Carbohydrates (kg COD·m ⁻³)	Proteins (kg COD·m ⁻³)	Lipids (kg COD·m ⁻³)	Sugar degraders (kg COD·m ⁻³)	Amino acid degraders (kg COD·m ⁻³)	LCFA degraders (kg COD·m ⁻³)	Butyrate and valerate degraders (kg COD·m ⁻³)	Propionate degraders (kg COD·m ⁻³)	Acetate degraders (kg COD·m ⁻³)	Hydrogen degraders (kg COD·m ⁻³)	Particulate inerts (kg COD·m ⁻³)	Inhibitor factors: $I_1 = I_{pH} I_{N,lim}$ $I_2 = I_{pH} I_{N,lim} I_{h2}$ $I_3 = I_{pH} I_{N,lim} I_{NH3, Xac}$	

Table 3 Stoichiometric parameter values of the ADM1 biofilm model

Symbol	Description	Value	Unit	Reference
Carbon content of:				
C_{aa}	amino acids	0.03000	moleC·gCOD ⁻¹	Batstone et al. (2004)
C_{ac}	acetate	0.03125	moleC·gCOD ⁻¹	Batstone et al. (2004)
C_{biom}	biomass	0.03125	moleC·gCOD ⁻¹	Batstone et al. (2004)
C_{bu}	butyrate	0.02500	moleC·gCOD ⁻¹	Batstone et al. (2004)
C_{ch4}	methane	0.01563	moleC·gCOD ⁻¹	Batstone et al. (2004)
C_{fa}	LCFA	0.02170	moleC·gCOD ⁻¹	Batstone et al. (2004)
C_{li}	lipids	0.02200	moleC·gCOD ⁻¹	Batstone et al. (2004)
C_{pro}	propionate	0.02679	moleC·gCOD ⁻¹	Batstone et al. (2004)
C_{SI}	soluble inert	0.03000	moleC·gCOD ⁻¹	Batstone et al. (2004)
C_{su}	sugars	0.03125	moleC·gCOD ⁻¹	Batstone et al. (2004)
C_{va}	valerate	0.02404	moleC·gCOD ⁻¹	Batstone et al. (2004)
C_{Xc}	complex particulate	0.02790	moleC·gCOD ⁻¹	Batstone et al. (2004)
C_{XI}	particulate inert	0.03000	moleC·gCOD ⁻¹	Batstone et al. (2004)
Nitrogen content of:				
N_{aa}	amino acids	0.00700	moleN·gCOD ⁻¹	Batstone et al. (2004)
N_{biom}	biomass	0.00625	moleN·gCOD ⁻¹	Batstone et al. (2004)
N_{SI}	S_I	0.00200	moleN·gCOD ⁻¹	Batstone et al. (2004)
N_{Xc}	X_C	0.00200	moleN·gCOD ⁻¹	Batstone et al. (2004)
N_{XI}	X_I	0.00200	moleN·gCOD ⁻¹	Batstone et al. (2004)
Yield of product from degradation of substrate:				
$f_{ac,aa}$	acetate from amino acid	0.40000	-	Batstone et al. (2002)
$f_{ac,su}$	acetate from sugar	0.40755	-	Batstone et al. (2002)
$f_{bu,aa}$	butyrate from amino acids	0.26000	-	Batstone et al. (2002)
$f_{bu,su}$	butyrate from sugar	0.13280	-	Batstone et al. (2002)
$f_{ch,xc}$	carbohydrates from particulates	0.15000	-	Batstone et al. (2002)
$f_{fa,li}$	LCFA from lipid	0.95000	-	Batstone et al. (2002)
$f_{h2,aa}$	H ₂ from amino acid	0.06000	-	Batstone et al. (2002)

$f_{h_2, su}$	H ₂ from sugar	0.19055	-	Batstone et al. (2002)
$f_{li, xc}$	lipids from particulates	0.25000	-	Batstone et al. (2002)
$f_{pr, xc}$	proteins from particulates	0.15000	-	Batstone et al. (2002)
$f_{pro, aa}$	propionate from amino acid	0.05000	-	Batstone et al. (2002)
$f_{pro, su}$	propionate from sugar	0.26910	-	Batstone et al. (2002)
$f_{SI, xc}$	S _I from particulates	0.10000	-	Batstone et al. (2002)
$f_{va, aa}$	valerate from amino acid	0.23000	-	Batstone et al. (2002)
$f_{XI, xc}$	X _I from particulates	0.35000	-	Batstone et al. (2002)

Biomass yield coefficient on:

Y_{aa}	uptake of amino acids	0.0800	gCOD·gCOD ⁻¹	Batstone et al. (2004)
Y_{ac}	uptake of acetate	0.0500	gCOD·gCOD ⁻¹	Batstone et al. (2004)
Y_{c4}	uptake of valerate and butyrate	0.0600	gCOD·gCOD ⁻¹	Batstone et al. (2004)
Y_{fa}	uptake of LCFA	0.0600	gCOD·gCOD ⁻¹	Batstone et al. (2004)
Y_{h_2}	uptake of H ₂	0.0600	gCOD·gCOD ⁻¹	Batstone et al. (2004)
Y_{pro}	uptake of propionate	0.0400	gCOD·gCOD ⁻¹	Batstone et al. (2004)
Y_{su}	uptake of monosaccharide	0.1000	gCOD·gCOD ⁻¹	Batstone et al. (2004)

Table 4 Kinetic parameters of ADM1biofilm model

Symbol	Description	Value	Unit	Reference
Threshold value of pH inhibition: (UL = no inhibition, LL = full inhibition)				
$I_{pH, ac, LL}$	LL for ac ⁻ degradation	6	-	Batstone et al. (2004)
$I_{pH, ac, UL}$	UL for ac ⁻ degradation	7	-	Romli et al. (1995)
$I_{pH, biom, LL}$	LL for biomass	4	-	Batstone et al. (2004)
$I_{pH, biom, UL}$	UL for biomass	5.5	-	Batstone et al. (2004)
$I_{pH, h_2, LL}$	LL for H ₂ degradation	5	-	Romli et al. (1995)
$I_{pH, h_2, UL}$	UL for H ₂ degradation	6	-	Romli et al. (1995)
Decay rate of:				
$k_{dec, X_{aa}}$	X_{aa}	0.050	d ⁻¹	Batstone et al. (2004)
$k_{dec, X_{ac}}$	X_{ac}	0.100	d ⁻¹	Batstone et al. (2004)
$k_{dec, X_{c4}}$	X_{c4}	0.100	d ⁻¹	Batstone et al. (2004)

$k_{dec,Xfa}$	X_{fa}	0.100	d^{-1}	Batstone et al. (2004)
$k_{dec,Xh2}$	X_{h2}	0.100	d^{-1}	Batstone et al. (2004)
$k_{dec,Xpro}$	X_{pro}	0.100	d^{-1}	Batstone et al. (2004)
$k_{dec,Xsu}$	X_{su}	0.100	d^{-1}	Batstone et al. (2004)
Disintegration and hydrolysis first rate constant of:				
k_{dis}	particulate disintegration	0.5	d^{-1}	Batstone et al. (2004)
$k_{hyd,ch}$	carbohydrate hydrolysis	106	d^{-1}	Gavala and Lyberatos (2001)
$k_{hyd,li}$	lipid hydrolysis	0.4	d^{-1}	Gujer and Zehnder (1983)
$k_{hyd,pr}$	protein hydrolysis	2.7	d^{-1}	Gavala and Lyberatos (2001)
Inhibitory concentration of:				
$k_{I,h2,c4}$	H_2 for X_{c4}	$1.0 \cdot 10^{-5}$	$kg \text{ COD } m^{-3}$	Batstone et al. (2004)
$k_{I,h2,fa}$	H_2 for X_{fa}	$5.0 \cdot 10^{-6}$	$kg \text{ COD } m^{-3}$	Batstone et al. (2004)
$k_{I,h2,pro}$	H_2 for X_{pro}	$3.5 \cdot 10^{-6}$	$kg \text{ COD } m^{-3}$	Batstone et al. (2004)
$k_{I,NH3,ac}$	NH_3 for X_{ac}	$1.8 \cdot 10^{-3}$	$kmole \text{ N } m^{-3}$	Batstone et al. (2004)
Maximum uptake rate of:				
$k_{m,aa}$	X_{aa}	250	$g \text{ g}^{-1} \text{ d}^{-1} \text{ (COD)}$	Batstone et al. (2004)
$k_{m,ac}$	X_{ac}	40	$g \text{ g}^{-1} \text{ d}^{-1} \text{ (COD)}$	Batstone et al. (2004)
$k_{m,c4}$	X_{c4}	100	$g \text{ g}^{-1} \text{ d}^{-1} \text{ (COD)}$	Batstone et al. (2004)
$k_{m,fa}$	X_{fa}	30	$g \text{ g}^{-1} \text{ d}^{-1} \text{ (COD)}$	Batstone et al. (2004)
$k_{m,h2}$	X_{h2}	175	$g \text{ g}^{-1} \text{ d}^{-1} \text{ (COD)}$	Batstone et al. (2004)
$k_{m,pro}$	X_{pro}	65	$g \text{ g}^{-1} \text{ d}^{-1} \text{ (COD)}$	Batstone et al. (2004)
$k_{m,su}$	X_{su}	150	$g \text{ g}^{-1} \text{ d}^{-1} \text{ (COD)}$	Batstone et al. (2004)
Half-saturation constant for:				
$K_{S,aa}$	amino acid degradation	$3.0 \cdot 10^{-1}$	$kg \text{ COD } m^{-3}$	Batstone et al. (2004)
$K_{S,ac}$	acetate degradation	$1.5 \cdot 10^{-1}$	$kg \text{ COD } m^{-3}$	Batstone et al. (2002)
$K_{S,c4}$	C4 degradation	$2.0 \cdot 10^{-1}$	$kg \text{ COD } m^{-3}$	Batstone et al. (2002)
$K_{S,fa}$	LCFA degradation	$4.0 \cdot 10^{-1}$	$kg \text{ COD } m^{-3}$	Batstone et al. (2004)
$K_{S,h2}$	hydrogen degradation	$7.0 \cdot 10^{-6}$	$kg \text{ COD } m^{-3}$	Batstone et al. (2002)
$K_{S,pro}$	propionate degradation	$1.0 \cdot 10^{-1}$	$kg \text{ COD } m^{-3}$	Batstone et al. (2004)

$K_{S,su}$	monosaccharide degradation	$5.0 \cdot 10^{-1}$	kg COD m^{-3}	Batstone et al. (2004)
------------	----------------------------	---------------------	-----------------	------------------------

Table 5 Physico-chemical parameters of ADM1 biofilm model

Symbol	Description	Value	Unit	Reference
Acidity constants (K_a) and acid-Base reaction constants (K_{AB})				
$K_{a,ac}$	acetic acid	$10^{-4.76}$	M	Lide (2003)
$K_{a,bu}$	butyric acid	$10^{-4.83}$	M	Lide (2003)
$K_{a,co2}$	CO ₂	$10^{-6.35} \exp\left(\frac{7646}{100 \cdot R} \cdot \left(\frac{1}{T_{std}} - \frac{1}{T}\right)\right)$	M	Lide (2003) Batstone et al. (2002)
$K_{a,h2o}$	H ₂ O	$10^{-13.995} \exp\left(\frac{55900}{100 \cdot R} \cdot \left(\frac{1}{T_{std}} - \frac{1}{T}\right)\right)$	M	Lide (2003) Batstone et al. (2002)
$K_{a,nh4}$	NH ₄ ⁺	$10^{-9.25} \exp\left(\frac{51965}{100 \cdot R} \cdot \left(\frac{1}{T_{std}} - \frac{1}{T}\right)\right)$	M	Lide (2003) Batstone et al. (2002)
$K_{a,pro}$	propionic acid	$10^{-4.87}$	M	Lide (2003)
$K_{a,va}$	valeric acid	$10^{-4.80}$	M	Lide (2003)
$K_{AB,CO2}$	CO ₂	10^8	d ⁻¹	Batstone et al. (2002)
Henry's law constants				
$K_{H,ch4}$	CH ₄	$0.00140 \cdot R \cdot T \cdot \exp\left(\frac{-14240}{100 \cdot R} \cdot \left(\frac{1}{T_{std}} - \frac{1}{T}\right)\right)$	-	Batstone et al. (2002) Lide (2003)
$K_{H,co2}$	CO ₂	$0.03400 \cdot R \cdot T \cdot \exp\left(\frac{-7646}{100 \cdot R} \cdot \left(\frac{1}{T_{std}} - \frac{1}{T}\right)\right)$	-	Batstone et al. (2002) Lide (2003)
$K_{H,h2}$	H ₂	$0.00078 \cdot R \cdot T \cdot \exp\left(\frac{-4180}{100 \cdot R} \cdot \left(\frac{1}{T_{std}} - \frac{1}{T}\right)\right)$	-	Batstone et al. (2002) Lide (2003)
Diffusivity in water of:				
D_{aa}	amino acids	$8.62 \cdot 10^{-6}$	m ² d ⁻¹	Batstone et al. (2004)
D_{ac}	acetate	$6.48 \cdot 10^{-6}$	m ² d ⁻¹	Batstone et al. (2004)
D_{bu}	butyrate	$5.04 \cdot 10^{-6}$	m ² d ⁻¹	Batstone et al. (2004)
D_{ch4}	methane	$1.36 \cdot 10^{-4}$	m ² d ⁻¹	Lide (2003)
D_{co2}	carbon dioxide	$1.71 \cdot 10^{-4}$	m ² d ⁻¹	Reid et al. (1977)

D_{fa}	LCFA	$5.33 \cdot 10^{-6}$	$m^2 d^{-1}$	Batstone et al. (2004)
D_{h2}	hydrogen	$4.02 \cdot 10^{-4}$	$m^2 d^{-1}$	Verhallen et al. (1984)
D_{ion}	cations and anions	$1.17 \cdot 10^{-4}$	$m^2 d^{-1}$	Batstone et al. (2004)
D_{nh3}	ammonia	$1.52 \cdot 10^{-4}$	$m^2 d^{-1}$	Reid et al. (1977)
D_{pro}	propionate	$6.00 \cdot 10^{-6}$	$m^2 d^{-1}$	Batstone et al. (2004)
D_{SI}	soluble inerts	$8.62 \cdot 10^{-6}$	$m^2 d^{-1}$	Batstone et al. (2004)
D_{su}	monosaccharide	$4.56 \cdot 10^{-6}$	$m^2 d^{-1}$	Batstone et al. (2004)
D_{va}	valerate	$5.00 \cdot 10^{-6}$	$m^2 d^{-1}$	Batstone et al. (2004)

Other physico-chemical parameters:

P_{atm}	atmosphere pressure	1.013	bar	standard
P_{h2o}	pressure of water	$0.0313 \cdot \exp\left(5290 \cdot \left(\frac{1}{T_{std}} - \frac{1}{T}\right)\right)$	bar	Rosen and Jeppsson (2006)
R	gas law constant	0.08314	$bar M^{-1} K^{-1}$	standard
T	temperature (25°C)	298.15	K	measured

B. Calculation of pH

Kinetic reaction rates and stoichiometric coefficients for acid-base reaction is calculated by implementing a differential equation (DE). For DE implementation, the free form S_{hva} , S_{hbu} , S_{hpro} , S_{hac} , S_{co2} , and S_{nh4} should be substituted for the total ionic forms (Batstone et al., 2002). Stoichiometric matrix and kinetic rate equation for acid-base reactions in a DE implementation is presented in Table 6. The following equation for calculating hydrogen ion concentration:

$$\theta = S_{CAT} + S_{NH_4^+} + S_{H^+} - \frac{S_{AC^-}}{64} - \frac{S_{PRO^-}}{112} - \frac{S_{BU^-}}{160} - \frac{S_{VA^-}}{208} - S_{HCO_3^-} - \frac{K_w}{S_{H^+}} + -S_{AN}$$

$$S_{H^+} = -\frac{\theta}{2} + \frac{1}{2}\sqrt{\theta^2 + 4K_w}$$

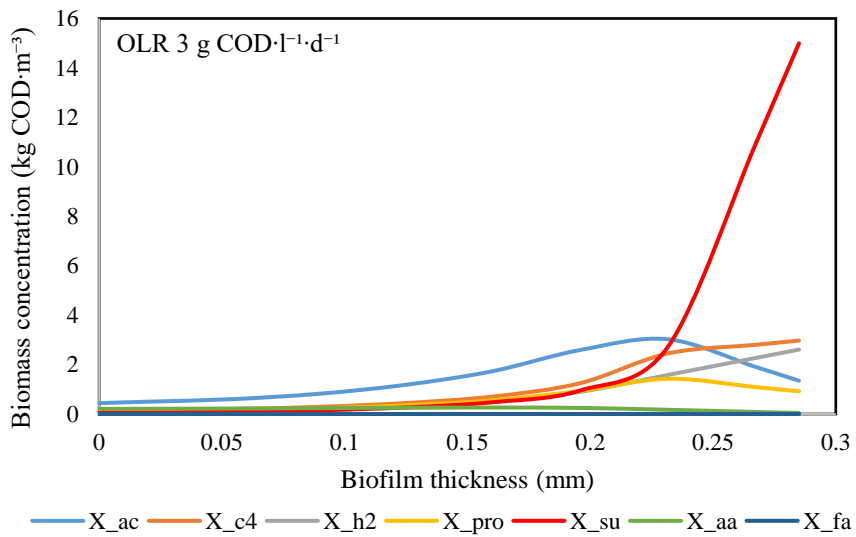
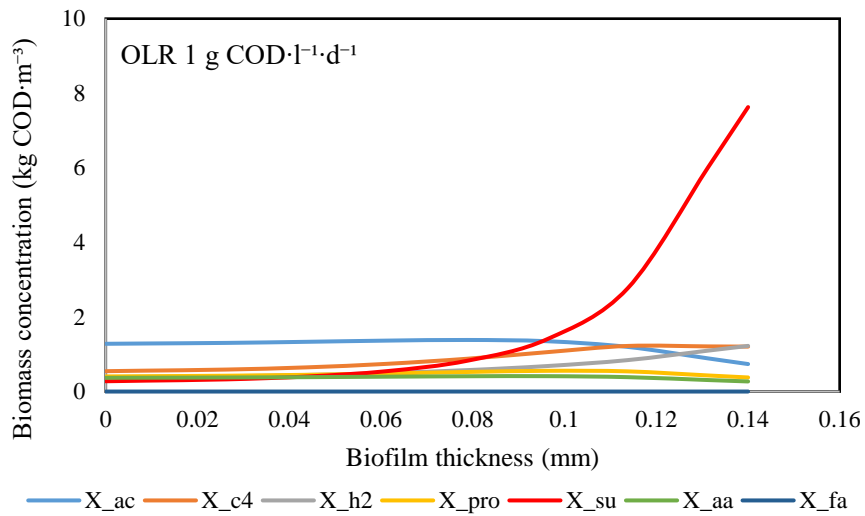
Where θ is the net charge in the system resulting from all acid-bases considered in the model.

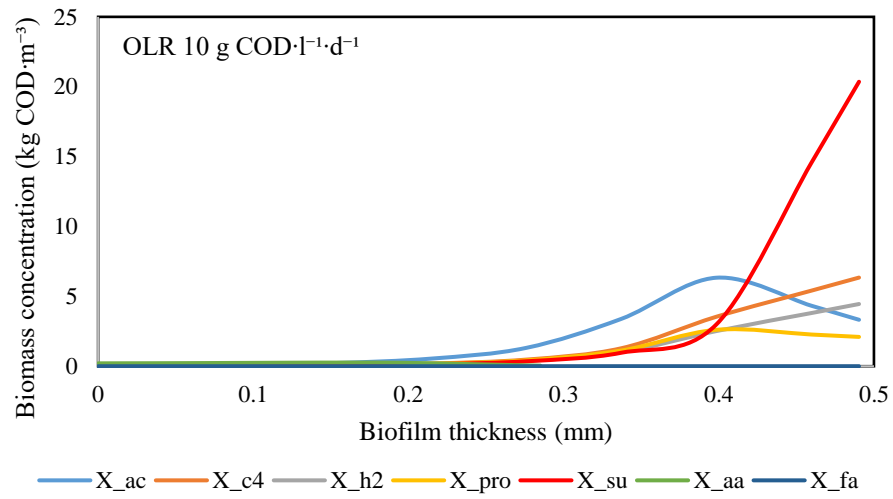
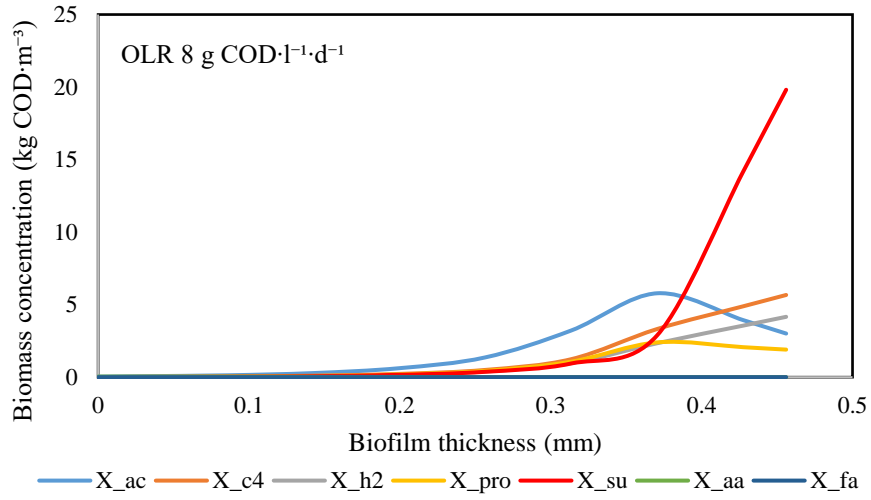
Table 6 Rate coefficients ($\nu_{i,j}$) and kinetic rate equation (ρ_j) for acid-base reactions in a DE implementation

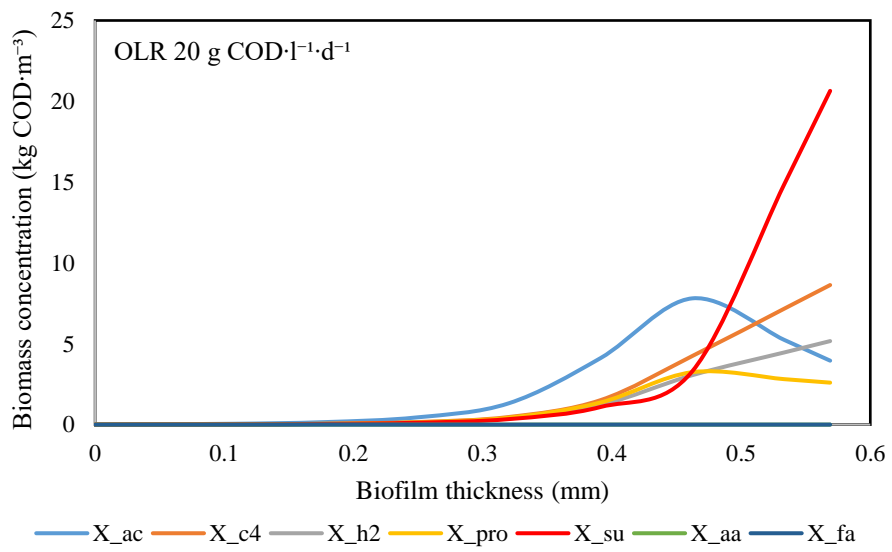
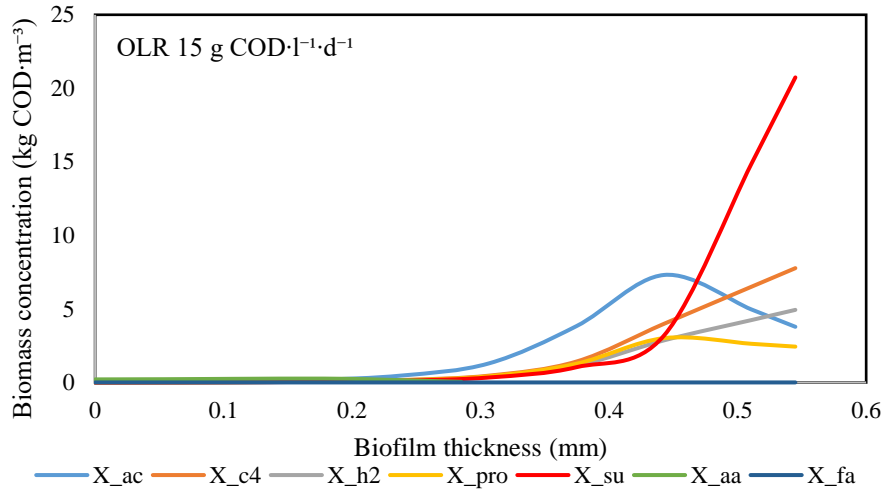
Component →		i	2	4	6	8	9	10	11	13	Rate (ρ_j , kg COD·m ⁻³ ·d ⁻¹)
j	Process ↓	S_{va^-}	S_{bu^-}	S_{pro^-}	S_{ac^-}	S_{co2}	S_{hco3^-}	S_{nh4^+}	S_{h^-}		
1	Valerate ion production	1									$\left[S_{va} - \frac{(K_{A,va} + S_{h^-}) \cdot S_{va^-}}{K_{A,va}} \right] K_{A/B}$
2	Butyrate ion production		1								$\left[S_{bu} - \frac{(K_{A,bu} + S_{h^-}) \cdot S_{bu^-}}{K_{A,bu}} \right] K_{A/B}$
3	Propionate ion production			1							$\left[S_{pro} - \frac{(K_{A,pro} + S_{h^-}) \cdot S_{pro^-}}{K_{A,pro}} \right] K_{A/B}$
4	Acetate ion production				1						$\left[S_{ac} - \frac{(K_{A,ac} + S_{h^-}) \cdot S_{ac^-}}{K_{A,ac}} \right] K_{A/B}$
5	Inorganic carbon production					1	-1				$[S_{hco3^-} \cdot S_{h^-} - K_{A,co2} \cdot S_{co2}] K_{A/B}$
6	Inorganic nitrogen production								1		$\left[S_{IN} - \frac{(K_{A,nh4} + S_{h^-}) \cdot S_{nh4}}{S_{h^-}} \right] K_{A/B}$
		Valerate ion (kgCOD·m ⁻³)	Butyrate ion (kgCOD·m ⁻³)	Propionate ion (kgCOD·m ⁻³)	Acetate ion (kgCOD·m ⁻³)	Carbon dioxide (kmoleC·m ⁻³)	Bicarbonate (kmoleC·m ⁻³)	Ammonium (kmoleN·m ⁻³)	Hydrogen ion (M)		Kinetic parameters: $K_{a/BI}$, rate coefficient for the base to acid reaction. Initially set to 10 ⁹ m ⁻¹ ·d ⁻¹ (Batstone et al., 2002).

C. Biomass and substrate profile results

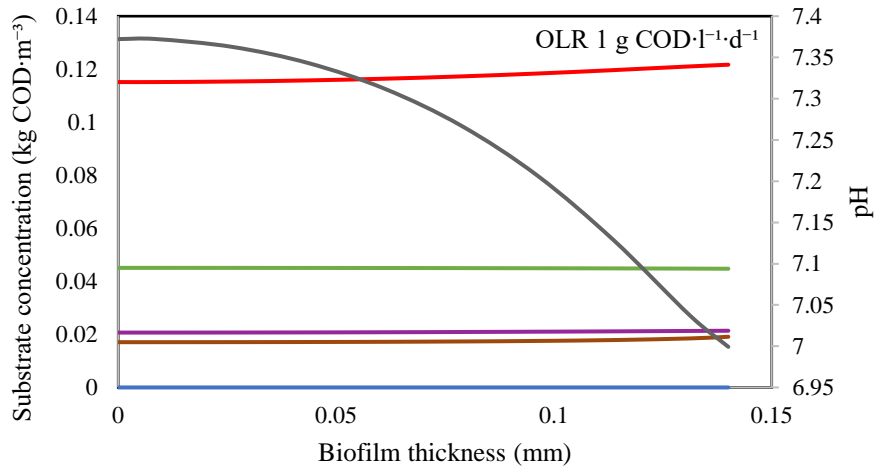
Biomass profile along the granule in UASB reactor during steady-state condition:



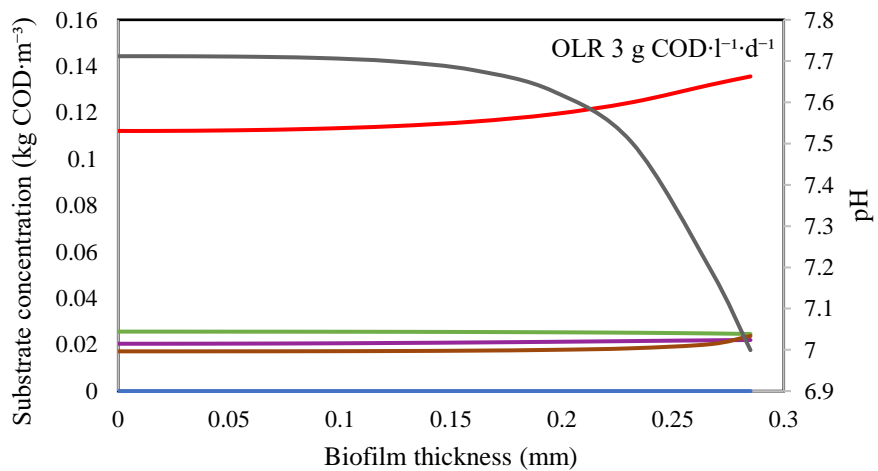




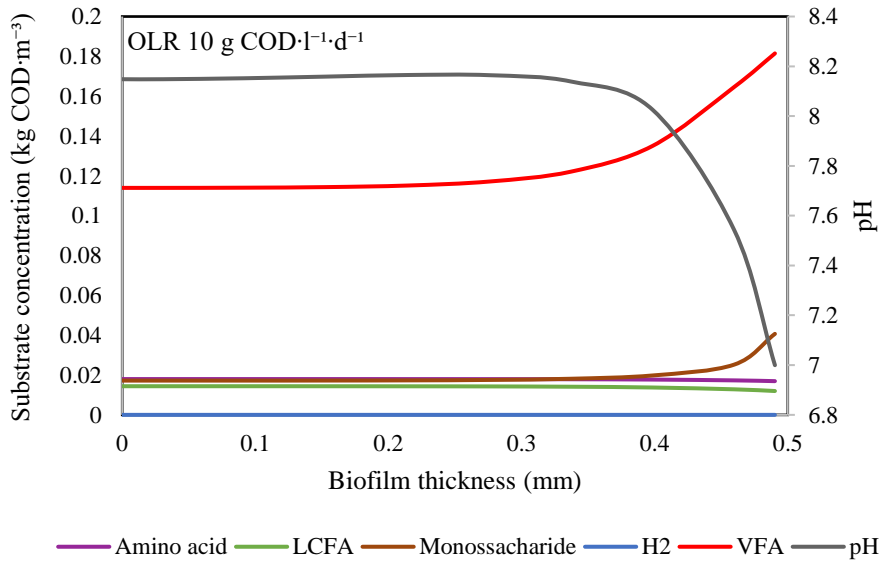
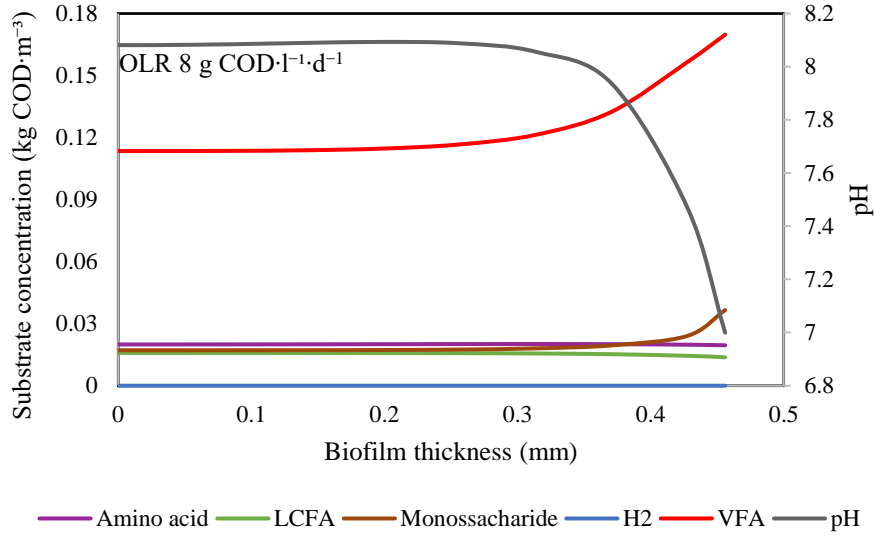
Substrate profile along the granule in UASB reactor during steady-state condition:

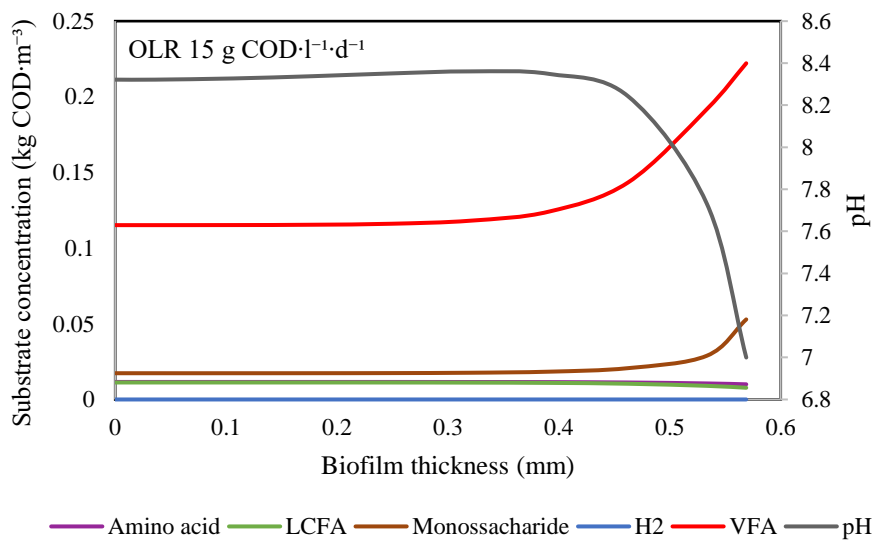
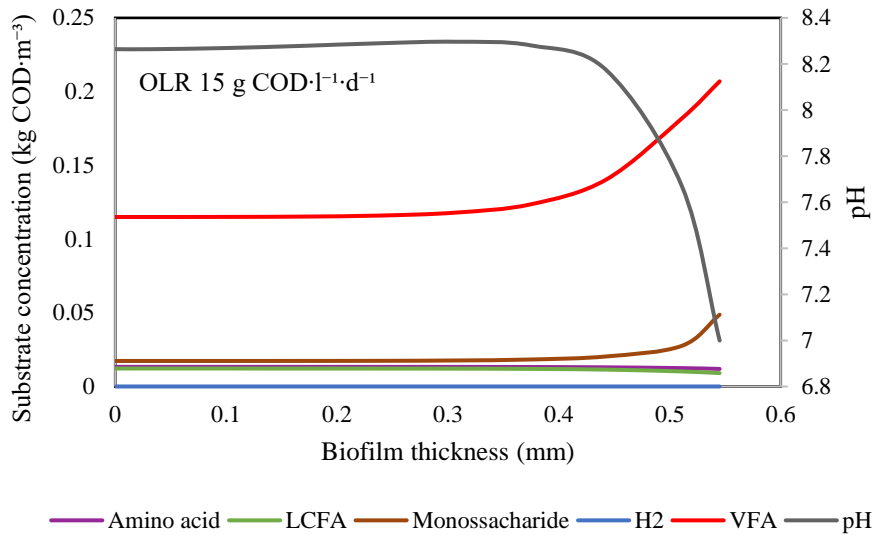


— Amino acid — LCFA — Monossacharide — H₂ — VFA — pH



— Amino acid — LCFA — Monossacharide — H₂ — VFA — pH





References

Batstone, D. 2006. Mathematical Modelling of Anaerobic Reactors Treating Domestic Wastewater: Rational Criteria for Model Use.

Reviews in Environmental Science and Bio/Technology, 5(1), 57-71.

Batstone, D.J., Keller, J., Angelidaki, I., Kalyuzhnyi, S.V., Pavlostathis, S.G., Rozzi, A., Sanders, W.T.M., Siegrist, H., Vavilin, V.A. 2002. Anaerobic Digestion Model No. 1 (ADM1). IWA Scientific and Technical Report No. 13, London SW1H 0QS, UK.

Batstone, D.J., Keller, J., Blackall, L.L. 2004. The influence of substrate kinetics on the microbial community structure in granular anaerobic biomass. *Water Research*, 38(6), 1390-1404.

Cunningham, A.B., Lennox, J.E., Ross, R.J. 2011. Biofilms: The Hypertextbook, Retrieved from (http://www.hypertextbookshop.com/biofilmbook/working_versionOld/).

de Heyder, B., Vanrolleghem, P., van Langenhove, H., Verstraete, W. 1997. Kinetic characterization of mass transfer limited biodegradation of a low water soluble gas in batch experiments—Necessity for multiresponse fitting. *Biotechnology and Bioengineering*, 55(3), 511-519.

Fedorovich, V., Lens, P., Kalyuzhnyi, S. 2003. Extension of Anaerobic Digestion Model No. 1 with processes of sulfate reduction. *Applied Biochemistry and Biotechnology*, 109(1-3), 33-45.

Gavala, H.N., Lyberatos, G. 2001. Influence of anaerobic culture acclimation on the degradation kinetics of various substrates. *Biotechnology and Bioengineering*, 74(3), 181-95.

Gujer, W., Zehnder, A.J.B. 1983. *Conversion Processes in Anaerobic Digestion*. IAWPRC ; Pergamon. Oxford, United Kingdom.

Lide, D.R. 2003. *CRC Handbook of Chemistry and Physics*, 84th Edition. Taylor & Francis. Bethesda, Maryland.

- Nishimura, S., Yoda, M. 1997. Removal of hydrogen sulfide from an anaerobic biogas using a bio-scrubber. *Water Science and Technology*, 36(6–7), 349-356.
- Reid, R.C., Prausnitz, J.M., Sherwood, T.K. 1977. *The properties of gases and liquids*. McGraw-Hill. New York, US.
- Reis, M.A., Almeida, J.S., Lemos, P.C., Carrondo, M.J. 1992. Effect of hydrogen sulfide on growth of sulfate reducing bacteria. *Biotechnology and Bioengineering*, 40(5), 593-600.
- Romli, M., Keller, J., Lee, P.L., Greenfield, P.F. 1995. Model prediction and verification of a two-stage high-rate anaerobic wastewater treatment system subjected to shock loads. *Process Safety and Environmental Protection*, 73, 151-154.
- Rosen, C., Jeppsson, U. 2006. Aspects on ADM1 Implementation within the BSM2 Framework. in: *Industrial Electrical Engineering and Automation (IEA)*, Lund Institute of Technology (LTH). Lund, Sweden.
- Sander, R. 1999. *Compilation of Henry's Law Constants for Inorganic and Organic Species of Potential Importance in Environmental Chemistry*. Max-Planck Institute of Chemistry. Frankfurt, Germany.
- Shen, C.F., Guiot, S.R. 1996. Long-term impact of dissolved O₂ on the activity of anaerobic granules. *Biotechnology and Bioengineering*, 49(6), 611-620.
- Tchobanoglous, G., Burton, F.L., Metcalf, Eddy. 1991. *Wastewater engineering: treatment, disposal, and reuse*. McGraw-Hill. New York, US.
- van der Lans, R.G.J.M. 2000. *Advanced course on environmental biotechnology*. Chapter 21: Gas-liquid interphase transport. Biotechnological sciences Delft Leiden. The Netherlands.

- Verhallen, P.T.H.M., Oomen, L.J.P., Elsen, A.J.J.M.v.d., Kruger, J., Fortuin, J.M.H. 1984. The diffusion coefficients of helium, hydrogen, oxygen and nitrogen in water determined from the permeability of a stagnant liquid layer in the quasi-s. *Chemical Engineering Science*, 39(11), 1535-1541.
- Wilhelm, E., Battino, R., Wilcock, R.J. 1977. Low-pressure solubility of gases in liquid water. *Chemical Reviews*, 77(2), 219-262.
- Xu, X., Chen, C., Lee, D.J., Wang, A., Guo, W., Zhou, X., Guo, H., Yuan, Y., Ren, N., Chang, J.S. 2013. Sulfate-reduction, sulfide-oxidation and elemental sulfur bioreduction process: modelling and experimental validation. *Bioresource Technology*, 147, 202-1